1401184490

43/446
CRANFIELD UNIVERSITY
LIBRARY

CRANFIELD INSTITUTE OF TECHNOLOGY

COLLEGE OF AERONAUTICS

AERODYNAMICS DEPARTMENT

PhD THESIS

S. B. V. GOMES

An Investigation of the Flight Dynamics of Airships with Application to the YEZ-2A

Supervisor: Mr M. V. Cook

October 1990

CRANFIELD UNIVERSITY
LIBRARY

A B S T R A C T

In order to construct a flight dynamics computer simulation model of airship flight with a high degree of fidelity in the aerodynamic modelling, extensive wind tunnel testing was carried out. This was aimed at, first developing some specific airship wind tunnel testing techniques and then to obtain aerodynamic data for the YEZ-2A project airship being designed and built by Airship Industries for the US Navy. The wind tunnel testing techniques so developed insured a good matching between wind tunnel results and flight test data from existing airships.

The next step consisted in the construction of the flight dynamics computer simulation model. This was a full six-degree-of-freedom (6 DOF) non-linear model written in the simulation language ACSL, and the wind tunnel generated data for the YEZ-2A airship provided the aerodynamic data base.

The computer simulation model was then used to study the YEZ-2A aerodynamic stability modes, to obtain a catalogue of vehicle responses to both aerodynamic and power control inputs and finally to predict some of its longitudinal handling qualities characteristics.

ACKNOWLEDGEMENTS

This research programme would not have been possible without the help and encouragement of many people. It would be impossible to thank everyone by name, but my thanks to anyone who has contributed to the programme.

I am greatly indebted to virtually all the technicians of the Aerodynamics Department of the College of Aeronautics. Their vital participation in the design, construction and then wind tunnel testing of the various airship models, frequently at unsocial times will always be remembered with great affection.

My thanks also go to Dr Kevin Garry and Barry Anderson, for their warm support during the wind tunnel test programme and to Dr Sandra Fairs for the great help received during and after the wind tunnel data processing.

I am also greatly indebted to the supervisors of this work, i.e., Mike Cook, Ian Harris and Pete Thomasson. Only with their continuous and unabated support was it possible to carry out the multidisciplinary tasks required by this research programme.

Finally, none of this would have been possible without the support given by two sponsors, CNPq (the National Research Council of Brazil) and Airship Industries (UK) Ltd, the latter being behind the extensive airship wind tunnel test programme carried out. My personal thanks to Ken Nippress, David Speirits, Crispin Belcher and Mike Pilkington of the Airship Industries Aerodynamics Department for their invaluable support.

CONTENTS

Page

LIST OF FIGURES

NOTATION

1. OVERVIEW 1
   1.1 Introduction 1
   1.2 Background 5
   1.3 The Purpose of this Work 7

2. THE AERODYNAMIC MODEL 10
   2.1 Introduction 10
   2.2 Results from the Tasks 11
      2.2.1 Task 1 11
      2.2.2 Task 1A 15
      2.2.3 Task 2 18
      2.2.4 Task 3 21
      2.2.5 Task 4 21
   2.3 The YEZ-2A Weight, Buoyancy and Environmental Conditions Cases 22
   2.4 Concluding Remarks 23

3. THE SIMULATION CONCEPT 25
   3.1 Introduction 25
   3.2 The Adaptation to the Airship Case 26
      3.2.1 Axes and Assumptions 26
      3.2.2 Equations of Motion (EOM) 28
      3.2.3 The Mass Matrix M 29
      3.2.4 The Dynamics Vector F_d 30
      3.2.5 The Aerodynamics Vector A 31
      3.2.6 The Gravity & Buoyancy Vector G 32
      3.2.7 The Propulsion Vector P 34
   3.3 The Solution 34

4. THE SIMULATION MODEL 37
   4.1 The Computer Simulation and ACSL 37

Page

4.2 Axes Transformation 40
4.3 The Mass Matrix 41
4.3.1 The Airship Mass m 42
4.3.2 Moments and Product of Inertia 44
4.3.3 Centre of Gravity Position 44
4.3.4 Virtual Masses and Inertias 45
4.4 Dynamics 48
4.5 Aerodynamics 49
4.5.1 Importing the Wind Tunnel Data into the Simulation 50
4.5.2 The Input Parameters 51
4.5.3 Static Forces and Moments 54
4.5.4 Damping Terms 56
4.5.5 Aerodynamic Control 57
4.6 Gravity and Buoyancy 58
4.7 Propulsion 59
4.8 The Solution 62
4.9 Initial Conditions and Trimming 64
4.10 Model Running in ACSL 68

5. STABILITY INVESTIGATION AND MODE DEMONSTRATION 75
5.1 Introduction 75
5.2 Longitudinal Stability 76
5.2.1 Mode Demonstration 79
5.3 Lateral Stability 89
5.3.1 Mode Demonstration 92
5.4 Comparison and Concluding Remarks 101

6. RESPONSE TO CONTROLS 106
6.1 Introduction 106
6.2 Elevator Type of Input 107
6.3 Rudder Type of Input 117
6.4 Response to Thrust Change 128
6.5 Sensitivity to Flight Speed 134

Page

6.6 Concluding Remarks 147

7. HANDLING QUALITIES INVESTIGATION 150
7.1 Introduction 150
7.2 Experiments and Results 152
7.3 Analysis 162
7.4 Conclusions 163

8. CONCLUSIONS AND RECOMMENDATIONS 167
8.1 Conclusions 167
8.2 Recommendations 168

9. REFERENCES 170

APPENDIX-1 - DATA BASE SUMMARY 178
A1.1 Introduction 179
A1.2 YEZ-2A General Data 179
A1.3 Test Rigs 180
A1.4 Task 2 Data Base 185
A1.5 Task 3 Results 253
A1.6 YEZ-2A Mass & Inertia Tables 255
A1.7 Propulsion 259
A1.8 The Atmospheric Model 259

APPENDIX 2 - COMPUTER SIMULATION: ADDITIONAL ALGORITHMS AND PROCEDURES 262
A2.1 Introduction 263
A2.2 The Quaternion Method 263
A2.3 From Wind Tunnel Axes to Body Axes 265
A2.4 The Solution to the Aileron Cases 268
A2.5 The Solution to the $\beta < 0$ Problem 271

Page

A2.6 Tail Deflection Configuration Due to Pilot Demand 274

APPENDIX 3 - DERIVATION OF THE YEZ-2A MODES OF MOTION 276

A3.1 Introduction 277

A3.2 Eigenvalues & Eigenvectors 280

A3.3 Derivation of the Longitudinal Modes 288

A3.4 Derivation of the Lateral Modes 295

A3.5 Non-neutral Buoyancy Effects 300

LIST OF FIGURES

		Page
Fig. 1.1	: YEZ-2A Airship General Features	4
Fig. 2.1	: Skyship-600 Model Wind Tunnel Test Results: C_D, C_L and C_m versus α	14
Fig. 2.2	: Drag Comparison	17
Fig. 3.1	: The Body Axes System	27
Fig. 3.2	: The Simulation Model Structure	36
Fig. 4.1	: Program Regions of the Computer Simulation Model	38
Fig. 4.2	: Internal Arrangement of the Air Ballonets inside the Gas Envelope of the YEZ-2A	46
Fig. 4.3	: α, β, u, v, w and V_{Total} in relation to the body axes system	53
Fig. 4.4	: Ruddervator Deflection Scheme	53
Fig. 4.5	: Engine thrust lines with respect to body axes system	60
Fig. 4.6	: Computer Simulation Program Flow Chart	71
Fig. 5.1	: YEZ-2A Airship Longitudinal Stability (Eigenvalues), Case 1	77
Fig. 5.2	: YEZ-2A Airship Longitudinal Stability, Frequency versus Damping Ratio / Pendulum Mode	78
Fig. 5.3	: YEZ-2A Airship Longitudinal Hover / Heave Mode	81
Fig. 5.4	: YEZ-2A Airship Longitudinal Hover / Pendulum Mode	82
Fig. 5.5	: YEZ-2A Airship Longitudinal Surge Mode, U0 = 25 m/s	84

Page

Fig. 5.6 : YEZ-2A Airship Longitudinal Pitch Subsidence Mode, U0 = 25 m/s 86

Fig. 5.7 : YEZ-2A Airship Longitudinal Pendulum Mode, U0 = 25 m/s 87

Fig. 5.8 : YEZ-2A Airship Longitudinal Pendulum Mode, U0 = 5 m/s 88

Fig. 5.9 : YEZ-2A Airship Lateral Stability (Eigenvalues), Case 1 90

Fig. 5.10 : YEZ-2A Airship Lateral Stability, Frequency versus Damping Ratio / Roll Mode 91

Fig. 5.11 : YEZ-2A Airship Lateral Yaw Subsidence and Sideslip Subsidence Modes in Hover 94

Fig. 5.12 : YEZ-2A Airship Lateral Roll Mode in Hover 95

Fig. 5.13 : YEZ-2A Airship Lateral β-subsidence Mode, U0 = 5 m/s 98

Fig. 5.14 : YEZ-2A Airship Lateral Yaw Subsidence Mode, U0 = 5 m/s 99

Fig. 5.15 : YEZ-2A Airship Lateral Roll Mode, U0 = 5 m/s 100

Fig. 6.2.1 : YEZ-2A Airship Response to Elevator, 5° up for 15 sec, U0 = 25 m/s 109

Fig. 6.2.2 : YEZ-2A Airship Response to Elevator, 6° up for 15 sec, U0 = 25 m/s 110

Fig. 6.2.3 : YEZ-2A Airship Response to Elevator, 20° up for 15 sec, U0 = 25 m/s 112

Fig. 6.2.4 : YEZ-2A Airship Response to Elevator, 21° up for 15 sec, U0 = 25 m/s 114

Fig. 6.2.5 : YEZ-2A Airship Response to Elevator Up, Elev. Pulse of 15 sec, 200 sec. Run, U0 = 25 m/s 115

Page

Fig. 6.2.6 : YEZ-2A Airship Response to Elevator Ramp, 0.25°/sec. up, U0 = 25 m/s 116

Fig. 6.2.7 : YEZ-2A Airship Tracking Response, Ramp of 0.25°/sec up, U0 = 25 m/s 118

Fig. 6.3.1 : YEZ-2A Airship Response to Rudder, 5° to starboard for 15 sec., U0 = 25 m/s 120

Fig. 6.3.2 : YEZ-2A Airship Response to Rudder, 6° to starboard for 15 sec., U0 = 25 m/s 122

Fig. 6.3.3 : YEZ-2A Airship Response to Rudder, 20° to starboard for 15 sec., U0 = 25 m/s 123

Fig. 6.3.4 : YEZ-2A Airship Response to Rudder, 21° to starboard for 15 sec., U0 = 25 m/s 124

Fig. 6.3.5 : YEZ-2A Airship Response to Right Rudder, Rudder Pulse of 15 sec., 200 sec. Run, U0 = 25 m/s 126

Fig. 6.3.6 : YEZ-2A Airship Response to Rudder Ramp, 0.25°/sec. of Starboard Rudder, U0 = 25 m/s 127

Fig. 6.3.7 : YEZ-2A Airship Lateral Tracking Ramp of 0.25°/sec., U0 = 25 m/s 129

Fig. 6.4.1 : YEZ-2A Response to Power Change Thrust Step of 10% above T0 for 15 sec, U0 = 25 m/s 130

Fig. 6.4.2 : YEZ-2A Response to Power Change Thrust Step of 75% above T0 for 15 sec, U0 = 25 m/s 132

Fig. 6.4.3 : YEZ-2A Response to Power Change Thrust Ramp of 1% of T0 increase/sec, U0 = 25 m/s 133

Fig. 6.5.1 : YEZ-2A Airship Response to Elevator, 20° up for 15 sec, U0 = 40 m/s 135

Page

Fig. 6.5.2 : YEZ-2A Airship Response to Elevator, 20° up for 15 sec, U0 = 5 m/s 137

Fig. 6.5.3 : YEZ-2A Airship Response to Elevator Up, Ramp of 0.25°/sec., θ and η versus Time 140

Fig. 6.5.4 : YEZ-2A Airship Response to Elevator Up, Ramp of 0.25°/sec., Height versus Time 141

Fig. 6.5.5 : YEZ-2A Airship Response to Rudder, 20° to starboard for 15 sec., U0 = 40 m/s 142

Fig. 6.5.6 : YEZ-2A Airship Response to Rudder, 20° to starboard for 15 sec., U0 = 5 m/s 144

Fig. 6.5.7 : YEZ-2A Airship Response to Right Rudder, Ramp of 0.25°/sec ζ and β versus Time 145

Fig. 6.5.8 : YEZ-2A Airship Response to Right Rudder, Ramp of 0.25°/sec North versus East 146

Fig. 7.2.1 : YEZ-2A Handling Qualities Investigation, 20° of Elevator Up for 30 sec., U0 = 40 m/s 154

Fig. 7.2.2 : Flight Path and Attitude Response YEZ-2A Airship, U0 = 40 m/s 155

Fig. 7.2.3 : YEZ-2A Handling Qualities Investigation, 20° of Elevator Up for 30 sec., U0 = 25 m/s 156

Fig. 7.2.4 : Flight Path and Attitude Response YEZ-2A Airship, U0 = 25 m/s 157

Fig. 7.2.5 : YEZ-2A Handling Qualities Investigation, 20° of Elevator Up for 30 sec., U0 = 5 m/s 158

Fig. 7.2.6 : Flight Path and Attitude Response YEZ-2A Airship, U0 = 5 m/s 159

Page

Fig. 7.2.7 : Typical longitudinal short period time responses for a conventional aircraft 160

Fig. 7.3.1 : The Gibson Criterion 164

Fig. A1.3.1 : Task 1 test rig 181

Fig. A1.3.2 : Task 2 test rig 182

Fig. A1.3.3 : Task 3 test rig 183

Fig. A1.3.4 : Task 4 test rig 184

Fig. A1.4.1 : YEZ-2A Drag Data / Elevator Cases, Lateral Incidence Psi = 0 Deg 187

Fig. A1.4.2 : YEZ-2A Drag Data / Elevator Cases, Lateral Incidence Psi = -5 Deg 188

Fig. A1.4.3 : YEZ-2A Drag Data / Elevator Cases, Lateral Incidence Psi = -10 Deg 189

Fig. A1.4.4 : YEZ-2A Drag Data / Elevator Cases, Lateral Incidence Psi = -20 Deg 190

Fig. A1.4.5 : YEZ-2A Drag Data / Elevator Cases, Lateral Incidence Psi = -30 Deg 191

Fig. A1.4.6 : YEZ-2A Side Force Data/Elevator Cases, Lateral Incidence Psi = 0 Deg 192

Fig. A1.4.7 : YEZ-2A Side Force Data/Elevator Cases, Lateral Incidence Psi = -5 Deg 193

Fig. A1.4.8 : YEZ-2A Side Force Data/Elevator Cases, Lateral Incidence Psi = -10 Deg 194

Fig. A1.4.9 : YEZ-2A Side Force Data/Elevator Cases, Lateral Incidence Psi = -20 Deg 195

Fig. A1.4.10: YEZ-2A Side Force Data/Elevator Cases, Lateral Incidence Psi = -30 Deg 196

Page

Fig. A1.4.11: YEZ-2A Lift Data / Elevator Cases, Lateral Incidence Psi = 0 Deg 197

Fig. A1.4.12: YEZ-2A Lift Data / Elevator Cases, Lateral Incidence Psi = -5 Deg 198

Fig. A1.4.13: YEZ-2A Lift Data / Elevator Cases, Lateral Incidence Psi = -10 Deg 199

Fig. A1.4.14: YEZ-2A Lift Data / Elevator Cases, Lateral Incidence Psi = -20 Deg 200

Fig. A1.4.15: YEZ-2A Lift Data / Elevator Cases, Lateral Incidence Psi = -30 Deg 201

Fig. A1.4.16: YEZ-2A Rolling Moment Data / Elevator Cases, Lateral Incidence Psi = 0 Deg 202

Fig. A1.4.17: YEZ-2A Rolling Moment Data / Elevator Cases, Lateral Incidence Psi = -5 Deg 203

Fig. A1.4.18: YEZ-2A Rolling Moment Data / Elevator Cases, Lateral Incidence Psi = -10 Deg 204

Fig. A1.4.19: YEZ-2A Rolling Moment Data / Elevator Cases, Lateral Incidence Psi = -20 Deg 205

Fig. A1.4.20: YEZ-2A Rolling Moment Data / Elevator Cases, Lateral Incidence Psi = -30 Deg 206

Fig. A1.4.21: YEZ-2A Pitching Moment Data / Elevator Cases, Lateral Incidence Psi = 0 Deg 207

Fig. A1.4.22: YEZ-2A Pitching Moment Data / Elevator Cases, Lateral Incidence Psi = -5 Deg 208

Fig. A1.4.23: YEZ-2A Pitching Moment Data / Elevator Cases, Lateral Incidence Psi = -10 Deg 209

Page

Fig. A1.4.24: YEZ-2A Pitching Moment Data / Elevator Cases, Lateral Incidence Psi = -20 Deg 210

Fig. A1.4.25: YEZ-2A Pitching Moment Data / Elevator Cases, Lateral Incidence Psi = -30 Deg 211

Fig. A1.4.26: YEZ-2A Yawing Moment Data / Elevator Cases, Lateral Incidence Psi = 0 Deg 212

Fig. A1.4.27: YEZ-2A Yawing Moment Data / Elevator Cases, Lateral Incidence Psi = -5 Deg 213

Fig. A1.4.28: YEZ-2A Yawing Moment Data / Elevator Cases, Lateral Incidence Psi = -10 Deg 214

Fig. A1.4.29: YEZ-2A Yawing Moment Data / Elevator Cases, Lateral Incidence Psi = -20 Deg 215

Fig. A1.4.30: YEZ-2A Yawing Moment Data / Elevator Cases, Lateral Incidence Psi = -30 Deg 216

Fig. A1.4.31: YEZ-2A Drag Data / Rudder Cases, Lateral Incidence Psi = 0 Deg 217

Fig. A1.4.32: YEZ-2A Drag Data / Rudder Cases, Lateral Incidence Psi = -5 Deg 218

Fig. A1.4.33: YEZ-2A Drag Data / Rudder Cases, Lateral Incidence Psi = -10 Deg 219

Fig. A1.4.34: YEZ-2A Drag Data / Rudder Cases, Lateral Incidence Psi = -20 Deg 220

Fig. A1.4.35: YEZ-2A Drag Data / Rudder Cases, Lateral Incidence Psi = -30 Deg 221

Fig. A1.4.36: YEZ-2A Side Force Data / Rudder Cases, Lateral Incidence Psi = 0 Deg 222

Page

Fig. A1.4.37: YEZ-2A Side Force Data / Rudder Cases, Lateral Incidence Psi = -5 Deg 223

Fig. A1.4.38: YEZ-2A Side Force Data / Rudder Cases, Lateral Incidence Psi = -10 Deg 224

Fig. A1.4.39: YEZ-2A Side Force Data / Rudder Cases, Lateral Incidence Psi = -20 Deg 225

Fig. A1.4.40: YEZ-2A Side Force Data / Rudder Cases, Lateral Incidence Psi = -30 Deg 226

Fig. A1.4.41: YEZ-2A Lift Data / Rudder Cases, Lateral Incidence Psi = 0 Deg 227

Fig. A1.4.42: YEZ-2A Lift Data / Rudder Cases, Lateral Incidence Psi = -5 Deg 228

Fig. A1.4.43: YEZ-2A Lift Data / Rudder Cases, Lateral Incidence Psi = -10 Deg 229

Fig. A1.4.44: YEZ-2A Lift Data / Rudder Cases, Lateral Incidence Psi = -20 Deg 230

Fig. A1.4.45: YEZ-2A Lift Data / Rudder Cases, Lateral Incidence Psi = -30 Deg 231

Fig. A1.4.46: YEZ-2A Rolling Moment Data / Rudder Cases, Lateral Incidence = 0 Deg 232

Fig. A1.4.47: YEZ-2A Rolling Moment Data / Rudder Cases, Lateral Incidence = -5 Deg 233

Fig. A1.4.48: YEZ-2A Rolling Moment Data / Rudder Cases, Lateral Incidence = -10 Deg 234

Fig. A1.4.49: YEZ-2A Rolling Moment Data / Rudder Cases, Lateral Incidence = -20 Deg 235

Page

Fig. A1.4.50: YEZ-2A Rolling Moment Data / Rudder Cases, Lateral Incidence = -30 Deg 236

Fig. A1.4.51: YEZ-2A Pitching Moment Data / Rudder Cases, Lateral Incidence = 0 Deg 237

Fig. A1.4.52: YEZ-2A Pitching Moment Data / Rudder Cases, Lateral Incidence = -5 Deg 238

Fig. A1.4.53: YEZ-2A Pitching Moment Data / Rudder Cases, Lateral Incidence = -10 Deg 239

Fig. A1.4.54: YEZ-2A Pitching Moment Data / Rudder Cases, Lateral Incidence = -20 Deg 240

Fig. A1.4.55: YEZ-2A Pitching Moment Data / Rudder Cases, Lateral Incidence = -30 Deg 241

Fig. A1.4.56: YEZ-2A Yawing Moment Data / Rudder Cases, Lateral Incidence = 0 Deg 242

Fig. A1.4.57: YEZ-2A Yawing Moment Data / Rudder Cases, Lateral Incidence = -5 Deg 243

Fig. A1.4.58: YEZ-2A Yawing Moment Data / Rudder Cases, Lateral Incidence = -10 Deg 244

Fig. A1.4.59: YEZ-2A Yawing Moment Data / Rudder Cases, Lateral Incidence = -20 Deg 245

Fig. A1.4.60: YEZ-2A Yawing Moment Data / Rudder Cases, Lateral Incidence = -30 Deg 246

Fig. A1.4.61: YEZ-2A Drag Data / Aileron Case, Lateral Incidence = 0 Deg 247

Fig. A1.4.62: YEZ-2A Side Force Data/ Aileron Case, Lateral Incidence = 0 Deg 248

Fig. A1.4.63: YEZ-2A Lift Data / Aileron Case, Lateral Incidence = 0 Deg 249

Page

Fig. A1.4.64: YEZ-2A Rolling Moment Data / Aileron Case, Lateral Incidence = 0 Deg 250

Fig. A1.4.65: YEZ-2A Pitching Moment Data / Aileron Case, Lateral Incidence = 0 Deg 251

Fig. A1.4.66: YEZ-2A Yawing Moment Data / Aileron Case, Lateral Incidence = 0 Deg 252

Fig. A1.7.1 : Power versus RPM curve for CRM engine 260

Fig. A2.3.1 : Axes transformation, wind tunnel axes to airship body axes 266

Fig. A2.4.1 : Axes transformation, Lift and Drag axes to airship body axes 270

Fig. A3.3.1 : Longitudinal Eigenvectors, YEZ-2A. U0 = Hover, Case 1, Pendulum Oscillation 290

Fig. A3.3.2 : Longitudinal Eigenvectors, YEZ-2A. U0 = 5 m/s, Case 1, Pendulum Oscillation 292

Fig. A3.3.3 : Longitudinal Eigenvectors, YEZ-2A. U0 = 25 m/s, Case 1, Pendulum Oscillation 294

Fig. A3.4.1 : Lateral Eigenvectors, YEZ-2A. U0 = Hover, Case 1, Roll Oscillation 297

Fig. A3.4.2 : Lateral Eigenvectors, YEZ-2A. U0 = 5 m/s, Case 1, Roll Oscillation 299

NOTATION

A	Aerodynamics vector (Chapter 4)
ACSL	Advanced Continuous Simulation Language
AFCS	Automatic Flight Control System
a_x, a_y, a_z	CG coordinates in the body axes system
B	Buoyancy force
CAP	Control Anticipation Parameter (Chapter 7)
C_D	Drag coefficient
C_L	Lift coefficient
C_l	Rolling moment coefficient
C_m	Pitching moment coefficient
C_n	Yawing moment coefficient
C_Y	Side force coefficient
CB	Centre of gross buoyancy
CG	Centre of Gravity
CV	Centre of Volume
d	Airship envelope maximum diameter
DB	Pitch attitude dropback angle (Chapter 7)
DCM	Direction Cosine Matrix
DOF	Degrees of freedom
EOM	Equations of motion
FCS	Flight Control System
F_d	Propulsion vector (Chapter 4)
G	Gravity vector (Chapter 4)
GRPATH	Distance travelled along ground path
g	Gravitational acceleration
Height	Altitude of airship above the ground
ISA	International Standard Atmosphere
L	Airship rolling moment about OX
l	Airship envelope length
M	Airship pitching moment about OY
M	Mass matrix (Chapter 4)
m	Airship total mass (Chapter 4)
M_q	Pitching moment derivative due to rate of pitch, $\partial M/\partial q$

m_q	Non-dimensional form of M_q (Appendix-1)
M_w	Pitching moment derivative due to velocity along OZ, $\partial M/\partial w$
m_w	Non-dimensional form of M_w (Appendix-1)
N	Airship yawing moment about OZ
N_{CB}	Airship load factor with respect to the CB
N_r	Yawing moment derivative due to rate of yaw, $\partial N/\partial r$
n_r	Non-dimensional form of N_r (Appendix-1)
N_v	Yawing moment derivative due to sideslip, $\partial N/\partial v$
n_v	Non-dimensional form of N_v
OX, OY, OZ	Airship body axes, with origin at CV
PIO	Pilot induced oscillations
p	Airship angular velocity in roll
q	Airship angular velocity in pitch
q_m	Peak pitch rate (Chapter 7)
q_{ss}	Steady pitch rate (Chapter 7)
r	Airship angular velocity in yaw
T	Period of oscillation
TDIESP	Thrust produced by port Diesel engine
$T\theta_2$	Time constant between airship pitch angle and flight path angle (Chapter 7)
t	Simulation time variable
t_d	Effective delay of pitch rate (Chapter7)
t_q	Time at pitch rate peak (Chapter 7)
$t_{\dot{q}}$	Time at pitch acceleration peak (Chapter 7)
t_γ	Flight path angle delay (Chapter 7)
U0	Airship initial total velocity at the beginning of a simulation run
u	Airship linear velocity along OX
v	Airship linear velocity along OY
V_{Tot}	Total airship linear velocity
W	Airship weight
w	Airship linear velocity along OZ
X	Airship force component along OX
Y	Airship force component along OY

Z	Airship force component along OZ
α (Alpha)	Airship longitudinal incidence with respect to OX
β (Beta)	Airship lateral incidence with respect to OY
γ (Gama)	Airship flight path angle with respect to horizontal plane ($\gamma = \theta - \alpha$)
δ_i (Delta)	Angular deflection of ruddervator i
ξ (Csi)	Total amount of aileron type of angular deflection present in any given tail deflection configuration (Chapter 4)
η (Eta)	Total amount of elevator type of angular deflection present in any given tail deflection configuration (Chapter 4)
η (Eta)	Angle of ruddervator deflection (all four) in elevator fashion (Chapter 6)
ζ (Zeta)	Total amount of rudder type of angular deflection present in any given tail deflection configuration (Chapter 4)
ζ (Zeta)	Damping ratio (Chapter 5)
ζ (Zeta)	Angle of ruddervator deflection (all four) in rudder fashion (Chapter 6)
θ (Theta)	Airship pitch angle (Euler)
λ_{ij} (Lambda)	Elements of the DCM
ρ (Rho)	Air density
τ (Tau)	Time constant
ϕ (Phi)	Airship bank angle (Euler)
ψ (Psi)	Airship yaw angle (Euler)
ω (Omega)	Angular frequency of oscillation
$\dot{(\ )}$	Derivative with respect to time

1. OVERVIEW

1.1 Introduction

In the history of world aviation the place occupied by the airship stands as a unique example of the successes and failures accumulated since man began to fly. The airship was the first vehicle used to demonstrate that controlled flight was possible, when the Brazilian aeronaut and sportsman Santos Dumont won the Deutsch prize in Paris in the beginning of this century.

The airship was also the first means of transcontinental air travel, when in the 1920s and 30s the German Zeppelins, operating for the DELAG airline, provided safe and regular trans-Atlantic crossings between Europe and North and South America (Ref. 1). The spectacular accident of 1936 with the Hindenburg put a sudden stop to the passenger carrying side of airship flight, but what is usually not so well known is the fact that the United States Navy continued to successfully operate their 'blimps' until the early 1960s in the anti-submarine warfare (ASW) role. During the Second World War, it is reported that no cargo ship was ever sunk by a German submarine in convoys being escorted by blimps.

The British efforts in the airship area culminated in the extraordinary R100 and R101 designs. Were it not for political influences which seriously compromised the R101 development program, resulting ultimately in its crash sixty years ago, they could have easily advanced this branch of aeronautical engineering beyond even what was being attempted in Germany at that time (Ref. 2). The R34 airship does stand, however, as the first aircraft ever to have crossed the Atlantic in both directions.

In the America of the 1920s and 30s, political problems also affected the destiny of the US Navy program of large rigid airships, which started with the ZR-1, the

'Shenandoah', and finished after the crash of the ZR-5, the 'Macon'. With the notable exception of the ZR-3, the German built 'Los Angeles' from the Zeppelin Company, all the others crashed ultimately due to causes largely attributable to political manipulation of an infant technology (Ref. 3). This took the form of flying into appalling weather conditions (ZR-1 and 4), expecting to show the airship's worth, executing manoeuvres well beyond the structural load limits (ZR-2) and even delaying mandatory structural reinforcement modifications (ZR-5).

In more recent times, interest in the airship arose after the oil crisis of 1973. The exceptionally low fuel consumption associated with the airship made it a subject of numerous studies carried out by major international institutions. An important international conference took place at the Massachusetts Institute of Technology in 1974 (Ref. 4) to discuss airship applications as well as its technical peculiarities, followed by similar events every two years organized by the American Institute of Aeronautics and Astronautics, the so called LTA (for lighter-than-air) Systems Technology Conferences. In Britain, the Airship Association in connection with the Royal Aeronautical Society has also been promoting yearly events of the same kind for quite a number of years now.

In 1981, the United Nations Organization for Industrial Development also sponsored a major gathering in Vienna between the representatives of developed and not so developed countries aimed at assessing the airship's potential as an agent to foster economic development.

However, as far as actual vehicle development is concerned the picture is not so bright. After a number of exploratory designs in the 70s, which ranged in applications from airships for natural gas transportation to those destined for cargo transportation in poor countries, the only significant designs to emerge were

those originated at Airship Industries in the United Kingdom (Ref. 5). The Skyship-500 was a late 70s design which was used for advertising and also underwent the most extensive series of concept evaluation trials that an airship has undergone in modern times (Ref. 6). Its updated and slightly larger version, the Skyship-600, has been successfully used for advertising, passenger sight-seeing, police patrol and crowd control duties, amongst other tasks, for a number of years now (Ref.7). It was also the chosen test bed for the first aircraft ever to fly with a full 'flight-by-light' type of flying controls (Ref. 8).

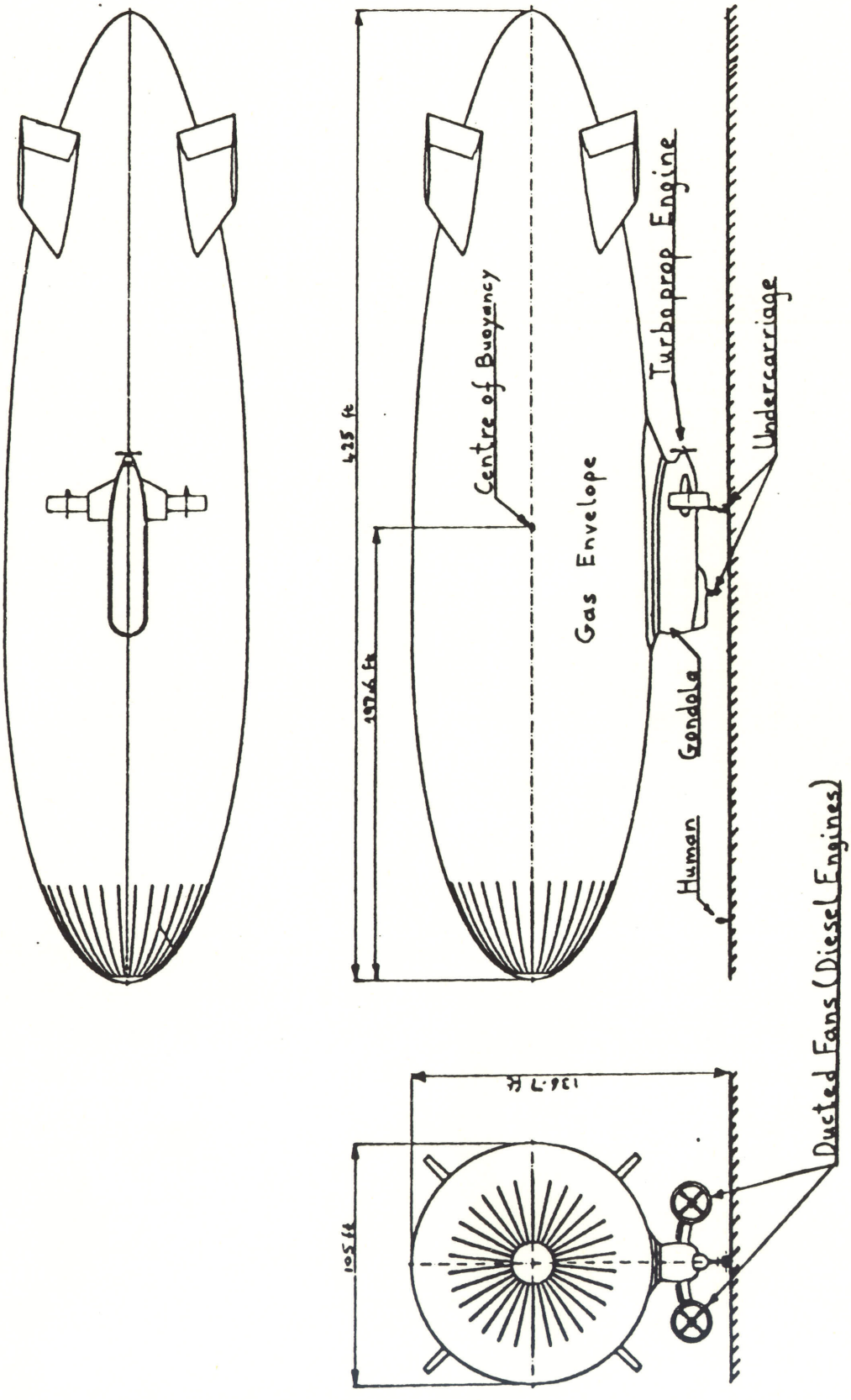
It was therefore considered a major breakthrough when, in 1987, the YEZ-2A contract was awarded to the consortium of Airship Industries and Westinghouse for the supply to the US Navy of an Airborne Early Warning (AEW) airship (Ref. 9). The so called Naval Airship Program (NASP) called for the design and construction of an Operational Development Model (ODM) whose main mission will be to demonstrate the airship capability in the AEW role, although other missions are already being considered for it (Ref. 10). The vehicle that is to fulfill the ODM requirements is called the YEZ-2A and it is the first large military non-rigid airship to be built in more than 25 years (Fig. 1.1).

In order to perform its AEW mission it is envisaged that it will be fitted with the radar and electronic suite already operational in the E2C 'Hawkeye' carrier based aircraft. The radar antenna is to be housed inside the gas envelope.

What is in effect outstanding in this event is the fact that a substantial proportion of the total US$ 170 million contract value is to go into research and development. In other words, for the first time in several decades money is being invested in upgrading airship technology to state-of-the-art levels.

It was therefore this set of circumstances that made

FIGURE 1.1 : YEZ-2A AIRSHIP GENERAL FEATURES



the research work here described not only possible but worth pursuing as well.

1.2 Background

With the resurgence in the 70s of world wide interest in the airship, one of the first aspects to be reassessed in the technical arena was, naturally enough, the subject of airship aerodynamics. Particular emphasis was placed on airship drag as this is the single most important design parameter in lighter than air technology (Ref. 11).

As a result of that, interest in the subject of airship flight dynamics came as a natural consequence. Airships had been considered unsuitable for flying in adverse weather conditions, of being difficult to handle near the ground and of being generally 'unstable' (Refs. 12 and 13). In order therefore to investigate these and other aspects, some notable attempts were made to model airship aerodynamics and to actually simulate airship flight with the aid of both digital and analogue computers.

Amongst the published work in this field, two research efforts in the field of flight dynamics of airships achieved a reasonable and deserved degree of prominence. The first originated at the University of Toronto Institute for Aerospace Studies (UTIAS), under the guidance of Professor James DeLaurier.

The scene was set with their 1979 paper "Airship Dynamic Stability" (Ref. 14), a landmark in the subject even to this day. After that, came the paper that is perhaps one of the most important in this field (Ref. 15), as it is actually an update and adaptation of the original formulation by Munk and others, based on slender body theory, to estimate the forces and moments acting along the airship hull and fins, with the use of modern digital computer techniques. The procedure that was outlined in this paper supplied the airship flight

dynamics researcher with a valuable tool for implementing the kind of simulation that is the main subject of this thesis, if only the geometrical characteristics together with the mass and inertias for the vehicle under study are known or estimated.

This procedure was put to good use by DeLaurier in association with other researchers (Refs. 16, 17, 18, 19, 20 and 21 amongst others) and applied to old as well as existing airships, resulting in the first major effort in contemporary times directed towards unraveling the peculiar flight dynamics aspects of airship flight. This included even airship response to turbulence.

The second research effort in this field which is worthy of praise is that undertaken by a California based company called Systems Technology Inc. Having been involved in the PACE trials of the Skyship-500 (Ref. 6), the company then used its earlier experience as consultants to NASA (the American National Aeronautics and Space Administration) in the field of airship flight simulation, to develop an airship full six degree of freedom non-linear simulation model. It has been applied to the Skyship-500 case, in order to compare its results with those from the PACE trials, especially in terms of transfer functions between control inputs and airship response in the frequency domain (Refs. 22 and 23).

The significance of the research efforts just described can better be gauged by the the realization that not only for the first time was it possible to predict airship flight characteristics but also that a certain degree of success was achieved between simulation predictions and flight test results when both simulation packages were applied to the Skyship-500 case (Refs. 20 and 22). However, to put these achievements in perspective, it must be understood that all the airship flight dynamics simulations described so far had to resort to analytical means in order to establish the aerodynamic model of the vehicles under consideration.

These analytical means were, as already mentioned, largely based on adaptations of slender body theory plus the cross-flow drag concept (Refs. 24, 25 and 26), which were originally developed in the 1920s and 30s at the height of world wide interest in airships. The main available experimental source used to compare the results from the theory was the series of wind tunnel trials carried out by Freeman using a 1:40 scale model of the 'Akron' (ZR-4) airship (Refs. 27, 28 and 29), as for some unknown reason, the excellent work reported in various Report & Memoranda of the British Aeronautical Research Committee, especially in connection with the R101, did not enjoy the same level of popularity. The Akron was a large rigid airship with a slenderness ratio (length over maximum diameter) of about six. Modern day non-rigid airships have a slenderness ratio of about 4.0 and so the original theory had to be suitably adapted in order to cater for this substantial change.

It was therefore with this background that the subject of this thesis was undertaken. In view of the importance of the YEZ-2A project, the need for the accurate modelling of airship aerodynamics had by then become an overwhelming consideration.

1.3 The Purpose of this Work

The purpose of this work was to construct an airship flight dynamics simulation with a high degree of fidelity in the aerodynamic modelling of the vehicle. In order to pursue this objective it was decided, early on in the project development, that the preferred source of data for the aerodynamic modelling would not come from the current analytical methods previously mentioned but from a wind tunnel test programme.

With the establishment of a cooperation scheme with Airship Industries linked with the YEZ-2A project (originally denominated 'Sentinel 5000', Ref. 30) the generation of an aerodynamic data base became the main

subject of interest for both parties. A mutually agreed programme of wind tunnel tests was therefore conceived and carried out (See Chapter 2), the result of which was a reasonably comprehensive aerodynamic data base that could and was used in the aerodynamic modelling of YEZ-2A in the way required to implement the flight dynamics simulation.

In contrast with the previously mentioned work in this field, where the simulation was first conceived, implemented and then checked against whatever flight test results became available, in the present case the overriding consideration was to try to correlate the wind tunnel test results with flight test data before the simulation was implemented. This type of approach was clearly justified in view of the original objective of a high fidelity simulation model.

Bearing in mind that the YEZ-2A was a project airship and that the option of having flight test data from it would not be available, the solution adopted was to carry out some initial wind tunnel tests with a model of an existing airship, the Skyship-600. The objective at this stage turned out to be the development of wind tunnel test techniques that would enable a good match between flight test data and tunnel data.

What happened eventually was that the more or less full confirmation of a reasonable match between flight test and tunnel data came only much later in the programme (See Section 2.4), although some encouraging early evidence was available from the PACE report (Ref. 6 and Fig. 2.2 of Chapter 2).

All in all, it was felt that the risks involved in this undertaking would be worth taking in view of the somewhat pioneering nature of generating a reasonably large wind tunnel aerodynamic data base for an airship whose slenderness ratio is of the order of 4.0, and which, as a consequence, has no known precedent as far as its scope and range of results are concerned.

As is often the case, this is the type of approach that has to be followed if the advancement of knowledge is the ultimate objective being pursued.

2. THE AERODYNAMIC MODEL

2.1 Introduction

The purpose of this Chapter is to give a brief outline on the aerodynamic data base that was used in support of the YEZ-2A flight dynamics simulation.

The generation of the afore mentioned data base occurred largely as a result of a cooperation between the College of Aeronautics and Airship Industries(UK) Ltd (Ref 30). The program of cooperation (Ref 31), which started in January of 1988 and finished in July of 1989, was organized around five so-called 'Tasks'. The basic principles that guided the concept of these five Tasks can be summarized as:

1. Gain experience in airship wind tunnel testing, given its specific peculiarities.

2. Provide Airship Industries with wind tunnel data resulting from investigating alternative hull shapes together with different fin sizes and locations on the hull tail cone. This was aimed at helping the preliminary design process at Airship Industries so that a basic design for the YEZ-2A could be evolved. The basic hull and fins design would therefore be employed in the work that followed.

3. Obtain wind tunnel static aerodynamic data on the YEZ-2A design, in terms of force and moment coefficients, pressure distribution around the hull and some of the fins, and control surface (ruddervator) hinge moments. This would enable Airship Industries to assess their design whilst at the same time supplying a substantial part of

the data base required by our flight dynamics simulation.

4. Obtain wind tunnel dynamic aerodynamic data on the YEZ-2A design, in terms of aerodynamic longitudinal and lateral rotary stability derivatives. This would eventually be incorporated into the flight dynamics simulation as the so-called damping terms.

5. Investigate the YEZ-2A response to turbulence, an area which is of particular relevance to airship flight, forms an important part of airship certification requirements (Ref 32), and is still lacking serious and comprehensive studies.

Finally, in order to be able to actually run the simulation model, it was necessary to obtain data regarding estimates on the moments of inertia, total mass and mass distribution as a function of environmental conditions. By the time the actual flight dynamics simulation started, the YEZ-2A project had seen enough progress at Airship Industries so that these estimates were available and could therefore be incorporated in the simulation model.

The following sections summarize the work performed in each of the Tasks and activities. These lead eventually to the aerodynamic model of the YEZ-2A used as the data base for the flight dynamics simulation.

2.2 Results from the Tasks

2.2.1 Task 1

The main purpose of this first Task was to try to obtain some degree of expertise in airship wind tunnel

testing. The main problems faced were:

1. Due to the relative large size of an airship, the results of airship wind tunnel testing are not always reliable in view of the large scale factors involved.
2. The thickness of the boundary layer on the aft portion of the envelope affects the fins and control surfaces effectiveness. This thickness is dependent upon the rate of growth of the boundary layer, i.e., to scale effects and the wind tunnel test Reynolds number relative to full size.

In view of these important aspects, it was decided that the the Task 1 investigation would incorporate the following points:

1. Boundary layer tripping and surface roughening techniques would be employed on the wind tunnel model so as to effectively raise the test Reynolds number. This would hopefully lead to turbulent flow over the whole model length and therefore avoid the unwanted effects of flow separation.
2. As the ultimate test for any wind tunnel result is a comparison with flight test results, and the YEZ-2A was a project airship, it was therefore decided that a 1:75 scale model of the existing Skyship-600 would be built and tested in the 8ft x 6ft wind tunnel of the College of Aeronautics. Since a small amount of flight test data was then available for the Skyship-500 and 600 airship series, these were to be used in the validation of the wind tunnel data.

The Skyship-600 model was therefore tested with four different kinds of surface roughening:

1. Model covered in fishnet type of stocking, for maximum surface roughness (Fig. A1.3.1 of Appendix-1).
2. Model covered in a fine mesh type of stocking, for minimum degree of surface roughness.
3. Model with bare hull but with a nose band for tripping the flow.
4. Model with the bare standard smooth wooden hull, for comparison purposes.

The results produced by the wind tunnel tests were analyzed in terms of drag, lift and pitching moment coefficients. Figure 2.1 shows these plotted as a function of incidence for the 'no control surface deflection' case.

These results were then compared with a previous set of wind tunnel test results (Ref. 33) and the small amount of flight test data then available (Ref 6). The conclusion reached was that the smallest amount of envelope surface roughening was to be used in all subsequent airship wind tunnel testing for the following reasons:

1. The Lift and Pitching Moment coefficient graphs show good agreement between the various surface condition results. The exception was the nose band case and this method was not therefore further pursued. The phenomenon of flow separation seems to have been avoided to a large extent, except in the range of extreme angles of longitudinal incidence where where some data scatter is evident in the pitching moment results. This last point is further substantiated by the pressure distribution measurements also carried out in the course of this work, and which were extensively analyzed in Reference 34.

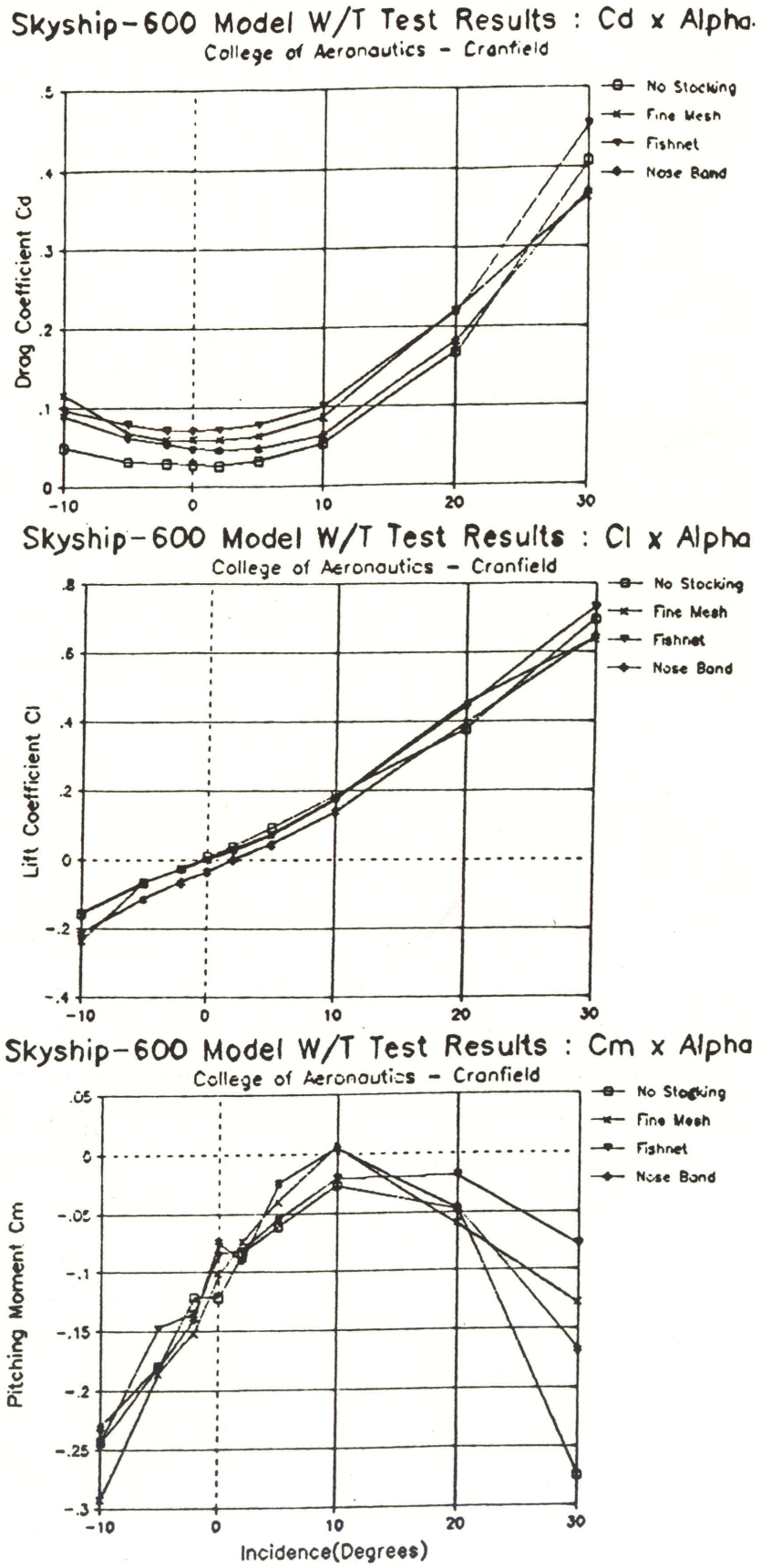

Skyship-600 Model W/T Test Results : Cd x Alpha
College of Aeronautics - Cranfield
No Stocking
Fine Mesh
Fishnet
Nose Band
Drag Coefficient Cd
.5
.4
.3
.2
.1
0
-10
0
10
20
30
Skyship-600 Model W/T Test Results : Cl x Alpha
College of Aeronautics - Cranfield
No Stocking
Fine Mesh
Fishnet
Nose Band
Lift Coefficient Cl
.8
.6
.4
.2
0
-.2
-.4
-10
0
10
20
30
Skyship-600 Model W/T Test Results : Cm x Alpha
College of Aeronautics - Cranfield
No Stocking
Fine Mesh
Fishnet
Nose Band
Pitching Moment Cm
.05
0
-.05
-.1
-.15
-.2
-.25
-.3
-10
0
10
20
30
Incidence(Degrees)

FIGURE 2.1

2. The Drag coefficient graph shows what was expected: Increasing surface roughness merely shifts the drag curve upwards as airship drag is, to a considerable extent, skin friction drag. The flight test drag coefficient estimate then available (Ref 6) indicated that the bare hull results were on the optimistic side, whereas the fine mesh stocking results fell on the pessimistic side by approximately 60%.

In this way, the minimum degree of surface roughness was concluded as being a must in the subsequent airship wind tunnel testing, with the proviso that drag coefficient results would probably need some fine tuning adjustment before they could be readily used. The complete set of methods employed and results achieved in this Task 1, which eventually resulted in approximately 2,500 force and moment coefficient data points and 500 pressure distribution data points, is given in Reference 35.

2.2.2 Task 1A

The main purpose of this Task was to help Airship Industries complete the preliminary design assessment of the YEZ-2A hull shape and fins. In order to achieve this, a 1:75 scale model of the YEZ-2A airship was built and tested in the 8ft x 6ft tunnel of the College of Aeronautics. Its method of assembly was such that it permitted three types of envelope tail cones (back ends) to be quickly interchanged, together with two types of fins, which in turn could be fitted at two different hull station positions.

Considering that the size of the model (1.72 m long) did not allow it to be covered in human stockings, the required degree of surface roughness was implemented by

painting the polyurethane made hull with grey spray paint from a distance of approximately 60 cm. This enabled a coarse type of surface finish to be achieved, which was felt to closely reproduce the fine mesh stocking type of surface roughness originally employed in the Task 1 wind tunnel tests.

The scope of the wind tunnel testing that was carried out was such that approximately 1,700 force and moment coefficient data points were obtained over a range of pitch and yaw angles. Some flow visualization trials were also carried out and Reference 36 gives a more detailed account of this Task 1A.

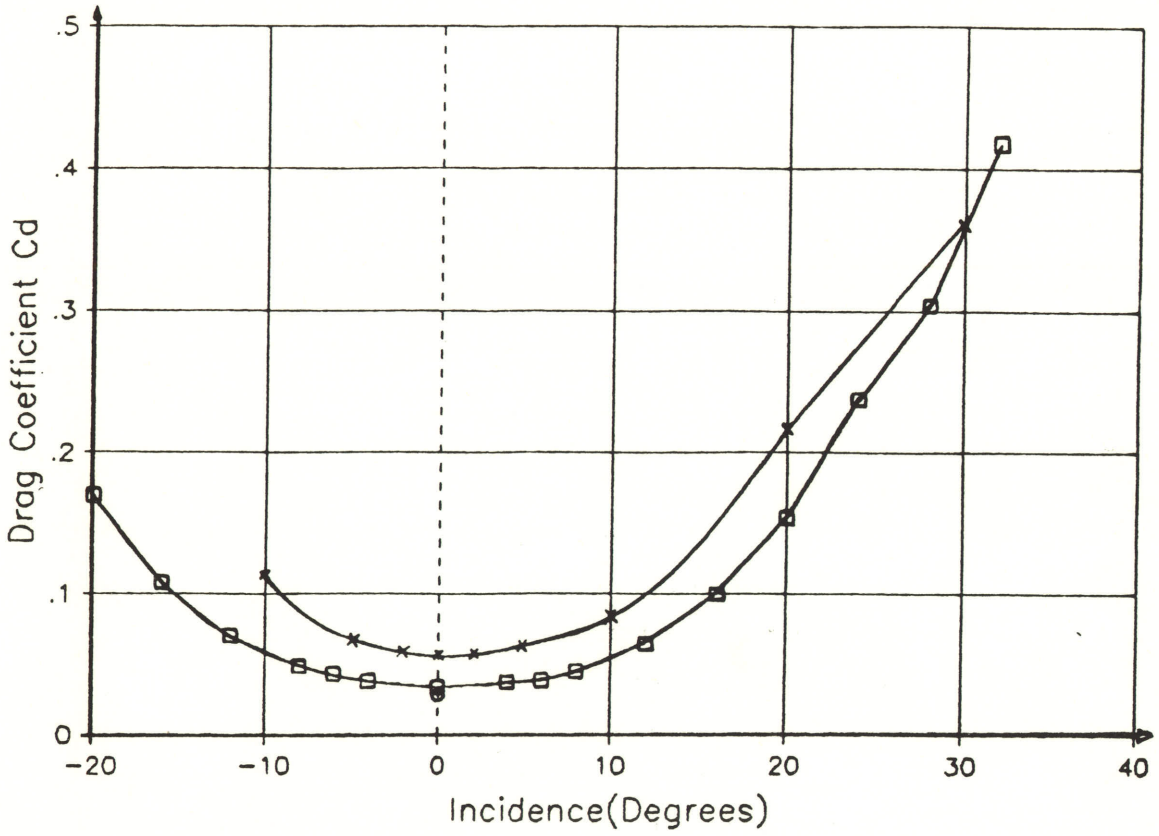
Two important results were achieved in this Task:

1. The drag coefficient result for the full flight straight and level condition (zero longitudinal and lateral incidences in terms of wind tunnel references) presented in Reference 6, is within less than 10% of the equivalent Task 1A result (Fig. 2.2).
2. The flow visualization wind tunnel tests indicated that flow separation only occurred when the airship model was set at extreme angles of longitudinal and/or lateral incidences.

These two important results lead to the conclusion that the degree of surface roughness implemented was not only adequate in view of the Task 1 investigation, but that no appreciable amount of drag curve fine tuning would be required in order to obtain reasonably realistic wind tunnel results.

Task 1A therefore served the purpose of helping Airship Industries to finalize the YEZ-2A preliminary design, as well as giving the required degree of confidence with which the subsequent Tasks, all aimed at establishing the aerodynamic characteristics of a more or less definitive design, could now be pursued.

FIG. 2.2-DRAG COMPARISON



X Task 1 Skyship-600 model with fine mesh stocking

□ Tasks 1A and 2 YEZ-2A model with roughened envelope surface

○ Skyship-500 full flight measured drag coefficient value (Ref.6)

Results for the 0° of sideslip and 0° of control surface deflection

2.2.3 Task 2

The main objective of this Task was to try to estimate the main aerodynamics characteristics of the YEZ-2A design project. This would enable Airship Industries to proceed in their design development, whilst at the same time providing the major part of the aerodynamic data base required by the flight dynamics simulation, which is the principal topic of this thesis.

The investigation carried out was concentrated around three main areas:

1. Force and Moment coefficients, i.e., obtaining the non-dimensional coefficients of Drag, Lift, Side Force, Rolling Moment, Pitching Moment and Yawing Moment.
2. Pressure distribution around the hull and along the quarter chord line of some of the fins.
3. Control surface (ruddervator) Hinge Moment coefficients.

The work was performed by incorporating the required modifications to the Task 1A 1:75 scale model of the YEZ-2A airship, and testing it in the 8ft x 6ft wind tunnel of the College of Aeronautics. (Fig. A1.3.2 of Appendix-1). The modifications included the fitting of a gondola (or 'car' in the US Navy vocabulary) to the underside of the model, fins with movable ruddervators, including two with strain gauge balances fitted to their deflection axes (for hinge moment measurements), and a total of 96 pressure tappings connected to two scanning valves for pressure distribution measurements.

A test Reynolds number of 6×10^6 was achieved in the wind tunnel, which is estimated to be about 35 times less than the full flight value, and this was considered to be quite an acceptable figure for airship model testing. Considering the tested range of the model longitudinal and lateral incidences, coupled with a

number of ruddervator deflection angles, a total of approximately 3,000 data points were produced for the various force, moment and hinge moment combinations, and 15,000 data points for the associated pressure distributions. A more detailed account of the Task 2 methods and results can be found in Reference 37.

It is important to note, however, that as far as the flight dynamics simulation is concerned, the relevant results produced by this Task were the force and moment coefficients produced. They were obtained as a result of testing the YEZ-2A scale model through a reasonably comprehensive range of longitudinal (α) and lateral ($\beta = -\psi$, in the wind tunnel axes system) incidences and ruddervator deflection angles. These were, in effect, the following:

* ψ angles: 0°, -5°, -10°, -20°, -30°
* α angles: -20°, -16°, -12°, -8°, -6°, -4°, 0°, 4°, 6°, 8°, 12°, 16°, 20°, 24°, 28°, 32°
* Ruddervator deflection angles (In both elevator and rudder configurations): -25°, -15°, 0°, 15°, 25°

In practice, the scheme of testing was achieved by setting the airship model at one of the ψ angles and running the wind tunnel while the model would be put through each of the stated α settings. This operation would be repeated for each ruddervator deflection angle, first in the pure elevator type of tail deflection configuration and then in the pure rudder type. Next, the model would be set at another ψ angle and the whole process repeated again until the complete range of ψ angles had been covered. The aerodynamic data base that resulted from following this procedure meant that for each set of a particular combination of ψ, α, and ruddervator deflection angles there would be, associated with it, three force coefficients (drag, lift and side force) and three moment coefficients (rolling, pitching

and yawing).

The processing of the raw data gathered in the wind tunnel was carried out using the model and test parameters required for the non-dimensionalization of the force and moment results (See Appendix-1). The resulting data base was presented in table form in ASCII type of files, one for each combination of ψ and ruddervator deflection, and containing the six coefficients as a function of α. In this way, the files were ready for visual inspection, by the use of a personal computer, they could be printed if so wished, or they could be used as input for a spread sheet type of software if the plotting of the coefficients were required.

The aerodynamic data base as here described was subsequently modified in its format, so as to suit the requirements of the simulation in general, and of the simulation language (ACSL) in particular. It is important to note, however, that data points were produced for the previously stated combinations of ψ, α, and ruddervator deflection angles only. Any simulation flight condition which fell in between any of the data points, or indeed outside the range covered, had its aerodynamic force and moment coefficients determined by a process of linear interpolation or extrapolation respectively (See Chapter 4).

In spite of this limitation, it was felt that the range of longitudinal and lateral incidences, together with the range of control surface deflection angles, was a set of data points comprehensive enough to support a good flight dynamics simulation, given the range of flight conditions that would be used in that investigation. The results of the Task 2 aerodynamic data base are presented in the form of graphs in Appendix-1.

2.2.4 Task 3

The main purpose of this Task was to estimate some of the aerodynamic damping derivatives of the YEZ-2A airship, namely m_q and n_r. In order to achieve this a special lightweight 1:75 scale model of the YEZ-2A airship was built and tested in the 8ft x 6ft wind tunnel of the College of Aeronautics (See Fig. A1.3.3 of Appendix-1). The rig assembly was such that the airship model could be made to oscillate in both pitch and yaw.

The usual technique for measurement in wind-on and wind-off conditions was carried out (Ref. 38). In practice, it is impossible to separate the virtual mass terms from the desired aerodynamic damping derivatives so that the values estimated were effectively for $m_q - m_{\dot{w}} u$ and for $n_r - n_{\dot{v}} u$. In the process, the values of the stiffness derivatives m_w and n_v were also determined.

A more detailed account of the Task 3 methods and results can be found in Reference 39. The relevant results for the flight dynamics simulation are presented in Appendix-1, together with the non-dimensionalization procedure adopted and a comparison with the equivalent results estimated for other airships. The relatively good agreement amongst these results allowed the Task 3 estimates to be used in the subsequent simulation work.

2.2.5 Task 4

The main objective of this final Task was to evaluate the YEZ-2A response to turbulence. In order to carry this out, an ultra-lightweight 1:200 scale model of the YEZ-2A airship was built and tested in the Earth Boundary Layer 8ft x 4ft wind tunnel of the College of Aeronautics (Fig. A1.3.4 of Appendix-1).

The simulated open field boundary layer velocity profile in the wind tunnel test section allowed a reasonably realistic representation of flight through a naturally turbulent atmosphere, with due consideration

being given to the airship model scale factor. Measurements of the instantaneous value of the vertical (gust) and horizontal velocity components were taken using hot wire anemometry. The airship response was measured in terms of Lift and Pitching Moment by the use of two strain-gauge balances fitted to the model's Centre of Volume (CV).

The results of this essentially dynamic type of experiment were subsequently analyzed in terms of the Transfer Function, the Phase Shift and the Coherence between input (the vertical gusts) and output (lift and pitching moment). The values of the spatial frequency Ω at which a peak occurred in the transfer function, followed by a marked phase shift and a value of the coherence function close to 1.0, were then noted down as the characteristic frequencies of response of the airship to turbulence. These results are likely to influence the design of the automatic flight control system once the appropriate scaling up procedure is followed.

Although the results of this Task are not directly applied in the subsequent flight dynamics simulation, the dynamic lift and pitching moment measurements constitute a data base that is relevant to the further work suggestions that are mentioned at the end of this document. A more detailed account of the Task 4 methods and results can be found in Reference 40.

2.3 The YEZ-2A Weight, Buoyancy and Environmental Conditions Cases

In order to complete the data base for the flight simulation work, typical examples of weight distribution, moments of inertia, and Centre of Gravity positions as a function of environmental conditions (temperature, pressure and altitude), were required. These estimates were eventually provided by the Weights Department of

Airship Industries and the 'Cases' effectively used are presented in table format in Appendix-1.

2.4 Concluding Remarks

As the results from Task 2 were used to provide the set of static force and moment coefficients required by the simulation, it is important to bear in mind that no attempt was made to carry out any data smoothing or curve fitting on them. The main reason for that is the fact that this is effectively a three-dimensional problem: Since each data point is a function of three variables, ψ, α and ruddervator deflection, the process would have to be carried out in each of the Task 2 graphs presented in Appendix-1 and, at the same time, from one graph to the next as the ψ angle varied. After that, the graph points would have to be restated in table format, in order to be suitable to be imported into the simulation. The scope of this type of work was clearly beyond our means, both in terms of the time required and the tools available.

On the other hand, a careful inspection of the Task 2 graphs presented in Appendix-1 shows that although in some situations a curve smoothing process would be a desirable feature to be incorporated into these results, in the majority of the cases this is not really a mandatory requirement. Although this is ultimately a matter largely for a subjective kind of discussion, it was felt that the lack of a curve fitting or smoothing process for the Task 2 results would not seriously compromise the simulation results to be obtained based upon them.

Finally, the previous sections have shown that, as far as the data base for running the simulation model is concerned, the results from Tasks 2 and 3 were the relevant ones. In retrospect, it can be argued that the other Tasks were not required for obtaining the

simulation aerodynamic data base.

Considering however that one of the objectives of this work was to construct a high fidelity aerodynamic model of the YEZ-2A airship, it was felt that the experience gained in the wind tunnel testing required by Tasks 1, 1A and 4 was of great importance in giving the necessary degree of confidence so that Tasks 2 and 3 could be adequately carried out. Besides, Task 1 and 1A provided the important link between the wind tunnel results and the small amount of flight test data available during the time when this work was being carried out. This link came in the form of the technique for airship wind tunnel testing developed as a consequence of performing these Tasks, and which was used in Tasks 2 and 3.

When further Skyship-600 airship flight test results became available more recently, they were compared with those produced by Task 1. The good degree of matching that was confirmed between the two sets of results (Ref. 41) can only be regarded as late confirmation that the wind tunnel test methodology employed was reasonably adequate in view of the high fidelity objective pursued.

3. THE SIMULATION CONCEPT

3.1 Introduction

The concept of the mathematical model that was used in the flight simulation work was derived from two previously published models by the College of Aeronautics staff (Refs. 42 and 43). The first one was conceived as a mathematical model to be used in the simulation of a Remotely Operated Underwater Vehicle (ROV), whereas the second one consisted in an adaptation of the former to obtain a small perturbation model for the study of airship flight dynamics. This background of work in buoyant vehicles led in 1988 to a Master of Science thesis based on a small perturbation model analogue simulation of an airship (Ref. 44).

In the present case, the primary objective was to obtain a full six-degree-of-freedom (DOF) non-linear mathematical model of airship flight, so that the flight dynamics simulation could be implemented. A major conditioning factor in the implementation was the fact that the aerodynamic forces and moments, including those used to control the airship, were to be determined from the results of the wind tunnel test programme (See Chapter 2), and not from analytic expressions based on the estimated values of some aerodynamic stability derivatives, as is usually the case in this type of work.

A second important condition was that the simulation was to be implemented digitally on a computer, using a high level language, so that different flight cases could be easily tried, as well as different types of control input.

It was decided therefore that, in order to satisfy the stated model requirements, the basic ROV mathematical model was to be used. Its very concept had already made possible simulation work of the kind sought here, and therefore just the necessary adaptations to the present

airship case had to be conceived and implemented.

3.2 The Adaptation to the Airship Case

3.2.1 Axes and Assumptions

The fundamental principle at the heart of the mathematical model of the simulation is the calculation of the three linear velocities, u, v and w, and the three angular velocities, p, q and r, with reference to X, Y and Z respectively. This is an orthogonal axes set, centered at the airship Centre of Volume (CV), and are called 'body axes'.

A second set of orthogonal axes is also used in this type of simulation concept: 'Inertial' or 'Earth' axes, where OX is aligned with the North direction, OY with the East and OZ points downwards towards the centre of the Earth. This axes set stays stationary throughout the simulation run, whereas the body axes set moves with the vehicle. For this simulation, the effects of Earth curvature were not taken into account ('flat Earth' assumption).

Once the velocities in body axes are calculated, the airship trajectory in three dimensional space, can be determined. This is achieved by a simple axes transformation, i.e., velocities in body axes are transformed into velocities in Earth axes, followed by a time integration, which, in Earth axes result in the displacements in the North, East and Vertical (height) directions respectively.

Figure 3.1 shows the set of body axes employed in the simulation. The CV is assumed to lie on the geometrical longitudinal axis of the envelope (its Centre Line), and the X-axis is aligned with it. The XZ plane defines the longitudinal plane of symmetry, since the body is assumed to be symmetric, and therefore the Centre of Gravity (CG) lies on this plane as well. Two important consequences arise from this assumption:

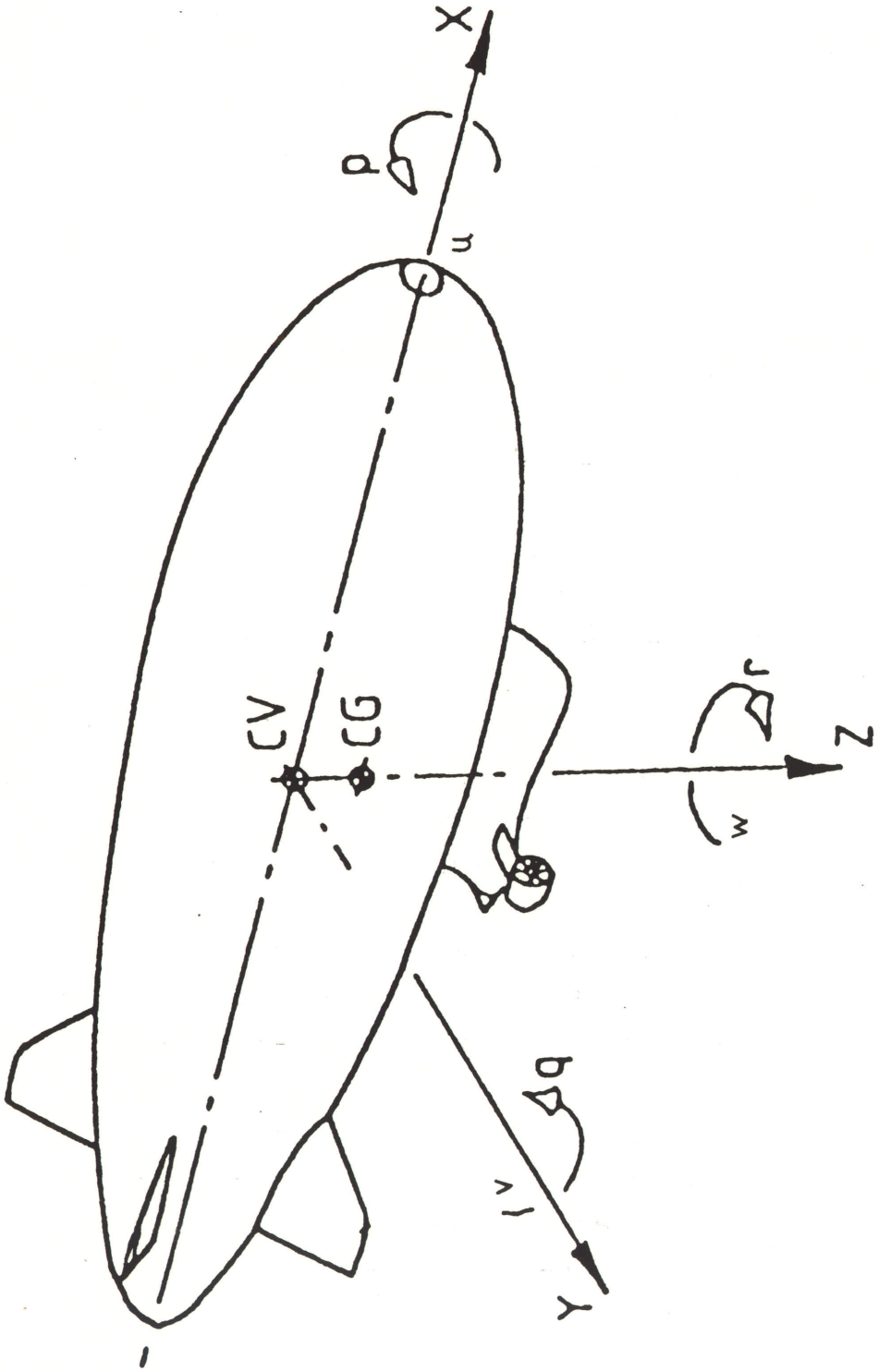


FIG 3.1 — The Body Axes System

i. If the CG coordinates, with respect to the stated axes system, are given by (a_x, a_y, a_z) then $a_y = 0$.

ii. The products of inertia I_{xy} and I_{yz} are both equal to zero.

Although the choice of axes set origin is arbitrary, in this case the CV was chosen because the wind tunnel gathered data on forces and moments was based on an equivalent set of axes. In this way, the transformation of force and moment coefficients in wind tunnel axes to simulation axes was avoided, greatly simplifying the Aerodynamics computation algorithm.

The remaining simulation model assumption made was that the airship is considered to be 'rigid', i.e., aeroelastic effects are ignored.

3.2.2 Equations of Motion (EOM)

The principle behind the concept of the equations of motion employed in the simulation is (Ref. 42) the formation of a Lagrangian from the energy of the airship and a large sphere of surrounding air. After some manipulations, the final format of the equation is given by:

$$M \begin{bmatrix} \dot{u} \\ \dot{v} \\ \dot{w} \\ \dot{p} \\ \dot{q} \\ \dot{r} \end{bmatrix} = F_d(u, v, w, p, q, r) + A(u, v, w, p, q, r) + G(\lambda_{31}, \lambda_{32}, \lambda_{33}) + P(\text{propulsion forces \& moments}) \qquad (3.1)$$

where

- M is the 6x6 Mass matrix
- F_d is the 6x1 matrix Dynamics vector
- A is the 6x1 matrix Aerodynamics vector
- G is the 6x1 matrix Gravitational and Buoyancy vector
- P is the 6x1 matrix Propulsion vector

The state variable format of the equations of motion (EOM) as here presented has been found, over the years, to be quite adequate for simulation model implementation using a high level computer language. One of the reasons is the fact that the whole problem of dealing with the six EOM is reduced to matrix manipulation procedures once the the elements of each matrix has been determined. It is mainly for this reason that this EOM format was employed in this work.

The following sections define the various matrices which were presented in Equation 3.1.

3.2.3 The Mass Matrix M

In the EOM formulation adopted additional terms that are specific to buoyant vehicles like airships, and are not usually considered in conventional aircraft simulation work, are incorporated in the Mass matrix. They are called 'added' or 'virtual' masses and inertias and arise due to the vehicle mass being of the same order of magnitude as the mass of displaced air (Ref. 22). The conventional modern formulation of using aerodynamic stability derivative notation to denote these terms has also been employed here, and they are therefore stated as equivalent aerodynamic acceleration derivatives (Ref. 45).

After incorporating the simplifications due to vehicle symmetry, the Mass matrix is given by

$$M = \begin{bmatrix} m_x & 0 & 0 & 0 & ma_z - X_{\dot{q}} & 0 \\ 0 & m_y & 0 & -ma_z - Y_{\dot{p}} & 0 & ma_x - Y_{\dot{r}} \\ 0 & 0 & m_z & 0 & -ma_x - Z_{\dot{q}} & 0 \\ 0 & -ma_z - L_{\dot{v}} & 0 & J_x & 0 & -J_{xz} \\ ma_z - M_{\dot{u}} & 0 & -ma_x - M_{\dot{w}} & 0 & J_y & 0 \\ 0 & ma_x - N_{\dot{v}} & 0 & -J_{xz} & 0 & J_z \end{bmatrix} \qquad (3.2)$$

where,

m = The airship mass

$m_x = m - X_{\dot{u}}$

$m_y = m - Y_{\dot{v}}$

$m_z = m - Z_{\dot{w}}$

$X_{\dot{u}}$, $Y_{\dot{v}}$ and $Z_{\dot{w}}$ are the virtual mass terms

$J_x = I_x - L_{\dot{p}}$

$J_y = I_y - M_{\dot{q}}$

$J_z = I_z - N_{\dot{r}}$

I_x, I_y and I_z are the moments of inertia about OX, OY and OZ, respectively

$L_{\dot{p}}$, $M_{\dot{q}}$ and $N_{\dot{r}}$ are the virtual inertia terms

$J_{xz} = I_{xz} + N_{\dot{p}} = I_{xz} + L_{\dot{r}}$

I_{xz} is the product of inertia about OY

$N_{\dot{p}}$ and $L_{\dot{r}}$ are virtual inertia terms

a_x and a_z are the CG coordinates with respect to OX and OZ respectively

$X_{\dot{q}}$, $Y_{\dot{p}}$, $Y_{\dot{r}}$ and $Z_{\dot{q}}$ are virtual mass terms

$L_{\dot{v}}$, $M_{\dot{u}}$, $M_{\dot{w}}$ and $N_{\dot{v}}$ are virtual inertia terms

In practice, some of the virtual masses and inertias have to be disregarded, whereas others can be estimated as will be shown in Chapter 4.

3.2.4 The Dynamics Vector F_d

The 6x1 column matrix that contains the dynamic terms associated with the inertial linear and angular velocities u, v, w, p, q and r can be expressed as

$$F_d = [\, f_1 \; f_2 \; f_3 \; f_4 \; f_5 \,]^T \qquad (3.3)$$

where,

$$f_1 = -m_z wq + m_y rv + m\left[\, a_x\left(q^2 + r^2\right) - a_z rp \,\right]$$

$$f_2 = -m_x ur + m_z pw + m\left[-a_x pq - a_z rq \,\right]$$

$$f_3 = -m_y vp + m_x qu + m\left[-a_x rp + a_z\left(q^2 + p^2\right) \,\right]$$

$$f_4 = -\left(J_z - J_y\right) rq + J_{xz} pq + ma_z\left(ur - pw\right)$$

$$f_5 = -\left(J_x - J_z\right) pr + J_{xz}\left(r^2 - p^2\right) + m\left[a_x\left(vp - qu\right) - a_z\left(wq - rv\right) \,\right]$$

$$f_6 = -\left(J_y - J_x\right) qp - J_{xz} qr + m\left[-a_x\left(ur - pw\right) \,\right]$$

In the above expressions the simplifications due to vehicle symmetry about the XZ plane have already been incorporated.

3.2.5 The Aerodynamics Vector A

The 6x1 column matrix that contains the aerodynamic forces and moments had its computation expressions and algorithm based entirely on the fact that, in the present airship simulation, these elements were to be determined directly from the results of the wind tunnel test programme carried out. In practice, if the aerodynamics vector is expressed as

$$A = \left[\, A_{X_B} \; A_{Y_B} \; A_{Z_B} \; A_{L_B} \; A_{M_B} \; A_{N_B} \,\right]^T \qquad (3.4)$$

where,

A_X = Aerodynamic total force on OX axis (Body axis)
A_Y = Aerodynamic total force on OY axis (Body axis)
A_Z = Aerodynamic total force on OZ axis (Body axis)
A_L = Aerodynamic total moment on OX axis (Body axis)
A_M = Aerodynamic total moment on OY axis (Body axis)
A_N = Aerodynamic total moment on OZ axis (Body axis)

then each one of the above matrix elements was determined from the associated wind tunnel measured non-dimensional coefficients. These were transformed into dimensional forces and moments using the appropriate factors. The dedicated expressions are presented in Chapter 4.

In summary therefore, the above expressions for total forces and moments, as implemented in the airship simulation model, incorporated the effects of:

i. The aerodynamic forces and moments due the vehicle air speed, and longitudinal and lateral incidences.

ii. Any control surface deflection effects, since the wind tunnel test programme results had this feature already built in. The A vector as stated contains, therefore, effectively the Aerodynamic Control vector, which is usually presented as a separate entity, especially in small perturbation simulation models.

iii. The dynamic force and moment damping terms, also estimated in the wind tunnel test programme (Chapter 2).

This approach to the solution of the Aerodynamic vector implied, therefore, that aerodynamic stability derivatives were not used in order to calculate the aerodynamic forces forces and moments, as is usually the case in flight dynamics simulation models. In fact, the state variable format of the EOM employed meant that the aerodynamic stability derivatives, for any particular flight regime, can be estimated, if required, from the system Jacobian, as is shown in Chapter 5.

3.2.6 The Gravity and Buoyancy Vector G

The 6x1 column matrix that contains the terms associated with the gravitational and buoyancy forces and moments is given by

$$G = \begin{bmatrix} \lambda_{31}\left(W - B\right) \\ \lambda_{32}\left(W - B\right) \\ \lambda_{33}\left(W - B\right) \\ -\lambda_{32}a_z W \\ \left(\lambda_{31}a_z - \lambda_{33}a_x\right)W \\ \lambda_{32}a_x W \end{bmatrix} \qquad (3.5)$$

where,

- W is the airship weight, acting at the CG
- B is the buoyancy force, acting at the CV
- a_x is the CG coordinate on the X-axis
- a_z is the CG coordinate on the Z-axis
- λ_{ij} are elements of the Direction Cosine Matrix (DCM, see Appendix-2)

In Equation (3.5) the simplifications due to vehicle symmetry about the XZ plane are already incorporated. The Direction Cosine Matrix (DCM) is the standard matrix used for axes transformation and for determining the airship attitude with respect to the horizontal and vertical planes (Appendix-2).

Unlike the conventional aircraft situation, the G vector in the airship case has only a secondary importance. This is largely due to the counteracting effect of the buoyancy force on the weight and the fact that, in normal circumstances, they differ by small amounts. Also, the CG in practice is made to rest at a certain distance directly below the CV, and therefore for small disturbances in pitch and roll, the value of the gravitational restoring moment tends to be small indeed. However,when the vehicle attitude has departed from the small angles condition the G vector becomes important,

and in a six-degree-of-freedom non-linear simulation its determination is, along with the other elements of Equation 3.1, essential.

3.2.7 The Propulsion Vector P

The 6x1 column matrix that contains the terms associated with the propulsive forces and moments had to be conceived as a function of the geometrical arrangement of the propulsive units around the established body axes set. It was therefore a function of the specific design of the YEZ-2A. For this reason, if P is expressed as

$$P = \left[X_{prop}, Y_{prop}, Z_{prop}, L_{prop}, M_{prop}, N_{prop} \right]^{T} \quad (3.6)$$

where,

X_{prop} = Total thrust along OX axis (Body axes)
Y_{prop} = Total thrust along OY axis (Body axes)
Z_{prop} = Total thrust along OZ axis (Body axes)
L_{prop} = Total thrust moment about OX axis (Body axes)
M_{prop} = Total thrust moment about OY axis (Body axes)
N_{prop} = Total thrust moment about OZ axis (Body axes)

then the derivation of the mathematical expressions that make up each element of P is presented in Chapter 4, where all the vehicle specific equations are developed.

3.3 The Solution

The solution to the type of simulation concept here presented is found by inverting the mass matrix M and multiplying both sides of Equation (3.1) by M^{-1}. Equation (3.1) will then have the form

$$\begin{bmatrix} \dot{u} \\ \dot{v} \\ \dot{w} \\ \dot{p} \\ \dot{q} \\ \dot{r} \end{bmatrix} = \begin{bmatrix} D \end{bmatrix} \qquad (3.7)$$

where,

D is a 6x1 matrix containing the numerical values of the state variable derivatives with respect to time

Once J is integrated over a small time interval Δt the values of the three linear and the three angular velocities in body axes are automatically found. Once the three linear velocities are transformed into Earth (inertial) axes and integrated over the same small time increment Δt, the displacements in the North, East and Vertical (height) directions are also found.

The body to Earth axes transformation is achieved by the use of the Direction Cosine Matrix (Appendix-2), which is also used to determine the set of Euler angles ϕ, θ and ψ which describe the airship attitude with respect to Earth axes.

The linear and angular velocities, together with the displacements in Earth axes and the Euler angles, are the basic flight dynamics simulation output parameters and Figure 3.2 summarizes the simulation concept here described.

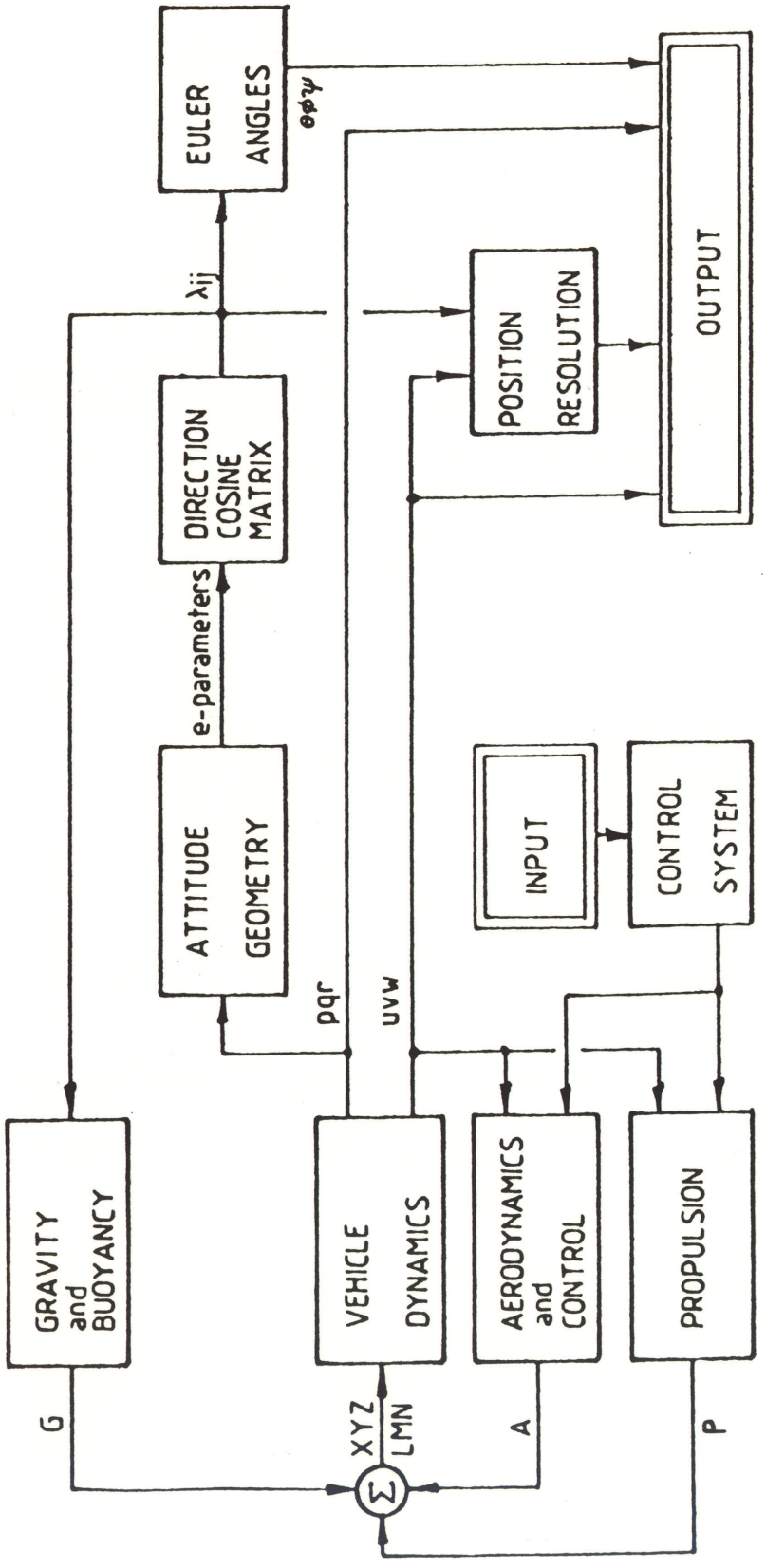


FIG 3.2 - The Simulation Model Structure

4. THE SIMULATION MODEL

4.1 The Computer Simulation and ACSL

Early in the development of the YEZ-2A simulation model, as presented in Chapter 3, a decision was taken regarding the simulation language to be used. The choice of ACSL (Advanced Continuous Simulation Language) seemed natural for the following main reasons:

i. It is a high level language conceived especially for simulation purposes. A program written in ACSL is already structured in terms of the Initial, Dynamic and Terminal regions since this is a requirement of the ACSL translator (Fig. 4.1). In other languages this structure has to be constructed manually with the use of logical flags and branching.

ii. ACSL has already built in the function INTEG which provides the time integration of the state variables using an integration algorithm specified by the user. This avoids the need to write, debug and implement Runge-Kutta type of subroutines to perform that task.

iii. As a substantial part of the flight dynamics investigation was concerned with stability and control, the ANALYZ package provided by ACSL seemed quite attractive with its built in capacity to calculate the system Jacobian matrix, the eigenvalues and associated eigenvectors.

iv. Being a FORTRAN based language, ACSL offers the facility of accepting subroutines written in that language to complement the main program features if so required.

In addition, to the stated reasons for using ACSL was another important one: The existence of an example

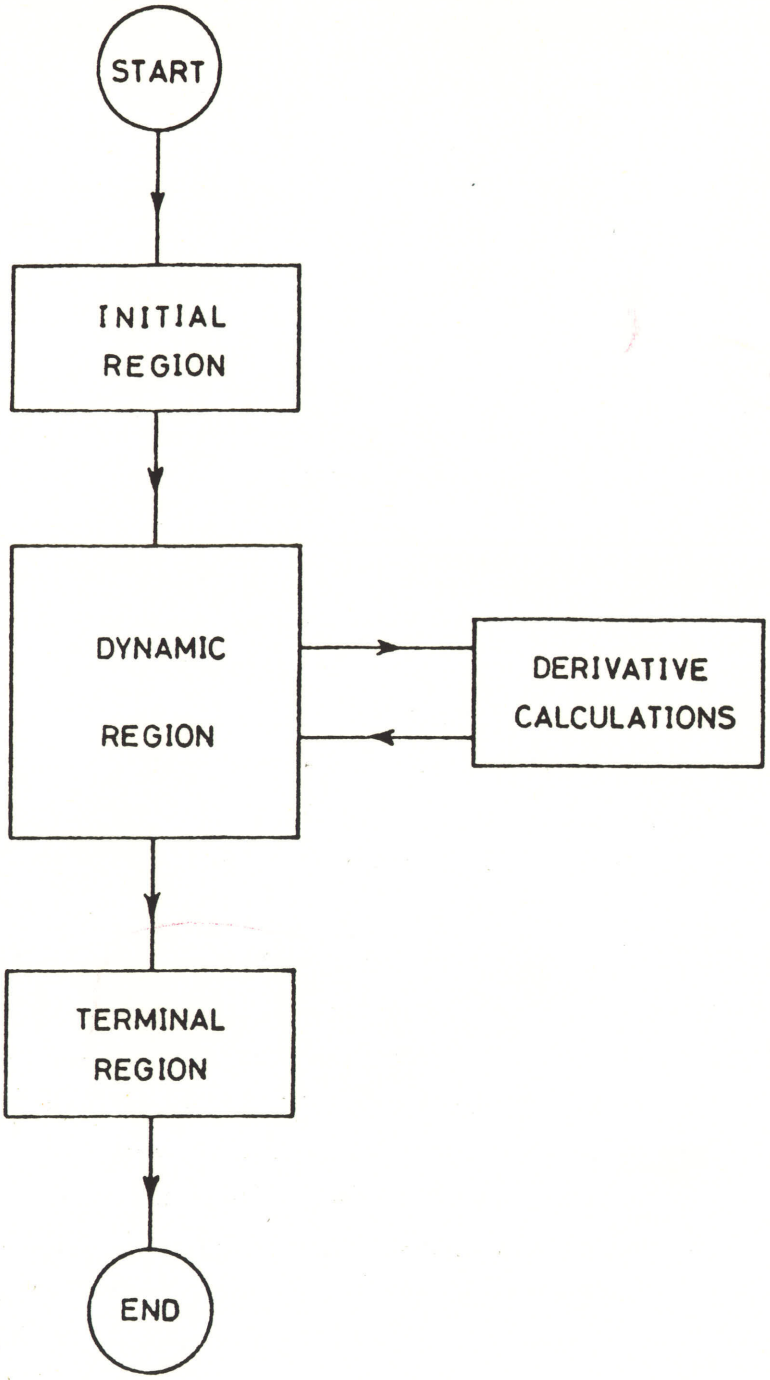


Figure 4.1 - Program regions of the computer simulation model. The ACSL language requires the program code to be conceived using this stucture, a feature not found in other commonly used high level languages.

program to simulate the firing of a torpedo, which is of course another kind of buoyant vehicle (Ref. 46). This program had already been debugged and implemented in ACSL, and although it was realized that extensive modifications would be required in order to adapt it to the airship case, it was felt that the torpedo simulation formed a very good starting point.

During program implementation, only two major inconveniences were found associated with the use of ACSL: The first was the need for the whole program to be compiled and linked as a single unit, preventing the separate development, debugging and implementation of program sub-units which would then be linked to the main program at compilation time. The second difficulty found was that the error reporting messages produced by ACSL are not as direct and explicit as those found in other languages, which made error identification and tracing a rather time consuming process. The combination of these two factors meant that the achievement of an error free simulation program was, most of the time, an all or nothing type of process, and this considerably delayed the stage when meaningful results started to appear.

The YEZ-2A simulation program consists essentially in the coding of the simulation model presented in Chapter 3. The mass matrix and the various vectors of the right-hand-side of Equation (3.1) are calculated in the Dynamics/Derivative region of the program at each integration step, so that the equivalent of Equation (3.7) is produced at each time step. The initial conditions regarding vehicle speed, attitude, weight and environmental conditions are all specified in the Initial region of the program, which acts therefore as the initial input to the actual running of the model in the Dynamic region. Matrix inversion and mass change, along with CG position change FORTRAN subroutines are called every time from the Derivative region in order to update these airship parameters as the simulation run is allowed

to proceed.

The simulation program was run from a command file in accordance with the options offered by the ACSL run-time syntax rules. In this way, the actual simulation program represented the coding of the simulation concept (seen in Fig. 3.2), along with the initial conditions that did not need to be changed, whereas the command file was used not only to specify the required parameters for each simulation run but changes in flight 'cases' as well, e.g., new environmental conditions, initial weight and buoyancy, speed or attitude, and aerodynamic and power control inputs.

An IBM Personal Computer AT fitted with a math coprocessor was used to develop, implement and run the YEZ-2A flight dynamics simulation.

The following sections present a summary of the relevant aspects in each of the main sections that make up the simulation program. A program flow-chart is presented at the end of the Chapter summarizing the way in which the simulation actually works.

4.2 Axes Transformation

The major axes transformation that the simulation required was, as seen in Chapter 3, between body axes and Earth axes. In order to achieve that a Direction Cosine Matrix (DCM) had to be calculated at each time interval Δt so that the necessary transformations could take place as the simulation run proceeded.

More specifically, the DCM or some of its elements were used in three main instances:

i. To obtain the velocities in the North, East and Vertical directions (Earth axes) once u, v and w were determined, so that

$$\begin{bmatrix} V_{North} \\ V_{East} \\ V_{Up} \end{bmatrix} = \begin{bmatrix} & DCM & \end{bmatrix} \begin{bmatrix} u \\ v \\ w \end{bmatrix} \qquad (4.1)$$

ii. To obtain the Gravity & Buoyancy vector G as in Equation (3.5).

iii. To obtain the Euler angles ϕ, θ and ψ, since they can be expressed as a function of the elements of the DCM.

The chosen way to calculate the DCM was by using the quaternion method (See Appendix-2), which is quite suitable for implementation in a digital type of simulation. This method assumes that the DCM can be expressed as

$$D\ C\ M = \begin{bmatrix} \lambda_{11} & \lambda_{12} & \lambda_{13} \\ \lambda_{21} & \lambda_{22} & \lambda_{23} \\ \lambda_{31} & \lambda_{32} & \lambda_{33} \end{bmatrix} \tag{4.2}$$

from which the relevant λ_{ij} values are used in the calculation of the G vector. On the other hand, the Euler angles are determined from

$$\phi = \arctan\left(\lambda_{32}/\lambda_{33}\right) \tag{4.3}$$

$$\theta = \arcsin\left(-\lambda_{31}\right) \tag{4.4}$$

$$\psi = \arctan\left(\lambda_{21}/\lambda_{11}\right) \tag{4.5}$$

A full derivation of the above expressions can be found in Reference 47.

4.3 The Mass Matrix M

The Mass matrix elements are those presented in Equation (3.2). For their determination the simulation program had to resort to different methods in accordance with the element being calculated.

The final calculation of M was accomplished in the ACSL program inside a PROCEDURAL block, a code section

which is not sorted by the ACSL translator and where the required output (M) and all the necessary inputs for its determination have to be precisely specified. An important property of the mass matrix is the fact that it is symmetrical about its diagonal elements. In the code implementation, therefore, only the diagonal elements and those above them were actually calculated. Once the latter were copied to the the array elements below the diagonal, observing of course the symmetry rules, the determination of M was completed.

After M had been obtained, a FORTRAN subroutine was called to perform the required inversion so as to obtain M^{-1}. The following sub-sections give a brief description of how each variable required to calculate each element of the Mass matrix was determined.

4.3.1 The Airship Mass m

One of the peculiarities of non-rigid airship flight is the considerable amount of vehicle total mass variation that can occur in a short time span. The usual condition for this to happen is the performance of a climb or descent manoeuvre, when the ballonets have to be emptied or filled with air respectively, so that the lifting gas has room inside the envelope to expand or contract in response to outside air density and pressure changes. Other situations which can potentially lead to sudden mass changes are the encountering of air masses that have a higher or lower temperature than that of the lifting gas inside the envelope. This will lead to adjustments in the amount of air allowed to remain inside each ballonet if constant height is to be maintained.

In the YEZ-2A simulation program the initial value of total airship mass is taken directly from the data base weight tables (Appendix-1). As the simulation run unfolds, the required mass variations are incorporated in the following way:

i. First, the air density ρ is calculated at each time step of the simulation. This is achieved by calling a subroutine directly from the Dynamic/Derivative region, whose inputs are the vehicle height and the ISA (International Standard Atmosphere) or off-ISA condition for the on-going simulation run. This subroutine effectively embodies a model of the atmospheric properties in accordance with the ISA convention (See Appendix-1).

ii. Second, the new ρ value is used to calculate the new value of the Buoyancy force B.

iii. Third, the difference between B (aerostatic buoyancy force) and W (airship total weight) is checked against the specified value of heaviness (weight larger than buoyancy) or lightness (buoyancy larger than weight) for that flight case. If that difference is greater than a specified tolerance, a mass change subroutine is immediately called and the mass m is changed to restore the original heaviness or lightness value specified.

iv. Fourth, in case m suffered any change, the mass change subroutine calls a CG position subroutine in order to determine the new CG position.

In the mass change subroutine, logical checks are carried out in order to determine whether, for example, in a climbing manoeuvre, there is still air to be pumped out of the ballonets. Otherwise a message saying that pressure height has been reached is displayed, which means that any height increase will only be possible by venting of the lifting gas, a situation which is normally avoided.

The implementation of the mass change algorithm as described was found to be satisfactory in keeping the

total airship mass constantly updated in response to changes in the flight operating conditions.

4.3.2 Moments and Products of Inertia

The weight tables (Appendix-1), present the moments and products of inertia referenced to the vehicle CG, i.e., I_x, I_y, I_z and I_{xz}, for each flight case. The simulation program had to alter these values in order to cater for the fact that the chosen reference body axes system had its origin at the CV, and to incorporate the necessary virtual inertia terms (See Section 3.2.3).

The first change was carried out by using the standard expressions for changing the moments and product of inertia from one reference frame to another. This was done in the Initial region of the program, since the CV position is assumed not to change during the simulation. After that, no changes were incorporated due to total airship mass variation as it was felt that, for the airship stability and response type of investigation and the associated vehicle manoeuvres that had to be performed (Chapters 5 and 6), the order of magnitude of the inertia changes due to this cause, would not make this a mandatory program requirement. For investigations in the area of vehicle performance, it is likely that these changes will have to be incorporated.

The second alteration to the inertias was incorporated in the Dynamic/Derivative region at each time step of the on-going simulation run. This is because the added inertias depend on the instantaneous value of the air density, which has to be calculated each time as well (See Section 4.3.4).

The final values of J_x, J_y, J_z and J_{xz} at each time step are obtained after the incorporation of the changes described to I_x, I_y, I_z and I_{xz}.

4.3.3 Centre of Gravity Position

The CG position with reference to the body axes

system, given by (a_x, a_y, a_z) where $a_y = 0$, is initially taken from the weight tables (Appendix-1). After the change imposed by the initial longitudinal trim procedure (See Section 4.9), the CG position is recalculated at each step of the simulation if, and only if, an airship total mass change had to be incorporated, as mentioned in Section 4.3.1. The subroutine that performs this task takes into account the following mass breakdown:

i. Airship airframe mass
ii. Lifting gas (helium) mass
iii. Forward ballonet mass
iv. Aft ballonet mass
v. Starboard pannier ballonet mass
vi. Port pannier ballonet mass

Although the airframe and lifting gas masses were assumed not to change in each given flight case, the four ballonet masses were allowed to change in response to the initial trim procedure and, as the simulation got going, in response to height (air density) changes. The coordinates of the CG of each one of the six elements given above were assumed to remain constant throughout the simulation.

Figure 4.2 shows the geometrical arrangement of the air ballonets inside the airship gas envelope and the relative positions of their CGs with respect to the airship CV.

4.3.4 Virtual Masses and Inertias

The estimation of the virtual masses and inertias followed the standard methods based on the original formulation by Lamb (Ref. 48) and Munk (Ref. 25). Referring to the Mass matrix definition (Equation 3.2), the associated virtual terms were estimated by using the following standard expressions:

$$X_{\dot{u}} = -k_1 \bar{m} \qquad (4.6)$$

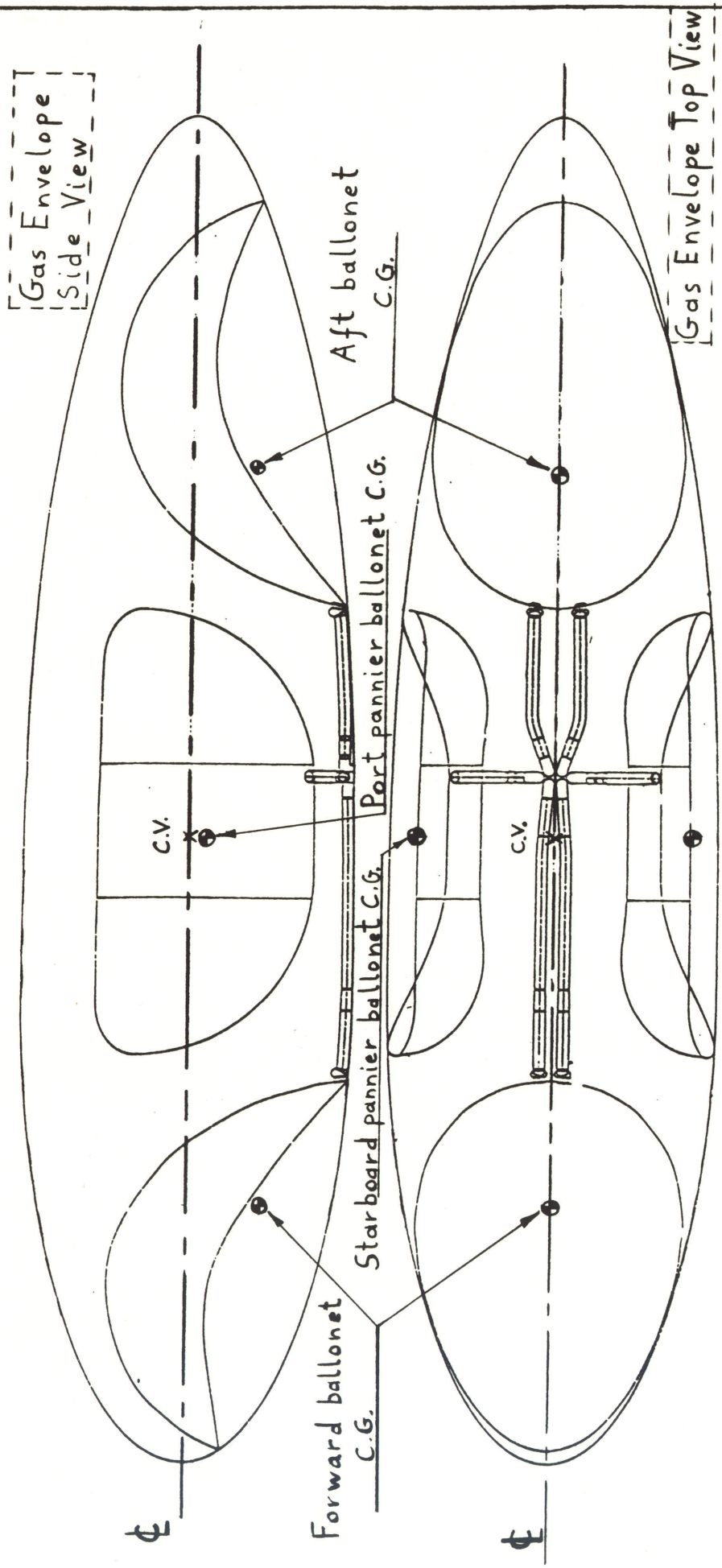


Figure 4.2 - Internal arrangement of the air ballonets inside the gas envelope of the YEZ-2A airship. The positions for the Centre of Gravity of each ballonet are also shown. C.V. is the Centre of Volume for the whole gas envelope.

$$Y_{\dot{v}} = -k_2 \bar{m} \tag{4.7}$$

$$M_{\dot{q}} = -k' \bar{I}_y \tag{4.8}$$

$$Z_{\dot{w}} = Y_{\dot{v}} \tag{4.9}$$

$$N_{\dot{r}} = M_{\dot{q}} \tag{4.10}$$

where,

k_1 is Lamb's inertia ratio for movement along the longitudinal axis (OX)

k_2 is Lamb's inertia ratio for movement along the lateral axis (OY)

k' is Lamb's inertia ratio for rotation about the lateral axis (OY)

$\bar{m} = B/g$

$$\bar{I}_y = \frac{\bar{m}\left(l^2 + d^2\right)}{20}$$

l = Airship length

d = Airship maximum diameter

In the expressions given, Equations (4.6), (4.7) and (4.8) are the original ones developed for a prolate spheroid. The YEZ-2A, for the purposes of estimating its virtual masses and inertias, was therefore considered to have a hull shape that approximated that of an ellipsoid of revolution, with a length to diameter ratio of approximately 4, as the is the usual practice.

Equations (4.9) and (4.10) are good approximations if the effects of the gondola are ignored, which is also the usual practice.

The effect of the fins was also ignored in view of the assumption that their contribution must be small as compared to that of the hull. An independent investigation in this area also estimated that, for fins

with an aspect ratio of the order of 3.0 (the YEZ-2A case), the two types of contributions to the virtual mass effects of fins cancel each other out, a result which lent further support to the original assumption (Ref. 15).

The remaining acceleration derivatives that are part of the Mass matrix were all assumed to have negligible values, after each one of them had been individually assessed, along with possible ways of estimating their values. In practice however, some additional values of acceleration derivatives were incorporated in the model (though not via the Mass matrix) with the use of damping term coefficients (Section 2.2.4) to calculate the Aerodynamics vector.

4.4 Dynamics

The calculation of the Dynamics vector F_d was achieved through relatively simple assignment statements, placed in the Dynamics/Derivative section of the simulation program, which were effectively the ACSL codification of Equation (3.3). The values of the required variables for this program section were all calculated elsewhere in the program, i.e.,

- m_x, m_y and m_z were estimated in the Mass matrix section
- a_x and a_z were initially estimated during the longitudinal trim procedure and then changed as required in the Mass matrix section
- u, v, w, p, q and r were calculated in the final part of the program (See Section 4.8)

After the values of each element of F_d were calculated using the expressions given in Equation (3.3), they were copied to the array elements that made up the Dynamics vector. This operation was carried out inside an

ACSL PROCEDURAL block, a practice used in the computation of all the 6x1 column matrices that were presented in the right-hand-side of Equation (3.1).

4.5 Aerodynamics

The calculation of the Aerodynamics vector A of Equation (3.1) is probably the most innovative part of the simulation investigation carried out. This is because this is the first time that, as far as we are aware, an airship simulation program has drawn directly on wind tunnel test results in order to determine the resultant aerodynamic forces and moments that are acting on the vehicle, including the contributions due to any control surface (ruddervator) deflection.

The basic idea was a relatively simple one: As the YEZ-2A wind tunnel test programme (Chapter 2) had yielded thousands of data points regarding the non-dimensional coefficients of Drag, Lift, Side Force, Rolling Moment, Pitching Moment and Yawing Moment for a number of lateral (β) and longitudinal (α) incidences, combined with rudder (ζ) and elevator (η) type of ruddervator deflection, these coefficients were to be used in order to estimate the actual aerodynamic forces and moments that would be acting on the airship, due to the simulation calculated values of α, β and the user input values for control surface deflections.

In order to implement this kind of solution to the Aerodynamics vector, the problem was divided into a number of smaller tasks. These were then tackled separately and eventually brought together under the Aerodynamics section of the simulation, in the Dynamics/Derivative region of the program.

The following sub-sections summarize the major challenges faced in each task and the associated solutions found for each one of them.

4.5.1 Importing the Wind Tunnel Data into the Simulation

The chosen way in which the wind tunnel coefficient results were to be used in the ACSL program was by implementing them in TABLEs. This decision was motivated by the fact that the ACSL TABLE function provides for automatic linear interpolation or extrapolation between or beyond the stated data points, avoiding therefore the need for a user supplied subroutine to carry out this task when the data base is constituted of discrete coefficient data points as in the present case. The TABLE function is also able to cope with a maximum of three independent variables associated with the dependent one, which was exactly the case in hand since each of the three force coefficients and the three moment coefficients were obtained as a function of α, β and ruddervator deflection.

In order to import the wind tunnel results into the ACSL program, a spread sheet type of software (SuperCalc) was used to read in from the ASCII type of files in which the original wind tunnel coefficient results were stored. The data points were then arranged in the format required by the ACSL syntax rules and subsequently exported to the simulation program, where each aerodynamic coefficient was assigned a specific TABLE. By doing the data transfer between the wind tunnel results and the simulation program in this way, the need of manually entering aerodynamic coefficient data to the simulation was avoided, preserving therefore the fidelity of the aerodynamic data base as originally stated.

A total of twelve TABLEs constituted the basic aerodynamic data base, since there were six aerodynamic coefficients, and for each one of them there were rudder type and elevator type of control surface deflection results.

Subsequently six more TABLEs were added to cater for the aileron (ξ) type of control surface deflection, a control function not normally found in airships. This

was motivated by the fact that, with this facility, the lateral roll oscillation mode could be more adequately excited (See Chapter 5). The fact that the YEZ-2A is to have a roll damping function incorporated in its auto stabilization system was behind the reason that lead to some exploratory wind tunnel trials using this type of unusual tail deflection configuration for an airship.

The 18 TABLEs created with the results from Task 2 (Chapter 2), constituted therefore the source of static aerodynamic force and moment coefficients. They came to be known as elevator, rudder and aileron TABLEs (six of each, for the three force and the three moment coefficients) and to enter them the current value, at each simulation time step, of α, β and η or ζ or ξ was required.

The Task 3 non-dimensional damping coefficients of pitching moment and yawing moment were used in the Aerodynamics section directly, after the static forces and moments had been determined, by applying the appropriate dimensionalization factors (See Appendix-2). Unfortunately the scope of the Task 3 tests could not accommodate equivalent rolling moment damping measurements and therefore the YEZ-2A roll damping coefficient was parametrically estimated from the results obtained for other airships in Reference 14. A value of $C_{l_p} = -0.012$ was used, a value which was found to be close to that estimated by Airship Industries for use in their own work.

4.5.2 The Input Parameters

As far as the algorithm (Section 4.5.3), and the aerodynamic coefficient data TABLEs were concerned, five parameters were required during each time step of the simulation run in order to calculate the static forces and moments. The first two were the following:

* Longitudinal Incidence α
  This was determined from the standard aerodynamic formulation
  $\alpha = \arctan(w/u)$ (4.11)
* Lateral Incidence β
  From the standard aerodynamic formulation
  $\beta = \arcsin\left(v/V_{Total}\right)$ (4.12)

Figure 4.3 shows the geometrical arrangement from which these parameters are calculated.

The next required parameters were associated with ruddervator deflections and therefore were user inputs. As the simulation model had been devised, amongst other reasons, to investigate the aerodynamic control response of the YEZ-2A, it was decided that it would be desirable that any of the four ruddervators could be deflected individually within the design limits, i.e.,with a maximum amplitude of $\pm 25^{\circ}$, where a positive deflection meant ruddervator down and vice-versa. So the four ruddervators were numbered by looking at the airship from the back and calling number one the high port side ruddervator, and progressing in a clockwise sense until number four was assigned to the low port side one.

The next step in this process was a determination of how much equivalent elevator, rudder and aileron deflection the four individual control surfaces would contribute to the total tail deflection configuration. This was achieved by first calling each ruddervator deflection δ_1, δ_2, δ_3 and δ_4 (Fig. 4.4) respectively. Then if the total amount of elevator deflection is called η, that of rudder is called ζ and that of aileron ξ, they were determined by imposing that

$$\eta = \frac{\delta_1 + \delta_2 + \delta_3 + \delta_4}{4} \qquad (4.13)$$

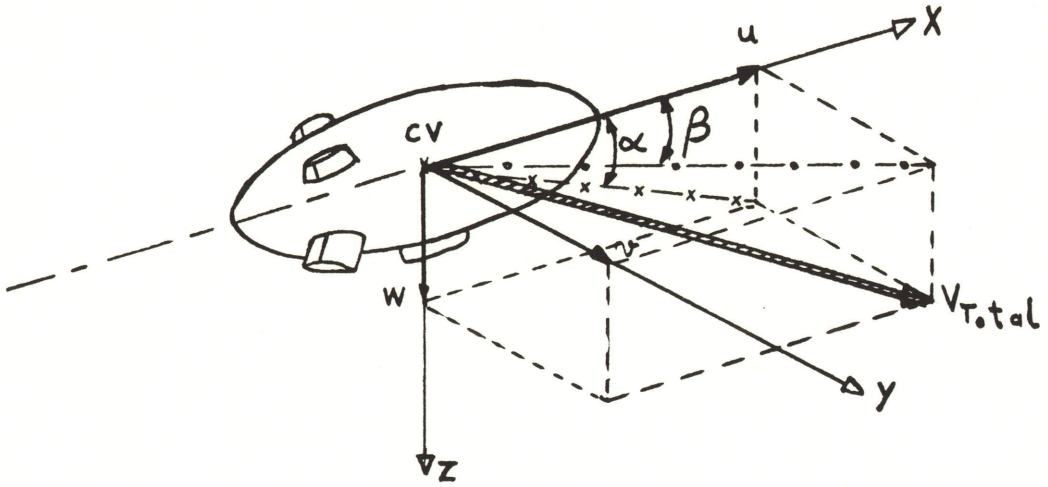


Figure 4.3 - The longitudinal incidence α and the lateral and the lateral incidence β shown together with the three linear velocities u,v and w, and the resultant velocity V_{Total} with respect to the body axes system.

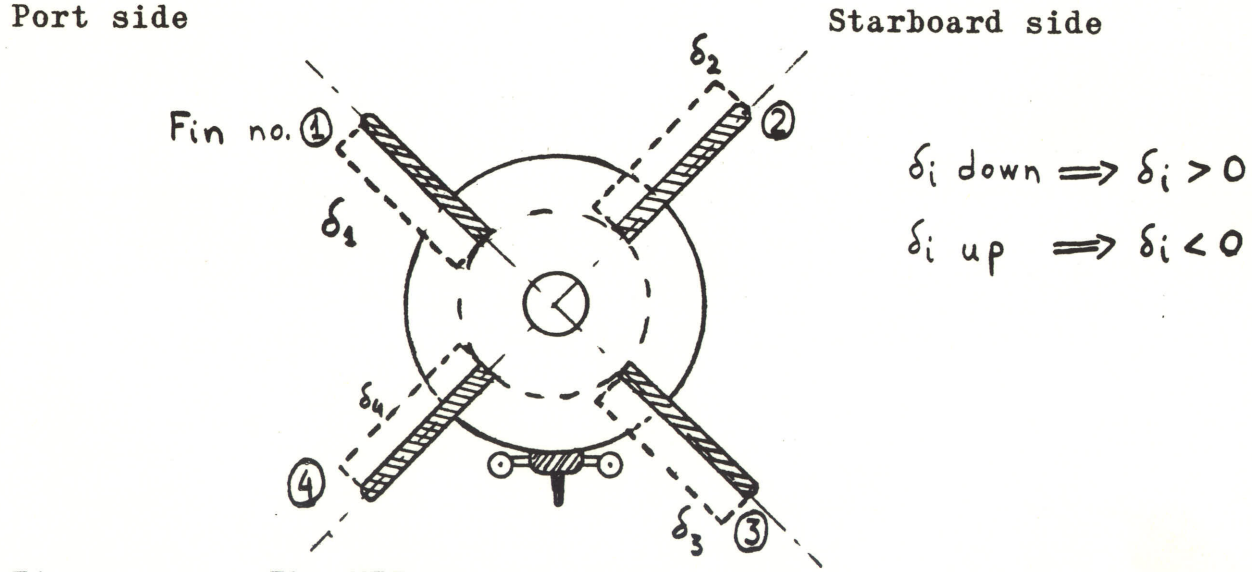


Figure 4.4 - The YEZ-2A viewed from the stern with the control surfaces (Ruddervators) deflection scheme. Each surface can be deflected either downwards or upwards up to $\pm$ 25 degrees. The configuration shown would be suitable for a turn to the starboard side.

$$\zeta = \frac{\delta_1 - \delta_2 + \delta_3 - \delta_4}{4} \tag{4.14}$$

$$\xi = \frac{\delta_1 - \delta_2 - \delta_3 + \delta_4}{4} \tag{4.15}$$

Having determined the five parameters required to enter the elevator, rudder and aileron TABLEs respectively, the next development step consisted in the concept and implementation of a calculation algorithm that would yield the resulting static forces and moments.

4.5.3 Static Forces and Moments

In trying to devise an algorithm that would best make use of the 18 aerodynamic data base TABLEs to calculate the static forces and moments, a number of different alternatives were tried out. Eventually, one was found to yield more consistent results for all the different airship manoeuvre possibilities and was therefore adopted.

The basic principle behind it is straightforward: Since all the TABLEs were constructed in a format that allowed the six aerodynamic coefficients to be obtained with and without any control surface deflection, each coefficient was to be calculated by considering the 'no control surface deflection' coefficient added to the incremental coefficient value due to any amount of rudder, elevator or aileron type of control surface deflection contribution, i.e.,

$$C(\alpha, \beta, \eta, \zeta, \xi) = C(\alpha, \beta, 0, 0, 0) + \Delta C(\alpha, \beta, \eta, \zeta, \xi) \tag{4.16}$$

where,

C is any of the six aerodynamic force & moment non-dimensional coefficients (Drag, Lift, Side Force, Rolling Moment, Pitching Moment or Yawing

Moment)

ΔC is the incremental C value due to the deflection of the ruddervators, i.e.,

$$\Delta C = \Delta C_{\eta} + \Delta C_{\zeta} + \Delta C_{\xi} \qquad (4.17)$$

In order to implement this formulation at each time step of the simulation program, first the aerodynamic TABLEs were entered with a zero value for ruddervator deflection, therefore obtaining the value of $C(\alpha, \beta, 0)$ (Any of the three types of TABLE will give the same C value if there are no control surface deflection and therefore, in this condition, C is a function of three rather than five independent variables).

Following this, the amount of elevator, rudder and aileron deflection associated with the complete tail deflection configuration, due to the deflection of each individual ruddervator as specified by the user, was determined using Equations (4.13-15). The next step consisted in entering the elevator, rudder and aileron TABLEs with the values of the independent variables (α, β, η), (α, β, ζ) and (α, β, ξ) respectively, therefore obtaining C_{η}, C_{ζ} and C_{ξ}. Once the subtraction of $C(\alpha, \beta, 0)$ from each one of these was carried out the respective values of ΔC_{η}, ΔC_{ζ} and ΔC_{ξ} were obtained.

They were then added together as in Equation (4.17) and the ΔC value arrived at was substituted in the equivalent ACSL coded form of Equation (4.16) to yield the value of the final static aerodynamic coefficient sought.

The corresponding full dimensional value of the three forces and three moments was obtained by multiplying the six coefficients by the associated non-dimensionalization factors (See Appendix-1).

In the actual implementation of this algorithm, three further problems had to be addressed:

i. Conversion of the aerodynamic coefficients to airship body axes, since these coincided with the wind tunnel axes only in the $\alpha = 0$ and $\beta = 0$ condition.

ii. The fact that the actual the wind tunnel test scope only accommodated zero and positive values of β (or, in wind tunnel jargon, negative ψ angles, since in the wind tunnel $\psi = -\beta$, see Appendix-1). This was justified in view of the vehicle being considered symmetrical about the XZ plane. The aerodynamic TABLEs therefore presented data only for $\beta \geq 0$.

iii. The fact that a rather small amount of data was available for the aileron type of tail control surface deflection configuration as this type of wind tunnel test had not been a high priority requirement.

The solution to these problems was incorporated in the simulation software, i.e., the aerodynamics section algorithm was conceived with specific sections devoted to addressing each one of them. The concept of the solutions found is presented in Appendix-2.

4.5.4 Damping Terms

The dynamic damping forces and moments were added to their static counterparts at the end of the aerodynamics section of the program, after being dimensionalized with the appropriate factors (Appendix-1). The non-dimensional moment coefficients used are those presented in Appendix-1 and Section 4.5.1.

For the corresponding values of the damping forces in yaw and in pitch a simplifying assumption had to be made in order to estimate them. This assumption was that most of the damping forces would be acting at the airship tail, and therefore the value of these forces was

estimated by dividing the value of the corresponding damping moment by the moment arm, i.e., the distance between the CV and the aerodynamic centre of the fins.

This calculation therefore concluded the aerodynamics section algorithm and supplied the six elements required by the 6x1 column matrix Aerodynamics vector.

4.5.5 Aerodynamic Control

As already mentioned, the amount of deflection of each ruddervator surface were configured as user input values (δ_1, δ_2, δ_3 and δ_4) from the ACSL command file. In this way, the tail deflection configuration could be made to change as required and and for as long as required during each simulation run.

However, since one of the major purposes of the simulation was to investigate the actual vehicle response to control inputs, the beginning of the aerodynamic section of the simulation program was fitted with four extra sections. These were designed so that as the simulation run proceeded, each ruddervator could be made to deflect in a precise way which would configure the standard control inputs of a STEP, a PULSE (i.e., a step of finite duration), and a RAMP.

This was achieved by using the ACSL built in functions of the same name in the appropriate way, and by introducing a slight modification to the use of the PULSE function, a Doublet type of control input law was achieved. The parameters that were required in order to obtain these types of input laws were all specified in the command file, where they could be easily changed before each new simulation run.

In order to achieve a particular type of input law from the four types given, the value of the logical flag associated with that input had to be set to TRUE. While it remained so only that part of the code associated with that particular kind of input law was executed at run

time, whilst the code sections associated with the other three types of inputs were skipped. This type of approach was found to be useful in shortening the total program execution time.

The solution given to the aerodynamic control problem of the airship was found to be adequate to study its aerodynamic response (Chapters 5 and 6).

A second version of the simulation program was also developed which accepted a pilot type of input in terms of demanded elevator and/or rudder type of control. An algorithm solved the pilot demand in terms of the four ruddervator deflections that would be adequate to meet it. Only one such algorithm was tried, but there is certainly scope for a wide range of experimentation in this area (See Appendix-2).

4.6 Gravity and Buoyancy

The Gravity and Buoyancy vector G was determined by a direct ACSL codification of Equation (3.5), since all the values of the variables required to calculate its constituent elements were determined in other sections of the simulation program.

The only exception to this was the determination of the total airship weight, which was not calculated by simply multiplying the current value of airship mass by g. In order to avoid the rounding-off type of numerical errors at every time step of the simulation, the value of the total airship weight in this section was determined as

$$\text{Weight} = (\text{Buoyancy Force}) + (\text{Heaviness}) \cdot g \qquad (4.18)$$

where,

Buoyancy Force = (Airship volume) . ρ . g

Heaviness = Airship heaviness value set by the simulation user in Kg (Positive for heaviness force greater than

airship weight and negative for the opposite)

ρ = Current value of air density

g = Acceleration due to gravity

By calculating W using the ACSL coded form of Equation (4.18), the value of heaviness set by the user was kept constant throughout the simulation run, irrespective of the kind of manoeuvres that the vehicle had to perform. This kind of solution was found to be more in line with the aims of the flight dynamics investigation than the other alternative mentioned, i.e. W = mg, which was initially tried but had to be abandoned for giving inconsistent values for the heaviness parameter as the simulation run proceeded.

4.7 Propulsion

The Propulsion vector P was calculated in the Dynamic /Derivative region of the program, and at each time step of the simulation, by assuming that the propulsive function is provided by pure thrusters located at fixed distances from the airship CV. Their geometrical arrangement with respect to the established system of body axes is shown in Figure 4.5.

From Figure 4.5 it can be seen that in the given body axes system the three propulsive forces and the three propulsive moments can be expressed as

$$X_{prop} = T_t + \left(T_{d_s} + T_{d_p} \right) \cos\mu \qquad (4.19)$$

$$Y_{prop} = 0 \qquad (4.20)$$

$$Z_{prop} = -\left(T_{d_s} + T_{d_p} \right) \sin\mu \qquad (4.21)$$

$$L_{prop} = \left(T_{d_p} - T_{d_s} \right) \sin\mu \cdot d_y \qquad (4.22)$$

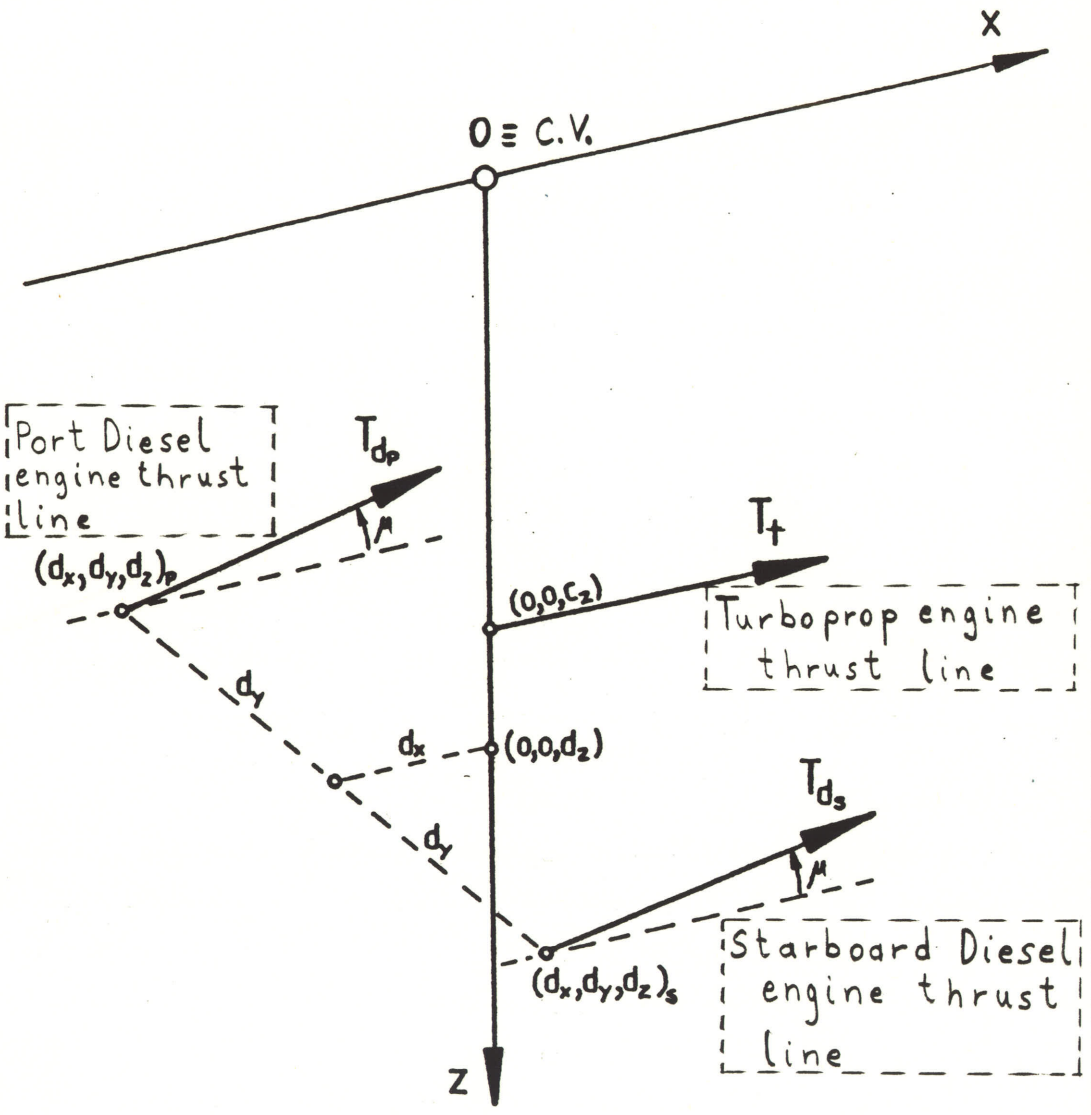


Figure 4.5 - Geometrical arrangement and coordinates of the engines thrust lines with respect to the YEZ-2A airship system of body axes.

$$M_{prop} = T_t \cdot c_z + \left(T_{d_s} + T_{d_p} \right) \left(d_z \cos\mu - d_x \sin\mu \right) \quad (4.23)$$

$$N_{prop} = \left(T_{d_p} - T_{d_s} \right) \cos\mu \cdot d_y \quad (4.24)$$

where,

T_t = Thrust of turboprop engine

T_{d_s} = Thrust of starboard side Diesel engine

T_{d_p} = Thrust of port side Diesel engine

μ = Angle of rotation through which the Diesel engines thrust vector directions can be varied synchronously in a plane parallel to OXZ

c_z = Vertical distance between the turboprop engine thrust line and the OX axis

d_x = Horizontal distance between the OZ axis and the line connecting the two Diesel engines thrust lines

d_y = Horizontal distance between the OXZ plane the Diesel engines thrust lines

d_z = Vertical distance between the OXY plane and the line connecting the two Diesel engines thrust lines

The thrust generated by the engines was estimated from the data supplied by Airship Industries (Appendix-1). Only the power available versus RPM curve was available for the Diesel engine selected, and the maximum continuous power figure for the turboprop engine. As the propellers for both the turboprop engine and the ducted fans connected to the Diesel engines had not been selected, a conservative figure of propeller efficiency of 60% was adopted in order to estimate the thrust of both types of engines from the power figures given. The standard expression

$$\text{Thrust} = \frac{\text{Power Available X Propeller Efficiency}}{\text{Total Air Vehicle Velocity}} \qquad (4.25)$$

was used to estimate the thrust generated by each engine type.

In normal circumstances only the Diesel engines thrust was considered, since the aim of the extra turboprop engine is to provide a 'dash' capability when and if required by the airship operational role.

The implementation of the propulsive model was achieved by the use of an ACSL TABLE in the propulsion section of the simulation program. This TABLE was simply the transcription to this format of the Power versus RPM curve given in Appendix-1. In this way, by selecting a desired RPM value the associated thrust value was obtained by first finding out the power available at that RPM figure from the power TABLE, and then using the ACSL coded form of Equation (4.25). After that, Equations (4.19-24) were used to determine the elements of the Propulsion vector P.

As in the Aerodynamics section case (Section 4.5.5) three extra sections were added so that thrust control input laws could be implemented in terms of the standard functions of STEP, PULSE and RAMP as already provided by ACSL. These were implemented in the same way and format as in the Aerodynamics case, and they provided for thrust change laws from the initial thrust value established in the longitudinal trim procedure (See Section 4.9). As before, the parameters required for this type of investigation could be changed from the command file, which made their use a relatively straightforward task (See Chapter 6 for some results).

4.8 The Solution

The previous sections have explained how each matrix, on both sides of Equation (3.1) was effectively

obtained in the simulation program. As already mentioned, the ACSL coded version of Equation (3.7) was obtained when both sides of Equation (3.1) were multiplied by M^{-1}, and this was accomplished in the program in a specific section of the Dynamic/Derivative region. It received the name 'Acceleration Calculations'.

The right hand side of Equation (3.7) could therefore be expressed as

$$\left[Acc\right]^T = \left[\begin{array}{cccccc} \dot{u} & \dot{v} & \dot{w} & \dot{p} & \dot{q} & \dot{r} \end{array}\right] \tag{4.26}$$

The next section in the same region of the simulation program, called 'Velocity Calculations', consisted in the use of the ACSL built in INTEG function which provided for the integration of each element of the Acc column matrix, yielding therefore

$$\left[Vel\right]^T = \left[\begin{array}{cccccc} u & v & w & p & q & r \end{array}\right] \tag{4.27}$$

Once the Vel matrix was obtained the total vehicle velocity could be calculated, using the standard expression

$$V_{Total} = \sqrt{u^2 + v^2 + w^2} \tag{4.28}$$

The final section of the Derivative region of the simulation program was called 'Position and Height'. It consisted first in the coded form of Equation (4.1), so as to obtain

$$\left[V_{Earth}\right]^T = \left[\begin{array}{ccc} V_{North} & V_{East} & V_{Up} \end{array}\right] \tag{4.29}$$

The INTEG function was again applied, now to the elements of the V_{Earth} matrix and the displacements of the airship in the North, East and Vertical directions

respectively were obtained. This was expressed as

$$\left[\text{Position}\right]^{T} = \left[\begin{array}{ccc} \text{North} & \text{East} & \text{H} \end{array}\right] \qquad (4.30)$$

The actual vehicle altitude from the ground was calculated as Height = -H, as the OZ axis, in the Earth axes system, is assumed to point toward the centre of the planet.

Two other variables that were determined at this stage were the ground path distance travelled and the absolute distance travelled since the start of the simulation run. These were calculated as

$$\text{Ground Path} = \sqrt{(\text{North})^2 + (\text{East})^2} \qquad (4.31)$$

$$\text{Total Distance} = \sqrt{(\text{North})^2 + (\text{East})^2 + (\text{Height})^2} \qquad (4.32)$$

These calculations concluded the Derivative region of the simulation program.

4.9 Initial Conditions and Trimming

The initial conditions associated with the state variables of the complete simulation equations, i.e., the initial values of u, v, w, p, q, r, e_0, e_1, e_2 ,e_3, North, East and H, were all stated in the Initial region of the simulation program as is the usual practice. As they were all declared as ACSL CONSTANTs, their values could be easily changed from the command file for each new simulation run.

In practice, and for the investigation here described, most runs started from an ISA sea-level condition, in which case the body axes system was made to coincide with the Earth axes system at t = 0. As in this condition V_{Total} is identical with u, basically only the initial value of u was changed between runs, although the

facility to change any of the other state variables was available. During the simulation run, however, conditions could change due to aerodynamic and/or power control inputs as already described.

Before the simulation run was allowed to actually start, the condition of longitudinal trim was imposed. This was a section of program code placed after the end of the Derivative region and before the end of the Dynamic region, in accordance with proven practice for ACSL (Ref. 49). The idea was that, while t was still equal to zero, the power setting would be changed in order to achieve trimmed flight at the initial value set for u, and the CG position would also be changed in order to counter the positive pitching moment due to the engines thrust line being a certain distance below the CV (origin of the body axes system).

The implementation of the two trimming procedures was achieved by enclosing their respective code sections inside regions delimited by logical flags. In this way, once the trimming conditions had been satisfied, the trimming flags were set to TRUE and those program sections were altogether skipped.

The power versus speed trimming was a straightforward procedure. As program execution went from the Initial region to the Dynamic/Derivative region at t = 0, the drag force for the initial set value of V_{Total} was calculated. This value was then multiplied by V_{Total} and divided by the assumed propeller efficiency factor and the result was made equal to the total engine power required. A Diesel engine RPM versus power available TABLE was then entered, and the RPM figure to be used in the initial part of the flight was therefore established. Finally, the logical flag for this section was set to TRUE, and it was never executed again from then on.

The next part of the trimming procedure, the CG trim, was slightly more involved. As already mentioned,

in normal circumstances the YEZ-2A airship will have a tendency to pitch nose up due to the engines thrust line being a certain distance below the CV. In some other airship designs this tendency is checked by having the horizontal fins set at a fixed predetermined incidence angle with respect to the vehicle Centre Line. With an X type of tail configuration as in the present case, this solution could still be used were it not for the fact that maximum endurance is a primary objective and a standard fin non-zero incidence angle generates enough trim drag as to be an unacceptable solution.

According to Airship Industries, the problem is likely to be solved in practice, and in principle, by shifting the CG position in such a way that the airship bow becomes 'heavy' enough to counter the existing pitch up moment. This forward shift of the CG is designed to occur by means of exchanging a certain amount of air between the bow and stern ballonets, so that the former ends up heavier than the latter for the initial longitudinal trim. This was therefore the solution implemented in the simulation program.

The CG trim procedure started by adding an extra variable to the right hand side of Equation (3.1), called Trimom (for trimming moment), which was allowed to assume a non-zero value only in the pitching moment equation of the set of six EOM. The idea was to arrive at Trimom value that would make the total pitching moment go to zero or, more realistically, a negligible specified value, whilst t = 0.

This idea was implemented in the simulation program by carrying out a number of iterations at t = 0, which calculated a new value for Trimom, each time program execution passed through the CG trim procedure region (just before the end of the Dynamic region). If the total pitching moment were still above the acceptable value, program execution would go back to the end of the Initial region and the Dynamic/Derivative region was

executed all over again with the new Trimom value. This process was repeated until the Trimom value made the total pitching moment negligibly small. Then the logical CG trim flags were set to TRUE, therefore making that program section a mandatory skip and allowing the actual simulation run to start ($t > 0$). For all practical purposes, the set maximum acceptable pitching moment value in this trimming procedure was of the order of 1.0 Nm, an empirical value that was arrived at after some considerable experimentation.

The value of Trimom was calculated at each iteration by using the expression

$$\text{Trimom} = -\left(\text{Mass}_{FB} - \text{Mass}_{AB}\right) g.x_{ball} \qquad (4.33)$$

where,

Mass_{FB} is the air mass in the forward ballonet
Mass_{AB} is the air mass in the aft ballonet
g is the acceleration due to gravity
x_{ball} is the horizontal distance between the CG of the forward or aft ballonets and the CV

The value of $\left(\text{Mass}_{FB} - \text{Mass}_{AB}\right)$ was calculated, at each iteration, as

$$\left(\text{Mass}_{FB} - \text{Mass}_{AB}\right) = \frac{\text{Total Pitching Moment}}{x_{ball} \cdot g} \qquad (4.34)$$

In the actual CG trim implementation an empirically determined gain factor (equal to 0.75) was introduced in the equivalent ACSL coded version of Equation (4.34), so as to achieve a rapid convergence to the final Trimom value. This was a necessary procedure since each new Trimom value determined also carried with it a new CG position, due to a new mass distribution inside the gas envelope.

Another measure that was introduced to speed up the

trimming process was the alternative way of terminating it once the value of $\dot{q}$ (pitch angular acceleration) had reached a negligibly small value. The acceptable $\dot{q}$ value was found empirically, after a trial and error process, to be of the order of 1.0×10^{-5} rad/sec^2.

Once these two measures were combined, the total program execution time spent in the trimming procedures, before the actual simulation run could start, was reduced to a period of approximately seven seconds on the average.

4.10 Model Running in ACSL

The YEZ-2A flight dynamics simulation was implemented in ACSL in the way described in the previous sections. In its final version, the source program had 1805 lines of code, of which approximately half were taken by the aerodynamic data base in the form of ACSL TABLEs. The translation plus compilation time of the source program took approximately 30 minutes to be accomplished, a factor that occasionally discouraged the introduction of more sophisticated refinements, bearing in mind the already mentioned error reporting difficulties associated with ACSL.

A typical simulation run of 200 seconds would take approximately 18 minutes to be accomplished, depending on the choice of integration control parameters. This gave an average ratio of approximately 5.5 between simulation time and real time.

It is important to notice that the figures given are for the Personal Computer already mentioned. Some tentative runs were occasionally carried out on more recently made and faster PCs, which resulted in dramatic reductions both in the compilation of the source program and the simulation run times. It is therefore recommended that future and more complex versions of the simulation program be run on the fastest equipment available so as to permit ever more sophisticated

simulation techniques to be implemented, if so desired.

In the actual running of the simulation model a considerable amount of time was spent in investigating the choice of parameters used by the ACSL integration control. These were mainly the integration algorithm (there are eight options available), the communication interval, i.e., the frequency at which the simulation results are output, and the maximum integration step size that is to be allowed.

After a reasonably extensive investigation process, during which a considerable number of spurious results were obtained and had subsequently to be discarded, the final set of integration parameters, that seemed to yield the most believable results, was arrived at. The choice of integration algorithm fell on the Runge-Kutta-Fehlberg (second order), complemented by a communication interval of half a second and a maximum integration step size of 0.1 second.

The given set of parameters meant that each simulation run would produce twice as many data points as its total run time in seconds, an output level which was found to produce graphs and tables with a reasonable degree of resolution.

The facilities provided by ACSL for outputting the results comprise the output file, in which the values of the variables specified in the PREPAR list of the command file are printed as text (ASCII characters), and its graphics package. The graphics package is able to produce both line and strip plots, and send them either to the computer screen or to a printer.

These facilities were considered adequate for most of the work carried out. The instructions on how to plot each graph, rather than being manually input to the system after each run, were all encoded inside PROCEDs in the command file, which not only saved a considerable amount of time but also helped to standardize the output of successive simulation runs.

The only drawback found, however, was that the ACSL system used was not able to combine the results of more than one run in a single plot. ACSL plots refer to a single run only. In order to overcome this problem a spread sheet type of package was used (SuperCalc), which was made to read in from the ACSL output file, after it underwent some modifications in order to allow this type of operation to be accomplished. Although not a straightforward process, it nevertheless worked as expected and avoided the need to re-enter data manually through the keyboard (when sometimes thousands of data points were involved), preserving therefore the accuracy of the original results.

FIGURE 4.6 - Flight dynamics computer simulation program flow chart.

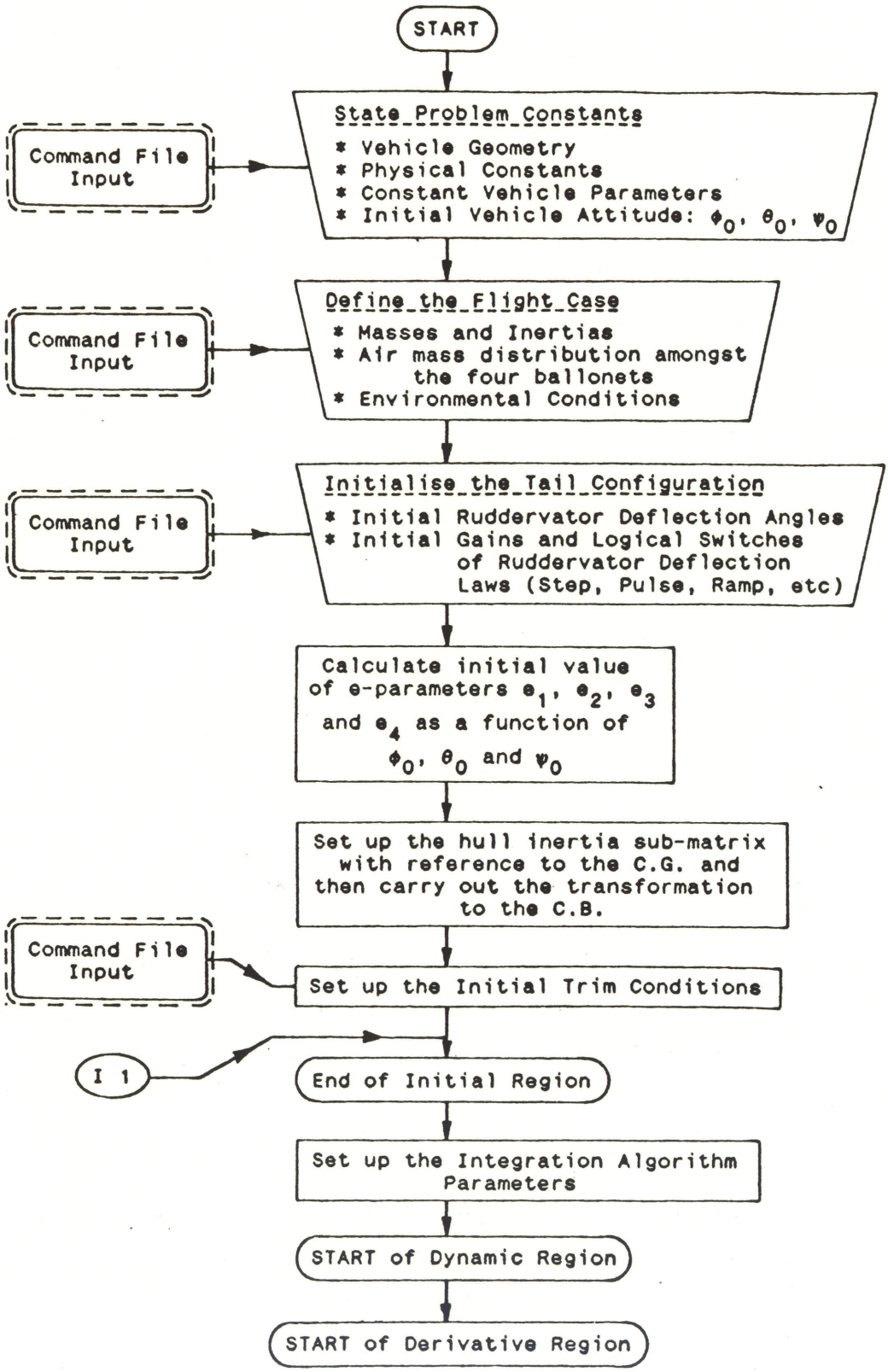


FIGURE 4.6 (cont.)

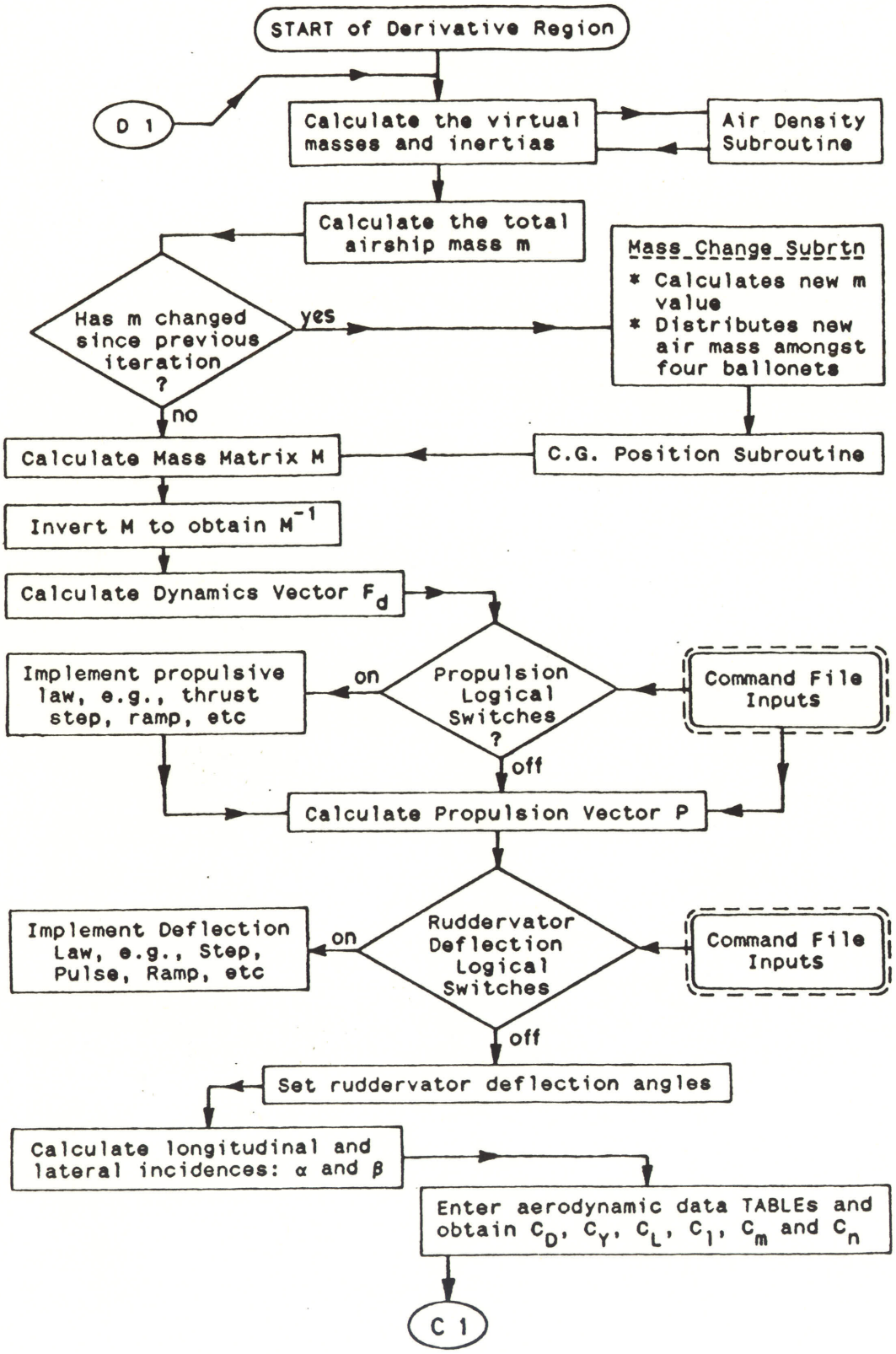


FIGURE 4.6 (cont.)

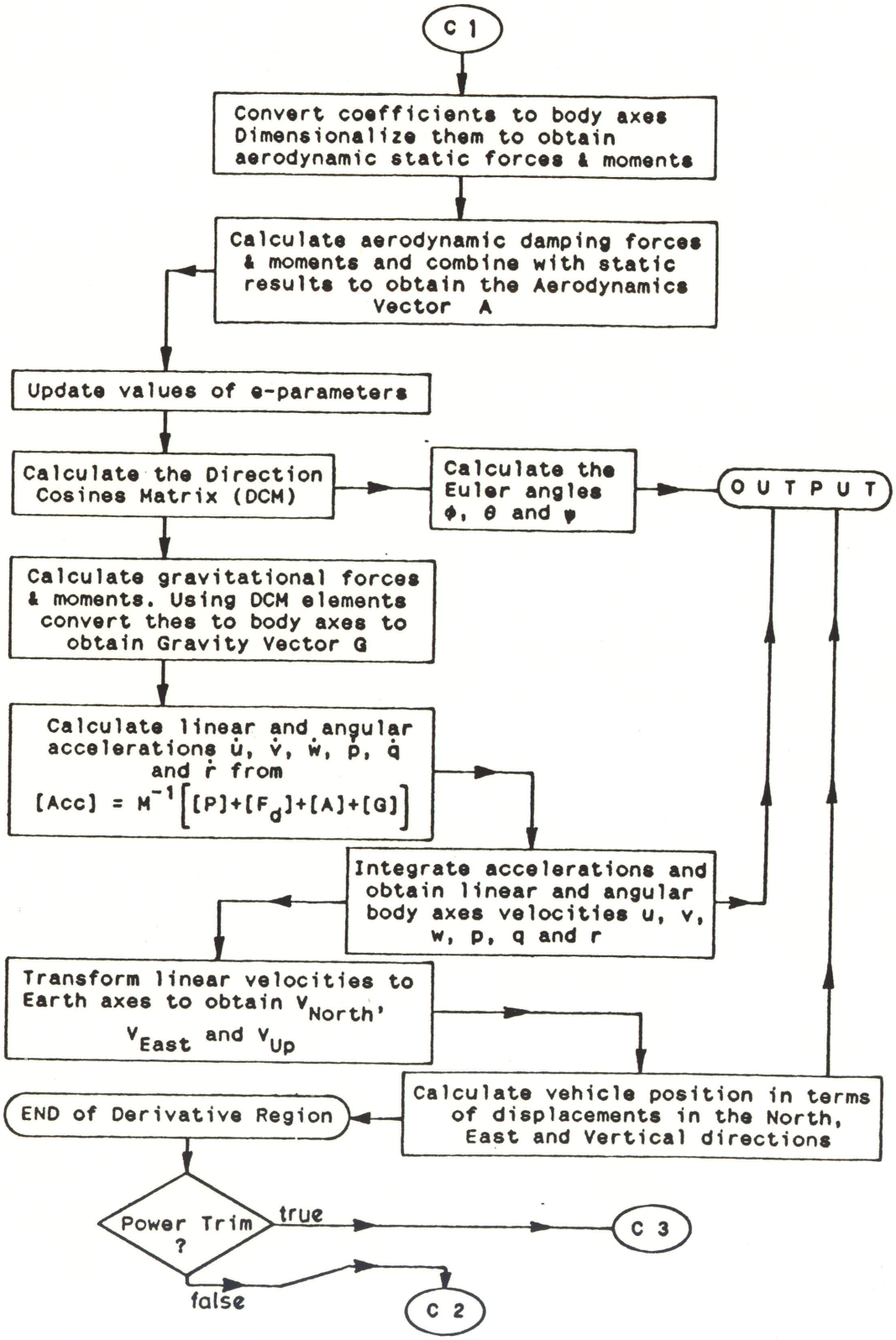
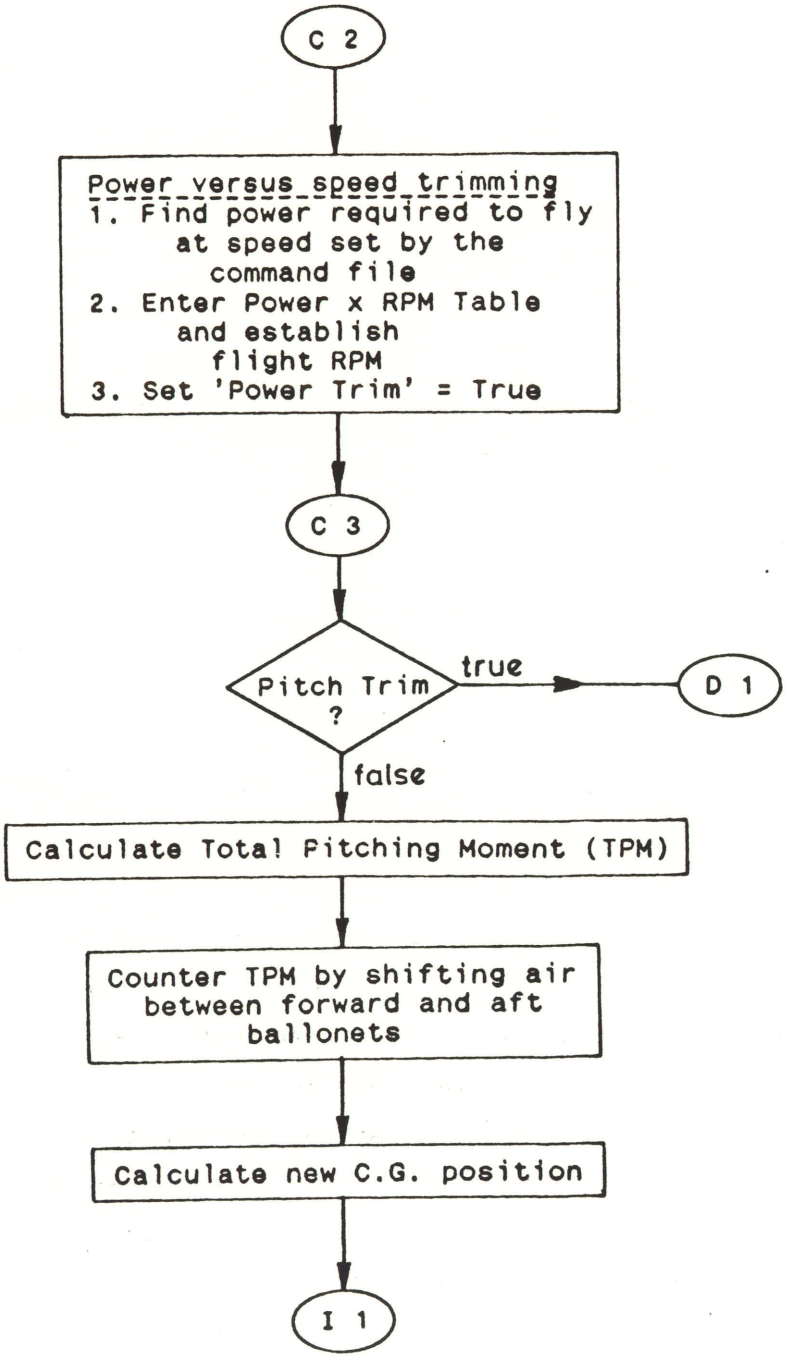


FIGURE 4.6 (cont.)



5. STABILITY INVESTIGATION AND MODE DEMONSTRATION

5.1 Introduction

The purpose of this Chapter is to present the results of the investigation on the stability and modes of motion of the YEZ-2A that was carried out using the developed flight dynamics simulation model.

Airships are known for their characteristically positive values of m_w (Cm_α) and negative values of n_v (Cn_β), which is certainly the case of the YEZ-2A (See Table A1.5.1 of Appendix-1). This would imply static instability for a conventional aircraft about its Centre of Gravity, with dynamic instability being a very likely consequence. In the case of the airship, however, with approximately neutral buoyancy, this might not be the case and therefore the need to investigate their specific stability characteristics (Ref. 14) was determined.

The investigation was divided up into two parts: The first was aimed at finding the eigenvalues and eigenvectors for a reasonable range of the YEZ-2A flight speeds. This would result in a general assessment of the YEZ-2A longitudinal and lateral stability characteristics, including an attempt to predict it modes of motion resulting from small perturbations.

The second part of the investigation was aimed at trying to demonstrate the longitudinal and lateral modes of motion of the YEZ-2A airship based on the information generated during the first part.

The methodology employed in the stability investigation, the resulting eigenvalues and eigenvectors, as well as the attempts to predict the airship modes of motion are all contained in Appendix-3. In particular, reference will be made here to the long sequence of Tables of eigenvalues and eigenvectors as functions of flight speed that form Section A3.2.

On the other hand, the mode demonstration investigation was carried out by running the simulation

model with different control inputs over different time intervals until the desired mode of motion was achieved. The results were then compared with the predictions generated in the first part of the investigation.

The next two sections present the results achieved for the longitudinal and lateral stability investigations. The last Section draws some conclusions and compares the results achieved with those estimated for other airships.

5.2 Longitudinal Stability

The eigenvalues for the YEZ-2A airship, Case 1 (neutral buoyancy, ISA, sea level conditions) are presented in Tables A3.2.1-15 of Appendix-3. Both the real and the complex values for the longitudinal case were plotted in the complex plane and are presented in Figure 5.1. The frequency of the oscillatory mode has also been plotted against its associated damping ratio and is shown in Figure 5.2.

From these results it can be concluded, in essence, that:

i. As all the eigenvalues are on the left hand side of the complex plane, with some of them virtually on the imaginary axis and/or its intersection with the real axis, the longitudinal stability of the YEZ-2A appears to vary from neutral to stable.

ii. In the hover condition the airship stability is virtually neutral, and this applies to the oscillatory mode as well. Considering that the damping of this mode is apparently non-existent, these indications suggest that unless some closed loop auto-stabilization feature can be incorporated into the flying controls and power throttles, the hover condition for an airship is not very much different from that faced by a free balloon.

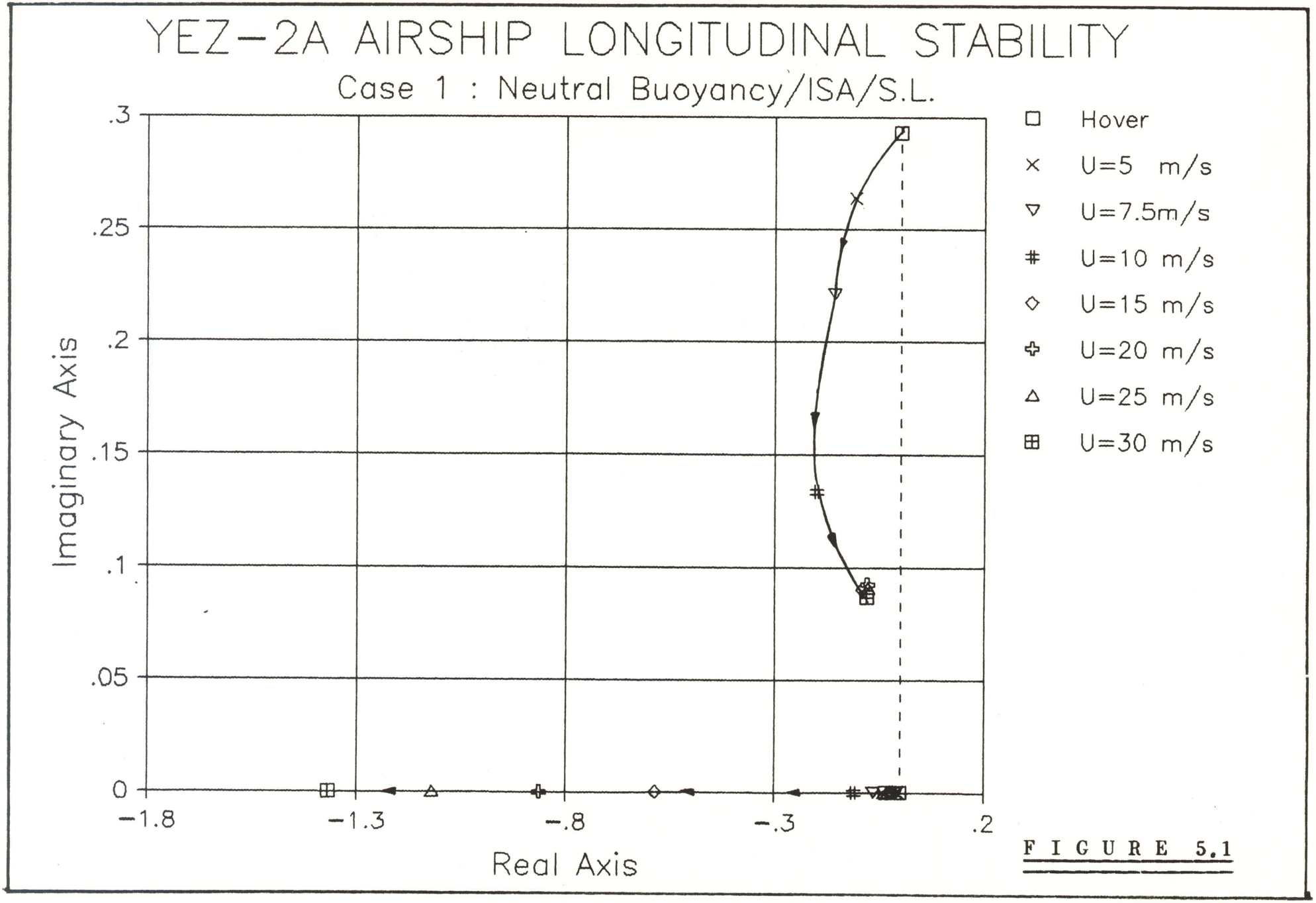

YEZ-2A AIRSHIP LONGITUDINAL STABILITY
Case 1 : Neutral Buoyancy/ISA/S.L.
Imaginary Axis
.3
.25
.2
.15
.1
.05
0
-1.8
-1.3
-.8
-.3
.2
Real Axis
Hover
U=5 m/s
U=7.5m/s
U=10 m/s
U=15 m/s
U=20 m/s
U=25 m/s
U=30 m/s

FIGURE 5.1

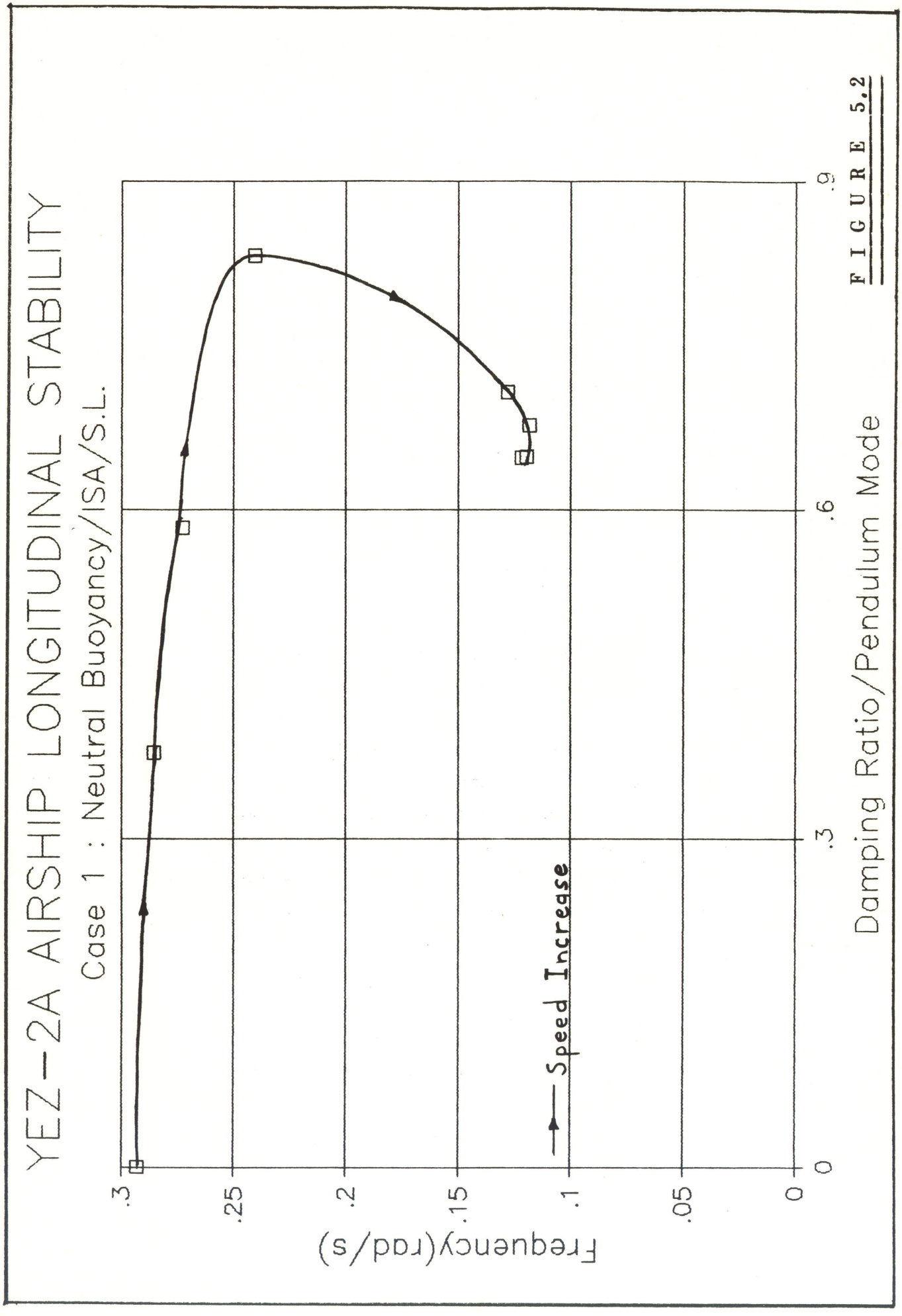

YEZ-2A AIRSHIP LONGITUDINAL STABILITY
Case 1 : Neutral Buoyancy/ISA/S.L.
Frequency(rad/s)
.3
.25
.2
.15
.1
.05
0
0
.3
.6
.9
Damping Ratio/Pendulum Mode
Speed Increase

FIGURE 5.2

iii. With the speed increase, the stability picture improves, since the damping ratio of the oscillatory mode increases and the eigenvalues of the subsidence modes become more negative.

iv. At the fast end of the speed range the oscillatory mode slows down, i.e., its frequency becomes smaller, but the damping ratio also gets slightly smaller and so the overall effect is probably a positive one.

v. The slow subsidence mode does not appear to be much affected by speed increases. It results in a nearly neutral mode with a long time constant and therefore should not present major difficulties in being dealt with by either a pilot or an automatic control system.

5.2.1 Mode Demonstration

In order to try to demonstrate the longitudinal modes of motion of the YEZ-2A airship, the command file that was used to drive the simulation was successively filled with instructions that would hopefully excite each mode in turn. In order to have a starting point, the mode derivation work presented in Sections A3.2-3 of Appendix-3 was used as a guide to conceive the mode demonstration experiments.

This type of work was carried out for a number of flight speeds as follows:

* Hover:

From Table A3.2.1, the hover heave mode eigenvalue is given by $s_2 = -7.6 \times 10^{-5}$ rad/s. If the usual exponential type of solution is assumed for this mode then its time constant τ_{heave} will be obtained from

$$s_2 = -1/\tau_{heave} \quad ===> \quad \tau_{heave} \cong 13{,}200 \text{ seconds}$$

An experiment was therefore devised in which the flight speed was set to 0.01 m/s (to avoid division by zero during program execution) and the four ruddervators were made to deflect in an 'elevator down' type of configuration of 25° for 19,500 seconds. The result is presented in the strip plot type of graph produced by ACSL in Figure 5.3.

It can be seen that both the vertical velocity w and the vehicle height appear to follow the assumed exponential law, as after 13,200 seconds of the applied disturbance both parameters have reached approximately 63% of their final steady state values. The mode denomination of 'heave' can therefore be considered to be adequate to describe the vehicle motion.

For the oscillatory mode, an experiment was conceived which comprised the application of an 'elevator' doublet, i.e., the four ruddervators were deflected upwards by 15° during 10 seconds and then immediately deflected downwards by the same amount and time. The result is shown in Figure 5.4.

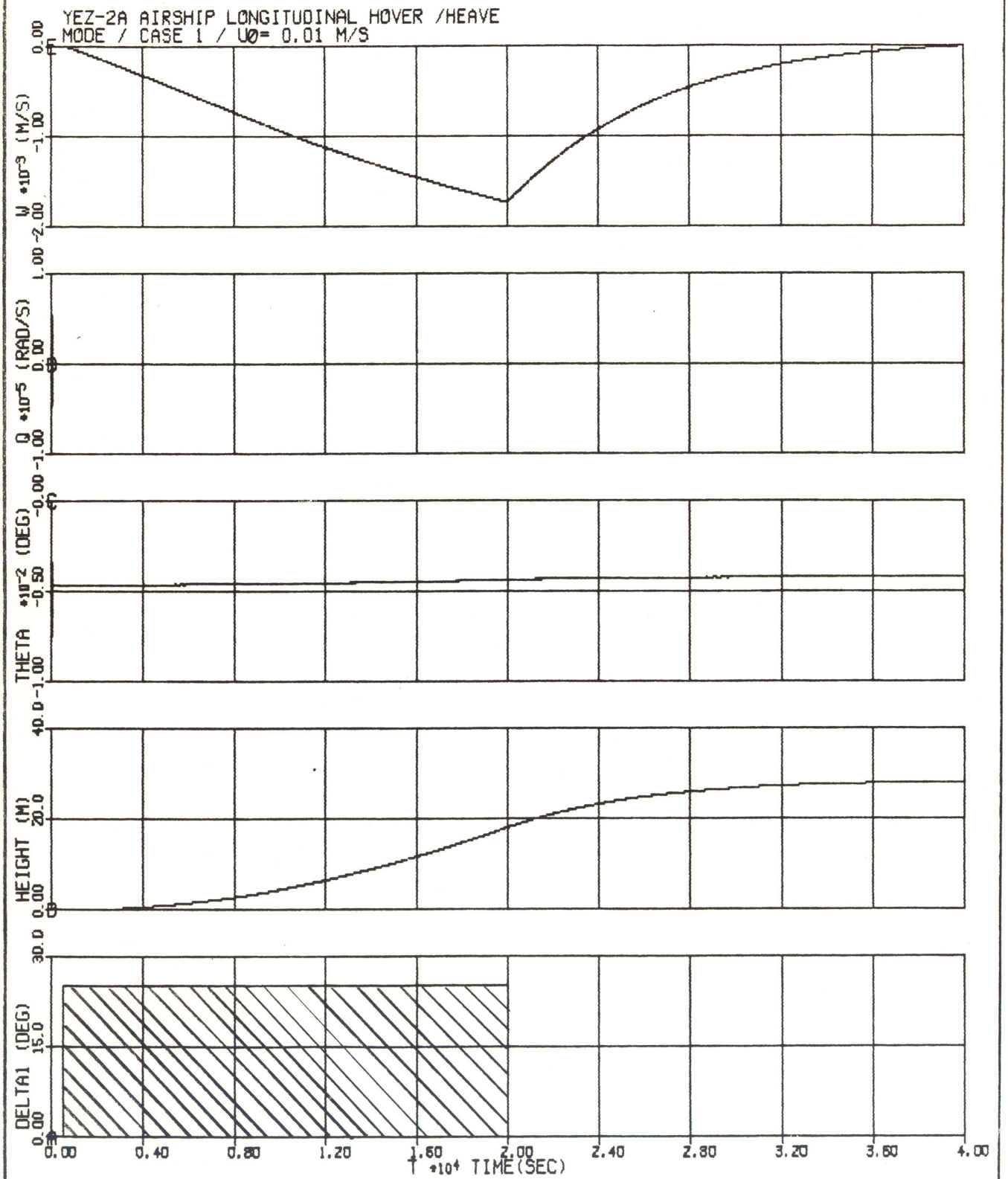
As predicted in Appendix-3, the oscillatory motion appears to have negligible damping characteristics. The time period of this mode can be estimated from the associated eigenvalue frequency, i.e.,

$$T_{pendulum} = 2\Pi/\omega = 2\Pi/0.293 = 21.4 \text{ seconds}$$

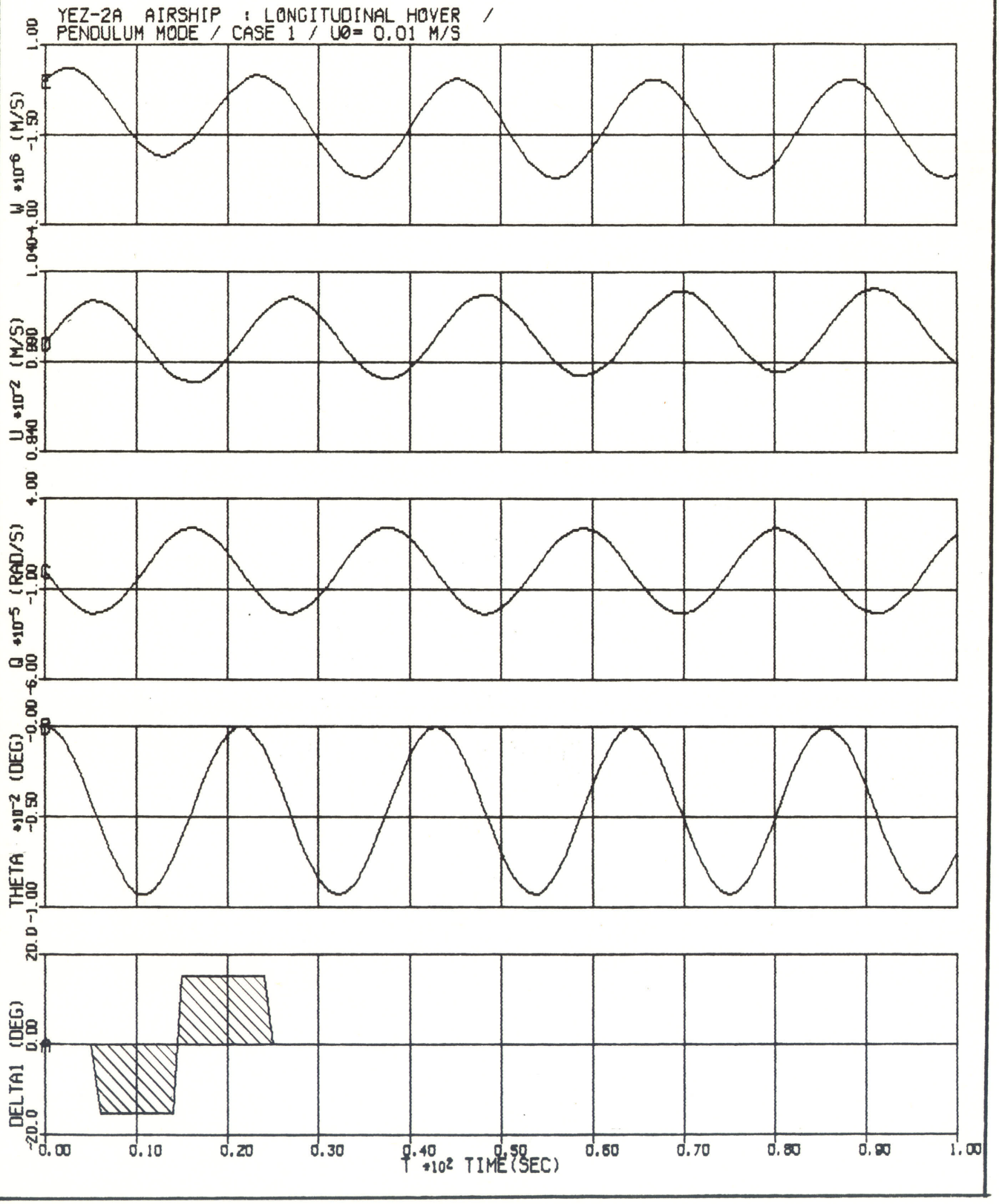
and this result is effectively confirmed in Figure 5.4. In addition, the phase relations predicted in Figure A.3.3.1 are all confirmed, i.e., q and θ are out of phase by 90°, and q and u are out of phase by 180°. In view of these results, it can be concluded that the assumed pendulum type of oscillation was in effect confirmed.

The physical explanation for its occurrence has long

F I G U R E 5.3


YEZ-2A AIRSHIP LONGITUDINAL HOVER /HEAVE
MODE / CASE 1 / U0= 0.01 M/S
W *10^-3 (M/S)
0.00
-1.00
-2.00
Q *10^-5 (RAD/S)
1.00
0.00
-1.00
THETA *10^-2 (DEG)
-0.00
-0.50
-1.00
HEIGHT (M)
40.0
20.0
0.00
DELTA1 (DEG)
30.0
15.0
0.00
0.00
0.40
0.80
1.20
1.60
2.00
2.40
2.80
3.20
3.60
4.00
*10^4 TIME(SEC)

F I G U R E 5.4


YEZ-2A AIRSHIP : LONGITUDINAL HOVER /
PENDULUM MODE / CASE 1 / U0= 0.01 M/S
W *10^-6 (M/S)
1.00
-1.50
-4.00
U *10^-2 (M/S)
1.040
0.980
0.940
Q *10^-5 (RAD/S)
4.00
-1.00
-6.00
THETA *10^-2 (DEG)
-0.00
-0.50
-1.00
DELTA1 (DEG)
20.0
0.00
-20.0
0.00
0.10
0.20
0.30
0.40
0.50
0.60
0.70
0.80
0.90
1.00
T *10^2 TIME(SEC)

been known to balloonists and it is due to the metacentric height of the CB, i.e., the fact that the Centre of Gravity is some distance below the Centre of Buoyancy. After a disturbance, this configuration induces an oscillatory motion caused by both the buoyancy force B and the vehicle weight W, about an axis that is located somewhere between the CG and the CB, and hence the mode denomination.

* Flight Speed = 25 m/s and 5 m/s:

From Table A3.2.13 the surge mode eigenvalue is given by $s_1 = -0.028$ rad/s. Therefore, the usually assumed exponential type of solution will yield

$$s_1 = -1/\tau_{surge} \quad \Longrightarrow \quad \tau_{surge} \cong 35 \text{ seconds}$$

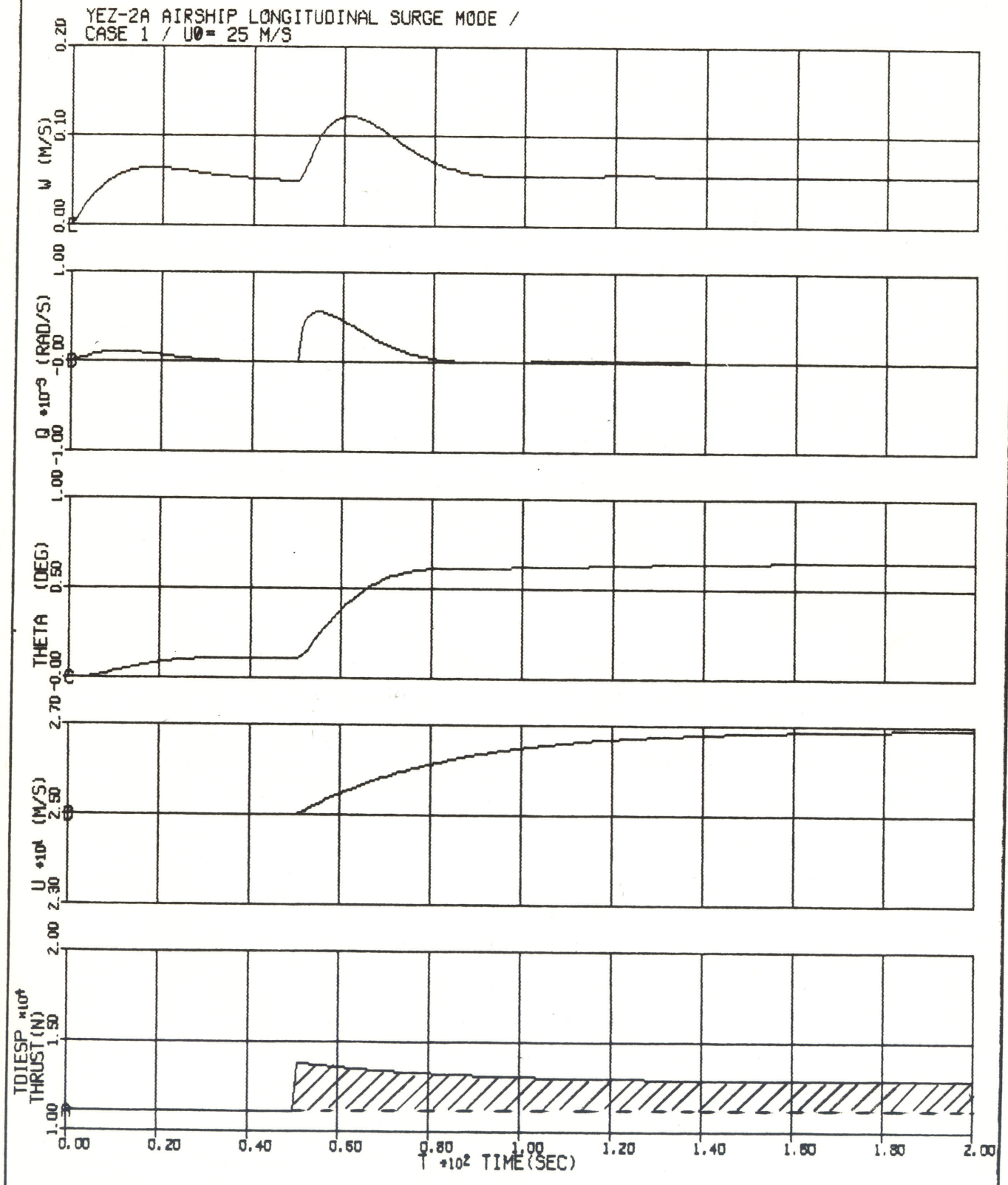
The experiment associated with the demonstration of this mode consisted in letting the airship fly for 50 seconds in the trimmed, straight and level condition. Then a thrust step was applied, whose value was 25% above the initial value. The results of the experiment are presented in Figure 5.5. It can be seen that the u-velocity appears to follow the assumed exponential law, as after approximately 35 seconds of the applied disturbance the value of this variable has reached about 63% of its final steady state value. The mode denomination of 'speed surge' or just 'surge' can therefore be considered to be adequate in describing the vehicle behaviour.

The second eigenvalue from the Table is given by $s_2 = -1.12$ and the assumed exponential solution will yield

$$\tau_{pitch} = -1/s_2 \cong 0.9 \text{ second}$$

For this much faster mode the experiment consisted in flying the airship in the trimmed, straight and level

F I G U R E 5.5


YEZ-2A AIRSHIP LONGITUDINAL SURGE MODE /
CASE 1 / U0= 25 M/S
W (M/S)
0.20
0.10
0.00
Q *10⁻³ (RAD/S)
1.00
-0.00
-1.00
THETA (DEG)
1.00
0.50
-0.00
U *10 (M/S)
2.70
2.50
2.30
TDIESP *10⁴
THRUST(N)
2.00
1.50
1.00
0.00
0.20
0.40
0.60
0.80
1.00
1.20
1.40
1.60
1.80
2.00
T *10² TIME(SEC)

condition for five seconds and then applying an elevator type of ruddervator deflection (all four surfaces) of 10° up for 10 seconds. As can be seen in Figure 5.6, after 0.9 second the value of the pitch rate variable q has reached approximately 63% of its final steady state value. It was therefore concluded that the 'pitch subsidence' denomination for this mode of motion was adequate in describing the vehicle behaviour.

For the oscillatory mode in Table A3.2.13 the indications are that the time period and the damping will be given by

$$T = 2\Pi/\omega = 2\Pi/0.119 \cong 53 \text{ seconds}$$
$$\zeta = 0.65$$

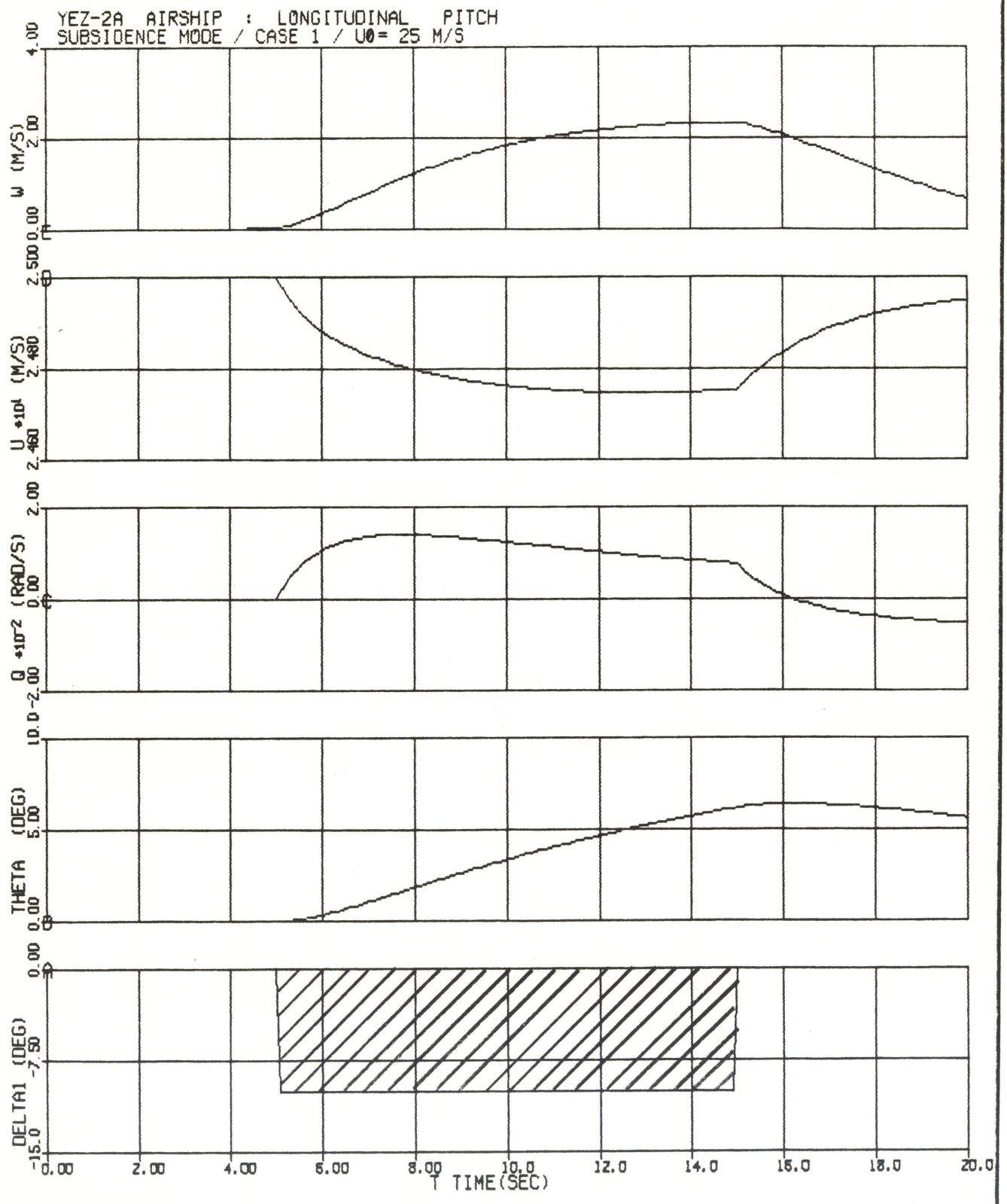
The relatively high damping value coupled with the long time period suggest a mode transition between an oscillatory type and a subsidence aperiodic mode of motion. The results from the associated experiment, which consisted in running the model initially for 5 seconds and then applying an elevator 'doublet' (all surfaces up and then down) of 15° in each direction for 10 seconds, confirm these predictions. They are shown in Figure 5.7 and, as pointed out in Section A3.3 (Appendix-3), 'pendulum oscillation' is a misnomer for this mode of motion at 25 m/s.

If however the speed is reduced to 5 m/s, as shown in Figure 5.8, then the characteristics of the pendulum oscillation, with a phase shift of approximately 90° between pitch rate q and pitch angle θ, become more evident. Furthermore, Table A3.2.3 indicates that at this speed the periodic time can be estimated from

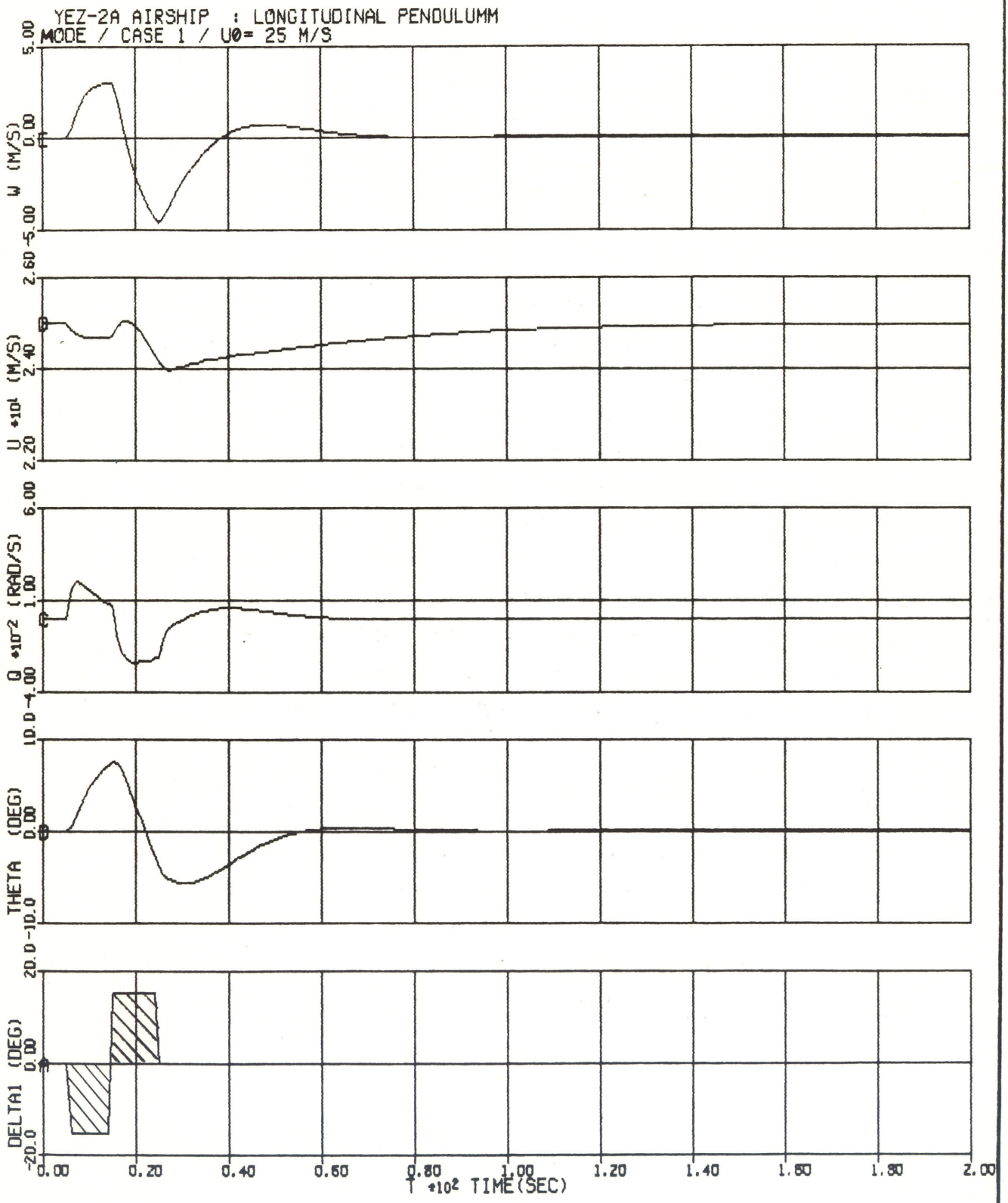
$$T = 2\Pi/\omega = 2\Pi/0.285 \cong 22 \text{ seconds}$$

and this can just about be confirmed in the θ versus time plot of Figure 5.8, before the damping ratio of $\zeta = 0.38$

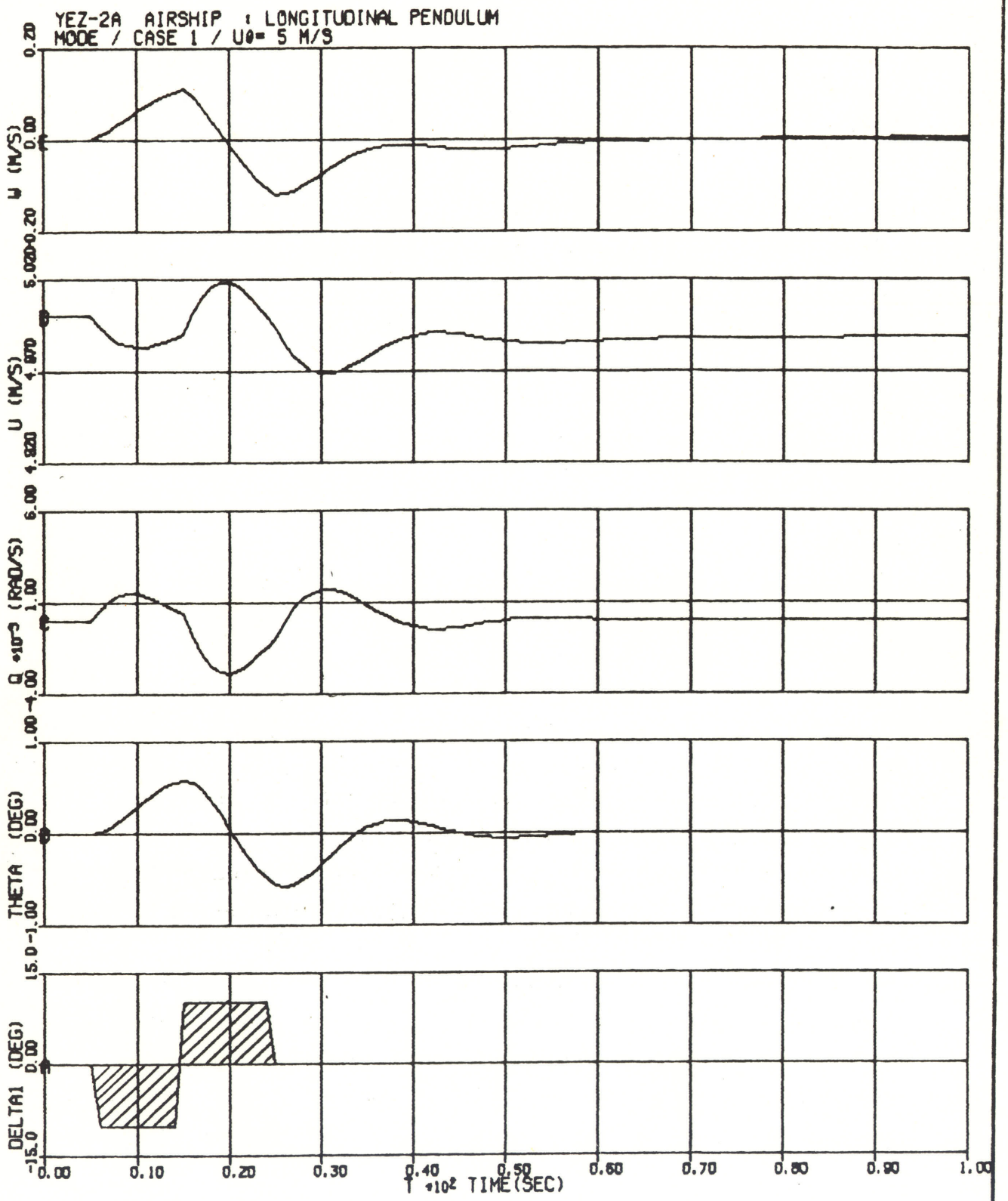
F I G U R E 5.6


YEZ-2A AIRSHIP : LONGITUDINAL PITCH
SUBSIDENCE MODE / CASE 1 / U0= 25 M/S
W (M/S)
U *10⁴ (M/S)
Q *10⁻² (RAD/S)
THETA (DEG)
DELTA1 (DEG)
T TIME(SEC)

F I G U R E 5.7


YEZ-2A AIRSHIP : LONGITUDINAL PENDULUMM
MODE / CASE 1 / U0= 25 M/S
W (M/S)
5.00
0.00
-5.00
U *10¹ (M/S)
2.60
2.40
2.20
Q *10⁻² (RAD/S)
6.00
1.00
-4.00
THETA (DEG)
10.0
0.00
-10.0
DELTA1 (DEG)
20.0
0.00
-20.0
0.00
0.20
0.40
0.60
0.80
1.00
1.20
1.40
1.60
1.80
2.00
T *10² TIME(SEC)

F I G U R E 5.8


YEZ-2A AIRSHIP : LONGITUDINAL PENDULUM
MODE / CASE 1 / U0= 5 M/S
W (M/S)
0.20
0.00
-0.20
U (M/S)
5.020
4.970
4.920
Q *10^-2 (RAD/S)
6.00
1.00
-4.00
THETA (DEG)
1.00
0.00
-1.00
DELTA1 (DEG)
15.0
0.00
-15.0
0.00
0.10
0.20
0.30
0.40
0.50
0.60
0.70
0.80
0.90
1.00
T *10^2 TIME(SEC)

reduces the amplitude of the oscillation to a negligible value. Under these conditions it was therefore felt that the pendulum oscillation denomination was adequate in describing the airship behaviour.

5.3 Lateral Stability

The lateral eigenvalues for the YEZ-2A airship, Case 1 (neutral buoyancy, ISA, sea level conditions) are presented in Tables A3.2.2-16 of Appendix-3. Both the real and the complex values for the longitudinal case were plotted in the complex plane and are presented in Figure 5.9. The frequency of the oscillatory mode has also been plotted against its associated damping ratio and is shown in Figure 5.10.

From these results it can be concluded, in essence, that:

i. As all the eigenvalues are on the left hand side of the complex plane, with some of them virtually on the imaginary axis and/or its intersection with the real axis, the lateral stability of the YEZ-2A appears to range from the neutral to the stable categories.

ii. In the hover condition the airship stability is virtually neutral, and this applies to the oscillatory mode as well. Considering that the damping of this mode is apparently non-existent, these indications suggest that, just like in the longitudinal case, unless some closed loop auto-stabilization feature can be incorporated into the flying controls and power throttles, the hover condition for an airship is not very much different from that faced by a free balloon.

iii. With the speed increase, the general stability picture improves, since the damping ratio of the oscillatory mode increases and the eigenvalues of the subsidence modes become more negative.

iv. However, in direct contrast to what happens in the

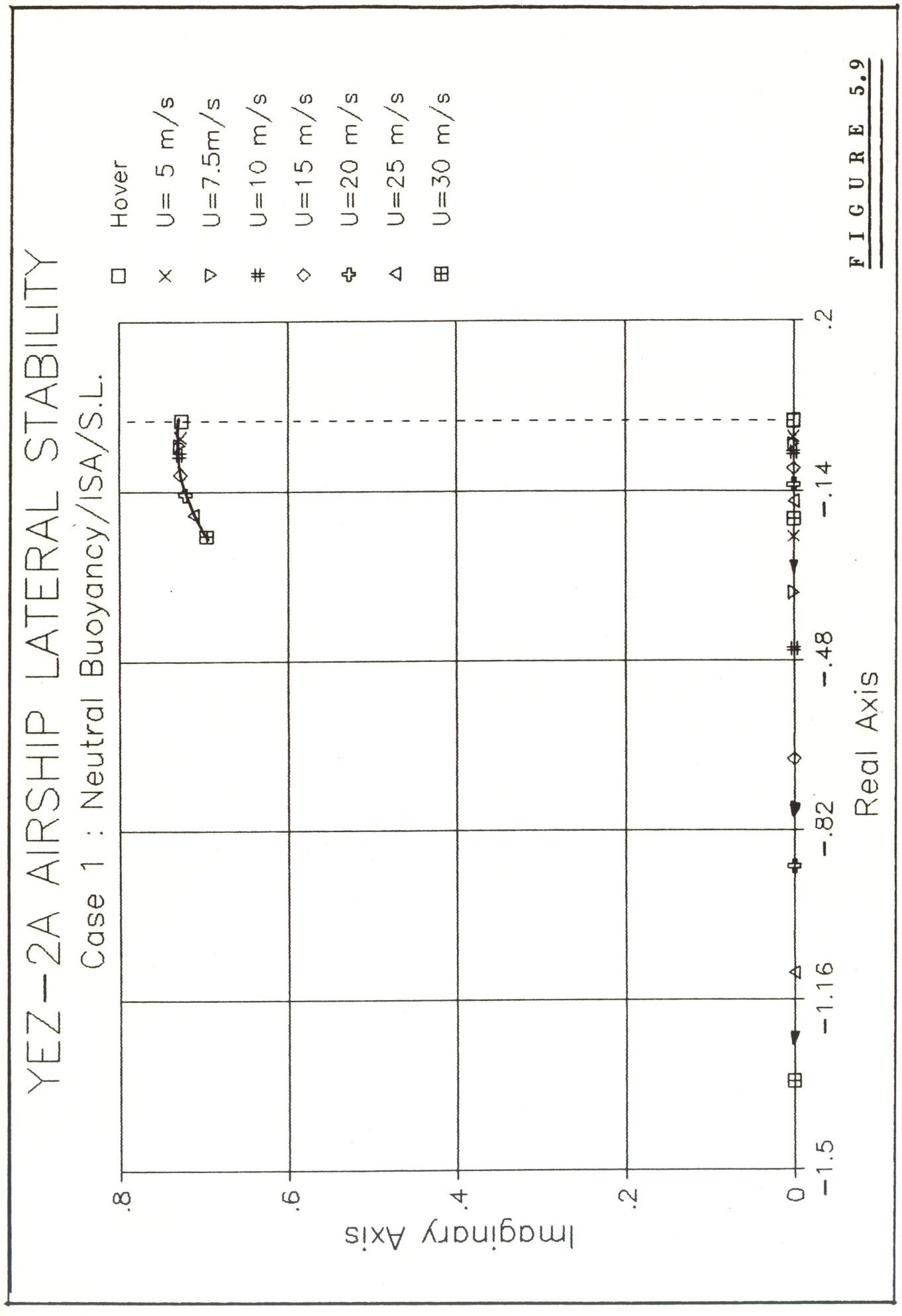

YEZ-2A AIRSHIP LATERAL STABILITY
Case 1 : Neutral Buoyancy//ISA/S.L.
Hover
U= 5 m/s
U=7.5m/s
U=10 m/s
U=15 m/s
U=20 m/s
U=25 m/s
U=30 m/s
Imaginary Axis
.8
.6
.4
.2
0
-1.5
-1.16
-.82
-.48
-.14
.2
Real Axis

FIGURE 5.9

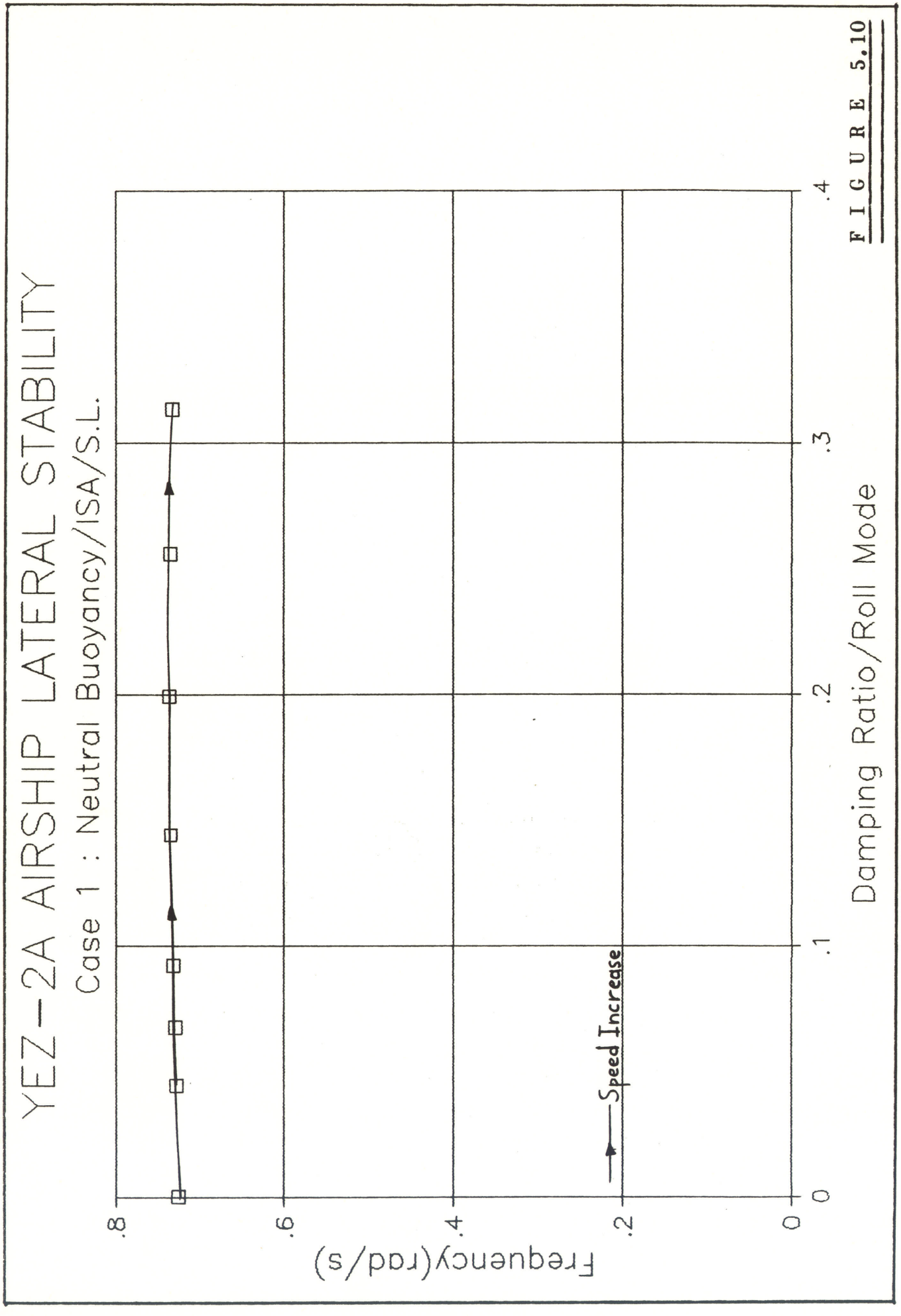

YEZ-2A AIRSHIP LATERAL STABILITY
Case 1 : Neutral Buoyancy/ISA/S.L.
Frequency(rad/s)
.8
.6
.4
.2
0
0
.1
.2
.3
.4
Speed Increase
Damping Ratio/Roll Mode

FIGURE 5.10

longitudinal case, the frequency of the oscillatory mode stays virtually unchanged throughout the speed range and only the damping ratio undergoes an increase, which in turn appears to be directly proportional to the speed variation.

v. The slow subsidence mode does not appear to be much affected by speed increases. It results in a nearly neutral mode with a long time constant and therefore should not present major difficulties in being dealt with by either a pilot or an automatic control system.

5.3.1 Mode Demonstration

In order to try to demonstrate the lateral modes of motion of the YEZ-2A airship, the command file that was used to drive the simulation was successively filled with instructions that would hopefully excite each mode in turn. In order to have a starting point, the mode derivation work presented in Section A3.4 of Appendix-3 was used as a guide to conceive the mode demonstration experiments.

In contrast to the longitudinal case, the increase in flight speed did not show any changes in the nature of the modes. Therefore, the mode demonstration investigation was carried out for two flight speeds only:

* Hover:

From Table A3.2.2, the hover sideslip subsidence and yaw subsidence mode eigenvalues are given respectively by $s_1 = -6.4 \times 10^{-5}$ rad/s and $s_2 = -4.7 \times 10^{-4}$ rad/s. If the usual exponential type of solution is assumed for these modes, then their time constants $\tau_{sidelip}$ and τ_{yaw} can be obtained from

$$s_1 = -1/\tau_{sideslip} \quad ===> \quad \tau_{sideslip} \cong 15{,}600 \text{ seconds}$$
$$s_2 = -1/\tau_{yaw} \quad ===> \quad \tau_{yaw} \cong 2{,}130 \text{ seconds}$$

An experiment was therefore devised in which the flight speed was set to 0.01 m/s (to avoid division by zero during program execution) and the four ruddervators were made to deflect in a 'rudder to port side' type of configuration of 25° for 15,000 seconds. The result is presented in the strip plot type of graph produced by ACSL in Figure 5.11.

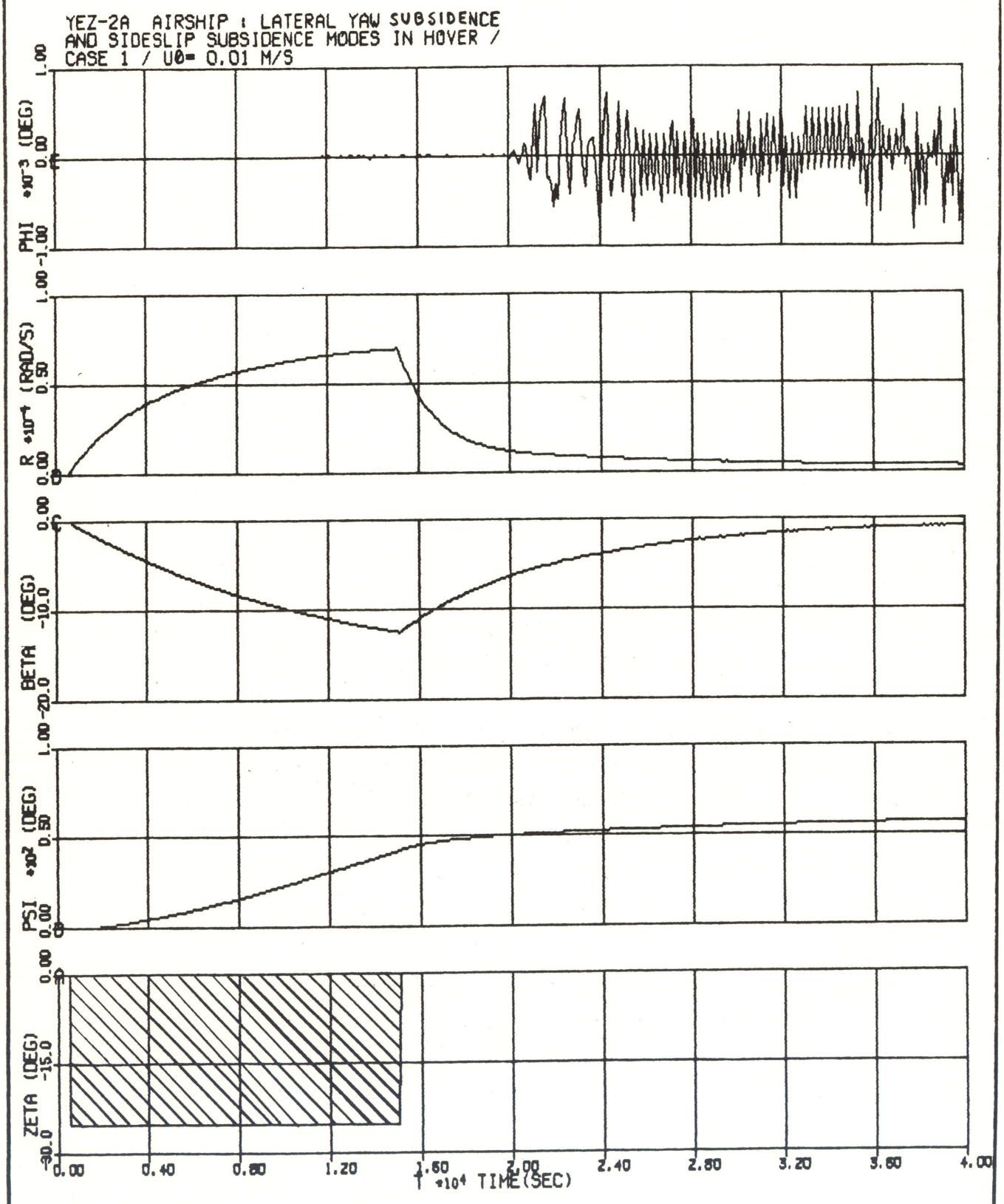
It can be seen that both the yaw rate r and the sideslip angle β appear to follow an exponential rule of convergence to their final steady state values. In addition, it can be seen that β has reached approximately 63% of its final estimated steady state value after its assumed time constant of 15,600 seconds had elapsed. The mode denomination of 'sideslip subsidence' was therefore considered to have been confirmed in the experiment.

As for the yaw rate r, it appears from Figure 5.11 that its associated time constant is about two times the predicted value of 2,130 seconds. This is probably due to the very hover conditions in which the experiment was carried out, which provide very little in terms of lateral motion damping, therefore allowing the yaw rate to develop up to a value higher than otherwise anticipated. The effective mode demonstration is consequently left for the forward flight condition in this particular case.

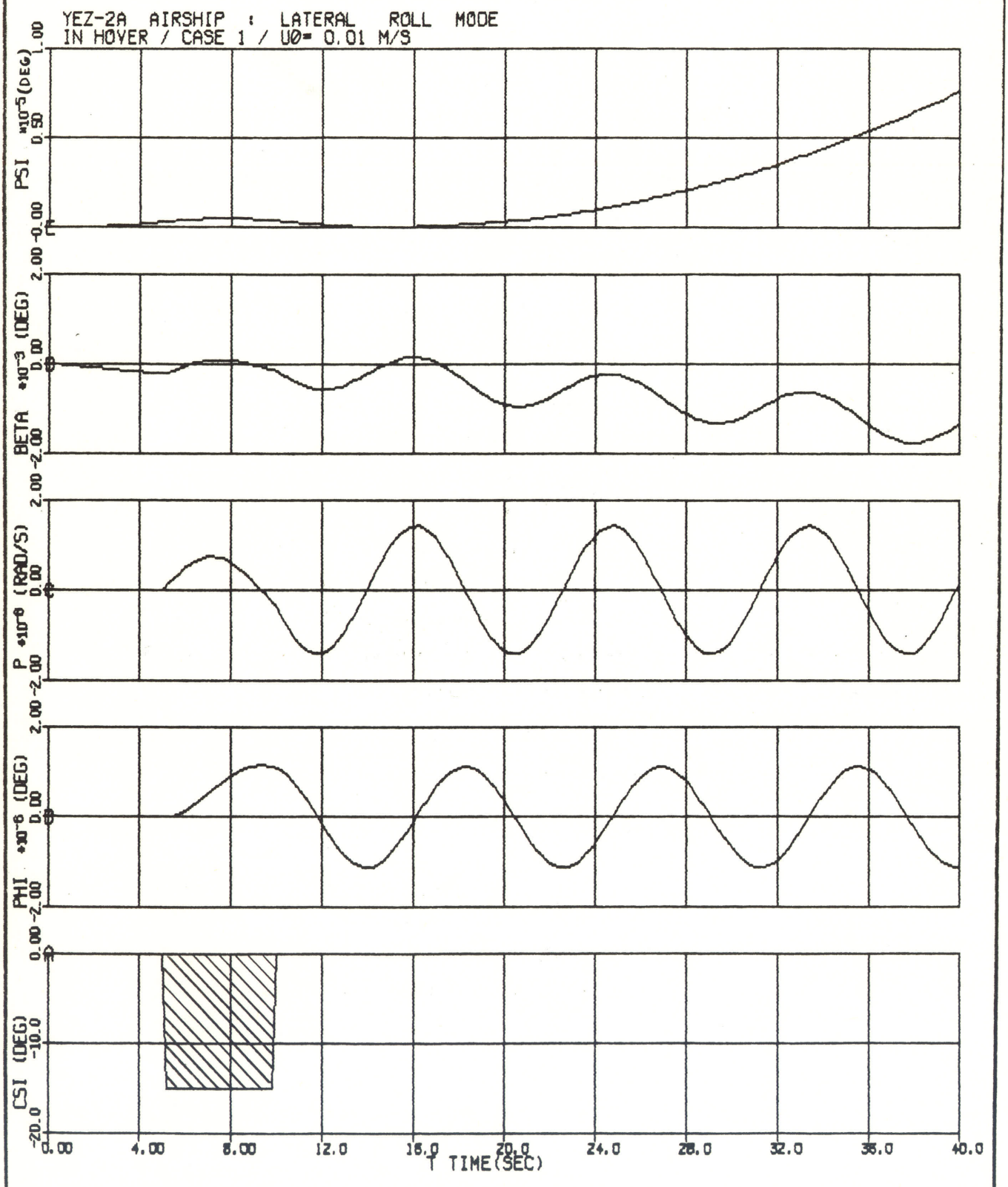
For the oscillatory mode, the experiment consisted in deflecting the four ruddervators in an aileron type of fashion, so as to give the vehicle a positive initial roll rate, of 15° for 5 seconds. The results are shown in Figure 5.12. The time period and damping ratio of the oscillation, if estimated from the Table A3.2.2 results, would be given by

$$T = 2\Pi/\omega = 2\Pi/0.727 \cong 8.6 \text{ seconds}$$
$$\zeta = 8.8 \times 10^{-5}$$

F I G U R E 5.11


YEZ-2A AIRSHIP : LATERAL YAW SUBSIDENCE
AND SIDESLIP SUBSIDENCE MODES IN HOVER /
CASE 1 / U0= 0.01 M/S
PHI *10^-3 (DEG)
1.00
0.00
-1.00
R *10^-4 (RAD/S)
1.00
0.50
0.00
BETA (DEG)
0.00
-10.0
-20.0
PSI *10^2 (DEG)
1.00
0.50
0.00
ZETA (DEG)
0.00
-15.0
-30.0
0.00
0.40
0.80
1.20
1.60
2.00
2.40
2.80
3.20
3.60
4.00
*10^4 TIME(SEC)

F I G U R E 5.12


YEZ-2A AIRSHIP : LATERAL ROLL MODE
IN HOVER / CASE 1 / U0= 0.01 M/S
PSI *10**-5 (DEG)
1.00
0.50
0.00
BETA *10**-3 (DEG)
2.00
0.00
-2.00
P *10**-6 (RAD/S)
2.00
0.00
-2.00
PHI *10**-6 (DEG)
2.00
0.00
-2.00
CSI (DEG)
0.00
-10.0
-20.0
0.00
4.00
8.00
12.0
16.0
20.0
24.0
28.0
32.0
36.0
40.0
T TIME(SEC)

These values appear to be appropriate in view of the results presented in Figure 5.12, including the fact that the amount of damping shown is negligible for all practical purposes, as predicted. In addition, the phase difference between the roll rate p and the roll angle ϕ is of the order of 90°, and v (or β) is in phase with p, as predicted in Figure A3.4.1 of Appendix-3. This type of motion can therefore be adequately described by the 'roll oscillation' denomination.

The roll oscillation is the lateral equivalent of the longitudinal pendulum oscillation and arises for similar reasons, i.e., the already mentioned metacentric height. However, as already shown by Figure 5.10, its frequency does not get lower with the increase of speed and only the damping ratio gets higher, in sharp contrast with what was shown for the longitudinal case. In addition, the lateral oscillatory mode is known to be excited whenever the airship starts a turn and under this light, the consideration of incorporating a roll damping feature in the Automatic Flight Control System acquires an added relevance in view of intended YEZ-2A primary mission.

* Flight Speed = 5 m/s:

For the forward flight condition, Table A3.2.4 of Appendix-3 gives the first eigenvalue as $s_1 = -0.0315$ and the second eigenvalue as $s_2 = -0.232$. The usual assumption of an exponential type of solution will yield the mode time constants as

$$s_1 = -1/\tau_{sideslip} \quad ===> \quad \tau_{sideslip} \cong 32 \text{ seconds}$$
$$s_2 = -1/\tau_{yaw} \quad ===> \quad \tau_{yaw} \cong 4.3 \text{ seconds}$$

In order to try to demonstrate these modes, two similar experiments were conceived. The first one, connected to the slow mode, consisted in deflecting the

ruddervators in a 'rudder to port' fashion of 15° for 150 seconds, after the airship had been flying in a trimmed condition for 10 seconds. The results are presented in Figure 5.13.

The second experiment, carried out in connection with the fast mode, consisted again in a rudder like ruddervator deflection of 15° for 20 seconds after the airship had been flying in a trimmed condition for 5 seconds only. The results are presented in Figure 5.14.

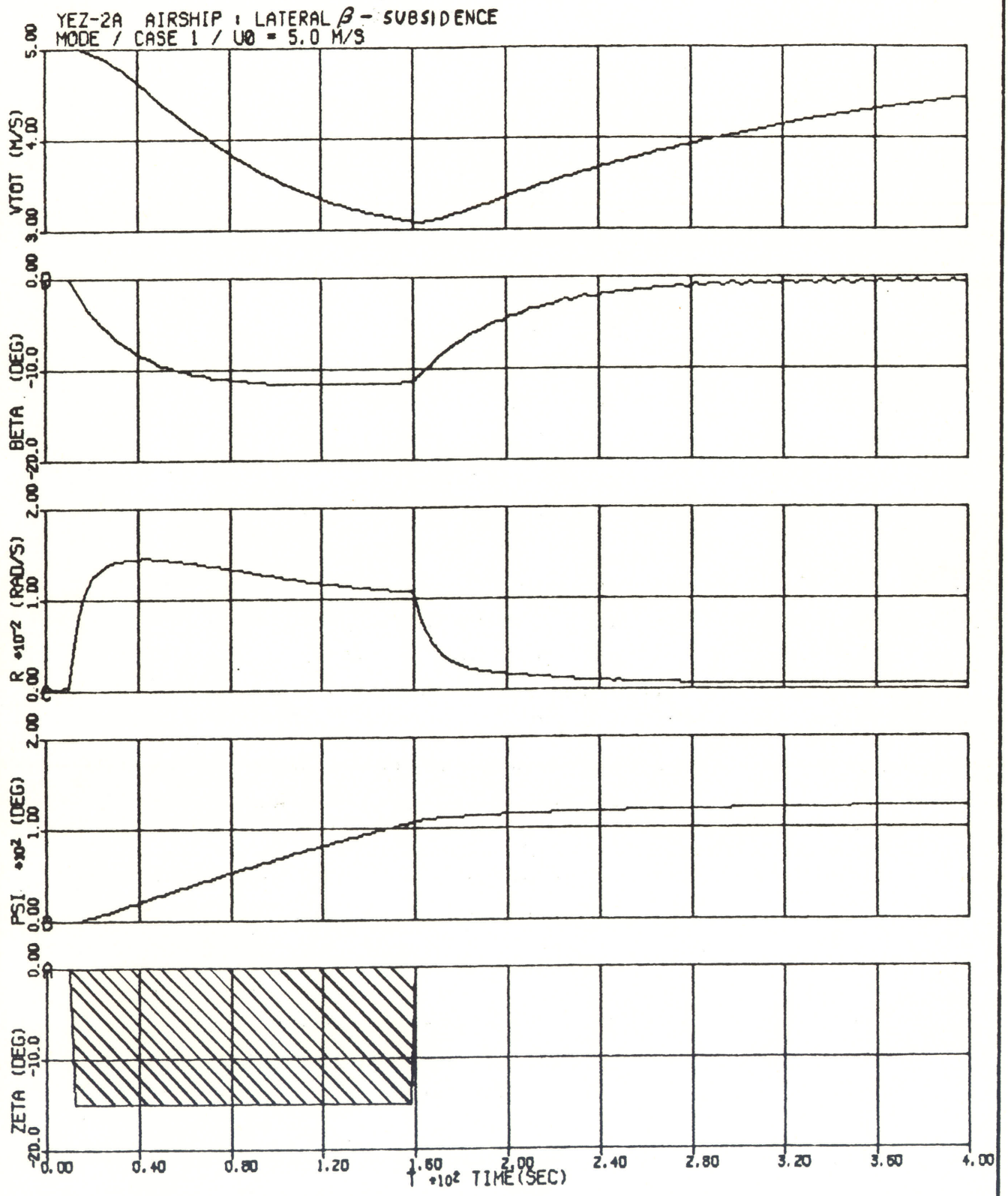
The analysis of both figures reveals that, in both situations, the sideslip angle β and the yaw rate r appear to follow an exponential law of convergence to their final steady state values. In addition, they both seem to have reached 63% of their final steady state values after a time interval that is reasonably close to their respective time constants. It was therefore concluded that the mode denominations of 'sideslip subsidence' and 'yaw subsidence' for the slow and fast subsidence modes respectively were adequate in describing their main characteristics.

Finally, in order to try to excite the lateral oscillatory mode, the experiment carried out consisted in deflecting the ruddervators in an 'aileron' type of fashion, so as to generate an initially positive roll rate r. They were deflected by 15° for 5 seconds and the results are presented as the set of strip plots of Figure 5.15. From Table A3.2.4 of Appendix-3, the anticipated mode time period and damping ratio would be given by

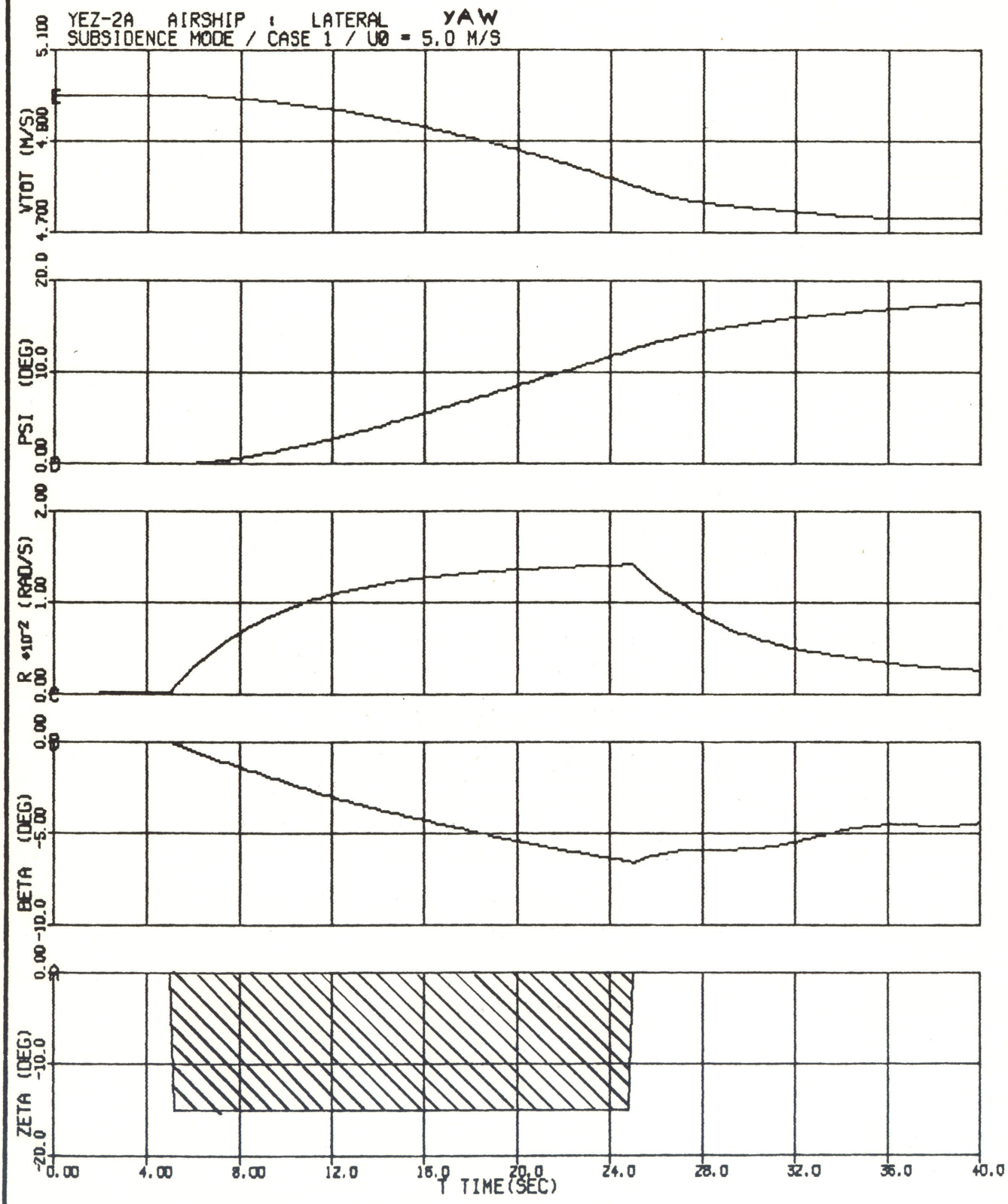
$$T = 2\Pi/\omega = 2\Pi/0.728 \cong 8.6 \text{ seconds}$$
$$\zeta = 0.044$$

These estimates appear to get a reasonable degree of confirmation from the results presented in Figure 5.15. The phase relations of Figure A3.4.2 (Appendix-3), i.e., a phase difference of 90° between the roll rate p and the roll angle ϕ, and p in phase with v (or sideslip angle

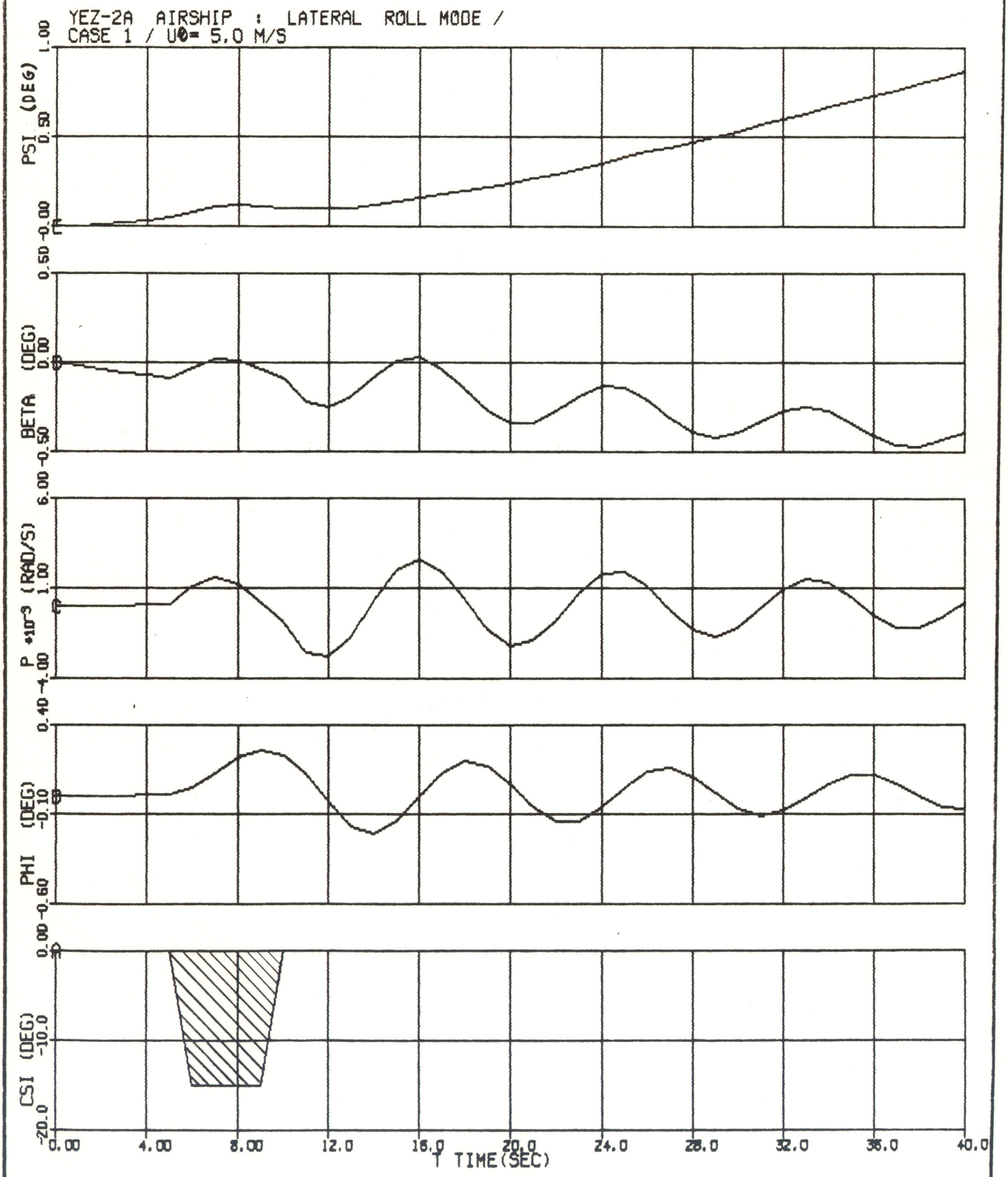
F I G U R E 5.13


YEZ-2A AIRSHIP : LATERAL β - SUBSIDENCE
MODE / CASE 1 / U0 = 5.0 M/S
VTOT (M/S)
5.00
4.00
3.00
BETA (DEG)
0.00
-10.0
-20.0
R *10^-2 (RAD/S)
2.00
1.00
0.00
PSI *10^2 (DEG)
2.00
1.00
0.00
ZETA (DEG)
0.00
-10.0
-20.0
0.00
0.40
0.80
1.20
1.60
2.00
2.40
2.80
3.20
3.60
4.00
*10^2 TIME(SEC)

F I G U R E 5.14


YEZ-2A AIRSHIP : LATERAL YAW
SUBSIDENCE MODE / CASE 1 / U0 = 5.0 M/S
VTOT (M/S)
5.100
4.800
4.700
PSI (DEG)
20.0
10.0
0.00
R *10^2 (RAD/S)
2.00
1.00
0.00
BETA (DEG)
0.00
-5.00
-10.0
ZETA (DEG)
0.00
-10.0
-20.0
0.00
4.00
8.00
12.0
16.0
20.0
24.0
28.0
32.0
36.0
40.0
T TIME(SEC)

F I G U R E 5.15


YEZ-2A AIRSHIP : LATERAL ROLL MODE /
CASE 1 / U0= 5.0 M/S
PSI (DEG)
1.00
0.50
0.00
BETA (DEG)
0.50
0.00
-0.50
P *10^-3 (RAD/S)
6.00
1.00
-4.00
PHI (DEG)
0.40
-0.10
-0.60
CSI (DEG)
0.00
-10.0
-20.0
0.00
4.00
8.00
12.0
16.0
20.0
24.0
28.0
32.0
36.0
40.0
T TIME(SEC)

β), are all reasonably confirmed in the results of the mode excitement experiment. It was therefore concluded that 'roll oscillation' was an adequate mode denomination.

5.4 Comparison and Concluding Remarks

The results presented in the previous Sections were aimed at providing a reasonable estimate of the open loop airship behaviour after longitudinal and lateral disturbances are encountered. In trying to draw comparisons with results published for other airships elsewhere, a fundamental difficulty is found due to the main fact that, as far as we are aware, there has never been an exactly similar effort directed towards unravelling airship modes and behaviour over the complete speed range of the vehicle as was the case here. What is found are results generated for only a particular speed or buoyancy condition, both in the case of flight test work as well as in the case of flight dynamics simulation work of the type here carried out.

If this difficulty is borne in mind, than some degree of comparison is possible with the results presented in the previous Sections. For easier reference, this was divided into two parts, the first one concerned with the results from other flight dynamics simulation work and the second part concerned with the small amount of flight test data available on this subject:

* Other Simulations

As pointed out in Chapter 1, the airship simulation work carried out at the University of Toronto Institute for Aerospace Studies (UTIAS) in the 70's until the mid-80's by J. DeLaurier and others, and that accomplished by various researchers at the Systems Technology Inc. (STI) company of California, USA, stand as the fundamental landmarks in this field. At the

College of Aeronautics, the work carried out by J. Lipscombe, although not formally published, was found particularly useful since it was aimed at the same objectives as those of this Chapter.

The DeLaurier stability and modes investigation (Ref. 14) concentrated on three airship types, the ZR-1, the ZR-4 and an inverted Y-tail blimp. The first two were rigid airships built before World War II with slenderness ratios of 6.0 or higher. The late 50's blimp design is consequently the one that most resembles the YEZ-2A characteristics.

Although DeLaurier's investigation was carried out for only one flight speed (the maximum in each case), his results for the blimp show a general agreement with those produced here for the YEZ-2A in the open-loop condition. The three longitudinal and the three lateral modes identified by him are qualitatively very similar to those detected for the YEZ-2A and only the phase relation between the u and the θ eigenvectors in the pendulum oscillation mode show some noticeable disagreement with our results. In the lateral case there is no substantial qualitative difference.

The results for the other rigid airships show significant differences when compared to those produced for the YEZ-2A, and this only reinforces the general feeling that each design configuration needs to be assessed separately.

The STI investigation (Ref. 22) consisted in a flight dynamics simulation model developed specifically for the Skyship-500 airship, aimed at checking out some of the flight test results obtained by STI during their participation in the PACE Skyship-500 flight test program (Ref. 6). Although the investigation was not directed towards stability and modes as in our case, concentrating rather more on the input/output relations resulting from frequency sweeps of both elevator an rudder types of command input, the resulting predictions for the angular

frequencies and damping ratios of the longitudinal and lateral oscillatory modes at the 25 Knots sped condition agree remarkably well with the YEZ-2A estimated values. In particular, the estimated values of ω_{roll} = 1.0 rad/s and ζ_{roll} = 0.11 for the angular frequency and damping ratio of the roll oscillation of the Skyship-500 are of the same order of magnitude as those anticipated for the YEZ-2A in Tables A3.2.8 and A3.2.10 (Appendix-3). Considering that the flight test results are plotted alongside the STI simulation predictions, and the clear similarities (e.g., slenderness ratio, hull shape) and differences (e.g., hull volume, tail configuration, total mass) between the YEZ-2A and SKS-500 designs, it appears that the YEZ-2A simulation is at least pointing towards some realistic direction.

Finally, J. Lipscombe's work (Ref. 55) was aimed at identifying airship modes of motion. It was based on a thorough theoretical analysis of the Jacobian matrix derived from the airship equations of motion, and it served as the starting point for the investigation which was presented in the previous Sections. However, due to the limited amount of reliable airship aerodynamic data available when it was carried out, the numerical results produced in the course of that work were very few. In this way, it was basically the characterization of the modes of motion, without even the benefits of the eigenvector analysis as presented here in Appendix-3, that were the fruits of this work. That mode characterization checked extremely well against the results of the present investigation.

* Flight Test

The only results taken from the PACE report (Ref. 6) that are directly relevant to the YEZ-2A stability and modes investigation are the detection of the longitudinal pendulum mode at approximately 0.3-0.4 rad/s and the lateral roll oscillation at 1.1 rad/s. Both figures are

for the 40 Knots flight speed regime, and the YEZ-2A corresponding results (Table A3.2.11-12 of Appendix-3) are 0.12 rad/s and 0.74 rad/s.

Therefore, if other differences are momentarily ignored, such as environmental conditions and location of the measuring instrumentation inside the Skyship-500, it appears that the YEZ-2A has slower modes than the Skyship-500. Considering the size and mass differences between both ships, this is a result that was to be intuitively expected.

Finally, in analysing the results presented in the previous Sections, two important points have to be remembered:

i. All the results presented were based on the established system of body axes, as introduced in Chapter 3. Therefore, the modes of motion here described were referenced to the Centre of Buoyancy (CB) of the YEZ-2A, and not to the Centre of Gravity (CG) as is usually the case in conventional aircraft work. As already pointed out, the longitudinal and lateral oscillatory modes do not occur about axes going through the CG (for further details see Ref. 22) and it was felt therefore that no loss of accuracy would result in staying with the set body axes system.

ii. As already remarked, it is believed that the investigation here presented is reasonably thorough and complete. In particular, it detected the change of characteristics of the longitudinal pendulum oscillation with the increase in flight speed, of which no previous published record was found.

In conclusion, it can be said that the definitive confirmation of these two points will only be possible

when further airship flight testing is carried out. However, the points raised here can be used as a starting point for the required investigation.

6. RESPONSE TO CONTROLS

6.1 Introduction

The purpose of this Chapter is to present the results of the investigation carried out with the objective of assessing the YEZ-2A's response to various types of control inputs. The inputs considered were, first, of the aerodynamic control type, i.e., the ruddervators were made to deflect in an elevator fashion and then in a rudder fashion, and the second type of input considered was that associated with power controls, i.e., thrust changes.

The response to these inputs was achieved by setting the appropriate parameters to the desired values of input in the command file of the ACSL flight dynamics simulation. The responses obtained, i.e., the time histories of the relevant flight parameters were then plotted using the ACSL graphics package. On some occasions, when the results of more than one run had to be combined then several ACSL output files were, after some careful manipulation, imported into a spread sheet software (SuperCalc 4), where the relevant results were suitably plotted.

For easier reference, the small catalogue of responses obtained as a result of the investigation is presented in the next Sections in accordance with the type of input that was used. Part of the investigation was also devoted to assessing the sensitivity to changes in the input amplitude, and the associated results are presented in the same Section of the relevant type of input, and to changes in the flight speed. The latter results are presented in a separate Section. The closing Section presents some brief conclusions and compares some of the results obtained with the small amount of published flight test data available for the Syship-500 airship.

6.2 Elevator Type of Input

The purpose of this part of the response investigation was to assess the behaviour of the airship once an elevator type of input was applied and then withdrawn. The short term as well as the medium to long term behaviour were felt to be of interest, and therefore the simulation run had to be sufficiently long in order to be able to show both the initial transient regime of the response as well as the ultimate steady state values assumed by the relevant flight parameters.

As the elevator type of input is the one directly responsible for the longitudinal airship response, the flight parameters that were selected as the relevant ones for this investigation were as follows:

η (Eta)	=	Angle of ruddervator deflection (all four) in degrees
θ (Theta)	=	Airship pitch angle in degrees
q	=	Airship pitch rate in rad/s
V_{Tot}	=	Total flight speed in m/s
w	=	Velocity along the OZ body axis in m/s
Height	=	Airship height above the ground in m
N_{CB}	=	Load factor with respect to the Centre of Buoyancy in g (gravitational acceleration)

In order to try and achieve a more thorough understanding of airship behaviour, two types of response experiments were carried out. The first had a small amplitude type of input and the second was aimed at investigating the large response type of behaviour. The initial flight speed was kept the same in both instances as well as the flight condition (masses, inertias and environmental conditions) so as to afford the required comparison. The results obtained were as follows:

* Small Perturbation

For an initial flight speed of 25 m/s, Case 1 (ISA,

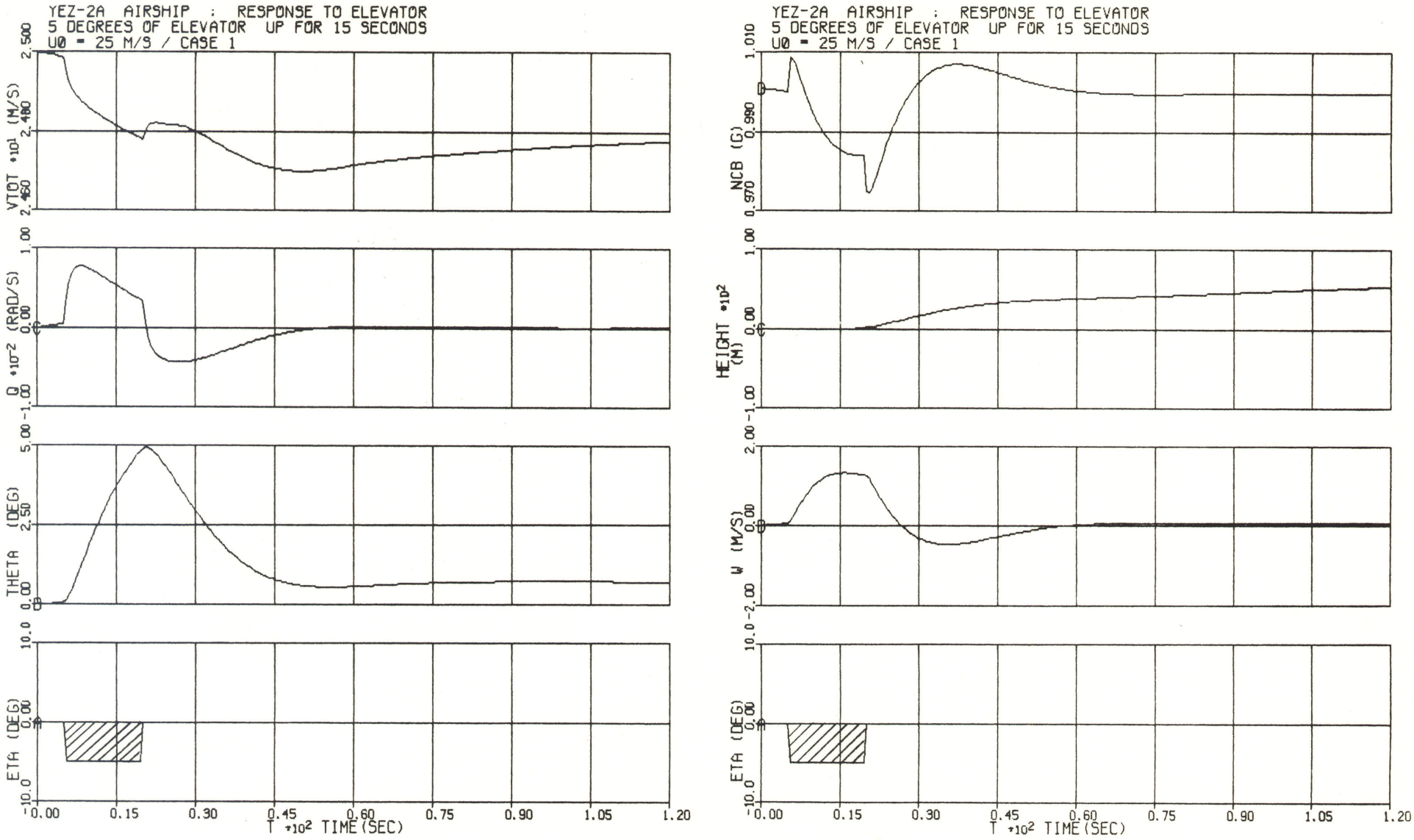
sea level, neutral buoyancy condition), with the airship flying level in a trimmed condition, an input of 5° of elevator up was applied during 15 seconds and then withdrawn. The results, for a total simulation run time of 120 seconds are shown in Figure 6.2.1.

The physical interpretation of the ACSL strip plot results is that the vehicle attitude angle slowly increased (nose up) up to 5°, with a corresponding drop in flight speed, a barely perceptible variation in the vertical load factor N_{CB} and a slow but steady increase in height. Upon removal of the input the airship nose went down, but did not reach quite the same attitude as before the application of the input. A residual θ value of about 1° remained, which implied a very low climb rate and very slow speed recovery. The load factor value returned to 1.0.

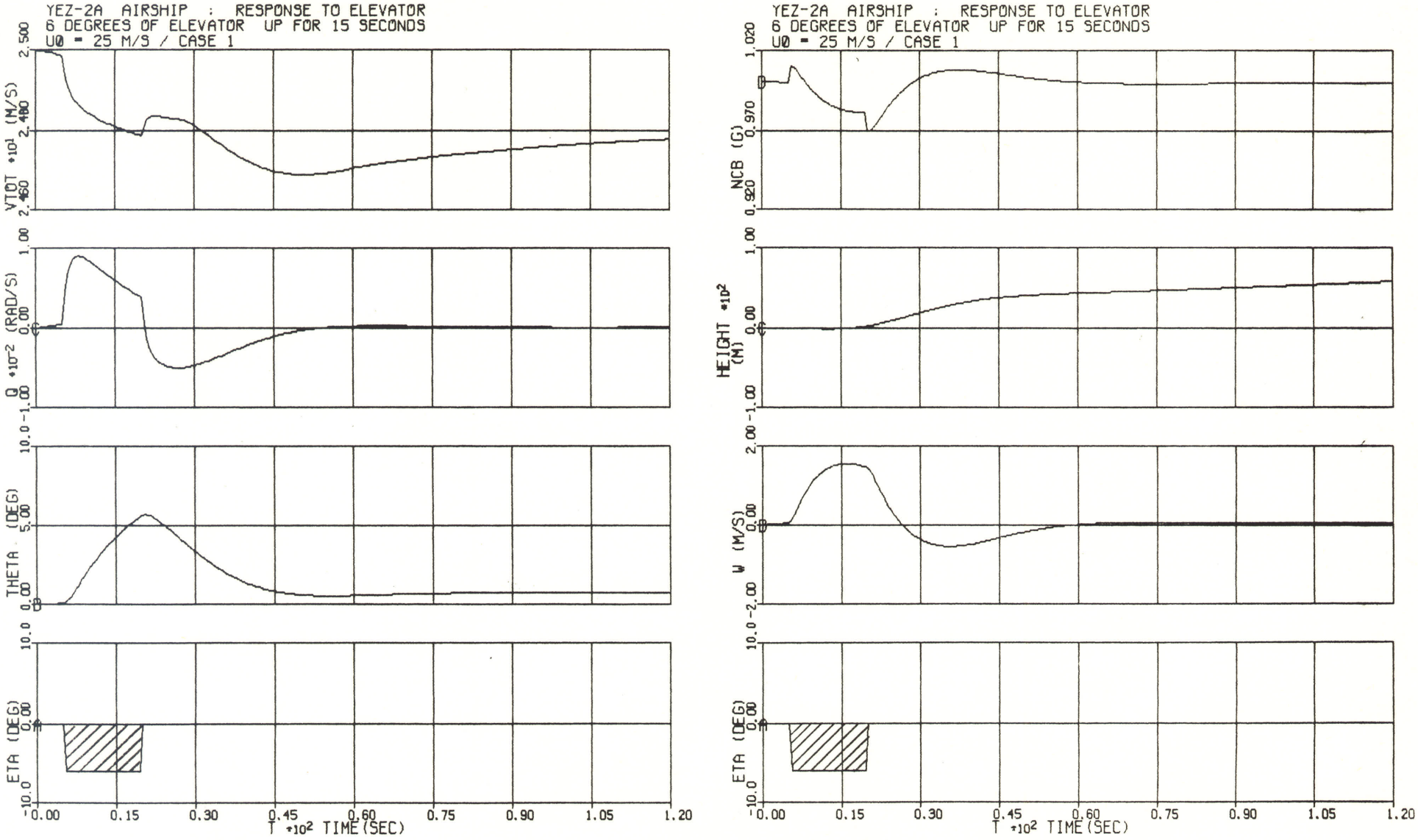
It is interesting to observe the behaviour of the pitch rate q throughout the exercise: A new pitch rate value was quickly acquired, in an approximate exponential fashion, as a result of the application of the elevator input, a result that is not surprising in view of the pitch subsidence mode described in the previous Chapter. Control removal brought it back to zero with approximately the same time constant as for the control application. Although the time constant value is different from that of general aviation aircraft, the type of q versus time curve obtained bears many similarities.

In order to assess the sensitivity to small perturbations, another simulation run was carried out, with exactly the same value for the initial conditions, except that now the elevator input applied was of 6°, rather than 5°. The results are shown in Figure 6.2.2.

The parameter that seemed to be most affected by the input amplitude increase was the pitch angle θ, which went up to nearly 6°, showing therefore a direct, nearly linear relationship between control input and vehicle


YEZ-2A AIRSHIP : RESPONSE TO ELEVATOR
5 DEGREES OF ELEVATOR UP FOR 15 SECONDS
U0 = 25 M/S / CASE 1
VTOT *10¹ (M/S)
Q *10⁻² (RAD/S)
THETA (DEG)
ETA (DEG)
T *10² TIME (SEC)
YEZ-2A AIRSHIP : RESPONSE TO ELEVATOR
5 DEGREES OF ELEVATOR UP FOR 15 SECONDS
U0 = 25 M/S / CASE 1
NCB (G)
HEIGHT *10²
(M)
W (M/S)
ETA (DEG)
T *10² TIME (SEC)

F I G U R E 6.2.1


YEZ-2A AIRSHIP : RESPONSE TO ELEVATOR
6 DEGREES OF ELEVATOR UP FOR 15 SECONDS
U0 = 25 M/S / CASE 1
VTOT *10¹ (M/S)
2.500
2.480
2.460
Q *10⁻² (RAD/S)
1.00
0.00
-1.00
THETA (DEG)
10.0
5.00
0.00
ETA (DEG)
10.0
0.00
-10.0
0.00
0.15
0.30
0.45
0.60
0.75
0.90
1.05
1.20
T *10² TIME (SEC)
YEZ-2A AIRSHIP : RESPONSE TO ELEVATOR
6 DEGREES OF ELEVATOR UP FOR 15 SECONDS
U0 = 25 M/S / CASE 1
NCB (G)
1.020
0.970
0.920
HEIGHT *10²
(M)
1.00
0.00
-1.00
W (M/S)
2.00
0.00
-2.00
ETA (DEG)
10.0
0.00
-10.0
0.00
0.15
0.30
0.45
0.60
0.75
0.90
1.05
1.20
T *10² TIME (SEC)

F I G U R E 6.2.2

response. The general nature of the response remained essentially the same and all the other parameters show time histories which are similar to the previous case.

The variation in the vertical velocity w is more apparent now, in the sense that it is positive at first and then slowly goes negative as initially demanded. The interpretation of this type of behaviour is that the application of elevator up generates a negative lift at the tail of the vehicle, which in turn makes it go down a few metres before climbing. This behaviour can barely be detected in the Height versus time plot.

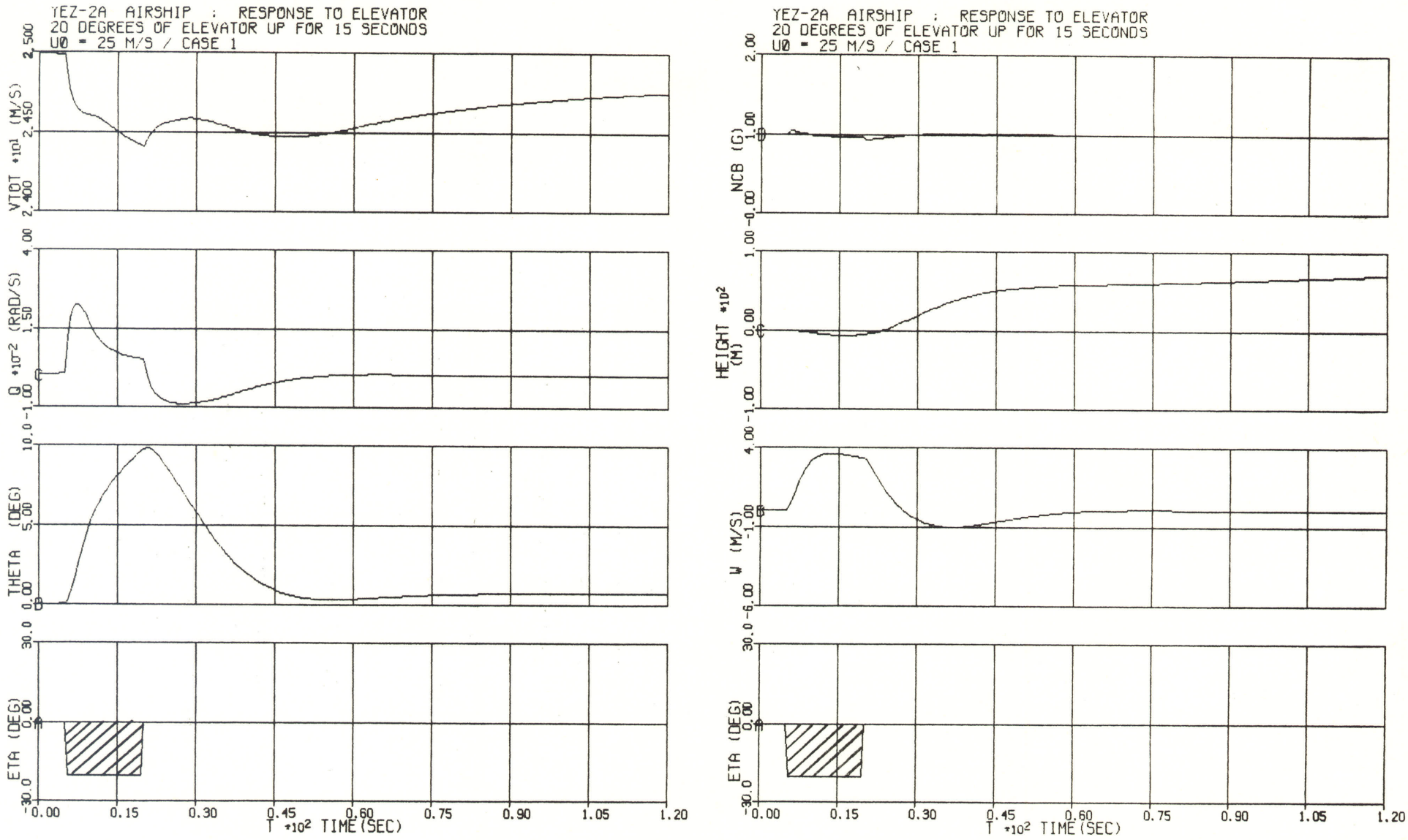
* Large Response

For an initial flight speed of 25 m/s, Case 1 (ISA, sea level, neutral buoyancy condition), with the airship flying level in a trimmed condition, an input of 20° of elevator up was applied during 15 seconds and then withdrawn. The results, for a total simulation run time of 120 seconds are shown in Figure 6.2.3.

Although the general shape of the vehicle response is the same as in the small perturbation case, there are now some marked differences. The pitch rate q decay, whilst the input was being applied, now has a nearly exponential type of behaviour, rather than the linear one shown previously. The maximum pitch angle θ, reached after 15 seconds, is only just under half of the applied input. The loss of height, immediately after control application, is now much more pronounced.

In summary, it appears that the large amplitude input has resulted in non-linear vehicle response. This airship characteristic has been known for some time, but it is only the type of investigation here presented that helps to quantify this aspect of lighter-than-air flight dynamics.

The large response sensitivity issue was tackled by running another simulation experiment with exactly the same initial conditions, except that now the input was

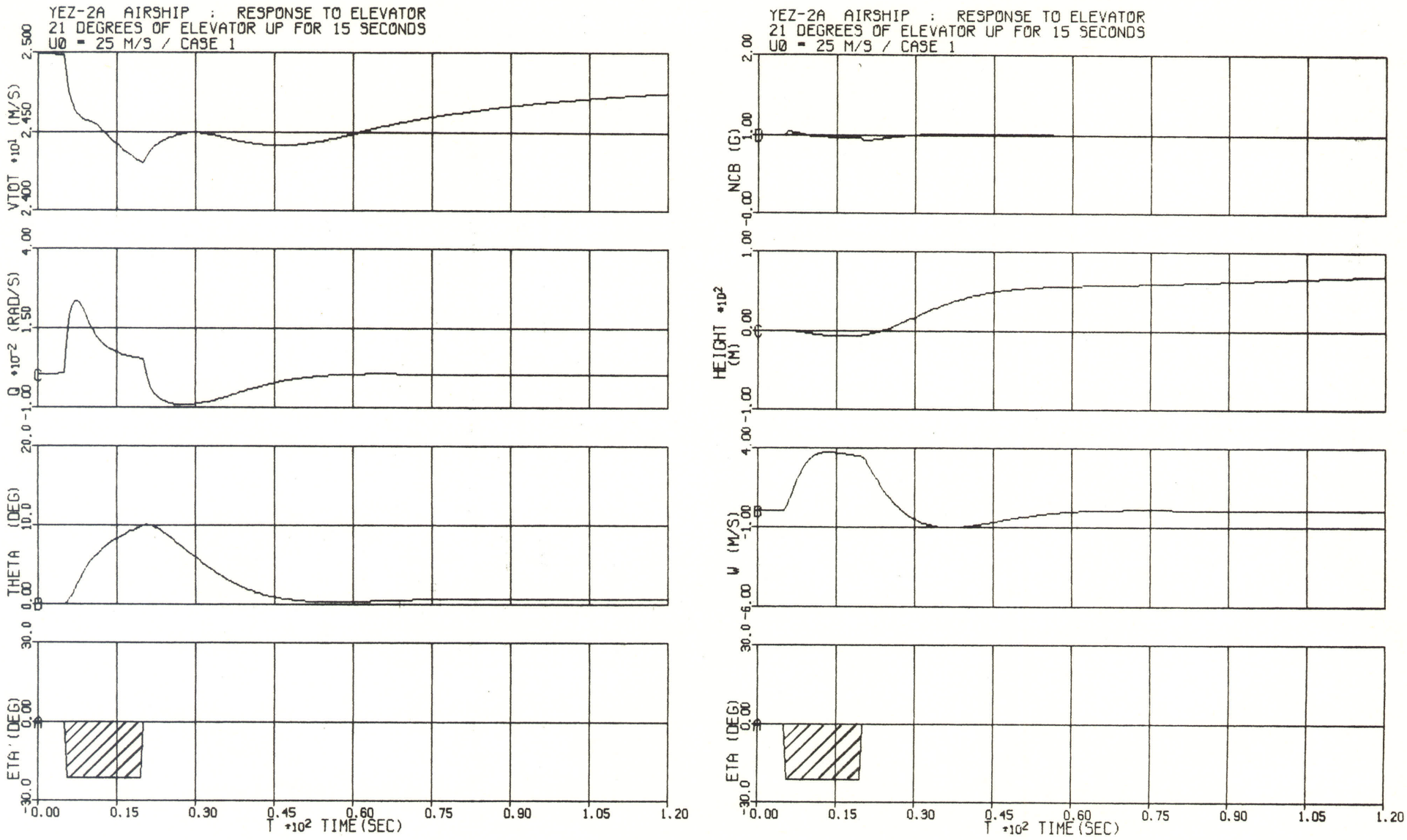

YEZ-2A AIRSHIP : RESPONSE TO ELEVATOR
20 DEGREES OF ELEVATOR UP FOR 15 SECONDS
U0 = 25 M/S / CASE 1
VTOT *10¹ (M/S)
2.500
2.450
2.400
Q *10⁻² (RAD/S)
4.00
1.50
-1.00
THETA (DEG)
10.0
5.00
0.00
ETA (DEG)
30.0
0.00
-30.0
0.00
0.15
0.30
0.45
0.60
0.75
0.90
1.05
1.20
T *10² TIME(SEC)
YEZ-2A AIRSHIP : RESPONSE TO ELEVATOR
20 DEGREES OF ELEVATOR UP FOR 15 SECONDS
U0 = 25 M/S / CASE 1
NCB (G)
2.00
1.00
-0.00
HEIGHT *10² (M)
1.00
0.00
-1.00
W (M/S)
4.00
-1.00
-6.00
ETA (DEG)
30.0
0.00
-30.0
0.00
0.15
0.30
0.45
0.60
0.75
0.90
1.05
1.20
T *10² TIME(SEC)

F I G U R E 6.2.3

changed to 21°of elevator up. The results thus obtained are presented in Figure 6.2.4 and it appears that when these are compared with the previous results the changes are small indeed, i.e., a 1° of input change goes practically unnoticed in the large amplitude regime.

In trying to better visualize the airship response to both the small perturbation and the large response cases, as well as the sensitivity investigation results, some of the results from the four simulation runs were combined in a single graph, which shows the airship trajectory during each run. This is shown in Figure 6.2.5. It can be seen that the sensitivity to input change is more pronounced in the small amplitude case than in the large response. As expected, although the climb gradient is the same in all cases after input removal, it is much steeper in the large amplitude case. The slight surprise was the final height reached in the 21° of elevator input case being a shadow inferior to the 20° case. Although this can easily be seen to have been caused by the larger negative lift generated at the early stages of control application, which made the vehicle sink further down in the former case, it is ultimately a demonstration of the non-linear characteristics of the response in the large amplitude condition.

Finally, this first part of the longitudinal response investigation was concluded by trying to assess the tracking response of the YEZ-2A. In order to achieve that, a simulation run was carried out in which after an initial flight in trimmed conditions, Case 1, with an initial speed of 25 m/s, an elevator input ramp of 0.25° per second was applied over 100 seconds, so that at the end of the run the maximum allowable control deflection angle would have been reached. The results are shown in Figure 6.2.6, where as expected, the input with a linear rate of increase generated a slow exponential type of response for most flight parameters.


YEZ-2A AIRSHIP : RESPONSE TO ELEVATOR
21 DEGREES OF ELEVATOR UP FOR 15 SECONDS
U0 = 25 M/S / CASE 1
VTOT *10¹ (M/S)
Q *10⁻² (RAD/S)
THETA (DEG)
ETA (DEG)
T *10² TIME(SEC)
YEZ-2A AIRSHIP : RESPONSE TO ELEVATOR
21 DEGREES OF ELEVATOR UP FOR 15 SECONDS
U0 = 25 M/S / CASE 1
NCB (G)
HEIGHT *10² (M)
W (M/S)
ETA (DEG)
T *10² TIME(SEC)

F I G U R E 6.2.4

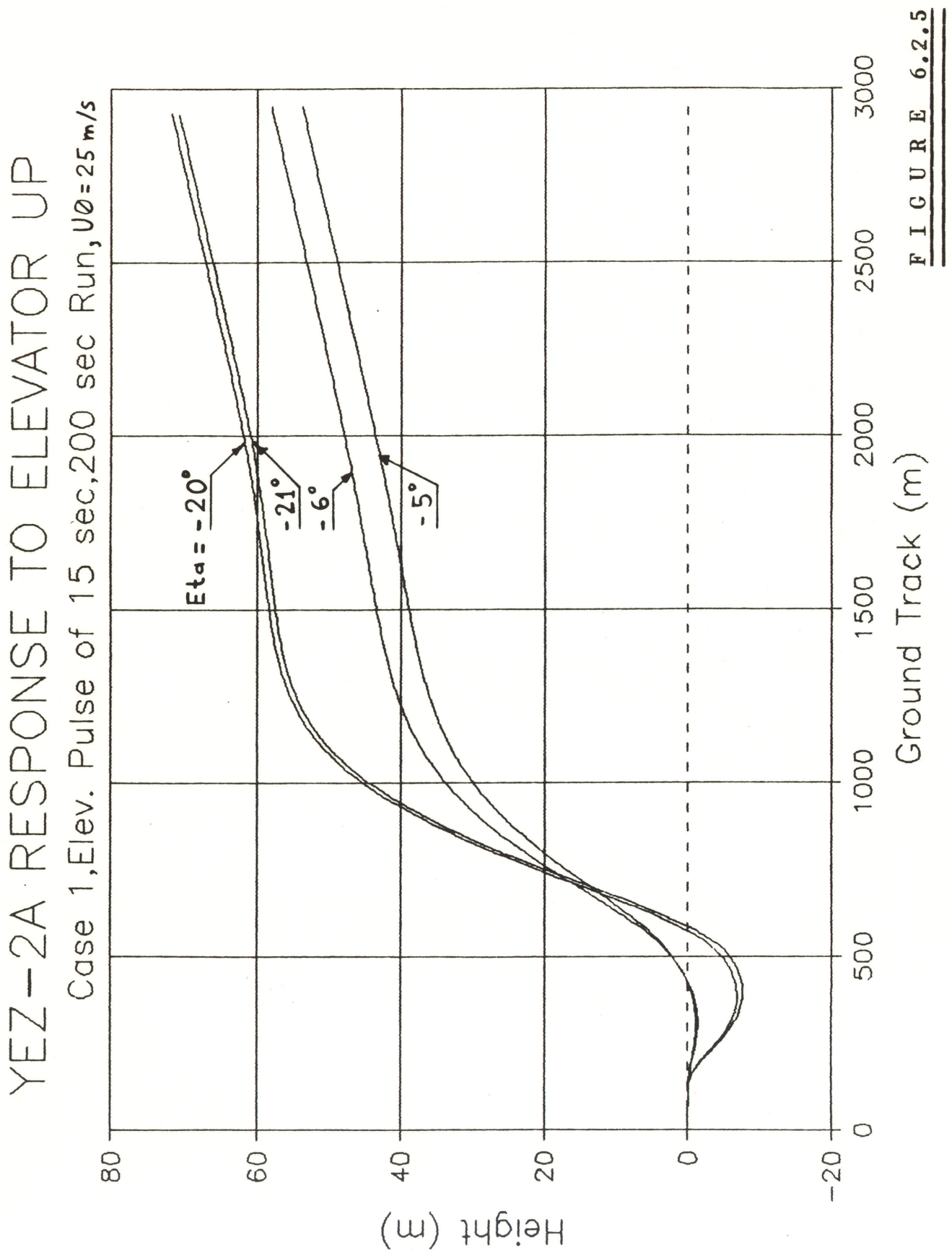
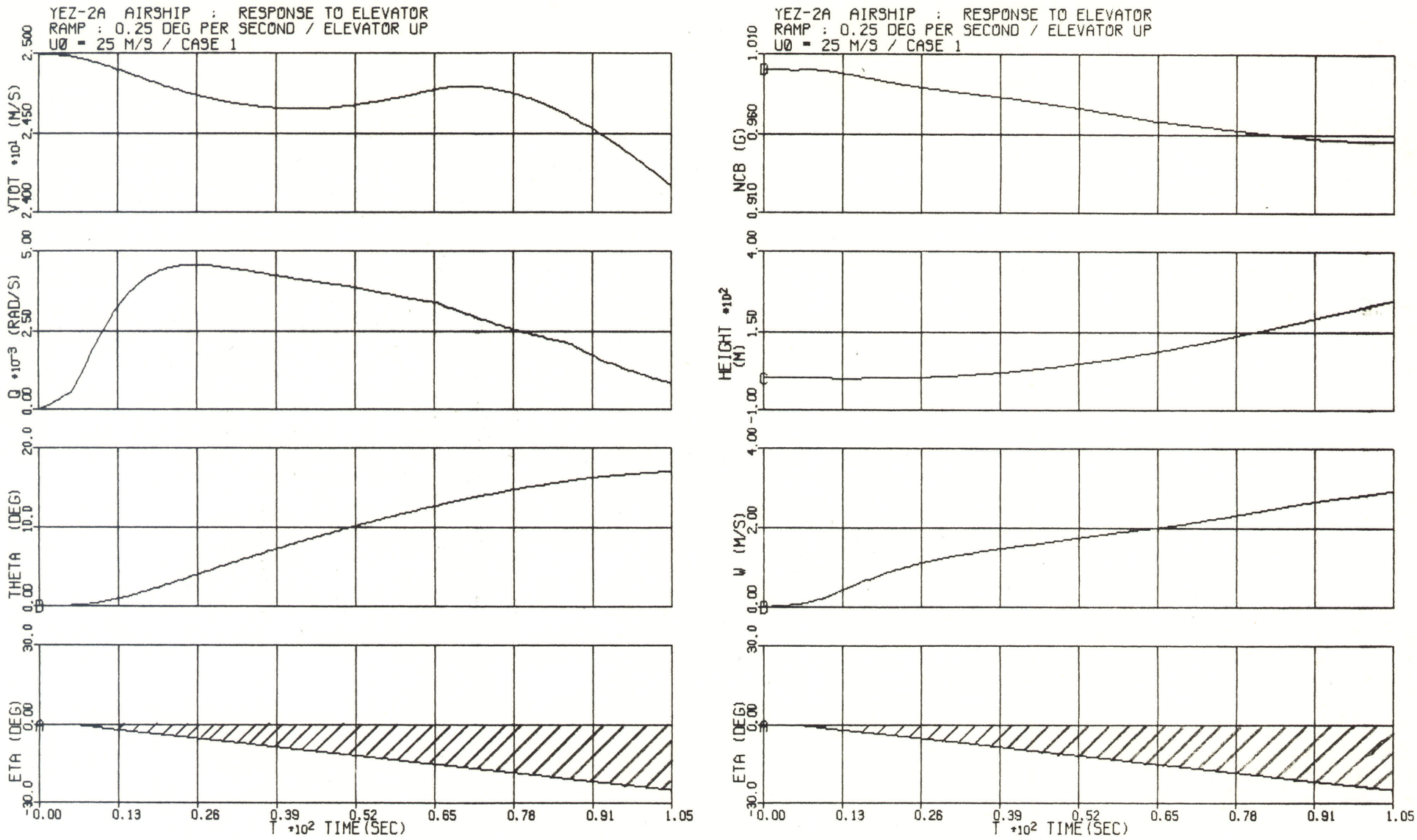

YEZ-2A RESPONSE TO ELEVATOR UP
Case 1,Elev. Pulse of 15 sec,200 sec Run, U0=25 m/s
Eta = -20°
-21°
-6°
-5°
Height (m)
80
60
40
20
0
-20
0
500
1000
1500
2000
2500
3000
Ground Track (m)

FIGURE 6.2.5


YEZ-2A AIRSHIP : RESPONSE TO ELEVATOR
RAMP : 0.25 DEG PER SECOND / ELEVATOR UP
U0 = 25 M/S / CASE 1
VTOT *10¹ (M/S)
Q *10⁻³ (RAD/S)
THETA (DEG)
ETA (DEG)
NCB (G)
HEIGHT *10² (M)
W (M/S)
T *10² TIME (SEC)
0.00
0.13
0.26
0.39
0.52
0.65
0.78
0.91
1.05

F I G U R E 6.2.6

The time histories of input elevator angle and the pitch angle θ are further plotted in Figure 6.2.7, where it can be seen that the time lag between input and output stays more or less constant up to about 8°, after which it increases exponentially. In other words, the pitch angle is said to 'track' behind the elevator deflection angle by a constant time lag up to about 8°, characterizing therefore a region of approximately linear type of response. After that, the region of non-linear response behaviour is reached, and the tracking time lag increases exponentially, so that at the extreme control surface deflection angle it has nearly reached infinity.

6.3 Rudder Type of Input

The purpose of this second part of the response investigation was to assess the behaviour of the airship once a rudder type of input was applied and then withdrawn. The short term as well as the medium to long term behaviour were felt to be of interest, and therefore the simulation run, just like in the previous longitudinal case, had to be sufficiently long in order to be able to show both the initial transient regime of the response as well as the ultimate steady state values assumed by the relevant flight parameters.

As the rudder type of input is the one directly responsible for the lateral airship response, the flight parameters that were selected as the relevant ones for this investigation were the following:

ζ (Zeta)	=	Angle of ruddervator deflection (all four) in degrees
ψ (Psi)	=	Airship pitch angle in degrees
r	=	Airship yaw rate in rad/s
β (Beta)	=	Airship sideslip angle in degrees
ϕ (Phi)	=	Airship bank angle in degrees
p	=	Airship roll rate in rad/s
u	=	Velocity along the OX body axis in m/s

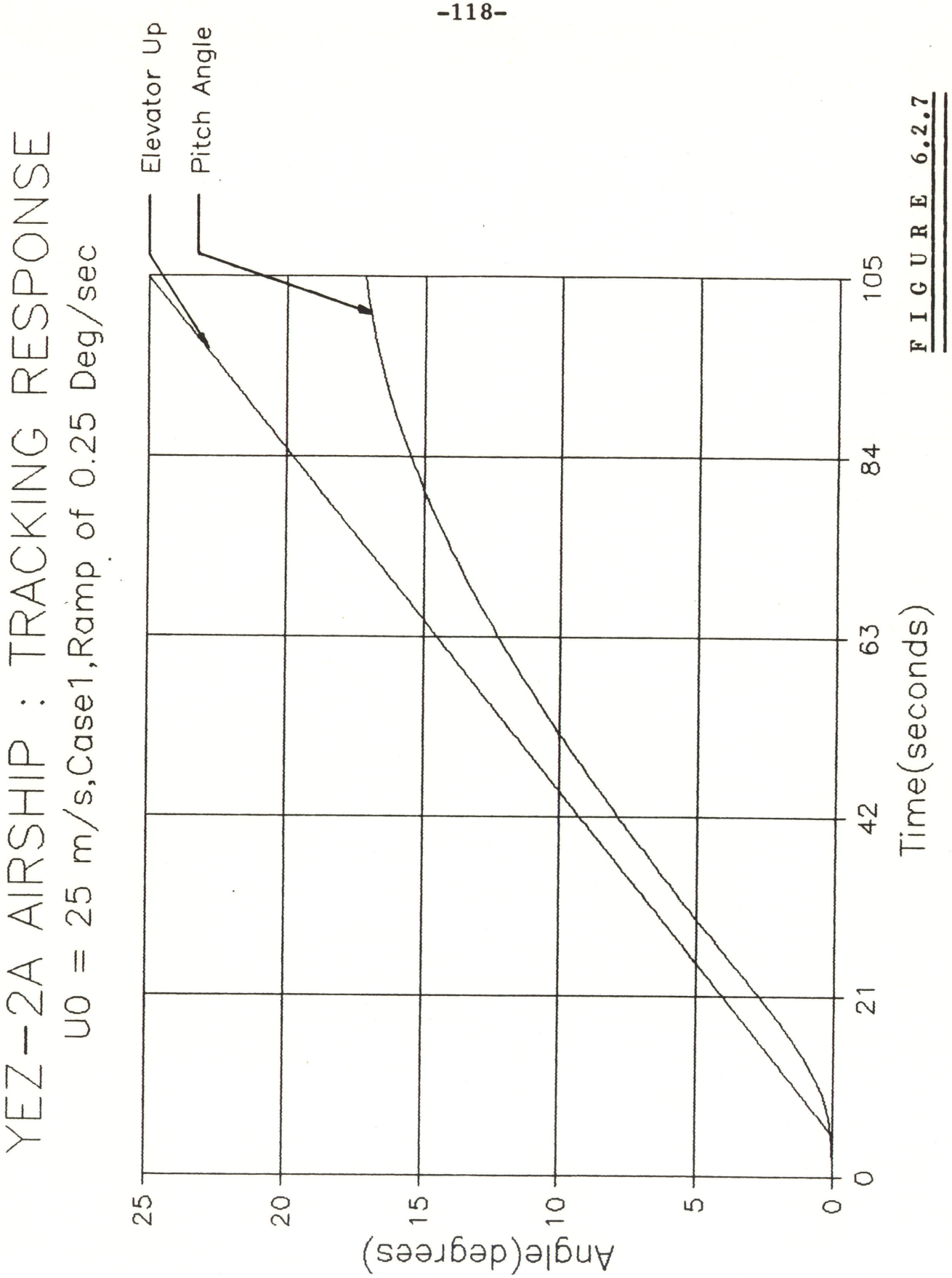

YEZ-2A AIRSHIP : TRACKING RESPONSE
U0 = 25 m/s,Case1,Ramp of 0.25 Deg/sec
Elevator Up
Pitch Angle
Angle(degrees)
25
20
15
10
5
0
0
21
42
63
84
105
Time(seconds)

FIGURE 6.2.7

As in the lateral case, two types of response experiments were carried out. The first had a small amplitude type of input and the second was aimed at investigating the large response type of behaviour. The initial flight speed was kept the same in both instances as well as the flight Case (masses, inertias and environmental conditions) so as to afford the required comparison. The results obtained were as follows:

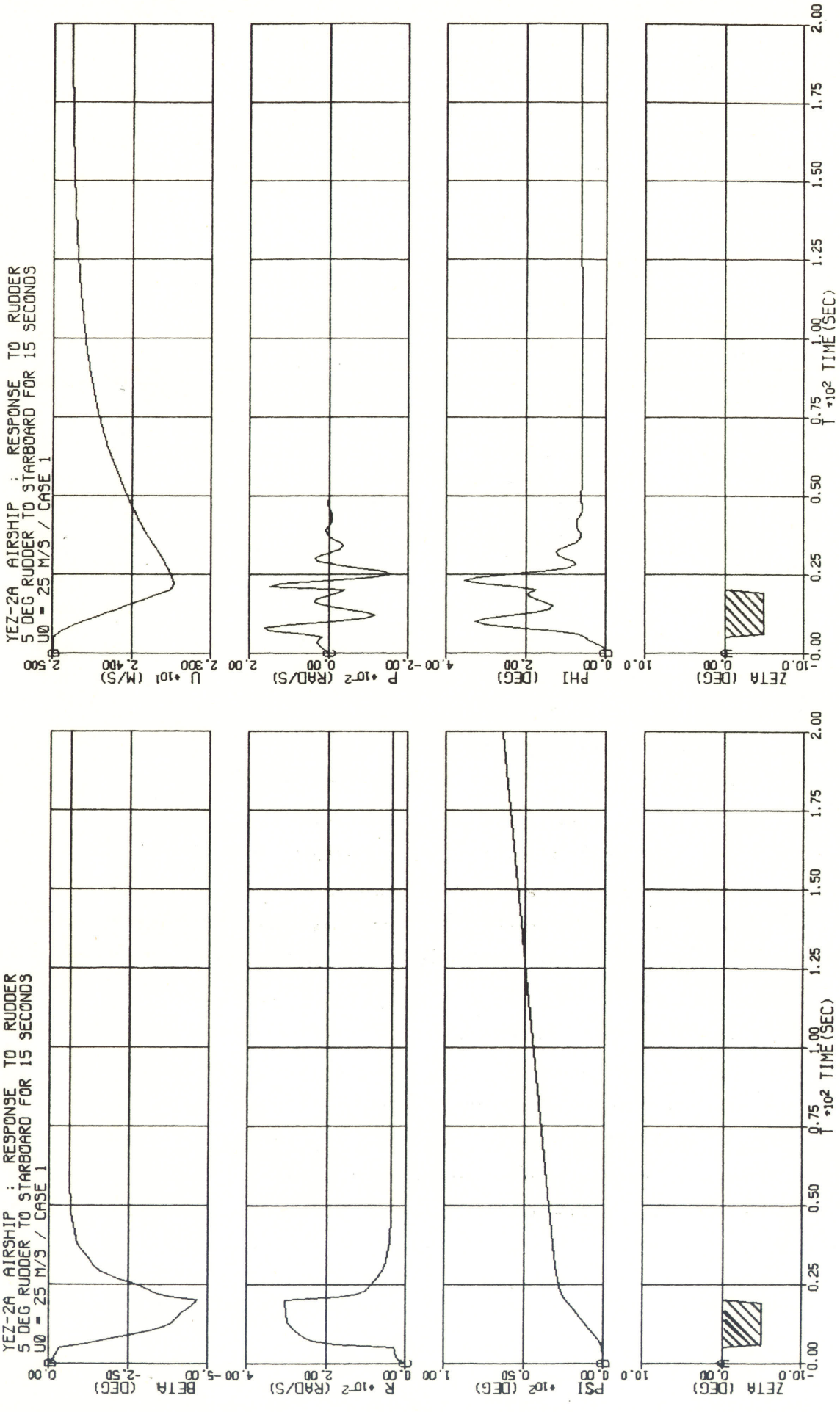
* Small Perturbation

For an initial flight speed of 25 m/s, Case 1 (ISA, sea level, neutral buoyancy condition), with the airship flying level in a trimmed condition, an input of 5° of rudder to starboard side was applied during 15 seconds and then removed. The results, for a total simulation run time of 200 seconds are shown in Figure 6.3.1.

It can be seen that, as expected, a new yaw rate r value was reached very quickly (the fast yaw subsidence mode shown in the previous Chapter), whereas the sideslip angle response was comparatively slower, with β_{max} having reached just under 5°. It is interesting to note that the initiation of the turn excited the roll oscillation mode, and a peak bank angle of just over 3° was reached. It should also be noted that these results show that a residual turn rate existed before control application. This merely reflects the fact that the wind tunnel gathered data had some residual side force and yawing moment even at the β = 0 condition, a fact that probably occurs even for the full size airship, as perfect longitudinal plane symmetry is virtually unattainable.

After control removal, the residual yaw rate ensures that a relatively steady turn will follow unless checked by another rudder input.

The sensitivity aspects of the lateral response were investigated by running the simulation once again, but this time increasing the rudder input to 6° of deflection


YEZ-2A AIRSHIP : RESPONSE TO RUDDER
5 DEG RUDDER TO STARBOARD FOR 15 SECONDS
U0 = 25 M/S / CASE 1
U *10¹ (M/S)
P *10⁻² (RAD/S)
PHI (DEG)
ZETA (DEG)
T *10² TIME (SEC)
YEZ-2A AIRSHIP : RESPONSE TO RUDDER
5 DEG RUDDER TO STARBOARD FOR 15 SECONDS
U0 = 25 M/S / CASE 1
BETA (DEG)
R *10⁻² (RAD/S)
PSI *10² (DEG)
ZETA (DEG)
T *10² TIME (SEC)

F I G U R E 6.3.1

to the starboard side. The results are shown in Figure 6.3.2. It can be seen that β_{max} has reached just under 6° now, with all the other flight parameters exhibiting slightly increased maximum values, but essentially the same kind of behaviour.

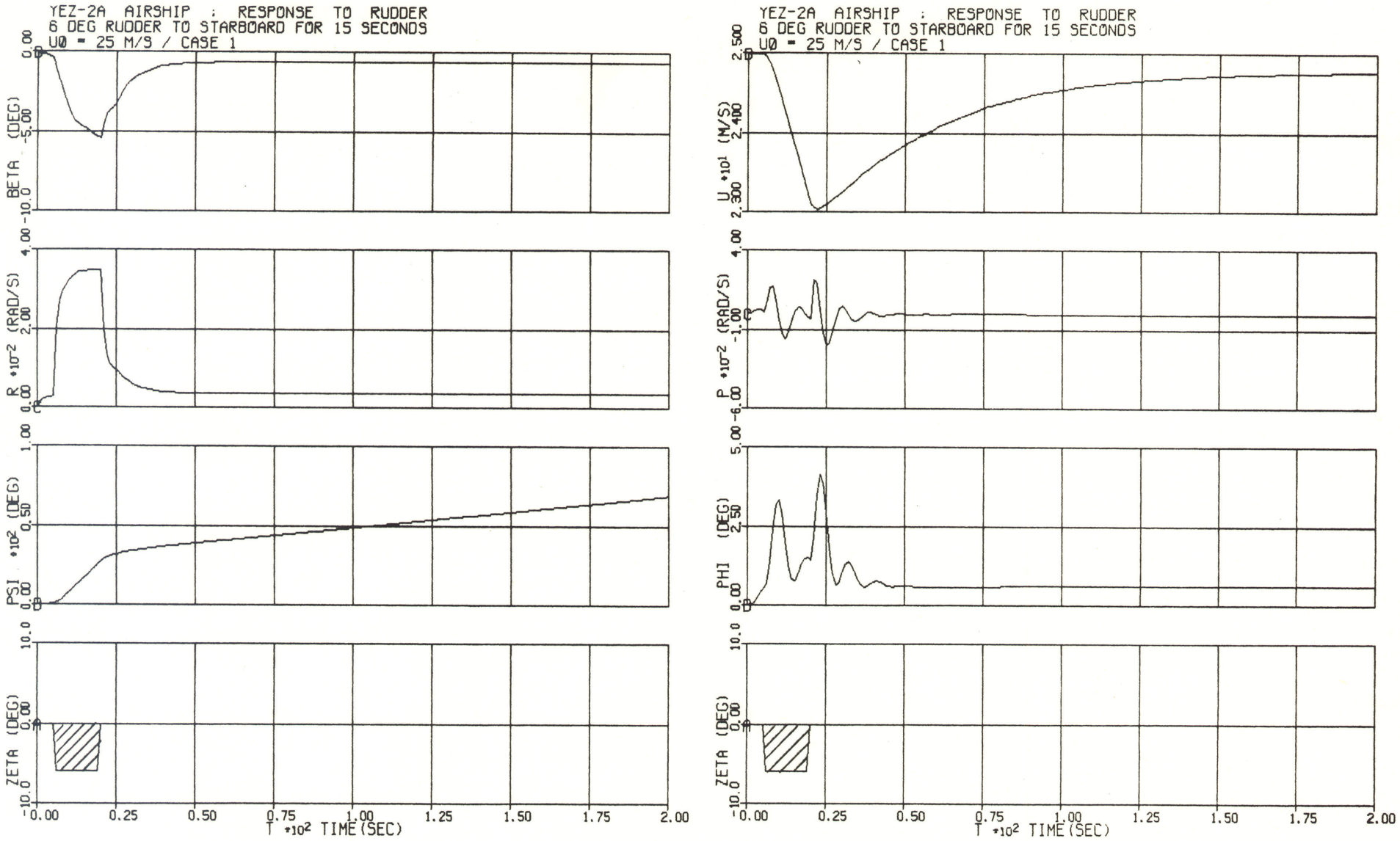
* Large Response

For an initial flight speed of 25 m/s, Case 1 (ISA, sea level, neutral buoyancy condition), with the airship flying level in a trimmed condition, an input of 20° of rudder to the starboard side was applied during 15 seconds and then removed. The results, for a total simulation run time of 200 seconds are shown in Figure 6.3.3.

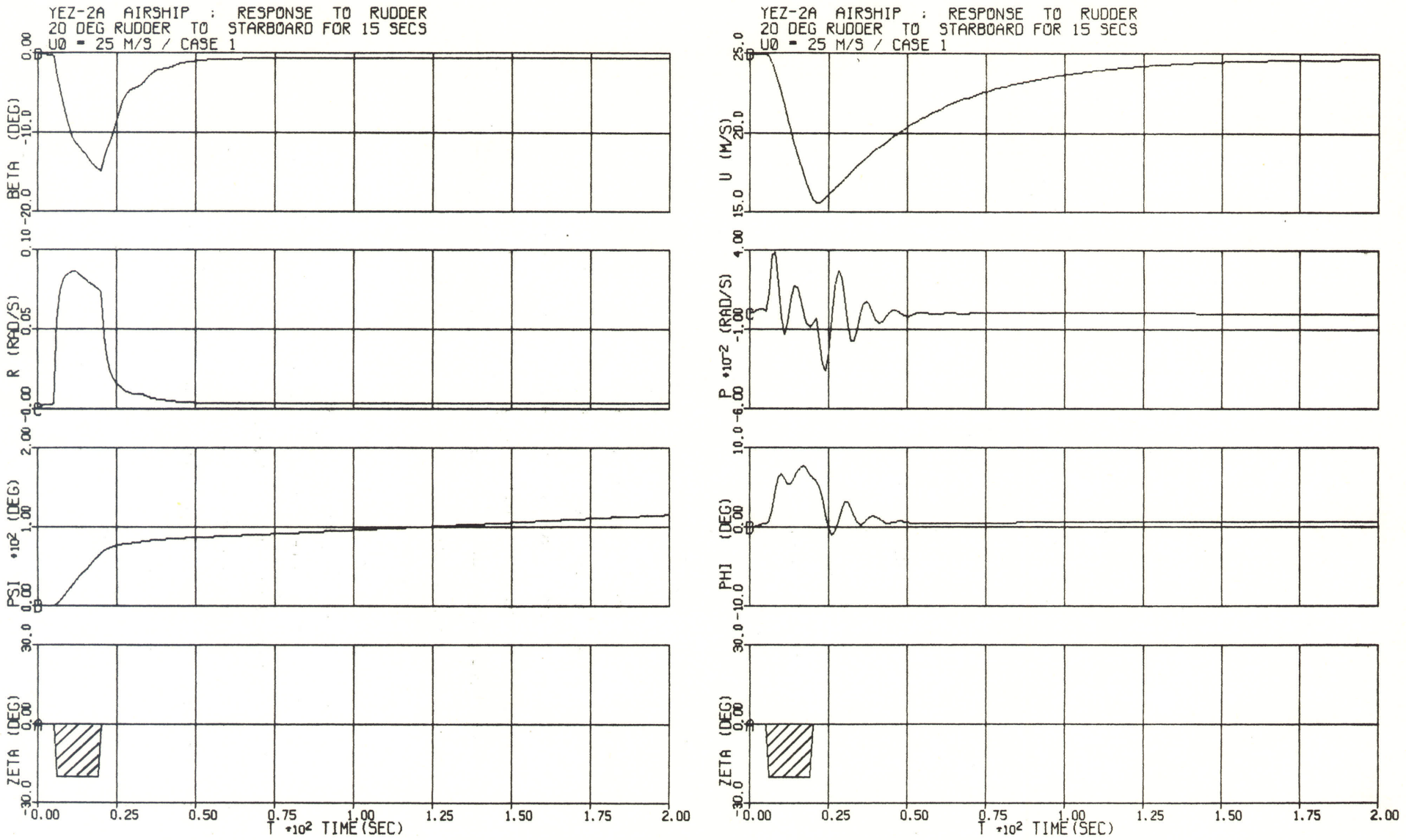
Although as in the longitudinal case, the general shape of the vehicle response is the same as in the small perturbation case, there are now some marked differences. The yaw rate r behaviour, whilst the input was being applied, now has a nearly linear type of decay law, rather than the constant value one previously seen. The maximum sideslip angle β, reached after 15 seconds, is now much lower than that of the applied input. The peak bank angle ϕ reached during control application, has now more than doubled.

In summary, it appears that the large amplitude input has resulted, just like in the longitudinal case, in a non-linear type of vehicle response being exhibited.

The large response sensitivity issue was tackled by running another simulation experiment with exactly the same initial conditions, except that now the input was changed to 21° of rudder to the starboard side. The results thus obtained are presented in Figure 6.3.4 and it appears that when these are compared with the previous results the changes are small indeed, i.e., a 1° of input change goes practically unnoticed in the large amplitude regime. Particularly noticeable is the β_{max} value which appears to have remained the same.


YEZ-2A AIRSHIP : RESPONSE TO RUDDER
6 DEG RUDDER TO STARBOARD FOR 15 SECONDS
U0 = 25 M/S / CASE 1
BETA (DEG)
R *10-2 (RAD/S)
PSI *10² (DEG)
ZETA (DEG)
T *10² TIME(SEC)
YEZ-2A AIRSHIP : RESPONSE TO RUDDER
6 DEG RUDDER TO STARBOARD FOR 15 SECONDS
U0 = 25 M/S / CASE 1
U *10¹ (M/S)
P *10-2 (RAD/S)
PHI (DEG)
ZETA (DEG)
T *10² TIME(SEC)

F I G U R E 6.3.2


YEZ-2A AIRSHIP : RESPONSE TO RUDDER
20 DEG RUDDER TO STARBOARD FOR 15 SECS
U0 = 25 M/S / CASE 1
BETA (DEG)
R (RAD/S)
PSI *10² (DEG)
ZETA (DEG)
U (M/S)
P *10⁻² (RAD/S)
PHI (DEG)
T *10² TIME(SEC)

F I G U R E 6.3.3

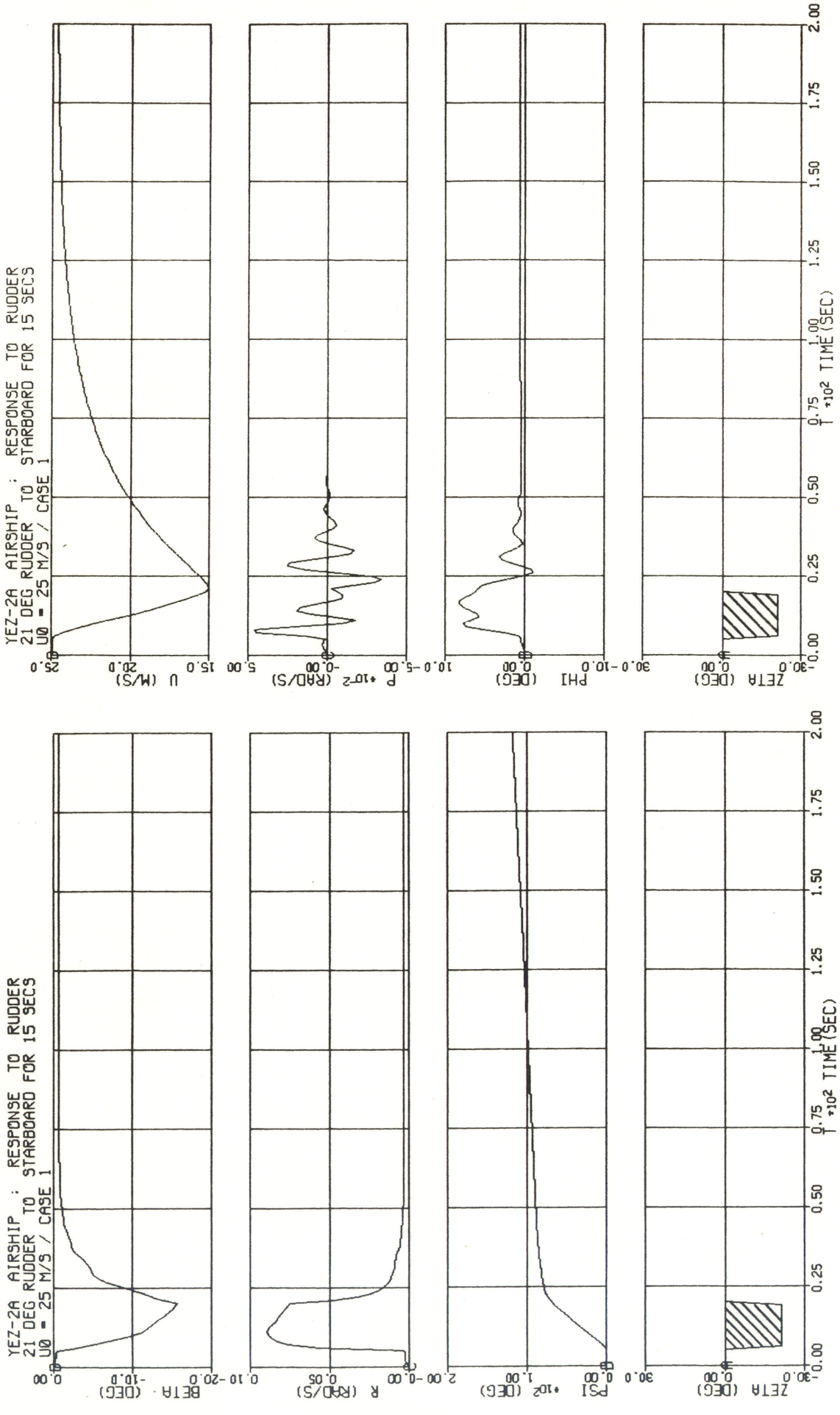

YEZ-2A AIRSHIP : RESPONSE TO RUDDER
21 DEG RUDDER TO STARBOARD FOR 15 SECS
U0 = 25 M/S / CASE 1
U (M/S)
P *10^-2 (RAD/S)
PHI (DEG)
ZETA (DEG)
T *10^2 TIME(SEC)
YEZ-2A AIRSHIP : RESPONSE TO RUDDER
21 DEG RUDDER TO STARBOARD FOR 15 SECS
U0 = 25 M/S / CASE 1
BETA (DEG)
R (RAD/S)
PSI *10^2 (DEG)
ZETA (DEG)
T *10^2 TIME(SEC)

FIGURE 6.3.4

In trying to better visualize the airship response to both the small perturbation and the large response cases, as well as the sensitivity investigation results, some of the results from the four simulation runs were combined in a single graph, which shows the airship trajectory during each run. As in this case it was lateral airship behaviour that was being investigated, the trajectory consists in the horizontal plane plot of the vehicle position, assuming that the initial condition is a north bound flight. This is shown in Figure 6.3.5.

As in the longitudinal case, it can be seen that the sensitivity to input change is more pronounced in the small amplitude regime than in the large response one although, as expected, the turn gradient is much larger in the large amplitude case.

Finally, this first part of the lateral response investigation was concluded by trying to assess the tracking response of the YEZ-2A. In order to achieve that, a simulation run was carried out in which after an initial flight in trimmed conditions, Case 1, with an initial speed of 25 m/s, a rudder input ramp of 0.25° per second was applied over 100 seconds, so that at the end of the run the maximum allowable control deflection angle would have been reached. The results are shown in Figure 6.3.6, where as expected, the input with a linear rate of increase generated a slow exponential type of response for most flight parameters. The roll behaviour in particular shows some interesting characteristics as it appears that once the control application starts, the already existing rolling tendency (due to the slightly untrimmed lateral condition) is first checked and then increased in the same direction. Then an oscillatory period follows, after which the positive rolling tendency only increases with the growing control input amplitude.

The time histories of input rudder angle and the corresponding sideslip angle β are further plotted in

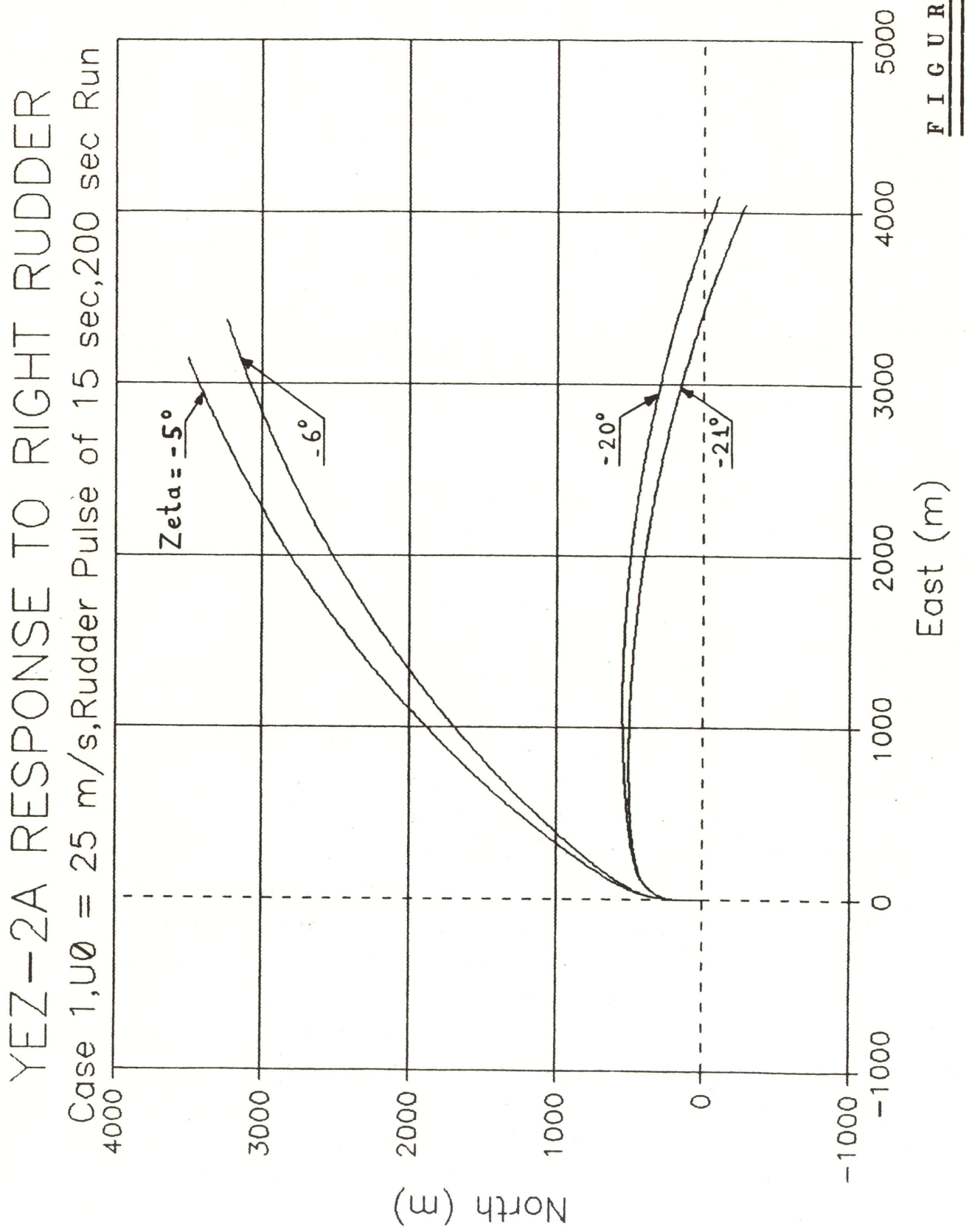

YEZ-2A RESPONSE TO RIGHT RUDDER
Case 1,U0 = 25 m/s,Rudder Pulse of 15 sec,200 sec Run
Zeta=-5°
-6°
-20°
-21°
North (m)
East (m)
4000
3000
2000
1000
0
-1000
-1000
0
1000
2000
3000
4000
5000

FIGURE 6.3.5

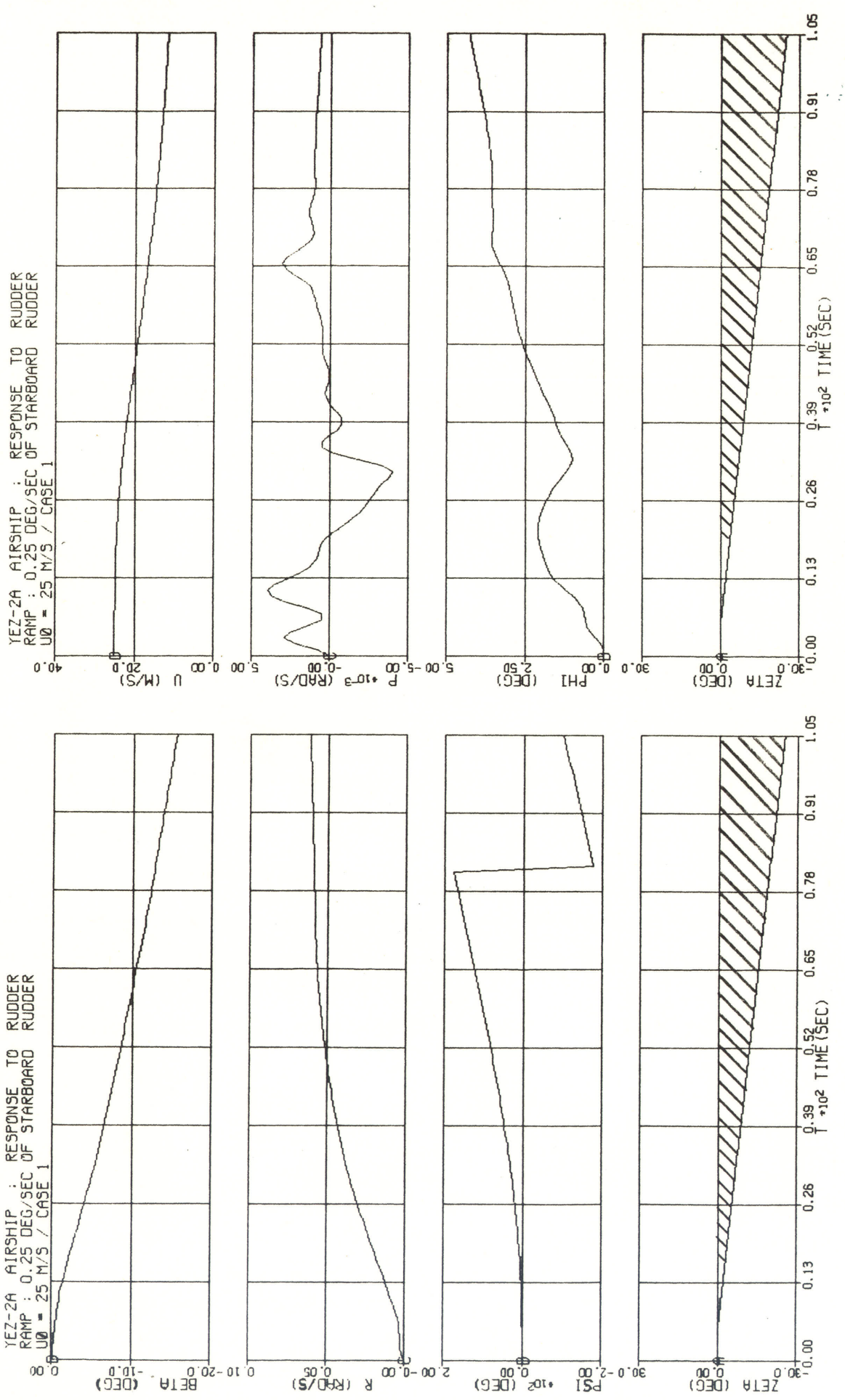

YEZ-2A AIRSHIP ; RESPONSE TO RUDDER
RAMP ; 0.25 DEG/SEC OF STARBOARD RUDDER
U0 = 25 M/S / CASE 1
U (M/S)
P *10-3 (RAD/S)
PHI (DEG)
ZETA (DEG)
T *10² TIME (SEC)
YEZ-2A AIRSHIP ; RESPONSE TO RUDDER
RAMP ; 0.25 DEG/SEC OF STARBOARD RUDDER
U0 = 25 M/S / CASE 1
BETA (DEG)
R (RAD/S)
PSI *10² (DEG)
ZETA (DEG)
T *10² TIME (SEC)

FIGURE 6.3.6

Figure 6.3.7, where, as in the longitudinal case, the response parameter (β) is shown to track behind the input (ζ). The region of constant time lag between input and output is, however, much smaller now and after about 4° of control input the time lag grows in an approximate exponential fashion, so that at the extreme rudder input angle it is getting close to infinity.

In summary, therefore, it appears that the region of non-linear behaviour for the airship starts much sooner in the lateral case than in the longitudinal case.

6.4 Response to Thrust Change

As the power control is the third type of control input available in the YEZ-2A airship, the last part of the response investigation was devoted to assessing the impact of thrust changes. As in the previous work reported, three types of input control law were successively tried out and their results carefully recorded. The first was a small step of increase on the trimmed value of engine thrust, the second was a large step of increase and the third was a ramp type of increase on the originally trimmed thrust value.

The first case started with the airship flying in a trimmed condition, Case 1 (ISA, sea level, neutral buoyancy), with an initial flight speed of 25 m/s. Then a step of increase of 10% above the trimmed thrust value was applied for 15 seconds and then removed. The simulation run was allowed to run for 120 seconds and the results obtained are presented in Figure 6.4.1. As thrust changes affect mainly the longitudinal motion of the vehicle, the chosen flight parameters were the same as for the longitudinal response investigation.

It can be seen that the effects of this small change in thrust result in the same pattern of response as for the elevator type of input. The magnitude of the changes in the flight parameters is however much smaller now, and the final steady state values that are obtained after the

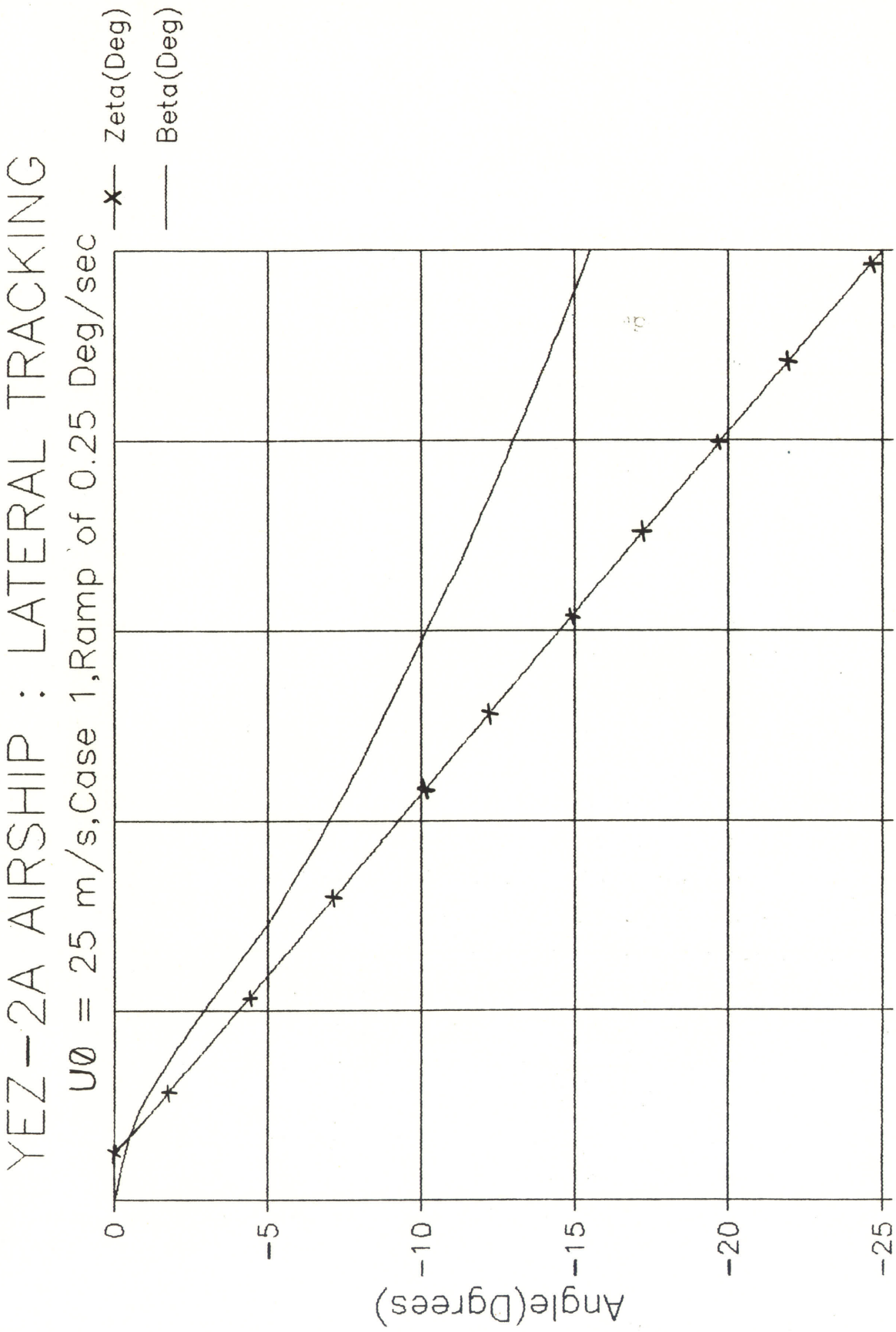
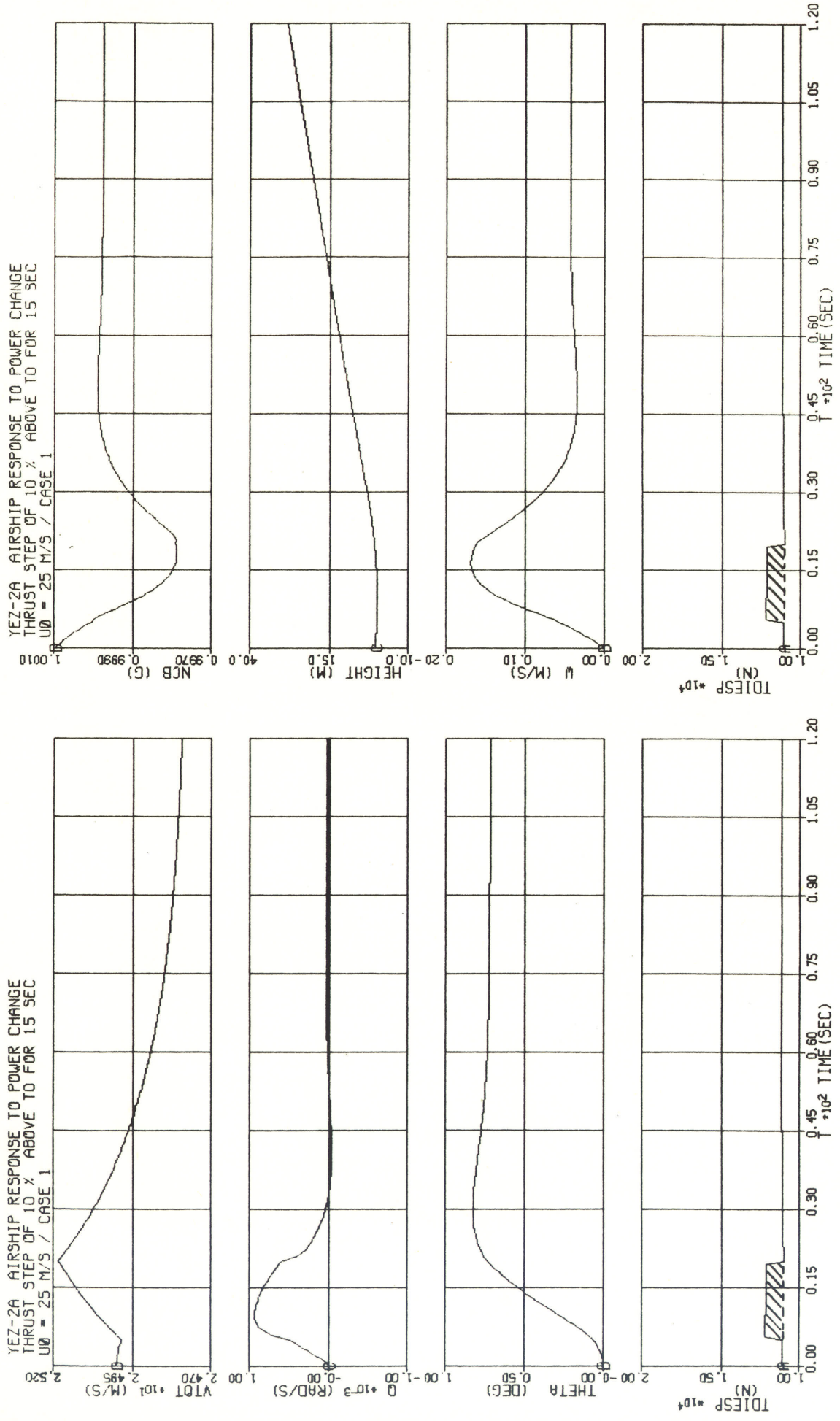

YEZ-2A AIRSHIP : LATERAL TRACKING
U0 = 25 m/s,Case 1,Ramp of 0.25 Deg/sec
Zeta(Deg)
Beta(Deg)
Angle(Dgrees)
0
-5
-10
-15
-20
-25
0
21
42
63
84
105
Time(Seconds)

FIGURE 6.3.7


YEZ-2A AIRSHIP RESPONSE TO POWER CHANGE
THRUST STEP OF 10 % ABOVE TO FOR 15 SEC
U0 = 25 M/S / CASE 1
NCB (G)
HEIGHT (M)
W (M/S)
TOIESP *10⁴ (N)
T *10² TIME (SEC)
YEZ-2A AIRSHIP RESPONSE TO POWER CHANGE
THRUST STEP OF 10 % ABOVE TO FOR 15 SEC
U0 = 25 M/S / CASE 1
VTOT *10¹ (M/S)
Q *10⁻³ (RAD/S)
THETA (DEG)
TOIESP *10⁴ (N)
T *10² TIME (SEC)

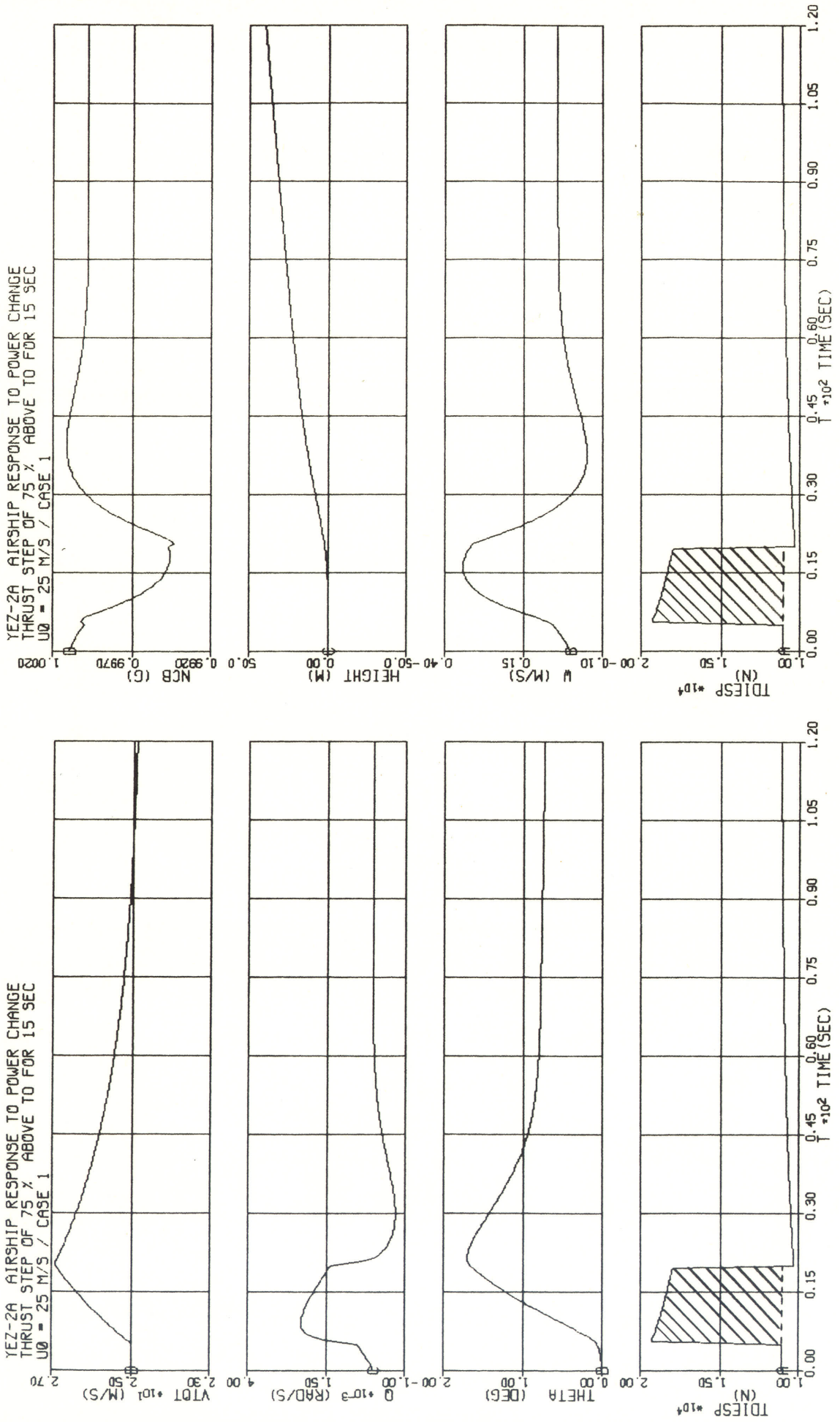
F I G U R E 6.4.1

control input removal are about the same as in the elevator up case. Since the YEZ-2A thrust lines are located some distance below both the CG and the CB the effect of a thrust increase is similar to that of pulling back on the control yoke, i.e., the bow rises, although the speed increases initially and then drops after input removal, and the vehicle gains height. It is just the scale of these effects that is much smaller now than in the elevator case.

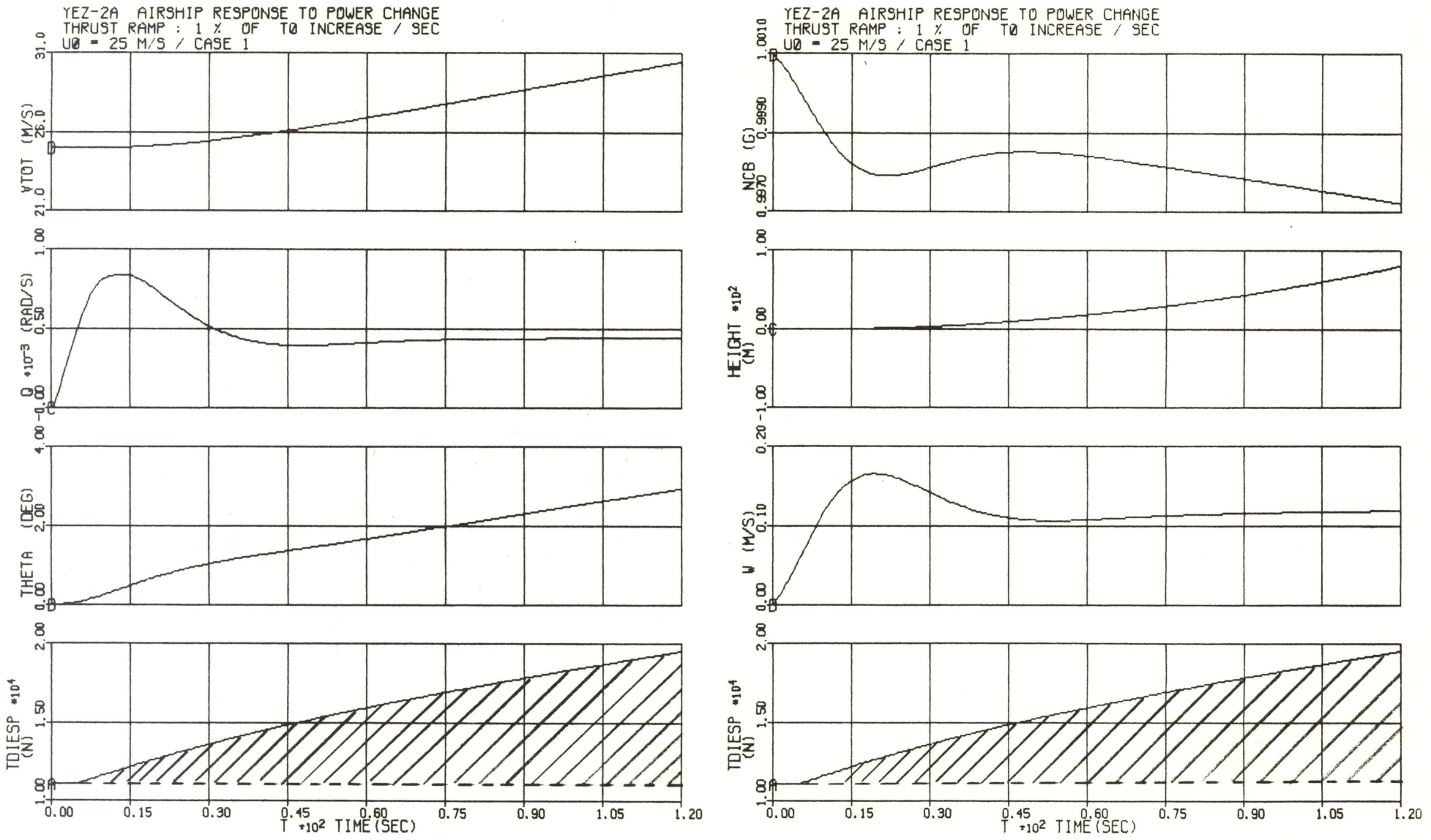
For the large step of increase, the initial conditions were set at the same values as in the previous case. A thrust step increase of 75% above the original thrust trim value was applied for 15 seconds and then removed. The results are presented in Figure 6.4.2.

It can be seen that the effect of increasing the thrust step was equivalent to having a larger elevator type of input, except for the flight speed increase during control application, although on a much smaller scale than if the actual elevator step were implemented. Evidence of that is the fact that at the end of the thrust step application period the bow of the airship had risen by under 2°. After input removal, the ultimate steady state values reached by all the flight parameters appear to be the same as in the previous case, except of course for the height reached which is somewhat higher now as could be expected.

Finally, for the thrust ramp the initial conditions were set at the same values as for the previous cases. Control input application consisted in a continuous increase of thrust of 1% of the initial trimmed, or basic, value over a period of 120 seconds. This basic value was slightly adjusted over the control application period (and the 1% increase was calculated as a fraction of the adjusted value) to account for changes in the flight speed that occurred, but its corresponding power figure remained constant. The results obtained are shown in Figure 6.4.3.


YEZ-2A AIRSHIP RESPONSE TO POWER CHANGE
THRUST STEP OF 75 % ABOVE TO FOR 15 SEC
U0 = 25 M/S / CASE 1
NCB (G)
HEIGHT (M)
W (M/S)
TDIESP *10⁴ (N)
T *10² TIME (SEC)
YEZ-2A AIRSHIP RESPONSE TO POWER CHANGE
THRUST STEP OF 75 % ABOVE TO FOR 15 SEC
U0 = 25 M/S / CASE 1
VTOT *10¹ (M/S)
Q *10⁻³ (RAD/S)
THETA (DEG)
TDIESP *10⁴ (N)
T *10² TIME (SEC)

F I G U R E 6.4.2


YEZ-2A AIRSHIP RESPONSE TO POWER CHANGE
THRUST RAMP : 1 % OF T0 INCREASE / SEC
U0 = 25 M/S / CASE 1
VTOT (M/S)
31.0
26.0
21.0
Q *10-3 (RAD/S)
1.00
0.50
0.00
-0.00
THETA (DEG)
4.00
2.00
0.00
TDIESP *10⁴ (N)
2.00
1.50
1.00
0.00
0.15
0.30
0.45
0.60
0.75
0.90
1.05
1.20
T *10² TIME(SEC)
YEZ-2A AIRSHIP RESPONSE TO POWER CHANGE
THRUST RAMP : 1 % OF T0 INCREASE / SEC
U0 = 25 M/S / CASE 1
NCB (G)
1.0010
0.9990
0.9970
HEIGHT *10² (M)
1.00
0.00
-1.00
W (M/S)
0.20
0.10
0.00
TDIESP *10⁴ (N)
2.00
1.50
1.00
0.00
0.15
0.30
0.45
0.60
0.75
0.90
1.05
1.20
T *10² TIME(SEC)

F I G U R E 6.4.3

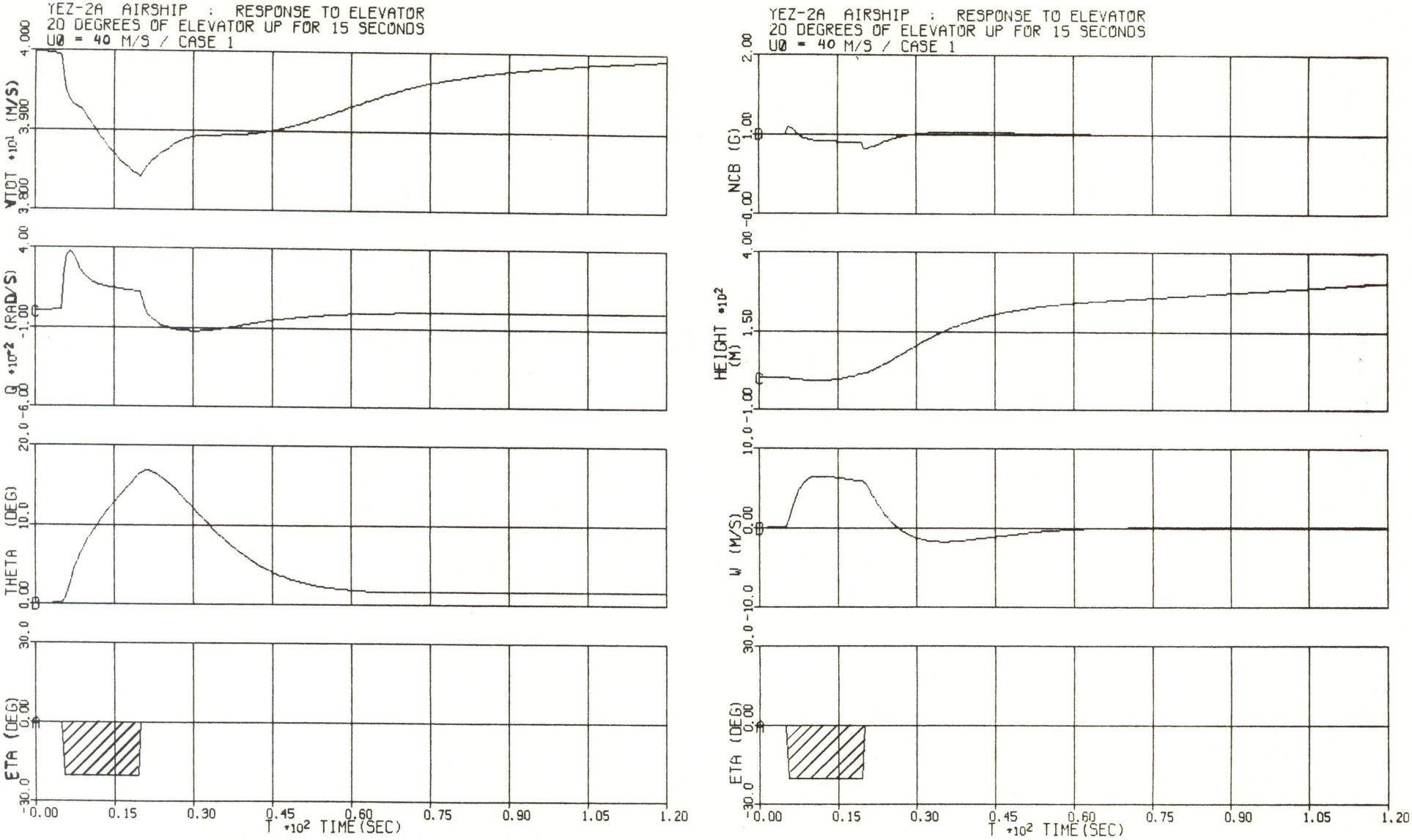
It can be seen that the slow application of an almost linear thrust increase (the slight deviation from a straight line is due to the basic thrust adjustment mentioned) results in approximately linear increases in both flight speed and pitch angle, whereas the other flight parameters exhibited the expected exponential behaviour. If left unchecked, this type of input will therefore result in a continuous pitch up motion with a very low and steady pitch rate, accompanied by speed and height increases. Considering however that all these changes occur in a relatively slow fashion, and that during this period the actual vehicle thrust nearly doubled, it does not appear to present any significant problems from a control point of view.

6.5 Sensitivity to Flight Speed

Having examined the basic vehicle response to the aerodynamic and power types of control inputs at the same initial flight speed, the next stage in the response to controls investigation consisted in trying to assess the effects of different flight speed regimes. A series of experiments were therefore devised and carried out, in which the change in flight speed was the main factor. In all cases, the Case 1 parameters (ISA, sea level, neutral buoyancy conditions) were used so as to have a common basis of comparison. As before, the investigation was divided into the longitudinal and lateral cases.

The first experiment of the longitudinal case consisted in simply running the large response experiment once again, with the same initial conditions except that now the initial velocity was set at 40 m/s, a value which is estimated to be very close to the maximum speed to be attained by the YEZ-2A. The results obtained are shown in Figure 6.5.1.

It can be seen that the shapes of the response curves are similar to those obtained for the initial speed of 25 m/s case (Fig. 6.2.3), and the curve peaks or


YEZ-2A AIRSHIP : RESPONSE TO ELEVATOR
20 DEGREES OF ELEVATOR UP FOR 15 SECONDS
U0 = 40 M/S / CASE 1
VTOT *10¹ (M/S)
Q *10² (RAD/S)
THETA (DEG)
ETA (DEG)
T *10² TIME(SEC)
NCB (G)
HEIGHT *10² (M)
W (M/S)

F I G U R E 6.5.1

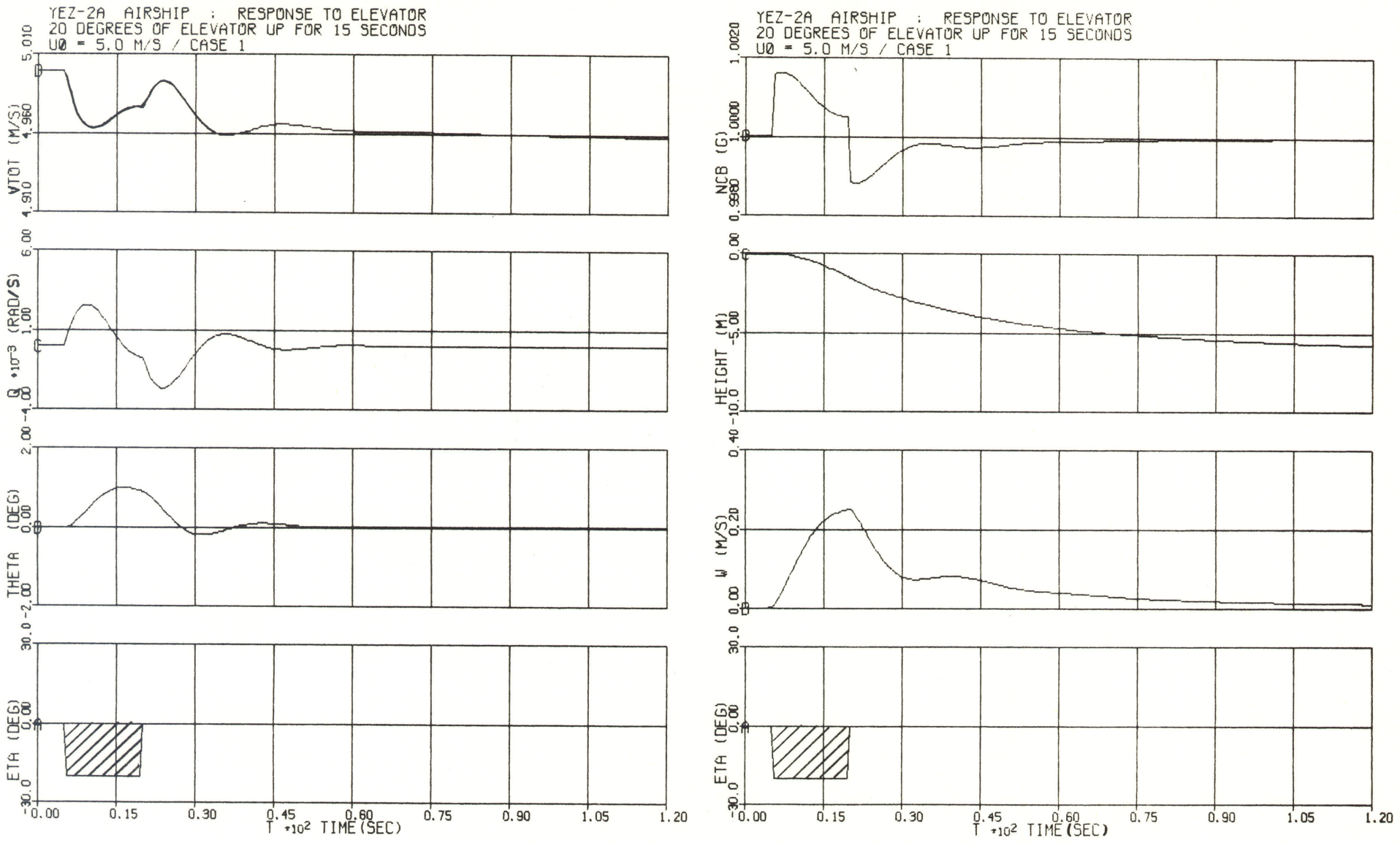
otherwise extreme values reached by the flight parameters are higher in this case. It is interesting to note that the speed recovery after control input removal is much faster now. In summary, it can be said that these results could well have been predicted from the previous U0 = 25 m/s case results.

The second experiment of the longitudinal case consisted in going in the opposite direction of the first experiment, i.e., having an initial flight speed of only 5 m/s, with the initial conditions remaining the same. The results obtained are shown in Figure 6.5.2.

It can be seen that as far as the vehicle attitude is concerned, the pendulum mode (See Chapter 5) was excited by the control input. However, the interesting finding here is the fact that during and after the elevator up type of control input the airship actually lost height, i.e., the opposite of what was to be expected. The interpretation for this fact seems to start with what was already detected in the U0 = 25 m/s case (Fig. 6.2.5): The elevator up input generates a down force that leads the pitching up moment, and so in the first instant the vehicle loses height for a few seconds. After this, the increasing longitudinal incidence causes the hull upward lift to predominate and the vehicle goes up, like a conventional aircraft.

However, when the forward flight speed is allowed to drop below a certain value, which seems to be the case in the U0 = 5 m/s instance, then the inertia to be overcome in pitching up the buoyant vehicle seems to be too high, and the downward pointing tail lift takes the whole vehicle down.

This result suggests the existence of a threshold speed, just like in the conventional aircraft case, above which the vehicle is controllable by the established aerodynamic type of controls. However, below that speed the conventional aircraft is hardly controllable and is very likely to stall and crash if the threshold is passed


YEZ-2A AIRSHIP : RESPONSE TO ELEVATOR
20 DEGREES OF ELEVATOR UP FOR 15 SECONDS
U0 = 5.0 M/S / CASE 1
VTOT (M/S)
5.010
4.960
4.910
Q *10-3 (RAD/S)
6.00
1.00
-4.00
THETA (DEG)
2.00
0.00
-2.00
ETA (DEG)
30.0
0.00
-30.0
NCB (G)
1.0020
1.0000
0.9980
HEIGHT (M)
0.00
-5.00
-10.0
W (M/S)
0.40
0.20
0.00
0.00
0.15
0.30
0.45
0.60
0.75
0.90
1.05
1.20
T *10² TIME(SEC)

F I G U R E 6.5.2

close enough to the ground. The airship on the other hand, if kept in a buoyant condition, will remain airborne but will have considerable difficulty in maintaining reasonable aerodynamic control characteristics. Below the aerodynamic control regime it appears that the solution has to be some form of vectored thrust control that permits the vehicle to move at least along the main body axes, as is done in the case of ROVs (Remotely Operated Underwater Vehicles).

The third and last experiment of the longitudinal case was conceived with the objective of throwing further light onto the aerodynamic controllability aspects as a function of flight speed. It consisted in effect in a series of simulation runs, each one having a different initial flight speed, and all having, as control input, a standard elevator up ramp of 0.25° per second extending over 100 seconds, so as to reach the limit of control surface deflection which is 25°. The combined relevant results of the various runs are presented in Figures 6.5.3 and 6.5.4.

In Figure 6.5.3 it can be seen how the longitudinal tracking characteristics are affected by flight speed. In the top speed case the response parameter θ first lags behind the control input η, then leads it for most of the input range and then lags behind again near the limit. At all the other flight speed cases the control input always leads the response, and the response lag increases sharply as flight speed is allowed to drop. At speeds below about 13 m/s it is not possible to pitch the vehicle up by more than 5° and the response time lag has become virtually infinite.

In Figure 6.5.4 it can be seen that as far as the vehicle trajectory is concerned, no gain in flight altitude will result from an elevator up type of control input if the speed is allowed to drop below about 13 m/s. In fact the airship is likely to loose height at the low speed range, a fact that could have disastrous

consequences if close to the ground or to surface vessels at sea, the latter being the likely operational environment for the YEZ-2A.

The first experiment of the lateral case consisted, like the corresponding one for the longitudinal case, in simply running the large response experiment once again, with the same initial conditions except that now the initial velocity was set at 40 m/s, a value which is estimated to be very close to the maximum speed to be attained by the YEZ-2A. The results obtained are shown in Figure 6.5.5.

It can be seen that again, the shapes of the response curves are similar to those obtained for the initial speed of 25 m/s case (Fig. 6.3.3), and the curve peaks or otherwise extreme values reached by the flight parameters are higher in this case. It is interesting to observe that after control input removal the tendency to continue the turn persists, although with a very low yaw rate r. This finding is associated with a well known aspect of airship stability, i.e., that their weathercock tendency is very low indeed, in contrast to the conventional aircraft. In the present simulation, this tendency is made even more obvious due to the already mentioned existence of a small side force and yawing moment at the $\beta = 0$ condition. The roll oscillation mode excitation resulted in a $\phi_{max} \cong 15^{\circ}$, which can therefore be regarded as an absolute maximum, since in practice the airship is not likely to fly continuously at this speed and much less likely to have a sudden rudder input of 20° without it being progressively applied and with the likely control lags.

In summary, it can be said that these results could well have been predicted from the previous U0 = 25 m/s case results, in the same way as for the longitudinal case.

The second experiment of the lateral case consisted, exactly as for the longitudinal case, in going in the

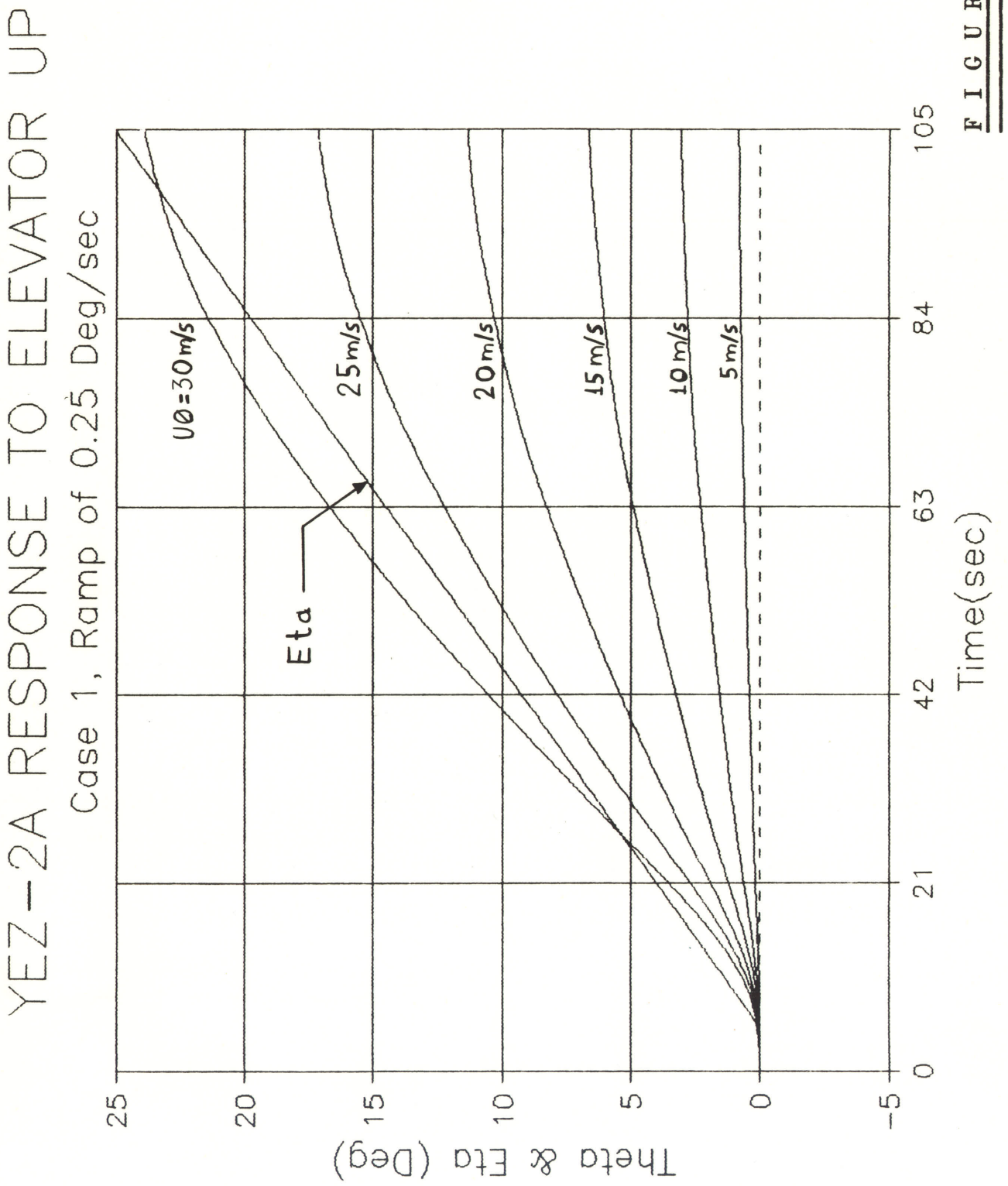

YEZ-2A RESPONSE TO ELEVATOR UP
Case 1, Ramp of 0.25 Deg/sec
U0=30m/s
25m/s
20m/s
15m/s
10m/s
5m/s
Eta
Theta & Eta (Deg)
Time(sec)
25
20
15
10
5
0
-5
0
21
42
63
84
105

FIGURE 6.5.3

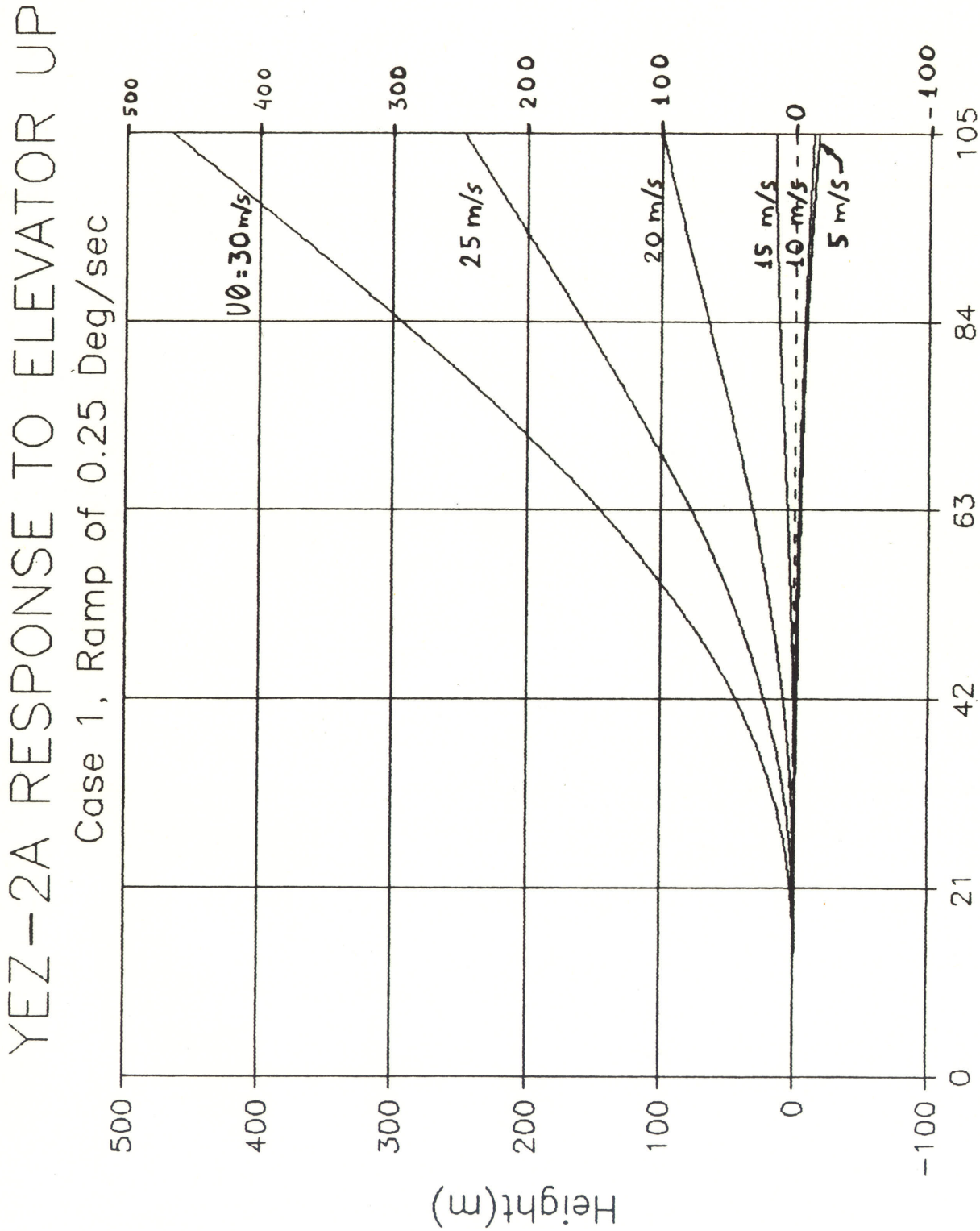

YEZ-2A RESPONSE TO ELEVATOR UP
Case 1, Ramp of 0.25 Deg/sec
Height(m)
Time(sec)
500
400
300
200
100
0
-100
0
21
42
63
84
105
V0=30 m/s
25 m/s
20 m/s
15 m/s
10 m/s
5 m/s

FIGURE 6.5.4

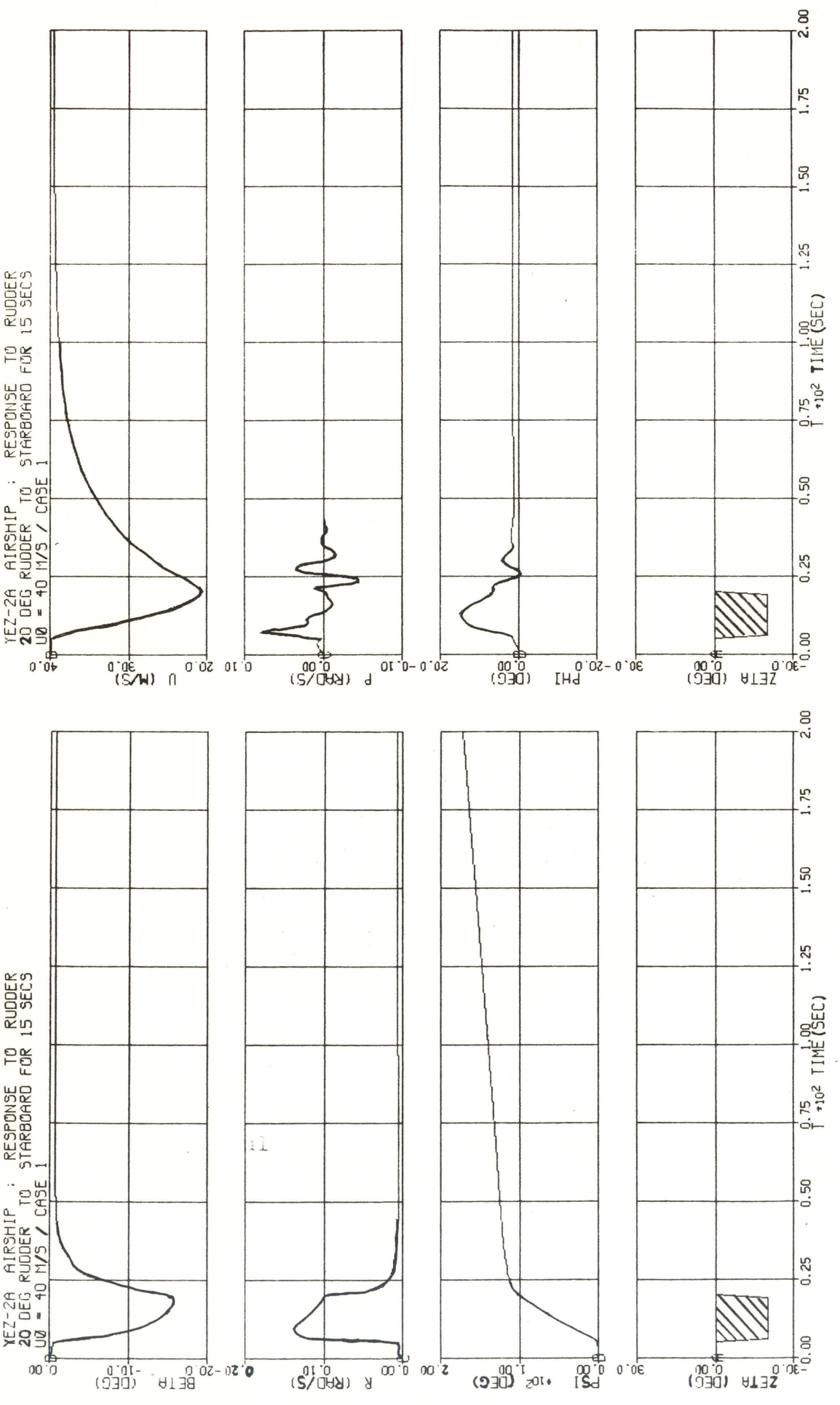

YEZ-2A AIRSHIP : RESPONSE TO RUDDER
20 DEG RUDDER TO STARBOARD FOR 15 SECS
U0 = 40 M/S / CASE 1
U (M/S)
P (RAD/S)
PHI (DEG)
ZETA (DEG)
T *10² TIME (SEC)
YEZ-2A AIRSHIP : RESPONSE TO RUDDER
20 DEG RUDDER TO STARBOARD FOR 15 SECS
U0 = 40 M/S / CASE 1
BETA (DEG)
R (RAD/S)
PSI *10² (DEG)
ZETA (DEG)
T *10² TIME (SEC)

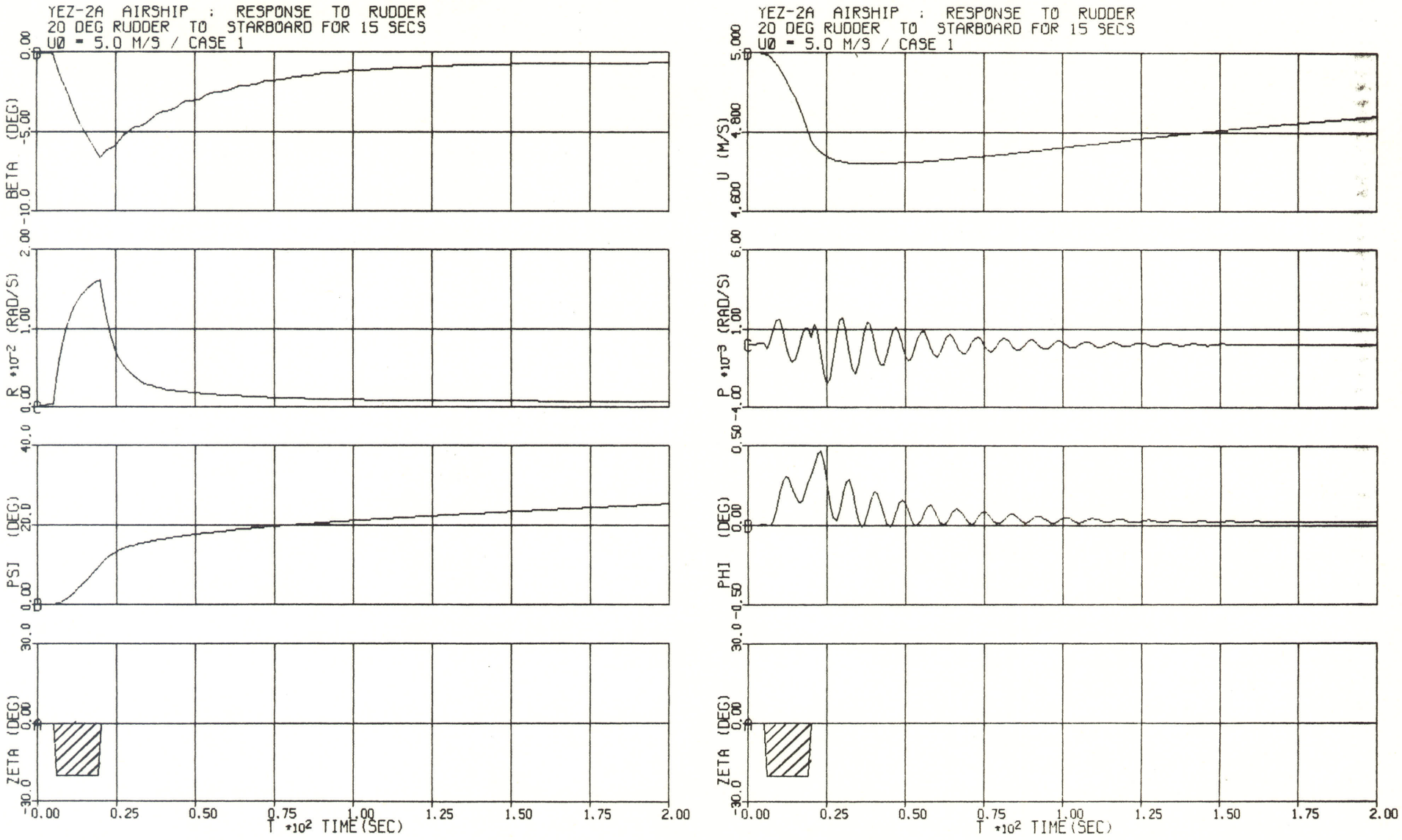
FIGURE 6.5.5

opposite direction of the first experiment, i.e., having an initial flight speed of only 5 m/s, with the initial conditions remaining the same. The results obtained are shown in Figure 6.5.6.

It can be seen that the general shapes of the response curves are essentially the same as in the previous case, except that the time constants for the recovery of the initial conditions are longer now. The damping of the oscillatory mode is, as expected, much lower in the present instance but so are the oscillation amplitudes. In summary therefore it appears that the turning of the vehicle will be possible at the low speed end of the speed range as it was possible at the high speed end.

The third and last experiment of the lateral case was conceived with the objective of throwing further light into the aerodynamic controllability aspects as a function of flight speed, using the same methodology as in the longitudinal case. It consisted therefore in a series of simulation runs, each one having a different initial flight speed, and all having, as control input, a standard rudder to starboard side ramp of 0.25° per second extending over 100 seconds, so as to reach the limit of control surface deflection which is 25°. The combined relevant results of the various runs are presented in Figures 6.5.7 and 6.5.8.

In Figure 6.5.7 it can be seen how the lateral tracking characteristics are affected by flight speed. In all cases the control input ζ leads the response parameter β by a time period that rises exponentially with the increase in control deflection angle. In addition, this time lag becomes virtually the same, at the extreme of rudder deflection angle, for all the flight speeds, except for lowest one of U0 = 5 m/s. The conclusion therefore was that it was always possible to make the airship turn, and that the turn configuration, in terms of the sideslip angle into the turn would be


YEZ-2A AIRSHIP : RESPONSE TO RUDDER
20 DEG RUDDER TO STARBOARD FOR 15 SECS
U0 = 5.0 M/S / CASE 1
BETA (DEG)
R *10-2 (RAD/S)
PSI (DEG)
ZETA (DEG)
T *10-2 TIME(SEC)
YEZ-2A AIRSHIP : RESPONSE TO RUDDER
20 DEG RUDDER TO STARBOARD FOR 15 SECS
U0 = 5.0 M/S / CASE 1
U (M/S)
P *10-3 (RAD/S)
PHI (DEG)
ZETA (DEG)
T *10-2 TIME(SEC)

F I G U R E 6.5.6

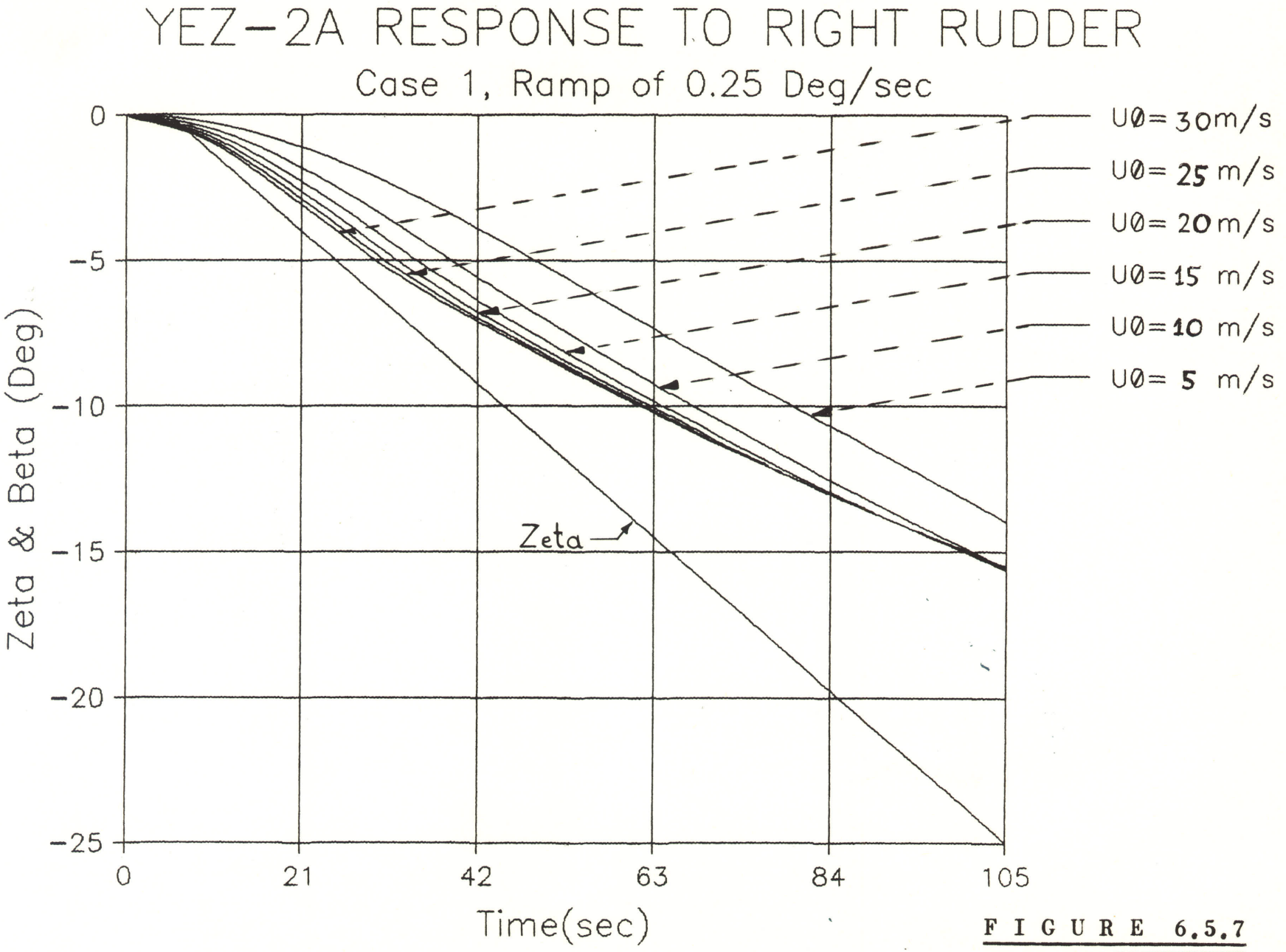

YEZ-2A RESPONSE TO RIGHT RUDDER
Case 1, Ramp of 0.25 Deg/sec
Zeta & Beta (Deg)
0
-5
-10
-15
-20
-25
0
21
42
63
84
105
Time(sec)
Zeta
U0= 30m/s
U0= 25 m/s
U0= 20 m/s
U0= 15 m/s
U0= 10 m/s
U0= 5 m/s

FIGURE 6.5.7

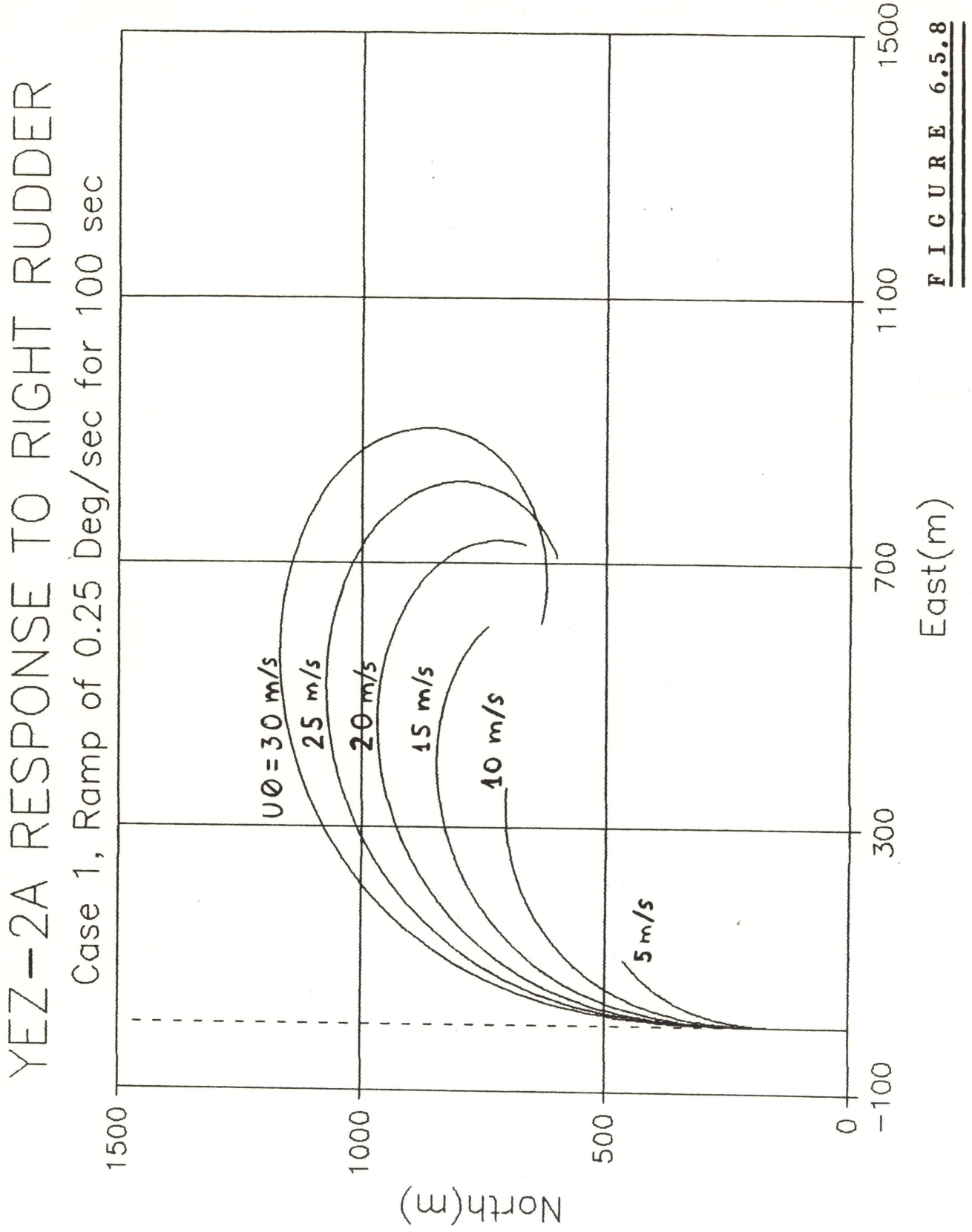

YEZ-2A RESPONSE TO RIGHT RUDDER
Case 1, Ramp of 0.25 Deg/sec for 100 sec
U0=30 m/s
25 m/s
20 m/s
15 m/s
10 m/s
5 m/s
North(m)
East(m)
1500
1000
500
0
-100
300
700
1100
1500

FIGURE 6.5.8

approximately the same irrespective of flight speed.

Figure 6.5.8 was produced with the objective of showing how the actual turns, achieved with the standard rudder ramp, would look like at the various initial flight speeds. As expected, the vehicle trajectory in the horizontal plane (North versus East) consists of turns of ever decreasing radii as a consequence of the progressive increase in the control input magnitude. Also, as expected the higher the initial flight speed the further the vehicle will fly during the standard 200 second run. It is, however, the striking geometrical similarity between the various turn trajectories that supports the stated assumption that the vehicle turn configuration is approximately the same, irrespective of initial flight speed.

6.6 Concluding Remarks

The simulation results gained further credibility when the small amount of flight test data from Reference 6 (the PACE Report) was used as a basis for comparison, if it is borne in mind that the data there presented is for the Skyship-500 airship, a much smaller airship than the YEZ-2A, but with a certain amount of hull geometrical similarity as both are non-rigid types and with a slenderness ratio of the order of four. Among the results that checked well between the two sets of data were:

i. The PACE trials estimated a sideslip angle β of 15-20° in a steady turn at 25° of rudder deflection angle, U0 = 25 and 40 Knots, a result similar to that shown in Figure 6.5.7.

ii. At those speeds, a residual turn rate of ± 1-2° at zero rudder deflection was found in the PACE trials, a result that is of the same order of magnitude as shown in the simulation results.

iii. The low level of directional stability found in the PACE trials is in good agreement with the results here presented, especially the noticeable continued increase in heading angle after rudder control input removal.

iv. The small amount of bank angle associated with steady turns detected in the PACE trials is in good agreement with the simulation results.

v. The PACE trials found that "At low speeds, the rudder and elevator seemed to be ineffective but eventually gave modest response." (Page 5-4), an assessment that is confirmed in Figures 6.5.4 and 6.5.8.

In the previous Sections an attempt has been made to present the major response characteristics of the YEZ-2A airship as originated from the application of aerodynamic types of control inputs (elevator-like and rudder-like) as well as the power type of control. It appears from this investigation that below a certain threshold speed, which bears some resemblance to the conventional aircraft V_{mca} (minimum control/air), aerodynamic control reversal is a definite possibility in the longitudinal case. Care in the operation of the vehicle at low speeds should therefore be exercised, as this condition is likely to exist close to the ground.

Furthermore, at the low speed regime vehicle control will probably have to be obtained from power control inputs. It is therefore recommended that further studies are carried out to ensure that this will be possible at least along the established main body axes. The first priority is motion control in the longitudinal plane, and the YEZ-2A vectored thrust feature with swivelling ducted fans is certainly a step in the right direction.

However, further refinements might still be needed for more precise lateral control in the low speed regime.

7. HANDLING QUALITIES INVESTIGATION

7.1 Introduction

In the literature surveyed in the course of this work it was practically impossible to find any significant material in the area of airship handling qualities, except for some brief comments by pilots on how they felt when in command of specific airship types. It was felt therefore that a systematic study of this important aspect of airship flight is currently required if the techniques developed for conventional aircraft over the past few decades (Ref. 57 and 58) are ever to be applied to the lighter-than-air case.

The purpose of this Chapter is to present the results of a short investigation on the handling qualities of the YEZ-2A airship, which was carried out using the ACSL flight dynamics computer simulation program. It is intended that this would be just the very first step towards trying to understand airship behaviour so that, in the future, specific airship handling qualities requirements can be developed and implemented.

The approach adopted was the one originally formulated by Gibson (Refs. 59 and 60). The main reasons behind this choice were as follows:

i. The only currently available handling qualities requirement, i.e., the American Military Specification 8785C (Ref. 61) was devised for conventional military aircraft. Therefore, the main parameters that are specified as relevant for assessing handling qualities are associated with conventional aircraft flight characteristics, e.g., short period pitching oscillation frequencies, normal acceleration change per unit change in angle of attack and others.

ii. Gibson, on the other hand, advocated the need for a set of longitudinal attitude criteria, which he successfully developed. The relationships associated with his criteria are fixed by the aerodynamics of the aircraft and are independent of the flight control system (FCS) design.

iii. Gibson further stresses the importance of this point by stating that the "...advent of full authority FCS has made the absence of attitude criteria unacceptable for several reasons:
* Additional high order response modes can result in poor or dangerous attitude behaviour.
* Attitude behaviour can be easily modified and so it is necessary to understand its acceptable limits.
* The historic link between flight path and attitude, that is $T\theta_2$, can be broken by the use of additional direct lift control."

Considering that most of these last points are directly relevant to the YEZ-2A airship case, the Gibson criterion was therefore chosen for the preliminary assessment of its longitudinal handling qualities.

However, as the Gibson criterion was developed based on pilots' comments and flight test data gathered using conventional aircraft, its applicability to the airship case has to be regarded with some degree of caution. It must be appreciated that it was aimed at highly manoeuvrable combat aircraft with high order flight control systems (FCS). Therefore, its application to the airship case might lead to a somewhat dubious assessment of lighter-than-air vehicle handling qualities, even though the principles involved in the application are

quite relevant.

7.2 Experiments and Results

In order to apply the Gibson criterion to the YEZ-2A case, a basic type of longitudinal manoeuvre was developed. This consisted of an elevator type of input of 20° applied over 30 seconds. The input was then removed and the simulation run was allowed to complete 60 seconds in total. The Case 1 set of weight and environmental conditions was used.

The same experiment was carried out for three values of initial flight speed: 40 m/s, 25 m/s and 5 m/s. The first value is very close to the estimated maximum flight speed, the second value represents a typical cruise speed and the last value represents a condition in which forward flight is just noticeable.

For the application of the Gibson criterion the output of the simulation consisted in the time histories of the following flight parameters:

η (Eta)	= Ruddervator deflection angle
θ (Theta)	= Airship pitch angle
γ (Gama)	= Airship flight path angle
q	= Airship pitch rate
$\dot{q}$ (Qdot)	= Airship pitch acceleration
α (alpha)	= Airship longitudinal incidence

The results from the simulation runs are presented in the following Figures 7.2.1-6. For the application of the Gibson criterion the identification of the following parameters is required:

CAP	= Control Anticipation Parameter, i.e., initial pitch acceleration/g
$t_{\dot{q}}$	= Time at pitch acceleration peak
q_m	= Peak pitch rate
q_{ss}	= Steady pitch rate

t_q = Time at pitch rate peak

t_d = Effective delay of pitch rate

DB = Pitch attitude dropback

t_γ = Flight path angle delay

Figure 7.2.7 shows how these parameters can be graphically identified in the case of the application of an elevator up type of input for a conventional aircraft. The corresponding numerical results from the YEZ-2A simulation runs are presented in Table 7.2.1.

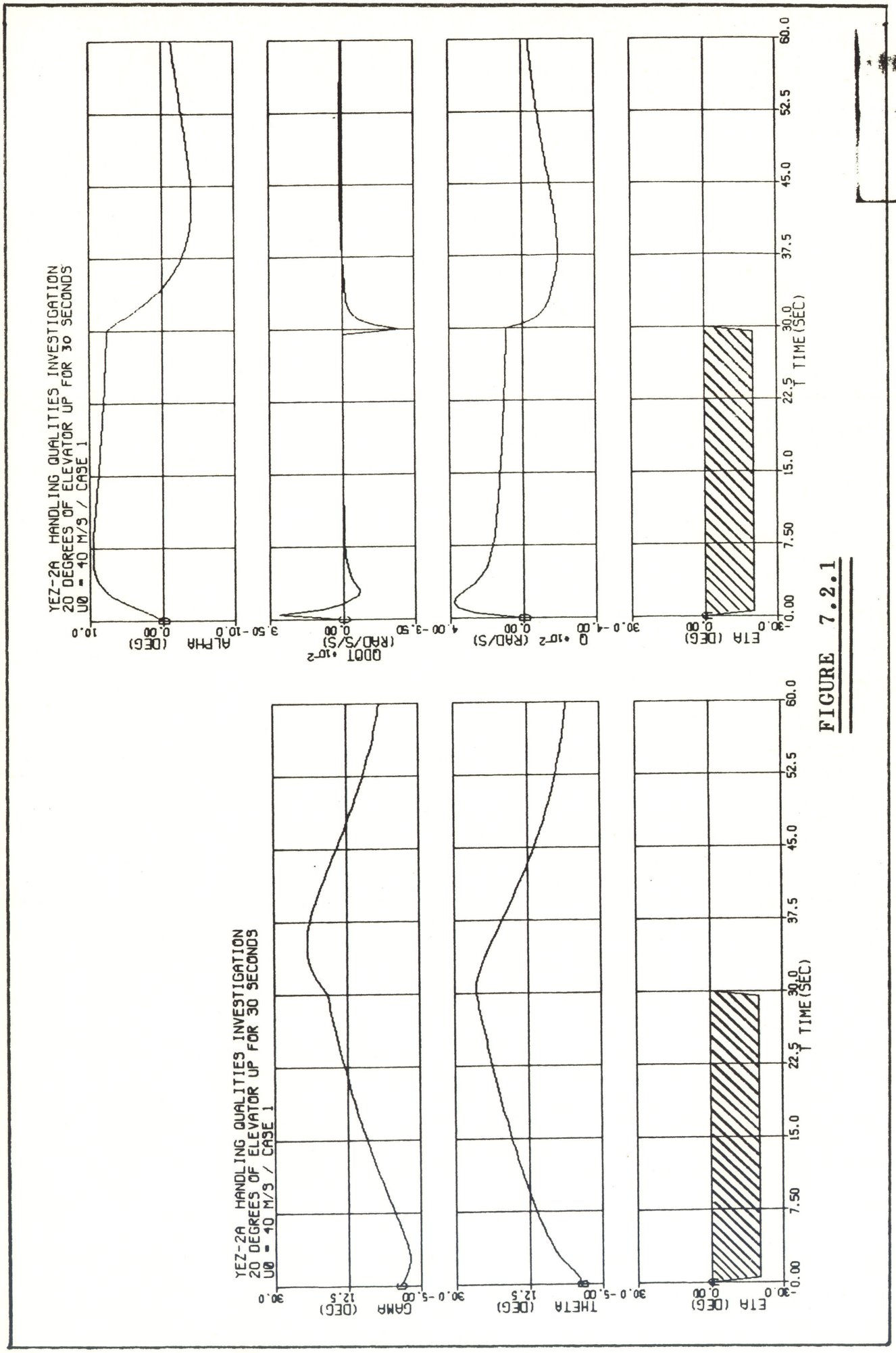

YEZ-2A HANDLING QUALITIES INVESTIGATION
20 DEGREES OF ELEVATOR UP FOR 30 SECONDS
U0 = 40 M/S / CASE 1
ALPHA (DEG)
10.0
0.00
-10.0
QDOT •10^-2 (RAD/S/S)
3.50
0.00
-3.50
Q •10^-2 (RAD/S)
4.00
0.00
-4.00
ETA (DEG)
30.0
0.00
-30.0
0.00
7.50
15.0
22.5
30.0
37.5
45.0
52.5
60.0
T TIME (SEC)
YEZ-2A HANDLING QUALITIES INVESTIGATION
20 DEGREES OF ELEVATOR UP FOR 30 SECONDS
U0 = 40 M/S / CASE 1
GAMA (DEG)
30.0
12.5
-5.00
THETA (DEG)
30.0
12.5
-5.00
ETA (DEG)
30.0
0.00
-30.0
0.00
7.50
15.0
22.5
30.0
37.5
45.0
52.5
60.0
T TIME (SEC)

FIGURE 7.2.1

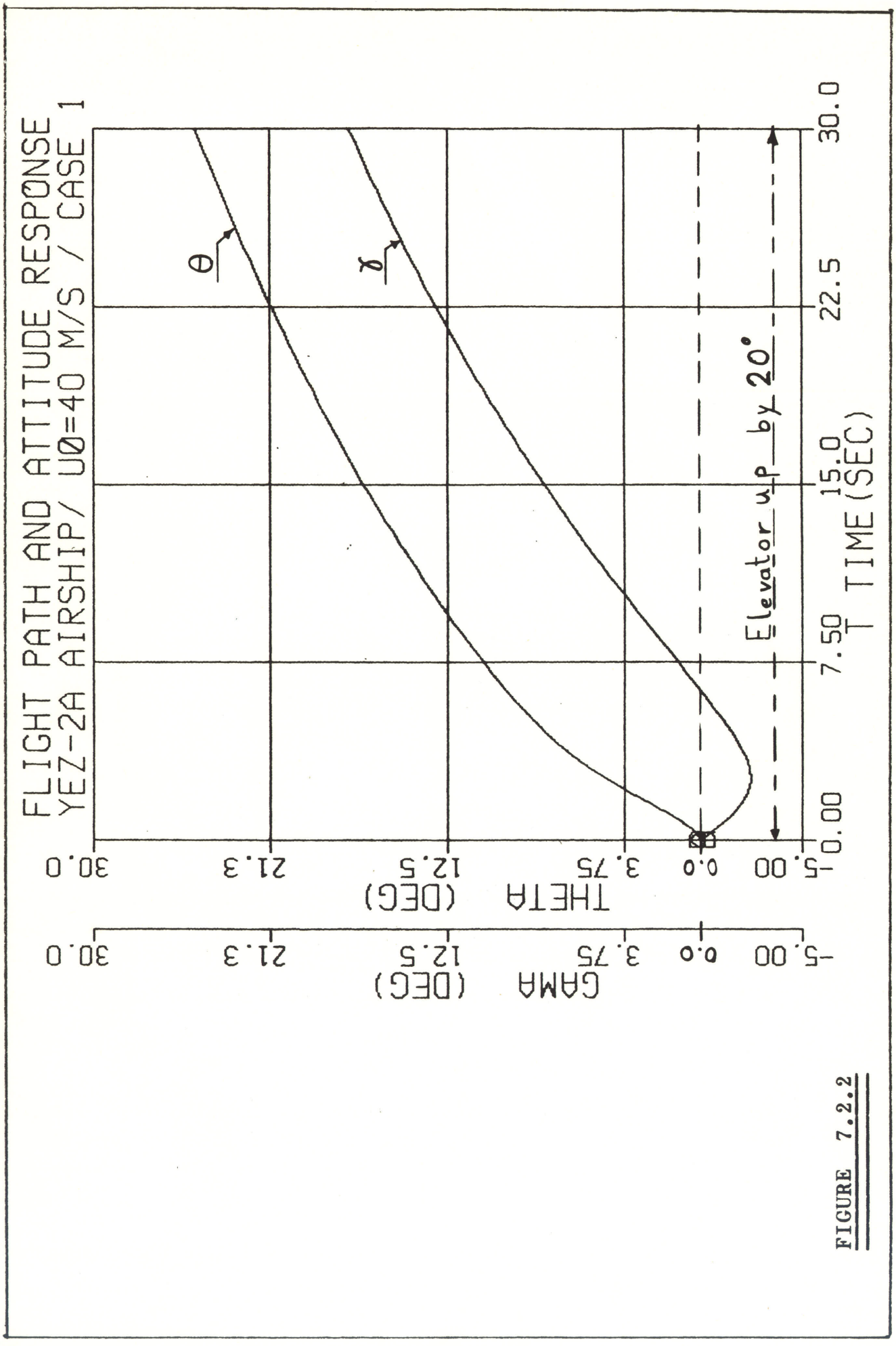

FLIGHT PATH AND ATTITUDE RESPONSE
YEZ-2A AIRSHIP/ U0=40 M/S / CASE 1
θ
γ
Elevator up by 20°
T TIME (SEC)
0.00
7.50
15.0
22.5
30.0
THETA (DEG)
GAMA (DEG)
-5.00
0.0
3.75
12.5
21.3
30.0

FIGURE 7.2.2

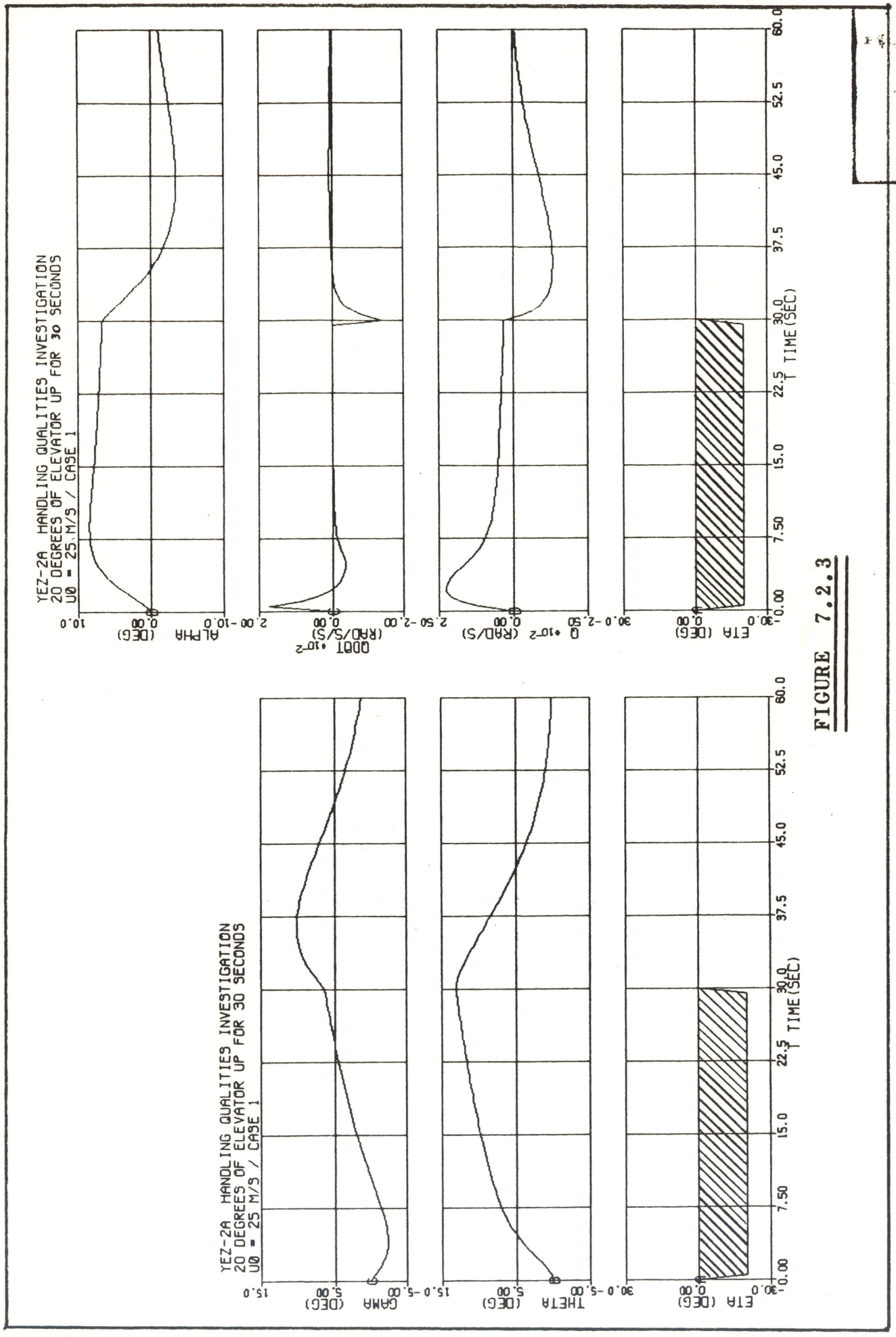

YEZ-2A HANDLING QUALITIES INVESTIGATION
20 DEGREES OF ELEVATOR UP FOR 30 SECONDS
U0 = 25 M/S / CASE 1
ALPHA (DEG)
10.0
0.00
-10.0
DDOT *10^-2 (RAD/S/S)
2.00
0.00
-2.00
Q *10^-2 (RAD/S)
2.50
0.00
-2.50
ETA (DEG)
30.0
0.00
-30.0
0.00
7.50
15.0
22.5
30.0
37.5
45.0
52.5
60.0
T TIME (SEC)
YEZ-2A HANDLING QUALITIES INVESTIGATION
20 DEGREES OF ELEVATOR UP FOR 30 SECONDS
U0 = 25 M/S / CASE 1
GAMA (DEG)
15.0
5.00
-5.00
THETA (DEG)
15.0
5.00
-5.00
ETA (DEG)
30.0
0.00
-30.0
0.00
7.50
15.0
22.5
30.0
37.5
45.0
52.5
60.0
T TIME (SEC)

FIGURE 7.2.3

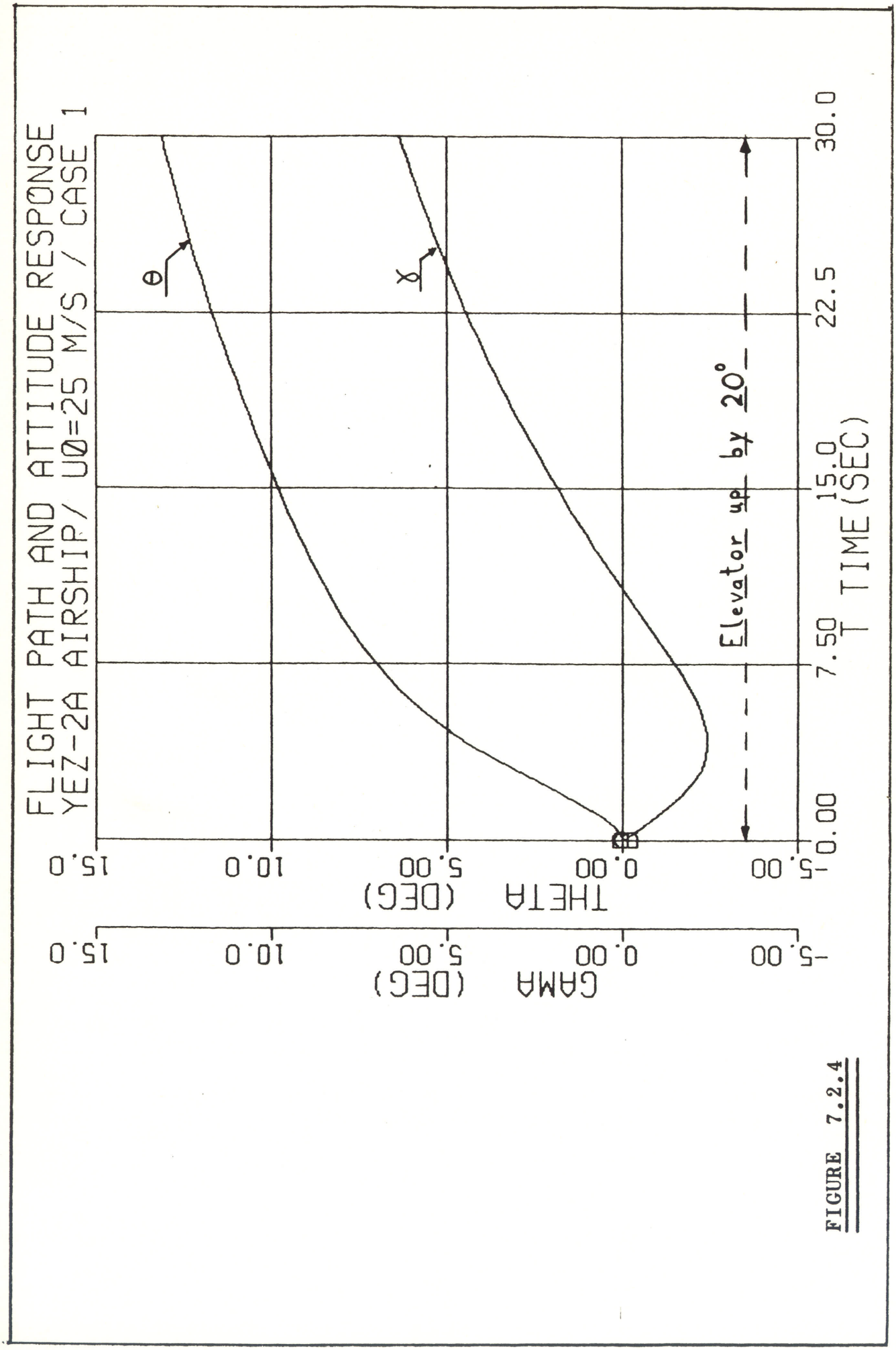

FLIGHT PATH AND ATTITUDE RESPONSE
YEZ-2A AIRSHIP/ U0=25 M/S / CASE 1
θ
γ
Elevator up by 20°
T TIME (SEC)
0.00
7.50
15.0
22.5
30.0
THETA (DEG)
GAMA (DEG)
-5.00
0.00
5.00
10.0
15.0

FIGURE 7.2.4

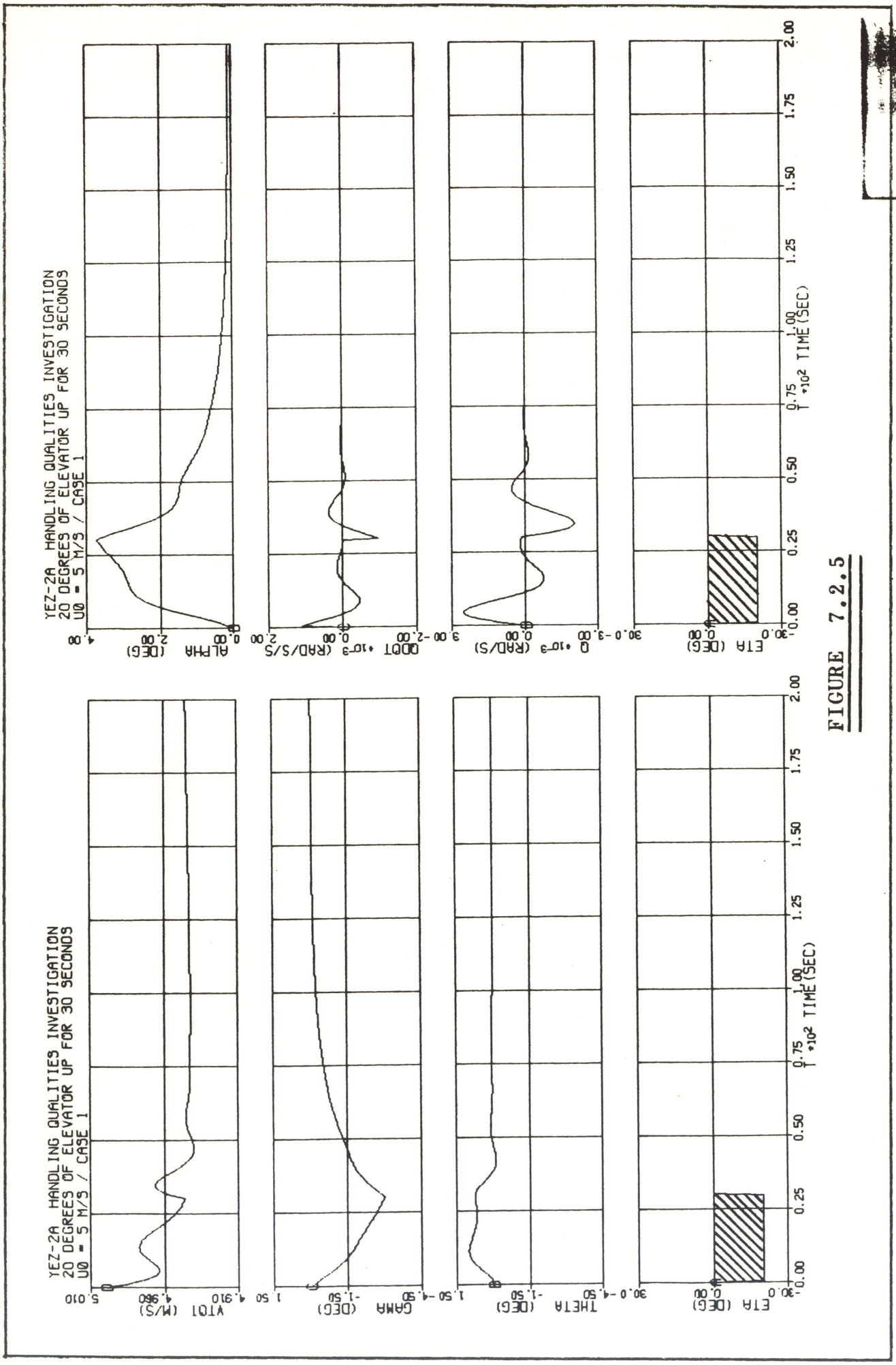

YEZ-2A HANDLING QUALITIES INVESTIGATION
20 DEGREES OF ELEVATOR UP FOR 30 SECONDS
U0 = 5 M/S / CASE 1
ALPHA (DEG)
DOOT *10-3 (RAD/S/S
Q *10-3 (RAD/S)
ETA (DEG)
T *10² TIME(SEC)
YEZ-2A HANDLING QUALITIES INVESTIGATION
20 DEGREES OF ELEVATOR UP FOR 30 SECONDS
U0 = 5 M/S / CASE 1
VTOT (M/S)
GAMA (DEG)
THETA (DEG)
ETA (DEG)
T *10² TIME(SEC)

FIGURE 7.2.5

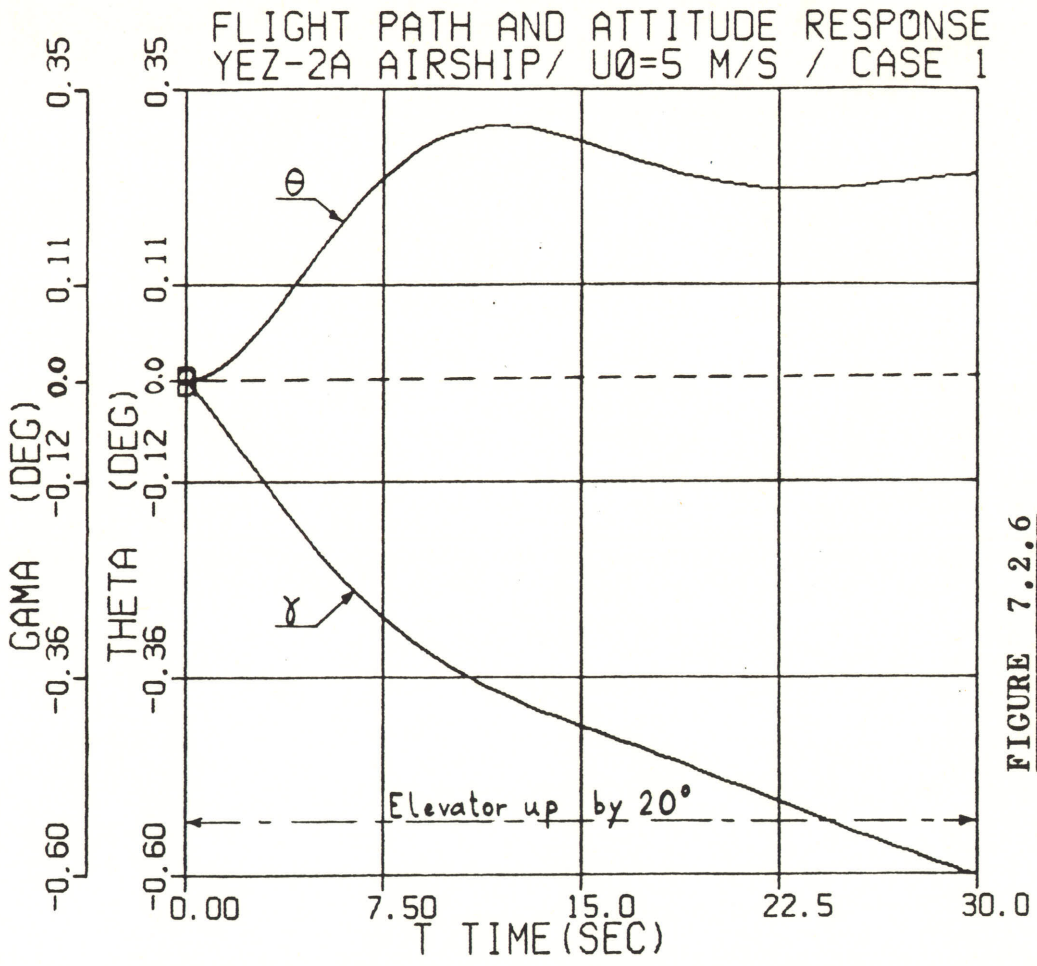

FLIGHT PATH AND ATTITUDE RESPONSE
YEZ-2A AIRSHIP/ U0=5 M/S / CASE 1
GAMA (DEG)
THETA (DEG)
0.35
0.11
0.0
-0.12
-0.36
-0.60
θ
γ
Elevator up by 20°
0.00
7.50
15.0
22.5
30.0
T TIME(SEC)

FIGURE 7.2.6

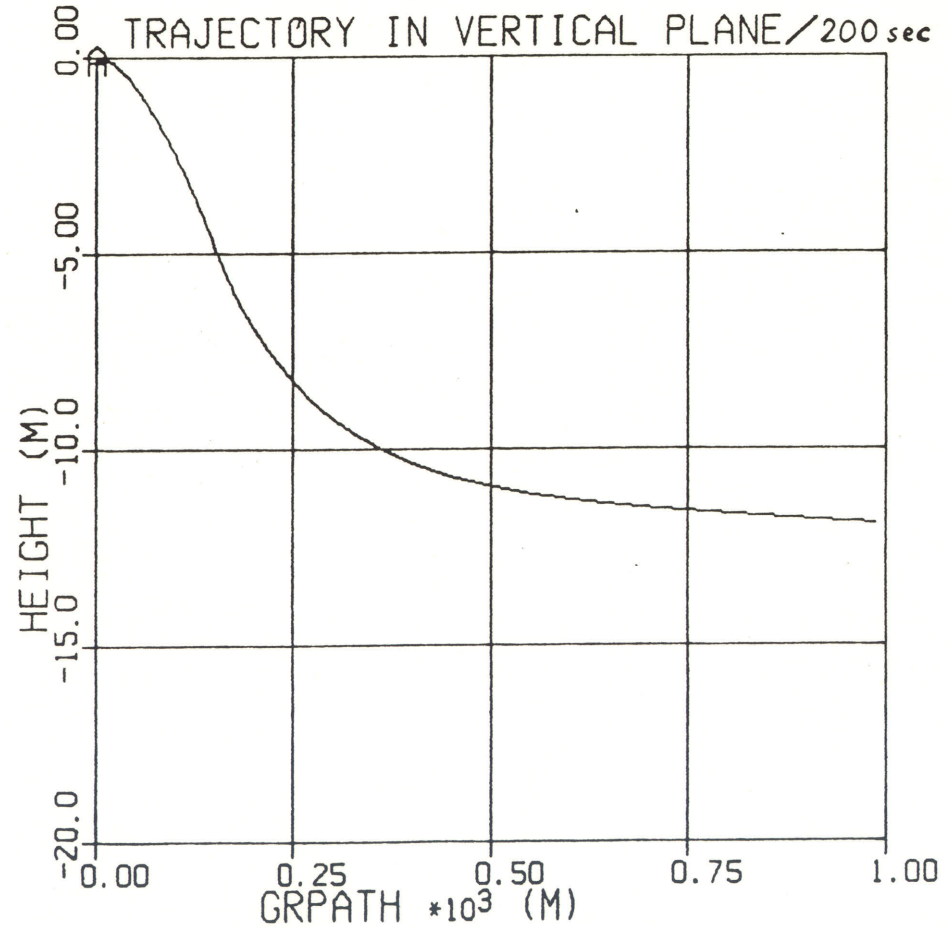
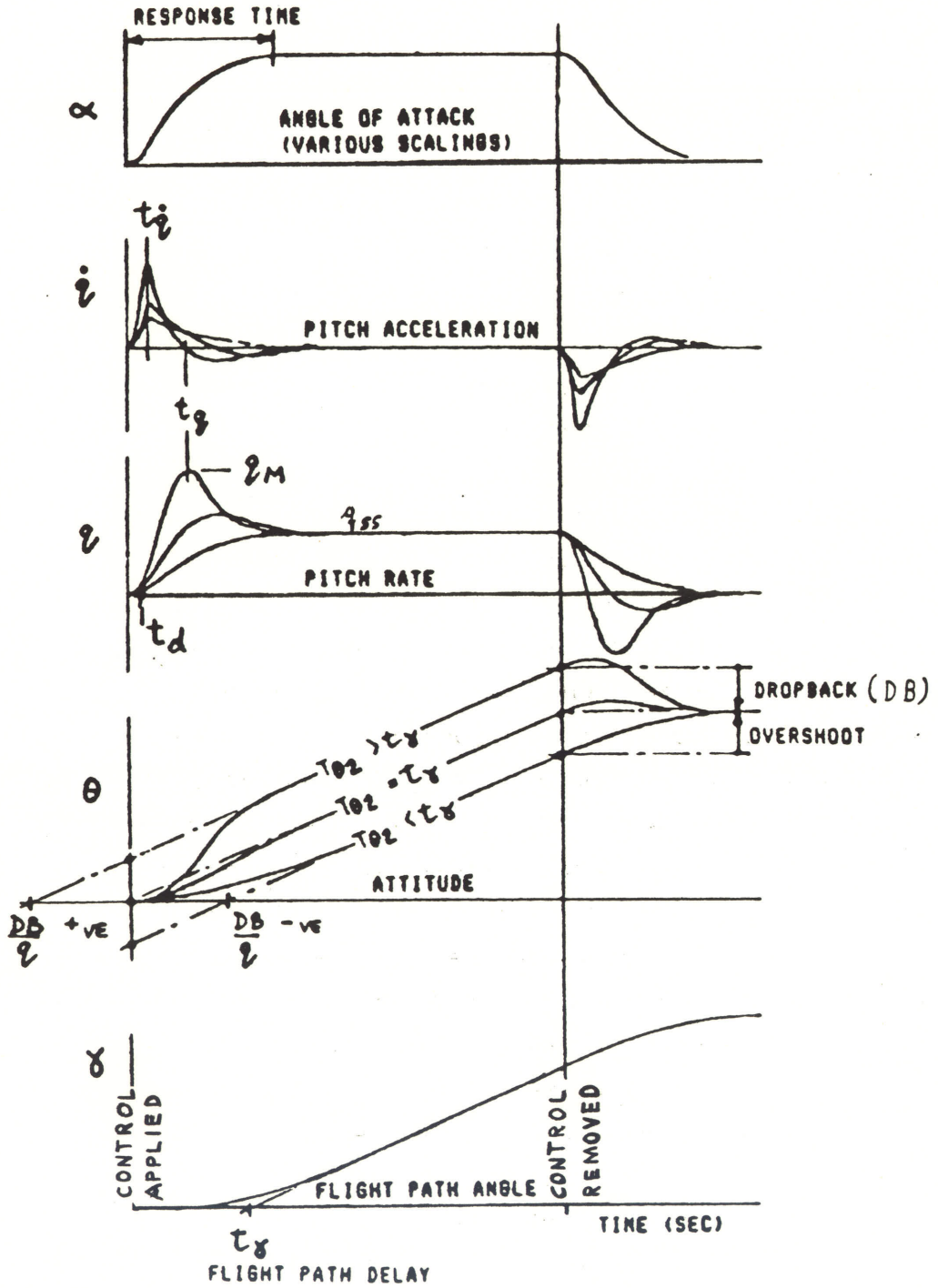

TRAJECTORY IN VERTICAL PLANE/200 sec
HEIGHT (M)
0.00
-5.00
-10.0
-15.0
-20.0
0.00
0.25
0.50
0.75
1.00
GRPATH *10³ (M)

FIGURE 7.2.7 - Typical longitudinal short period time responses for a conventional aircraft.



	U0 = 40 m/s	U0 = 25 m/s
CAP ($Deg/s^2/g$) ($Rad/s^2/g$)	1.7 0.03	0.94 0.02
$t_{\dot{q}}$ (sec)	0.5	0.5
q_m (Rad/s)	0.0385	0.0228
q_{ss} (Rad/s)	0.012	0.0051
q_m/q_{ss}	3.2	4.5
t_q (sec)	1.5	2.5
t_d (sec)	0	0
DB (Deg)	3	5
DB/q_{ss} (sec)	4.5	17
t_γ (sec)	6.3	10.5
$T\theta_2$ (sec)	12	25

TABLE 7.2.1 - The Gibson criterion parameters obtained in the flight dynamics simulation runs for the YEZ-2A airship (Case 1).

7.3 Analysis

The results presented in Table 7.2.1 are essentially all the parameters required in order to apply the Gibson criterion. Those for the initial flight speed of 5 m/s could not be presented since, as can be seen in Figures 7.2.5-6, in that case the vehicle response behaviour does not lend itself to the application of the Gibson criterion. As already pointed out in Chapter 6, at this low speed, vehicle control is to be obtained through power control, i.e., by changing the engine power settings and geometrical orientation of the ducted fan thrust lines. Therefore, for this condition a distinct type of handling qualities criterion should be developed and applied.

Although the airship operates under a clearly different set of rules as compared to conventional aircraft, e.g., lift is mainly aerostatically rather than aerodynamically generated, it is interesting to observe that the usual aerodynamic relations still apply. For instance:

i. The results presented in Table 7.2.1 show that the relation

$$\frac{DB}{q_{ss}} + t_{\gamma} \cong T\theta_2$$

still holds in the airship case.

ii. The results presented in Table 7.2.1 and Figures 7.2.2 and 7.2.4 show that the relation

$$\alpha_{ss} = T\theta_2 \cdot q_{ss}$$

where α_{ss} is the steady longitudinal incidence angle ($\alpha = \theta - \gamma$), is still applicable.

Figure 7.3.1 is the Gibson developed boundary for

satisfactory behaviour in the plane of normalized 'dropback', DB/q_{ss}, and pitch rate overshoot ratio, q_m/q_{ss}. The relevant results from Table 7.2.1 are also shown.

It can be seen that a 'continuous bobbling' type of handling is anticipated for the YEZ-2A case. The higher speed yielded a somewhat better result, but it is still far from the 'satisfactory' region.

Gibson (Ref. 59) further specified that:

i. "Attitude dropback had little effect within the range tested upon gross manoeuvring without target, landing approach or flight refuelling, provided it was not negative."

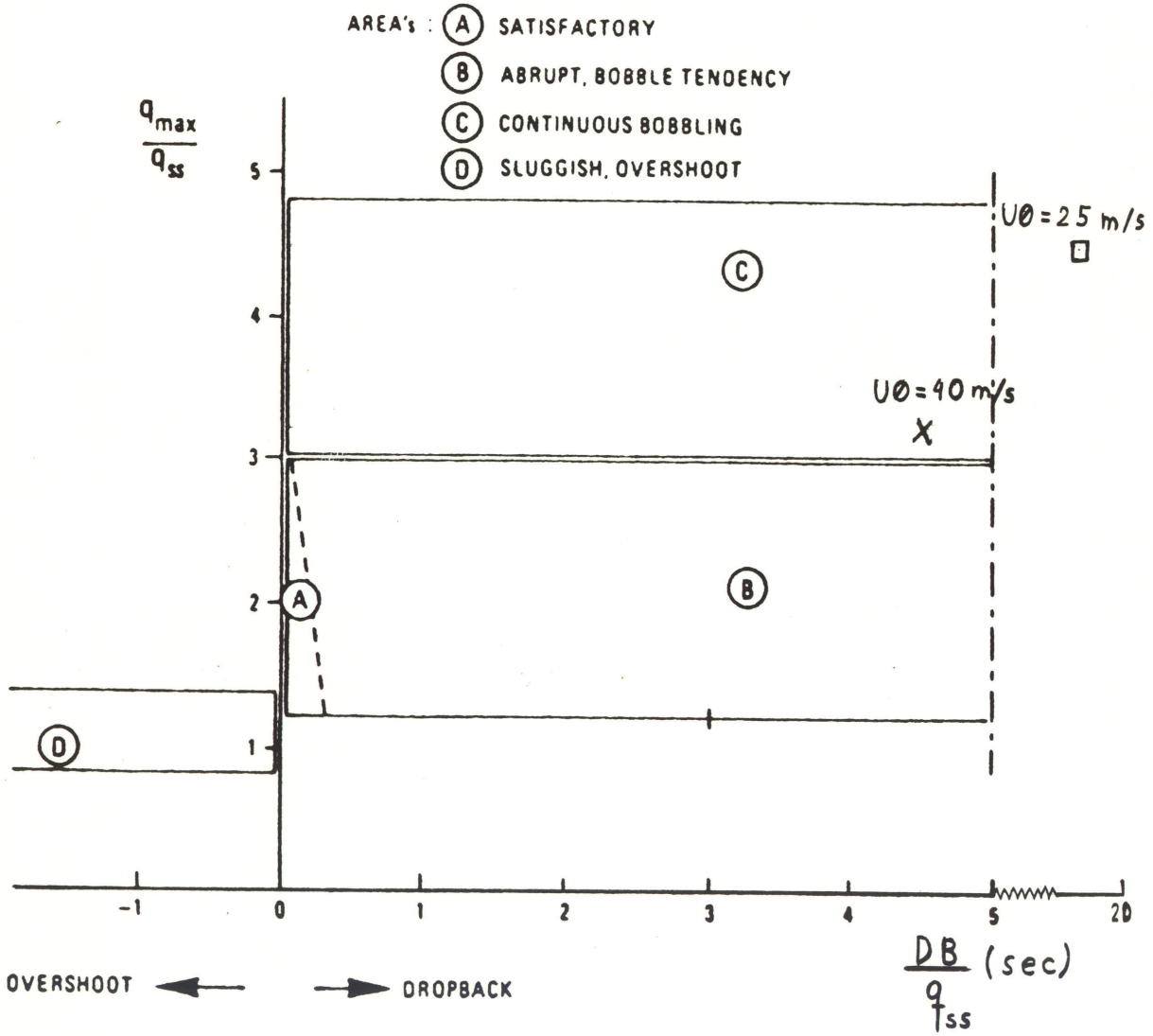
ii. "CAP up to 3.6 $rad/s^2/g$ was satisfactory for gross manoeuvring without a target but was unsatisfactory above 2 $rad/s^2/g$ for the landing approach, above 1 $rad/s^2/g$ for fine tracking, and below 0.28 $rad/s^2/g$ for any task."

iii. "Small values of flight path time delay were associated with excellent flight refuelling control, but were not essential for good gross manoeuvring and did not on their own ensure predictable behaviour."

7.4 Conclusions

Before reaching some tentative conclusions on the prediction of airship handling qualities based on the Gibson criterion, it is important to realize that it was developed over quite a few years based on flight test data and pilot rating and comment data. Its main objective was to try to present the significant low order aircraft handling characteristics so that current high order flight control systems would still exhibit the desirable low order handling qualities response

FIGURE 7.3.1 - The Gibson developed 'dropback' criterion in the plane of normalized dropback, DB/q_{ss}, and pitch rate overshoot ratio, q_m/q_{ss}.



characteristics.

In addition, the Gibson criterion is essentially aimed at combat aircraft, and more specifically at fighters. Not only its data base was obtained from such aircraft types, they also present the greatest challenge in terms of handling qualities characteristics in view of the nature of their missions.

Therefore, before a specific set of handling qualities is developed for the lighter-than-air case, the application of the Gibson criterion to the results of a flight dynamics computer simulation of the YEZ-2A airship yielded the following preliminary conclusions:

i. The positive dropback values found (3° for the U0 = 40 m/s case and 5° for the U0 = 25 m/s case) mean that a sluggish, unpredictable response, both in flight path control and in tracking, are not to be expected.

ii. The attitude dropback values found mean that the expected longitudinal response is characterized by "... abrupt response and bobbling, from 'slight tendency' to 'continuous oscillations', in tracking tasks. Sometimes this was called PIO (pilot induced oscillations) but it did not cause concern for safety" (Ref. 59). This assessment has been confirmed by observations carried out in existing airships, including the sensing of what appeared to be PIO. It is characterized by a slow frequency response to external disturbances, which makes it difficult to hold a set attitude and therefore can induce the pilot into over controlling the vehicle. From the results presented in Chapter 5 it can be concluded that if the pendulum mode is eventually excited by this handling qualities

characteristic its frequency range still allows a reasonable degree of control by the pilot or the AFCS (automatic flight control system).

iii. The CAP values found were unsatisfactory under the Gibson criterion, "...for any task", since in the airship case they were below the minimum value of 0.28 $rad/s^2/g$. This result was to be expected since the response time constants in the airship case are substantially greater than those associated with conventional aircraft, especially combat aircraft. It is felt however that since a typical airship cruising speed is much lower than any conventional aircraft speed, this might not have such a critical effect on its handling qualities.

Finally, it is important to remember that the conclusions reached were based on the open loop behaviour of the YEZ-2A airship. Being a project airship for which a 'fly-by-light' (optical signalling) type of flying controls is envisaged, coupled with an autopilot and an autostabilization system, it is very likely that its flight control system will exhibit high order characteristics that could result in a significant departure from the response behaviour here predicted. In that case the Gibson criterion will still be a valuable reminder of the low order handling qualities that are desirable and should be aimed for.

8. CONCLUSIONS AND RECOMMENDATIONS

8.1 Conclusions

The airship flight dynamics computer simulation model that was developed in the course of this work was used to provide the following type of information:

i. Describe and quantify the YEZ-2A airship longitudinal and lateral aerodynamic stability modes.

ii. Describe and quantify the airship response to both aerodynamic and power control inputs.

iii. Tentatively predict the kind of longitudinal handling qualities response that is to be expected for the YEZ-2A project design.

The results achieved in these three areas can be summarized as:

i. The airship was found to have three modes of longitudinal motion and three modes of lateral motion. In the longitudinal case these were demonstrated to be a surge mode, a pitch subsidence mode and a pendulum mode under forward flight conditions. In the hover condition however, the pitch subsidence mode became a simple heave mode. They were all stable modes, although stability became virtually neutral in the hover condition. In the lateral case the modes of motion were demonstrated to be a sideslip subsidence, a yaw subsidence and a roll oscillation. They were all stable modes, although again stability was found to become virtually neutral as the hover condition was approached.

ii. The airship was found to have a flight threshold speed of about 13 m/s, below which longitudinal aerodynamic control is not only not possible, but it will possibly result in a response that is the opposite of what was demanded by the pilot. Under these conditions, it appears that only the vectored thrust system will be able to provide acceptable response characteristics. This problem was not detected in the lateral case. Above the longitudinal threshold speed, aerodynamic control was found to be effective and reasonably adequate.

iii. The YEZ-2A airship was found to have handling characteristics of the "continuous bobbling" type when the Gibson criterion was applied. The Gibson criterion was originally developed for high performance combat aircraft and it seeks to optimize a "rate command attitude hold" type of longitudinal control. The "continuous bobbling" response found for the airship is characterized by a slow frequency response to external disturbances, which makes it difficult to hold a set attitude and can induce the pilot into over controlling the vehicle. Further work is definitely required in this field, in view of the inherent peculiarities of airship flight as compared to conventional aircraft handling characteristics.

8.2 Recommendations

The results and conclusions that were achieved in the course of this work constitute only a small part of what the simulation program is able to generate. Amongst the areas that could be further investigated are:

i. Extend the investigation to a few cases of non-neutral buoyancy conditions, so as to assess their impact on the three areas already covered.

ii. The investigation established the speed below which aerodynamic control of the vehicle is not possible or even advisable (Section 6.5). This is an aspect of airship flight that is well known to airship pilots but which, as far as we are aware, had not been properly quantified before. Therefore, the possibilities of manoeuvring using exclusively the power controls, including all the changes in the geometrical orientation of the ducted fans, need to be further investigated and quantified. The information thus obtained will be of special relevance for the design of the YEZ-2A auto-stabilization system, since it will also have to operate in the conditions of low altitude and very slow speed that will arise when the vehicle is refuelling and re-supplying from a fleet surface vessel.

iii. As already pointed out, a set of airship handling criteria needs to be developed. In this respect, the computer simulation program developed can play its part as far as the ground simulation is concerned, although flight test investigations coupled with pilot ratings and comments will also be required. Of special significance will be the lateral handling qualities criteria, since this is the area in which airships in general seem to attract a measure of criticism. In addition, one of the tasks that the YEZ-2A will be required to

perform is to refuel and re-supply from a surface vessel. This operation is to be carried out at low altitude and at a very slow forward speed. The handling qualities under these conditions require urgent research, since success in the accomplishment of the refuel and re-supply operations will be vital to the demonstration of the YEZ-2A capability. Assessment of how well a vehicle can perform a given task is, after all, the major objective of any handling qualities investigation.

All in all, it is felt that the high fidelity aerodynamic model of airship flight obtained in the course of this work served to characterize the airship as a perfectly controllable and manoeuvrable type of vehicle, given its inherent peculiarities that were also detected and, as far as possible, quantified. It is hoped that this contribution will go towards making the lighter-than-air vehicle concept a more viable proposition for air transportation, in a number of applications for which it is uniquely suited.

9. REFERENCES

1. Dick, H. G. and Robinson, D. H. - "Graf Zeppelin & Hindenburg - The Golden Age of the Great Passenger Airships", Smithsonian Institution Press, Washington, D.C., 1985.

2. Chamberlain, G. - "Airships Cardington", Terence Dalton Limited, Lavenham, Suffolk, 1984.

3. Smith, R. K. - "The Airships Akron and Macon", Naval Institute Press, Annapolis, Maryland, 1965.

4. Proceedings of the Interagency Workshop on Lighter than Air Vehicles, M.I.T. Flight Transportation Laboratory, FTL Report R75-2, January, 1975 (Edited by J. F. Vittek Jr).

5. Nayler, A. W. L. - "An Overview of Current British Airship Activity", AIAA 8th Lighter-than-Air Systems Technology Conference Proceedings, Jacksonville, Fl., October 5-7, 1989.

6. Bailey, D. B. - "Patrol Airship Concept Evaluation (PACE) Final Report", Executive Edition, prepared for the Naval Air System Command and US Coast guard Headquarters, Department of the Navy, Naval Air Development Center Rpt No. NADC-85019-60, 15 March 1985.

7. Rimell, R. L. - "Skyship", Albatros Productions Ltd, Berkhamstead, Herts, 1988.

8. Airship - The Journal of the Airship Association, No. 82, pp 3-4, December 1988.

9. Airship - The Journal of the Airship Association, No. 76, pp 14-15, June 1987.

10. Aviation Week & Space Technology, pp 65-70, December 5, 1988.

11. Curtiss Jr, H. C., Hazen, D. C. and Putman, W. F. - "LTA Aerodynamic Data Revisited", Journal of Aircraft, Vol. 13, No. 11, November 1976.

12. Brooks, P. W. - "Why the Airship Failed", Aeronautical Journal, pp 439-449, October 1975.

13. Owen, P.R. - "The Aerodynamics of Aircraft and Other Things", Aeronautical Journal, pp 383-405, August 1973.

14. DeLaurier, J. and Schenk, D. - "Airship Dynamic Stability", AIAA Lighter-than-Air Systems Technology Conference Proceedings, Palo Alto, Ca., July 11-13, 1979.

15. DeLaurier, J. and Jones, S.P. - "Aerodynamic Estimation Techniques for Aerostats and Airships", AIAA Lighter-than-Air Systems Technology Conference Proceedings, Annapolis, Maryland, July 8-10, 1981.

16. DeLaurier, J. and Evans, J.R. - "The Shenandoah Flies Again", AIAA Lighter-than-Air Systems Technology Conference Proceedings, Annapolis, Maryland, July 8-10, 1981.

17. DeLaurier, J. and Hui, K. C. K. - "Airship Survivability in Atmospheric Turbulence", AIAA Lighter-than-Air Systems Technology Conference Proceedings, Annapolis, Maryland, July 8-10, 1981.

18. DeLaurier, J., Wong, K. Y. and Zhiyoung, L. - "An Application of Source-Panel and Vortex Methods for Aerodynamic Solutions of Airships Configurations", AIAA 6th Lighter-than-Air Systems Technology Conference, Norfolk, Va., June 26-28, 1985.

19. DeLaurier, J. and King, A. - "An Experimental Investigation of the Aerodynamic Effects on a Body of Revolution in Turning Flight" AIAA 6th Lighter-than-Air Systems Technology Conference Proceedings, Norfolk, Va., June 26-28, 1985.

20. Amann, J. H. - "A Comparison of a Nonlinear Flight Dynamic Simulation of an Airship with Flight Test Results", AIAA 7th Lighter-than-Air Technology Conference Proceedings, Monterey, Ca., August 17-19, 1987.

21. DeLaurier, J. and Lowe, J. D. - "A Six-Degree of Freedom Heavy Lift Airship Flight Simulation", AIAA Lighter-than-Air Systems Conference Proceedings, Anaheim, Ca., July 25-27 1983.

22. Jex, H. R., Magdaleno, R.E., Gelhausen, P. and Tischler, M. P. - "Pre-and Post-Flight-Test Models Versus Measured Skyship-500 Control Responses", AIAA 7th Lighter-than-Air Technology Conference Proceedings, Monterey, Ca., August 17-19, 1987.

23. Jex, H. R., Magdaleno, R. E. and Johnson, W. A. - "LTASIM - A Desktop Nonlinear Airship Simulation", Systems Technology Inc. Paper No. 448, presented at Society of Flight Test Engineers Lighter-than-Air Test and Evaluation Workshop, Solomons, Md, 5-6 June 1990.

24. Munk, M. M. - "The Aerodynamic Forces on Airship Hulls", NACA Report No. 184, 1924.

25. Munk, M. M. - "Aerodynamics of Airships", in Aerodynamic Theory, Vol. 6, Durand, W. F., ed., Julius Springer, Berlin, 1936.

26. Upson, R. H. and Klikoff, W. A. - "Application of Practical Hydrodynamics to Airship Design", NACA Report No. 405, 1931.

27. Freeman, H. B. - "Measurements of Flow in the Boundary Layer of a 1/40 Scale Model of the US Airship Akron", NACA Report No. 430, April 1932.

28. Freeman, H. B. - "Force Measurements on a 1/40 Scale Model of the US Airship Akron", NACA Report No. 432, May 1932.

29. Freeman, H. B. - Pressure Distribution Measurements on the Hull and Fins of a 1/40 Scale Model of the US Airship Akron", NACA Report No. 443, June 1932.

30. Gomes, S. B. V. - "The College of Aeronautics to Cooperate in the Sentinel 5000 Airship Development Programme", Aerogram - The Newspaper of the College of Aeronautics, Vol. 5, No. 2, May 1988.

31. "Project Proposal - Flight Dynamics of Sentinel 5000", prepared by R. I. Harris, College of Aeronautics, C. I. T., November 1987.

32. Niedermayer, E. J. - "British Civil Airworthiness Requirements for Airships", AIAA Lighter-than-Air Systems Technology Conference Proceedings, Palo Alto, Ca., July 11-13, 1979.

33. Hurst, D. - "Wind Tunnel Tests for Airship Industries (UK) Limited", University of Southampton, Department of Aeronautics and Astronautics, December 1986.

34. Hamwi, S. - "Approximate Methods for Predicting the Lifting Characteristics of Wing-Body Combinations", PhD thesis, College of Aeronautics, Cranfield Institute of Technology, December 1989.

35. Gomes, S. B. V. - "Task 1 Report: Surface Roughening Technique Investigation for Airship Wind Tunnel Testing & Pressure Distribution Around a Skyship-600 Model", College of Aeronautics, Cranfield Institute of Technology, Cranfield, CoA Rpt. No. 8901, January 1989.

36. Gomes, S. B. V. - "Task 1A Report: Investigation of Alternative Hull and Fin Combinations for the Sentinel 5000 Aircraft", College of Aeronautics, Cranfield Institute of Technology, Cranfield, CoA Rpt. No. 8902, January 1989.

37. Gomes, S. B. V. - "Task 2 Report: Measurement of Forces and Moments, Pressure Distribution and Hinge Moments on a 1/75 Scale Model of the Sentinel 5000 Airship", College of Aeronautics, Cranfield Institute of Technology, Cranfield, CoA Rpt. No. 8903, January 1989.

38. Simmons, L. F. G. - "Note Relating Two Oscillation Methods in Use for Determining Rotary Derivatives of Models", Aeronautical Research Committee, Reports and Memoranda No. 711, January 1921.

39. Gomes, S. B. V. - "Task 3 Report: Measurement of Some

Aerodynamic Damping Derivatives for the YEZ-2A Airship", College of Aeronautics, Cranfield Institute of Technology, Cranfield, CoA Rpt. No. NFP 8909, May 1989.

40. Gomes, S. B. V. - "Task 4 Report: Measurement of a YEZ-2A Airship Model Response to Low-Altitude Turbulence", College of Aeronautics, Cranfield Institute of Technology, Cranfield, CoA Rpt. No. NFP 8910, July 1989.

41. Nippress, K. R. and Gomes, S. B. V. - "Estimation of Flight Dynamics Characteristics of the YEZ-2A", AIAA 8th Lighter-than-Air Systems Technology Conference, Paper, No. AIAA-89-3173, Jacksonville, Fl, October 5-7, 1989.

42. Lewis, D. J., Lipscombe, J. M. and Thomasson, P. G. - "The Simulation of Remotely Operated Underwater Vehicles", Proceedings of the ROV '84 Conference and Exposition, The Marine Technology Society, San Diego, Ca., 1984.

43. Cook, M. V. - "The Linearised Small Perturbation Equations of Motion for an Airship", Working Paper No. WP 8, Aerodynamics Department, College of Aeronautics, C. I. T., Cranfield, July 1987 (Revised January 1990).

44. Donnelly, S. L. - "An Analogue Simulation to Investigate Airship Dynamic Stability", MSc thesis, College of Aeronautics, Cranfield Institute of Technology, Cranfield, 1988.

45. Jones, R. and Williams, D. H. - "The Stability of Airships", Aeronautical Research Committee, Report

and Memoranda No. 751, June 1921.

46. Thomasson, P. G. - "ACSL Torpedo Simulation Program", internal communication, College of Aeronautics, Cranfield Institute of Technology, Cranfield.

47. Thomasson, P. G. - Lecture notes from the Flight Dynamics Simulation Course, College of Aeronautics, Cranfield Institute of Technology, Cranfield.

48. Lamb, H. - "The Inertia Coefficients of an Ellipsoid Moving in Fluid", Aeronautical Research Committee, Report and Memoranda No. 623.

49. Thomasson, P. G. - "F16 Simulation Program", internal communication, College of Aeronautics, Cranfield Institute of Technology, Cranfield.

50. Babister, A. W. - "Aircraft Dynamic Stability and Response", Pergamon Press, Oxford, 1980.

51. "Installation Manual: CT7-5A, -5A1, -5A2, -7,-7A, -7E and 7E1", General Electric Company, Aircraft Engine Business Group, SEI-585, May 1985.

52. Nelson, R. C. - "Flight Stability and Automatic Control", McGraw-Hill Book Company, 1989.

53. Ashley, H. - "Engineering Analysis of Flight Vehicles", Addison-Wesley, Reading, Mass., 1974.

54. Advanced Continuous Simulation Language (ACSL) Reference Manual, Mitchell and Gauthier Associates, Concord, Mass.,1986.

55. Lipscombe, J. M. - "Airship Modes at Hover",

"Longitudinal Modes of Airship Motion" and "Lateral Modes of Airship Motion", internal communications, College of Aeronautics, Cranfield Institute of Technology, Cranfield, June 1988.

56. Doetsch, K. H. - "The Time Vector Method for Stability Investigations", Reports and Memoranda No. 2945, August 1953.

57. Cooper, R. P. and Harper, G.E. - "Handling Qualities and Pilot Evaluation", Journal of Guidance, Vol. 9, No.5, Sept-Oct 1986, pp. 515-529.

58. Mooij, H. A. - Criteria for Low-Speed Longitudinal Handling Qualities of Transport Aircraft with Closed-Loop Flight Control Systems, Martinus Nijhoff Publishers, The Netherlands, 1985.

59. Gibson, J. C. - "Piloted Handling Qualities Design Criteria for High Order Flight Control Systems", in AGARD-CP-333 on Criteria for Handling Qualities of Military Aircraft, 1982, pp. 4.1-15.

60. Gibson, J. C. - "Handling Qualities for Unstable Combat Aircraft", Proceedings of the 15th Congress of the International Council of the Aeronautical Sciences (ICAS), London, 7-12 Sept, 1986.

61. Anon., "Flying Qualities of Piloted Airplanes", MIL-F-8785C, November 1980.

A P P E N D I X - 1

Data Base Summary

A1.1 Introduction

The purpose of this Appendix is to complement the description of the data base as employed in the flight dynamics simulation model of the YEZ-2A airship, and whose main features are presented in Chapter 2. The order of the material here presented follows the same sequence of Chapter 2 topics for easier reference.

A1.2 YEZ-2A General Data

* Total envelope volume = 70870.2 m^3
* Reference area = 1712.5 m^2 $\left(\text{i.e., Volume}^{2/3}\right)$
* Hull length = 129.5 m (≡ Reference length)
* Maximum hull diameter = 32.0 m
* Turboprop engine thrust line distance from the hull centre line c_z = 20.1 m (See Fig. 4.5)
* Diesel engines thrust point horizontal distance from the OYZ plane d_x = 3.5 m (See Fig.4.5)
* Diesel engines horizontal thrust line distance from the OXZ plane d_y = 7.87 m (See Fig. 4.5)
* Diesel engines thrust point vertical distance from the OXY plane d_z = 21.0 m (See Fig. 4.5)
* Centre of Volume distance from the airship bow, along the hull centre line = 60.2 m
* Distance between the aerodynamic centre of the tail fins and the CV = 41.4 m (i.e., tail moment arm)
* Lamb's inertia coefficients for movement along OX, OY and rotation about OY (See Section 4.3.4) were estimated, for the YEZ-2A case, as respectively
  k_1 = 0.085
  k_2 = 0.865
  k' = 0.61
* Diesel engine propeller efficiency (Equation 4.25 of Section 4.7) η_D = 0.6
* Turboprop engine propeller efficiency (Equation 4.25 of

Section 4.7) η_T = 0.6

* Coordinates of the forward ballonet CG with respect to the body axes system (See Fig. 4.2):

  FB_x = 34.96 m (along OX)
  FB_y = 0.0 m (along OY)
  FB_z = 7.07 m (along OZ)

* Coordinates of the aft ballonet CG with respect to the body axes system (See Fig. 4.2):

  AB_x = -34.96 m (along OX)
  AB_y = 0.0 m (along OY)
  AB_z = 6.31 m (along OZ)

* Coordinates of the starboard pannier ballonet CG with respect to the body axes system (See Fig. 4.2):

  PBS_x = 0.06 m (along OX)
  PBS_y = 13.21 m (along OY)
  PBS_z = 1.52 m (along OZ)

* Coordinates of the port pannier ballonet CG with respect to the body axes system (See Fig. 4.2):

  PBP_x = 0.06 m (along OX)
  PBP_y = -13.21 m (along OY)
  PBP_z = 1.52 m (along OZ)

A1.3 Test Rigs

The following pages present a picture of the test rigs used to obtain the aerodynamic data base in the form of Tasks 1, 2, 3 and 4. The Task 1A rig was essentially the same as that of Task 2 and therefore is not presented here.

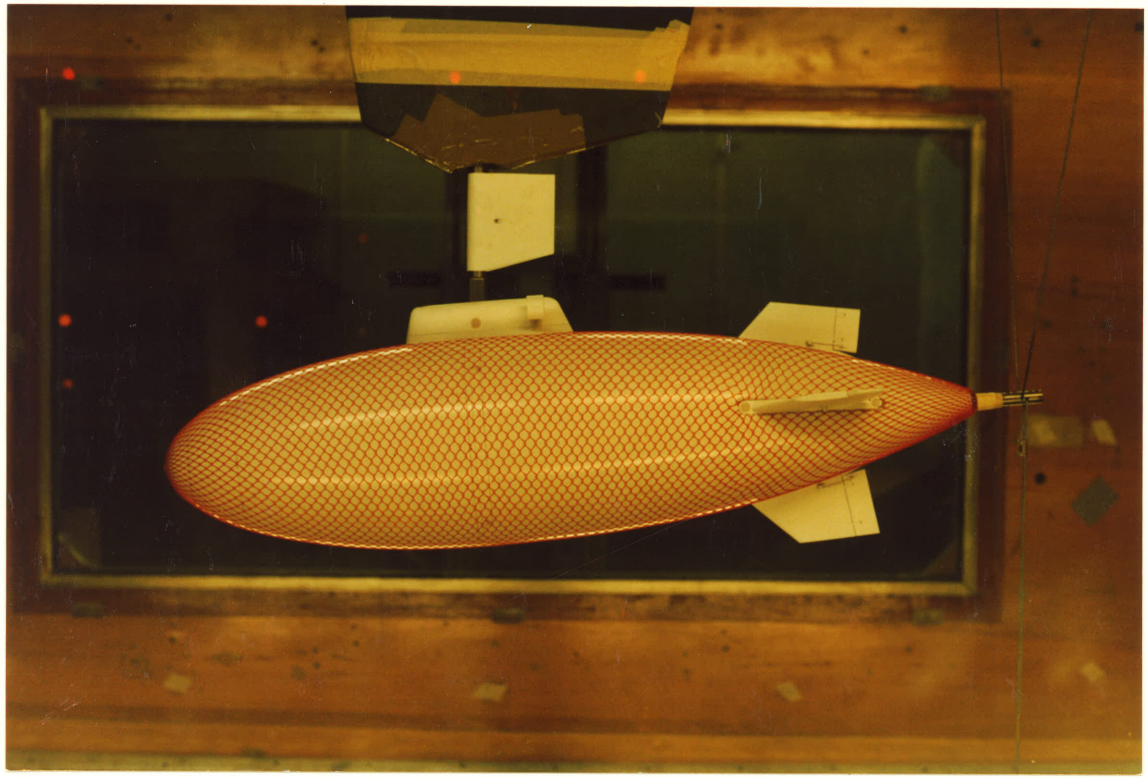


Figure A1.3.1 - The Skyship-600 1:75 scale model fitted with a fishnet stocking in the 8ft X 6ft wind tunnel of the College of Aeronautics. The model was monted upside down in the tunnel test section, the attachment point being the geometric centre of the gondola. This was the strongest type of surface roughness tried in the Task 1 series of tests.

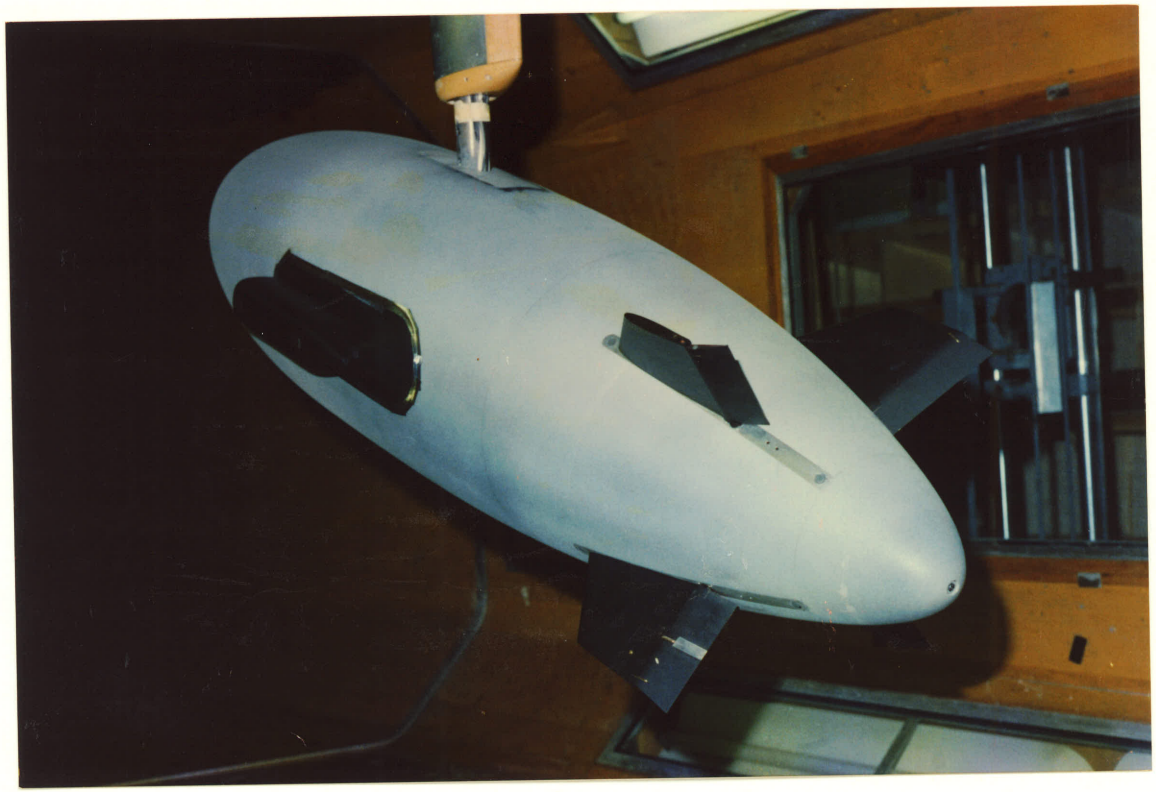


Figure A1.3.2 - The Task 2 YEZ-2A 1:75 scale model in the test section of the 8ft X 6ft wind tunnel of the College of Aeronautics. The model is suspended from the balance strut by its port side, the attachment point being the Centre of Volume inside the hull. It is shown here with 30 degrees of lateral incidence(vertical plane of the test section) and 0 degree of longitudinal incidence (horizontal plane of the test section). The ruddervators are deflected to generate an "elevators up by 25 degrees" case.



Figure A1.3.3 - The Task 3 YEZ-2A 1:75 scale model in the test section of the 8ft X 6ft wind tunnel of the College of Aeronautics. The model is configured for a yaw oscillation test, with the gondola fitted to its underside. For the pitch oscillation test the gondola was fitted to the model port side. The electric driving motor can be seen on the far left side. The picture is of the first series of trials. For the second series stiffer springs were fitted and the connecting piano wires were substituted with metal rods.

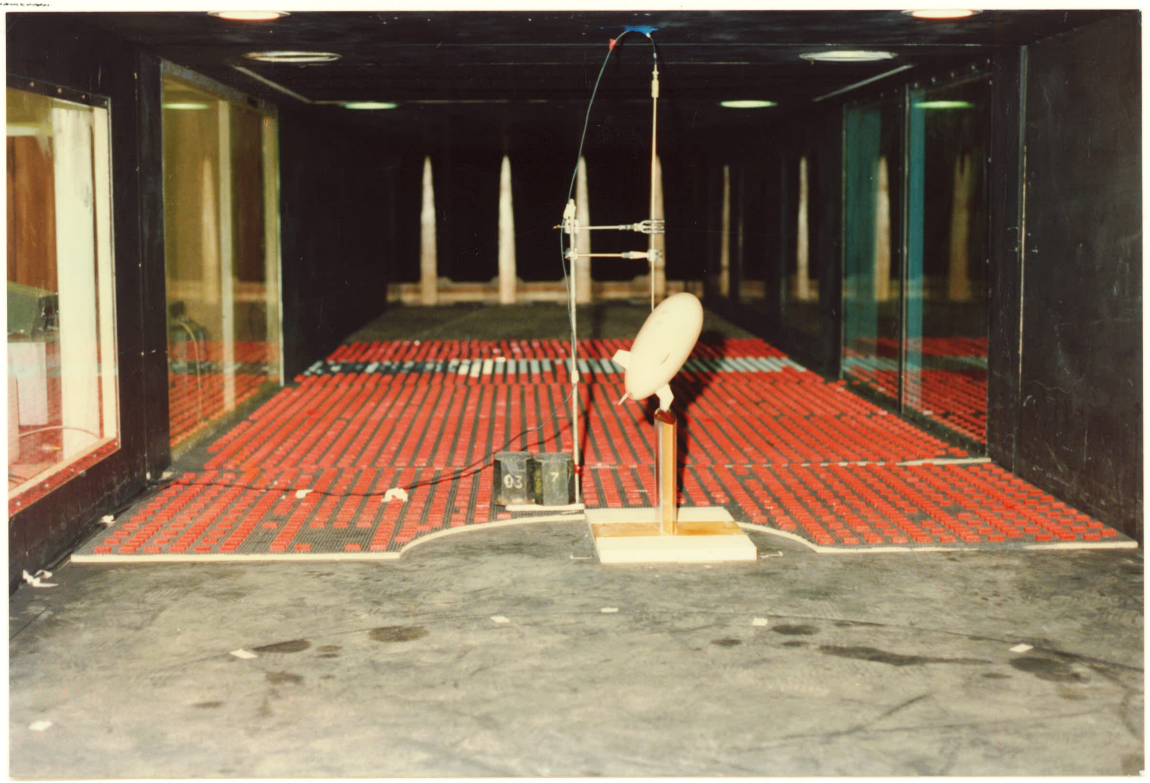


Figure A1.3.4 - The Task 4 1:200 scale model of the YEZ-2A airship in the test section of the 8ft X 4ft Earth Boundary Layer wind tunnel of the College of Aeronautics. The toy 'Lego' boards (foreground ahead of the model), the castellated wall and the Counihan teeth (background) were the devices employed to simulate the lower atmosphere turbulent boundary layer at the same scale as that of the model. The mast just in front of the model houses the hot-wire anemometer with which instantaneous readings of the u and w-velocity components were obtained. These were later correlated to the model response in terms of lift and pitching moment.

A1.4 Task 2 Data Base

The YEZ-2A aerodynamic data base obtained as a result of carrying out Task 2 is presented in the following pages in the form of graphs for easier inspection. The non-dimensional coefficients of forces and moments follow the standard convention for airships, i.e.,

* Drag Coefficient: $$C_D = \frac{D}{0.5 \times \rho \times U^2 \times S}$$

* Side Force Coefficient: $$C_Y = \frac{Y}{0.5 \times \rho \times U^2 \times S}$$

* Lift Coefficient: $$C_L = \frac{L}{0.5 \times \rho \times U^2 \times S}$$

* Rolling Moment Coefficient $$C_l = \frac{l}{0.5 \times \rho \times U^2 \times V}$$

* Pitching Moment Coefficient $$C_m = \frac{m}{0.5 \times \rho \times U^2 \times V}$$

* Yawing Moment Coefficient $$C_n = \frac{n}{0.5 \times \rho \times U^2 \times V}$$

where,

D = Drag force (N)
Y = Side force (N)
L = Lift force (N)
ρ = Air density (Kg/m^3)
V = Airship model volume (m^3)
l = Rolling moment (N.m)
m = Pitching moment (N.m)
n = Yawing moment (N.m)
U = Air speed in wind tunnel test section (m/s)
$S = V^{2/3}$ (m^2)

In the following graphs, the above coefficients are given as a function of the standard longitudinal incidence α. In each graph the value of the airship

model lateral incidence is also specified. This is given in terms of the model angle of yaw ψ in the tunnel test section, where (from Ref. 50, page 16)

$$\beta = -\psi \qquad \text{(A1.1)}$$

As far as the aerodynamics of the airship are concerned, it is of course the sideslip angle β that matters and, in the YEZ-2A flight dynamics simulation program, the change of sign given by Equation (A1.1) was incorporated in the algorithm.

Each graph also specifies the control surface (ruddervator) deflection test case. The model was tested so that all ruddervators would be up or down, i.e., a so called 'elevator' case, all ruddervators would be deflected to the starboard or port sides, i.e., a 'rudder' case, or, finally, all surfaces would be deflected to give the model a positive roll rate p about the OX axis, i.e., an 'aileron' case.

The test Reynolds number based on the airship model length that was achieved in the 8ft X 6ft wind tunnel was of the order of 6×10^6. The results presented in graph format in the following pages were imported directly into the YEZ-2A simulation program and they constituted the source of static force and moment coefficients for the simulation model aerodynamic data base.

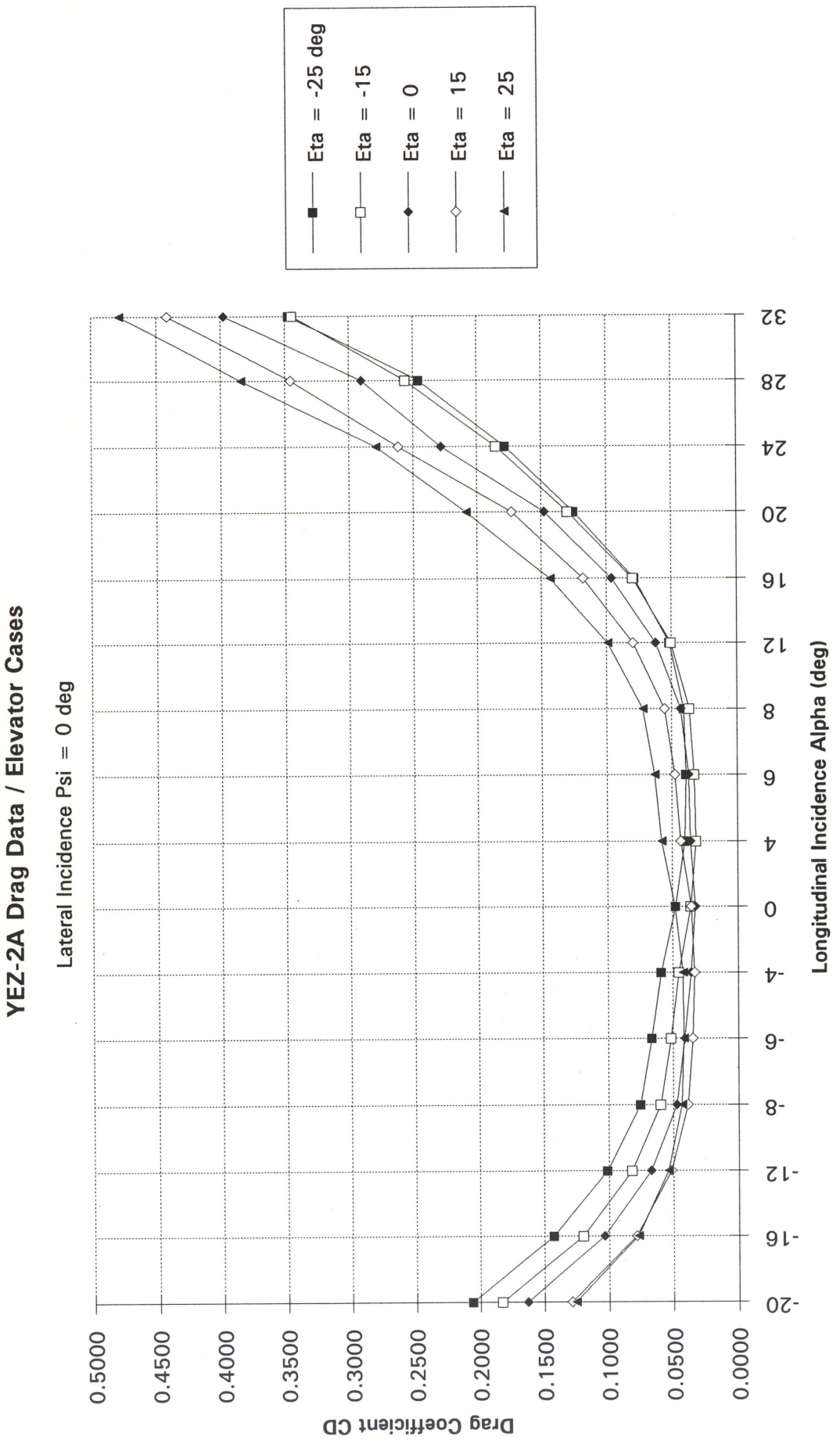

YEZ-2A Drag Data / Elevator Cases
Lateral Incidence Psi = 0 deg
Eta = -25 deg
Eta = -15
Eta = 0
Eta = 15
Eta = 25
Drag Coefficient CD
0.5000
0.4500
0.4000
0.3500
0.3000
0.2500
0.2000
0.1500
0.1000
0.0500
0.0000
Longitudinal Incidence Alpha (deg)
-20
-16
-12
-8
-6
-4
0
4
6
8
12
16
20
24
28
32

FIGURE A1.4.1

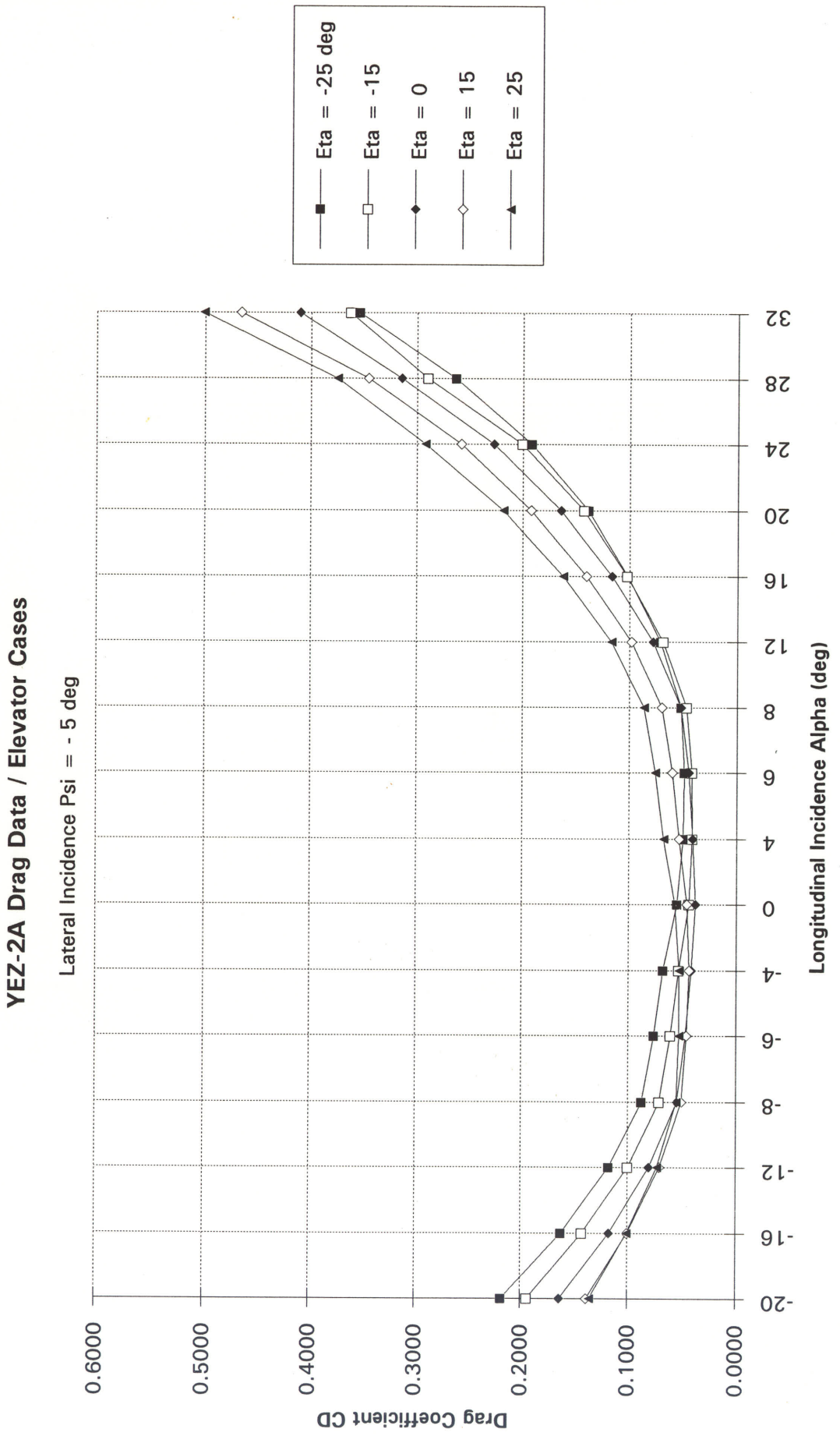

YEZ-2A Drag Data / Elevator Cases
Lateral Incidence Psi = - 5 deg
Eta = -25 deg
Eta = -15
Eta = 0
Eta = 15
Eta = 25
Drag Coefficient CD
0.6000
0.5000
0.4000
0.3000
0.2000
0.1000
0.0000
Longitudinal Incidence Alpha (deg)
-20
-16
-12
-8
-6
-4
0
4
6
8
12
16
20
24
28
32

FIGURE A1.4.2

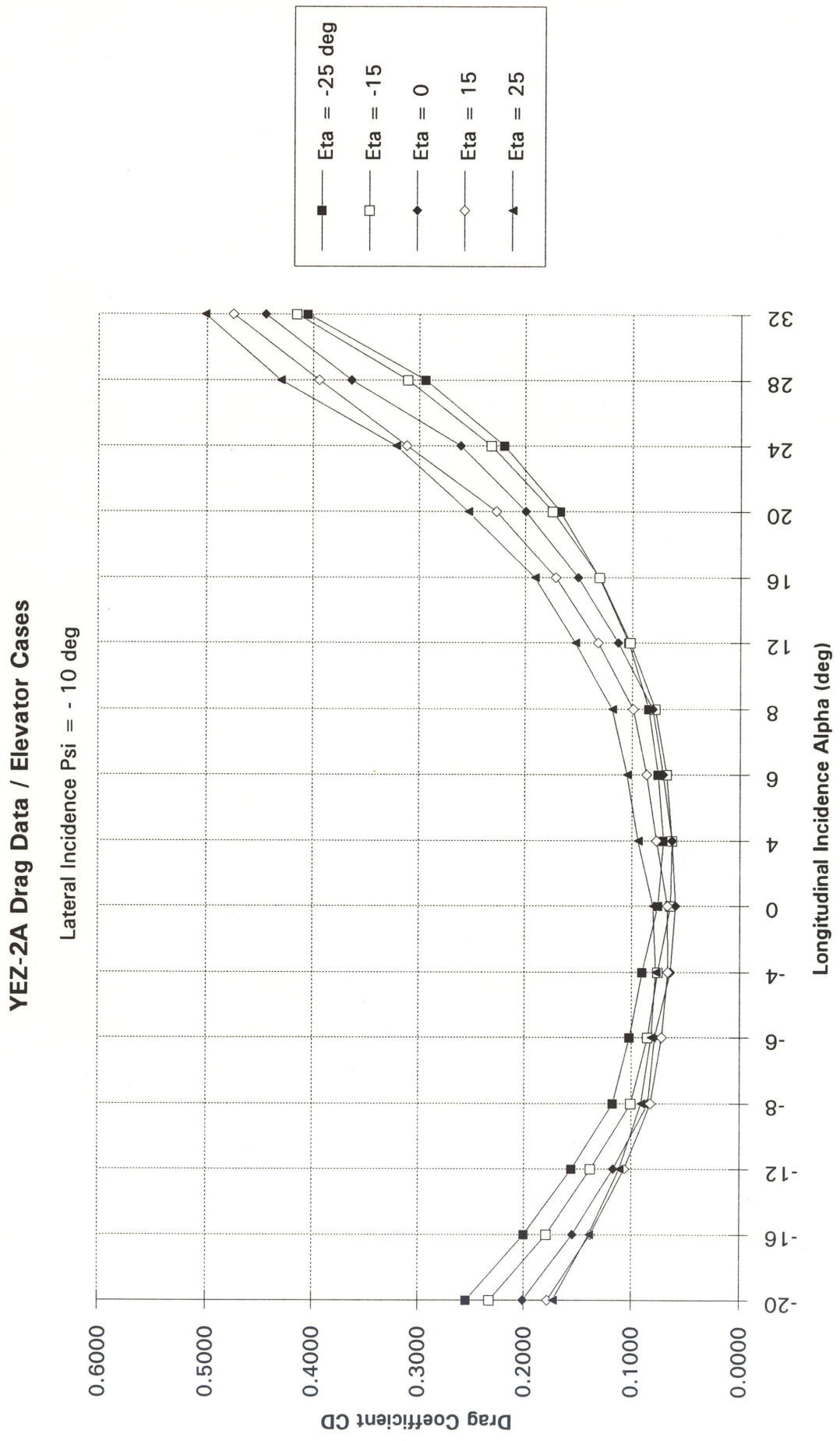

YEZ-2A Drag Data / Elevator Cases
Lateral Incidence Psi = - 10 deg
Eta = -25 deg
Eta = -15
Eta = 0
Eta = 15
Eta = 25
Drag Coefficient CD
0.6000
0.5000
0.4000
0.3000
0.2000
0.1000
0.0000
Longitudinal Incidence Alpha (deg)
-20
-16
-12
-8
-6
-4
0
4
6
8
12
16
20
24
28
32

FIGURE A1.4.3

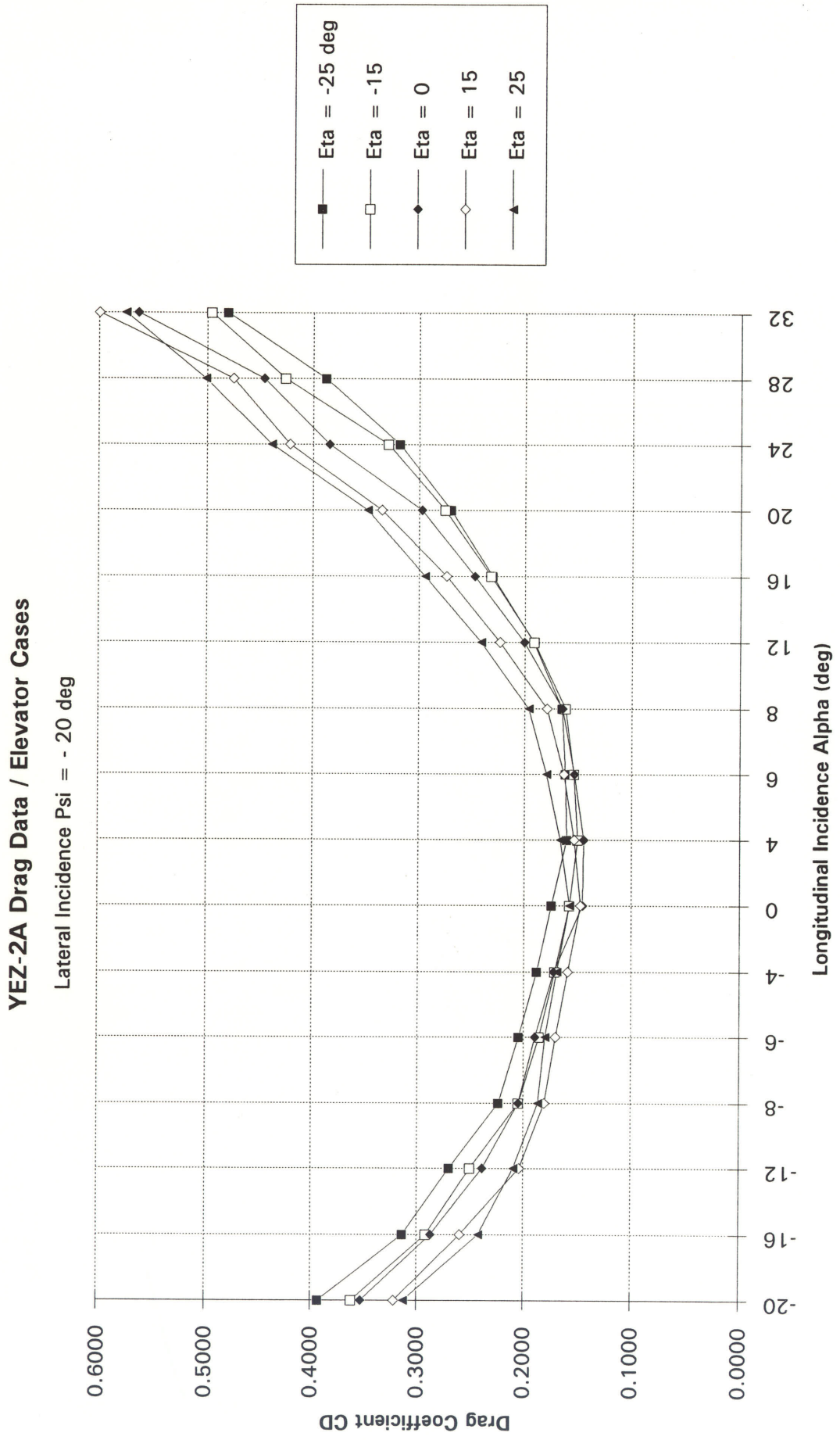

YEZ-2A Drag Data / Elevator Cases
Lateral Incidence Psi = - 20 deg
Eta = -25 deg
Eta = -15
Eta = 0
Eta = 15
Eta = 25
Drag Coefficient CD
0.6000
0.5000
0.4000
0.3000
0.2000
0.1000
0.0000
Longitudinal Incidence Alpha (deg)
-20
-16
-12
-8
-6
-4
0
4
6
8
12
16
20
24
28
32

FIGURE A1.4.4

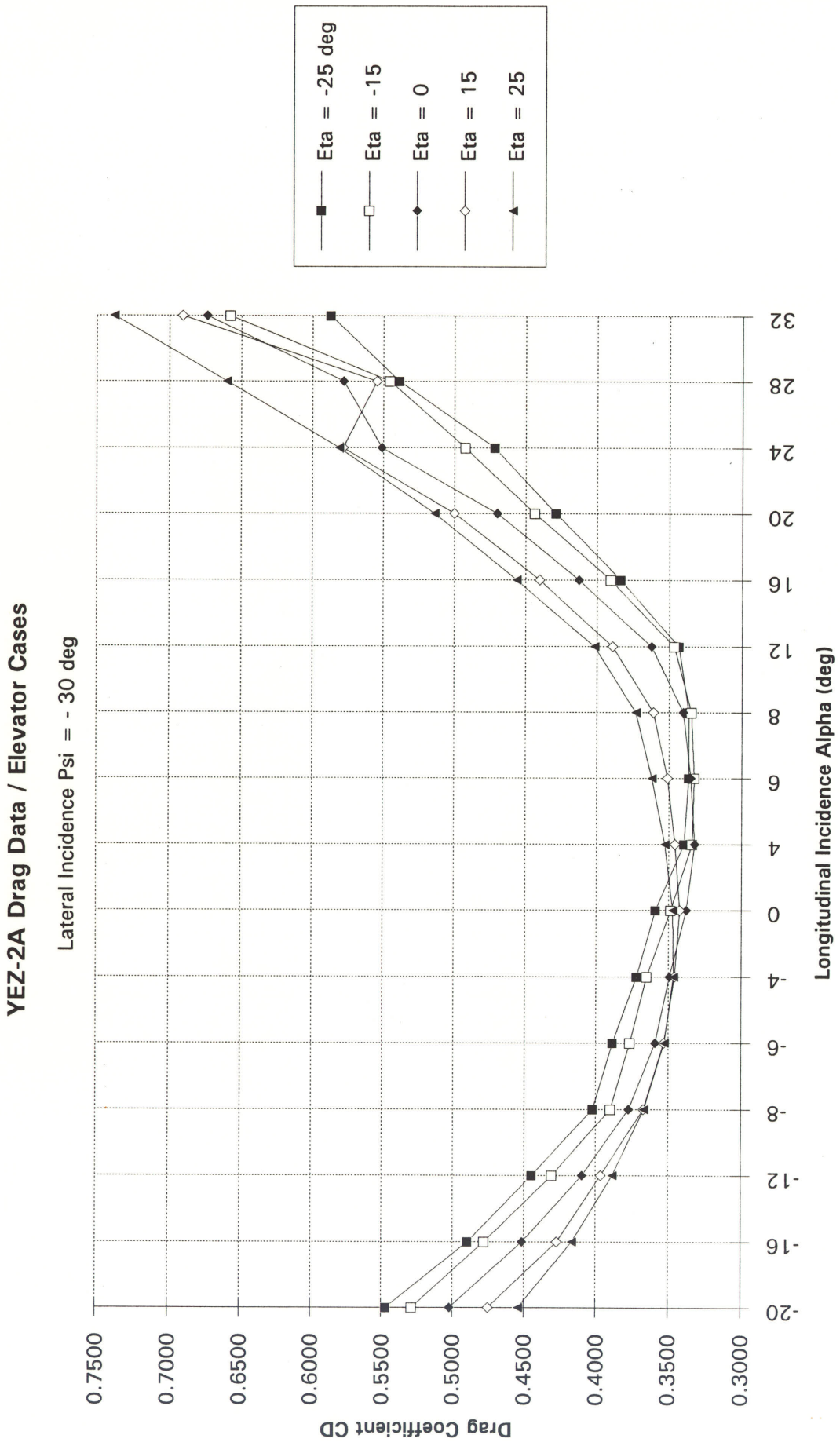

YEZ-2A Drag Data / Elevator Cases
Lateral Incidence Psi = - 30 deg
Eta = -25 deg
Eta = -15
Eta = 0
Eta = 15
Eta = 25
Drag Coefficient CD
0.7500
0.7000
0.6500
0.6000
0.5500
0.5000
0.4500
0.4000
0.3500
0.3000
Longitudinal Incidence Alpha (deg)
32
28
24
20
16
12
8
6
4
0
-4
-6
-8
-12
-16
-20

FIGURE A1.4.5

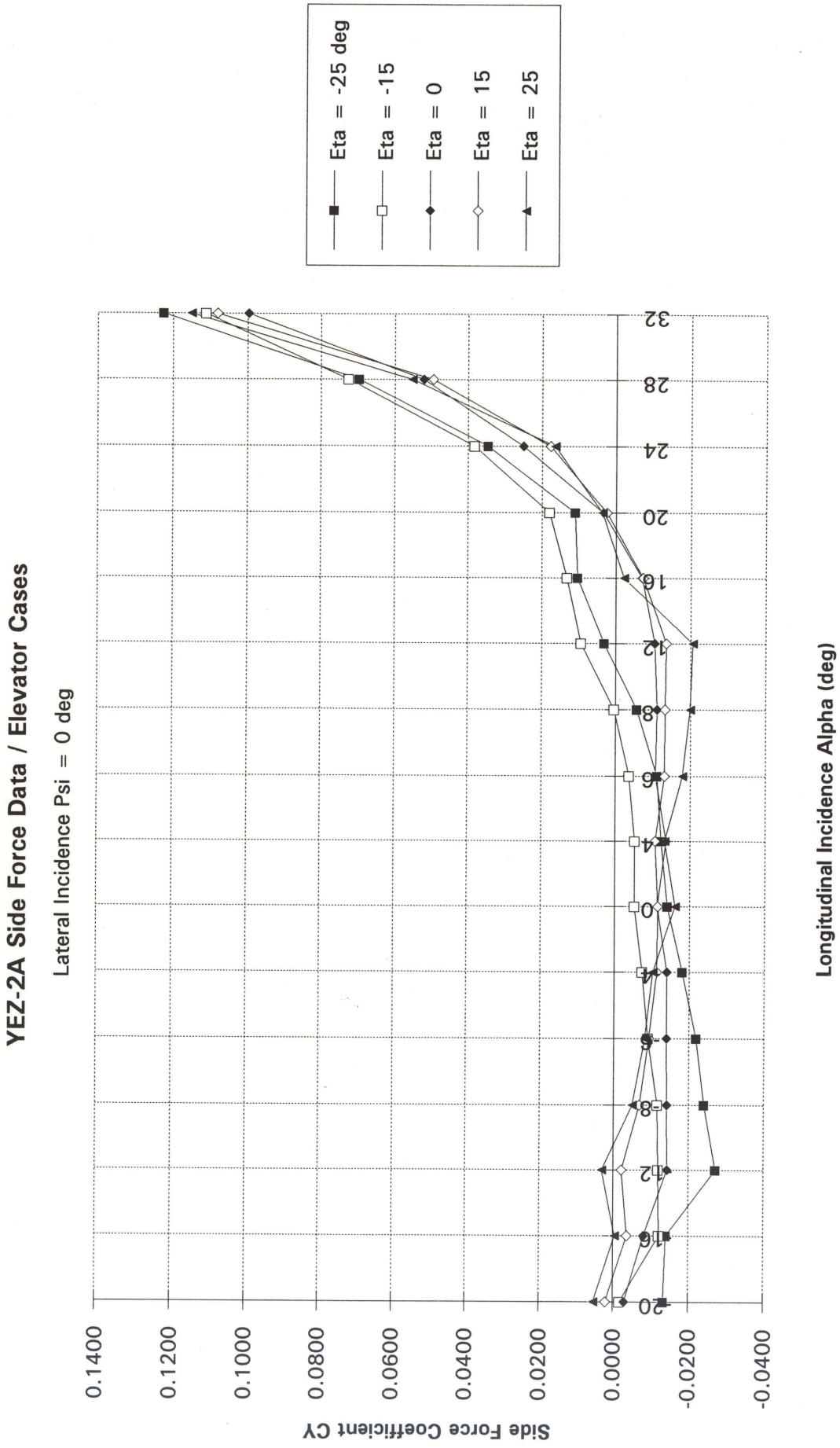

YEZ-2A Side Force Data / Elevator Cases
Lateral Incidence Psi = 0 deg
Eta = -25 deg
Eta = -15
Eta = 0
Eta = 15
Eta = 25
Side Force Coefficient CY
0.1400
0.1200
0.1000
0.0800
0.0600
0.0400
0.0200
0.0000
-0.0200
-0.0400
Longitudinal Incidence Alpha (deg)
32
28
24
20
16
12
8
4
0
-4
-8
-12
-16
-20

FIGURE A1.4.6

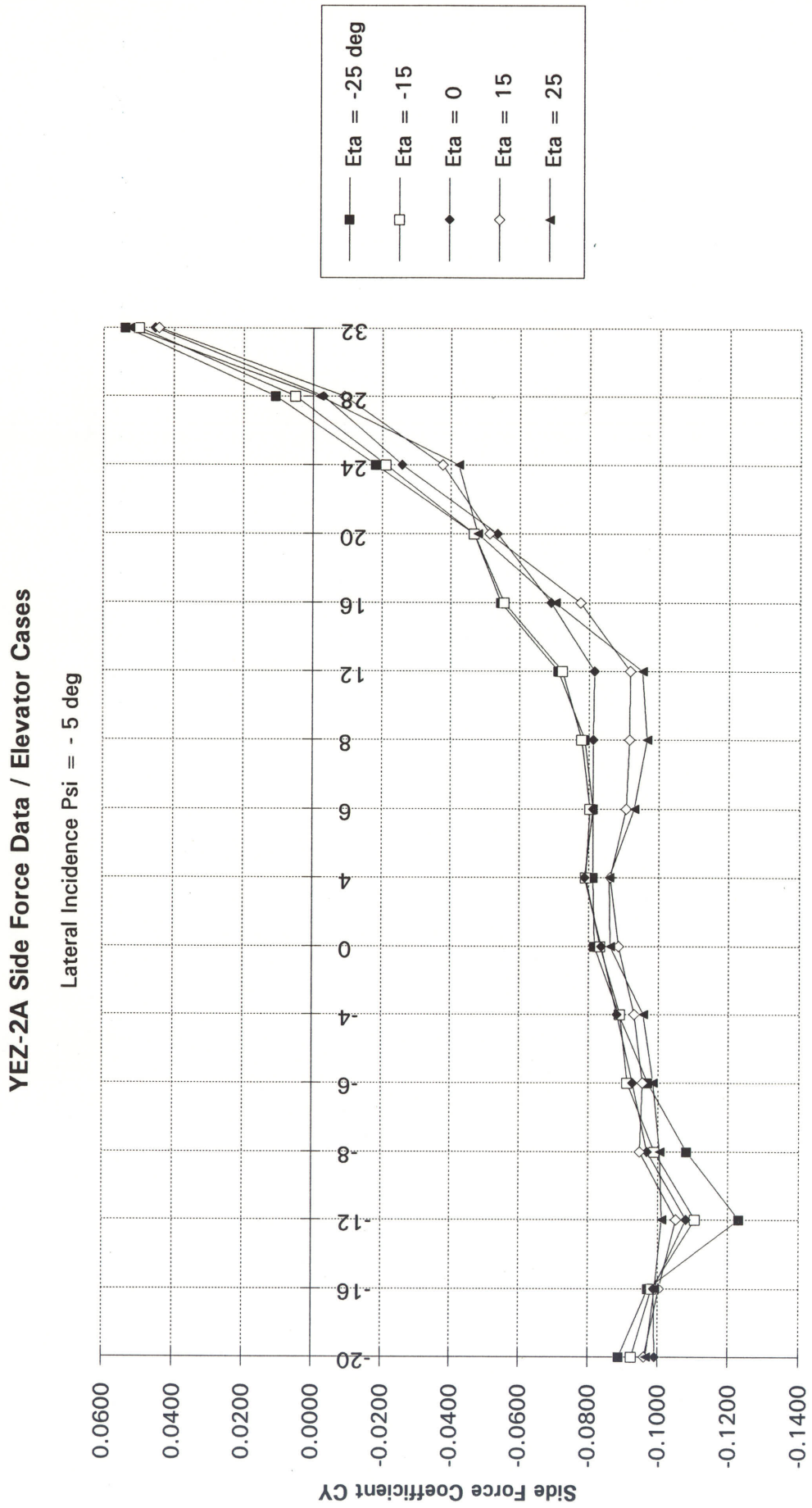

YEZ-2A Side Force Data / Elevator Cases
Lateral Incidence Psi = - 5 deg
Eta = -25 deg
Eta = -15
Eta = 0
Eta = 15
Eta = 25
Side Force Coefficient CY
0.0600
0.0400
0.0200
0.0000
-0.0200
-0.0400
-0.0600
-0.0800
-0.1000
-0.1200
-0.1400
Longitudinal Incidences Alpha (deg)
32
28
24
20
16
12
8
6
4
0
-4
-6
-8
-12
-16
-20

FIGURE A1.4.7

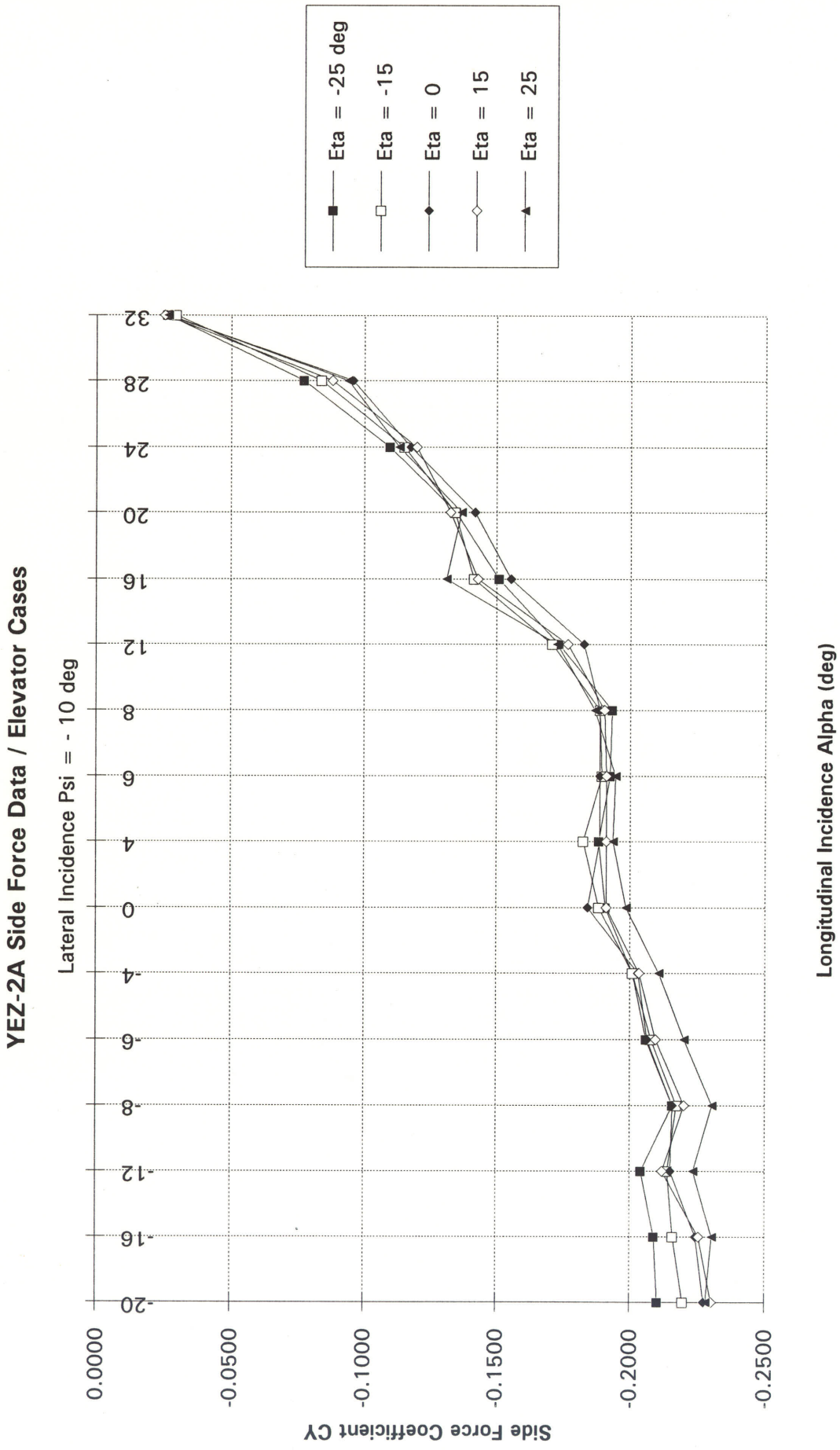

YEZ-2A Side Force Data / Elevator Cases
Lateral Incidence Psi = - 10 deg
Eta = -25 deg
Eta = -15
Eta = 0
Eta = 15
Eta = 25
Side Force Coefficient CY
0.0000
-0.0500
-0.1000
-0.1500
-0.2000
-0.2500
Longitudinal Incidence Alpha (deg)
32
28
24
20
16
12
8
6
4
0
-4
-6
-8
-12
-16
-20

FIGURE A1.4.8

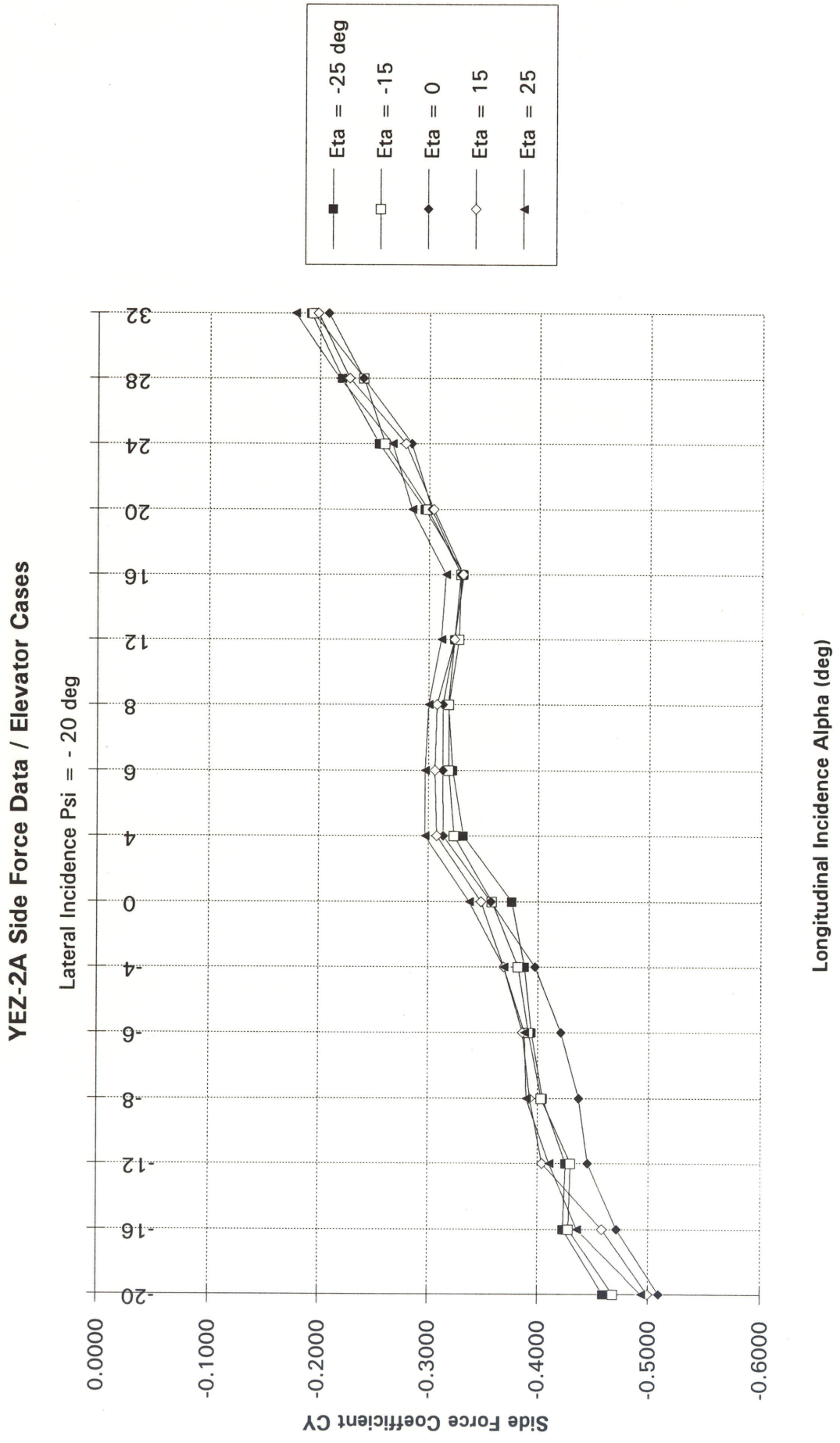

YEZ-2A Side Force Data / Elevator Cases
Lateral Incidence Psi = - 20 deg
Eta = -25 deg
Eta = -15
Eta = 0
Eta = 15
Eta = 25
Side Force Coefficient CY
0.0000
-0.1000
-0.2000
-0.3000
-0.4000
-0.5000
-0.6000
Longitudinal Incidence Alpha (deg)
32
28
24
20
16
12
8
6
4
0
-4
-6
-8
-12
-16
-20

FIGURE A1.4.9

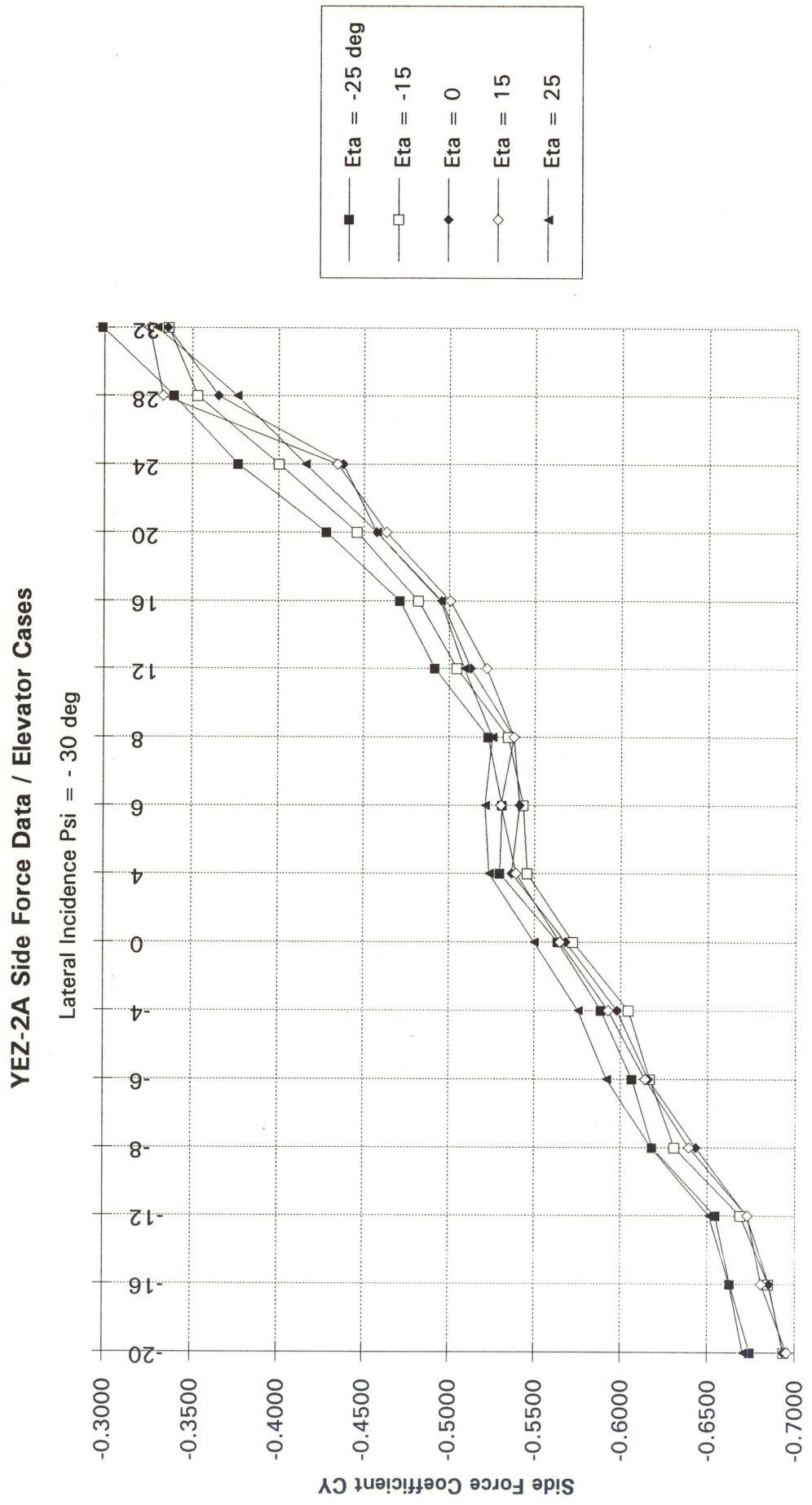


FIGURE A1.4.10

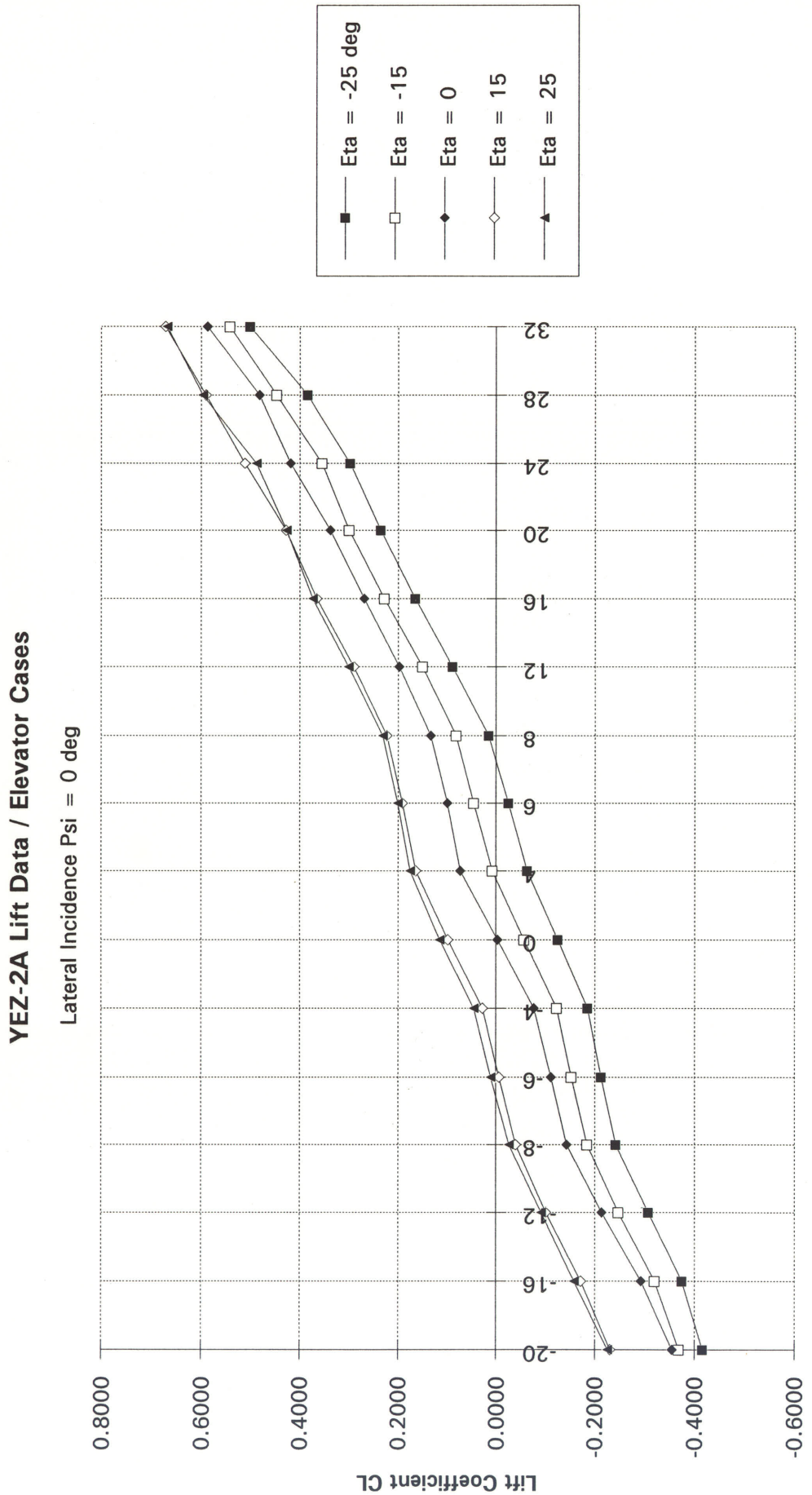


FIGURE A1.4.11

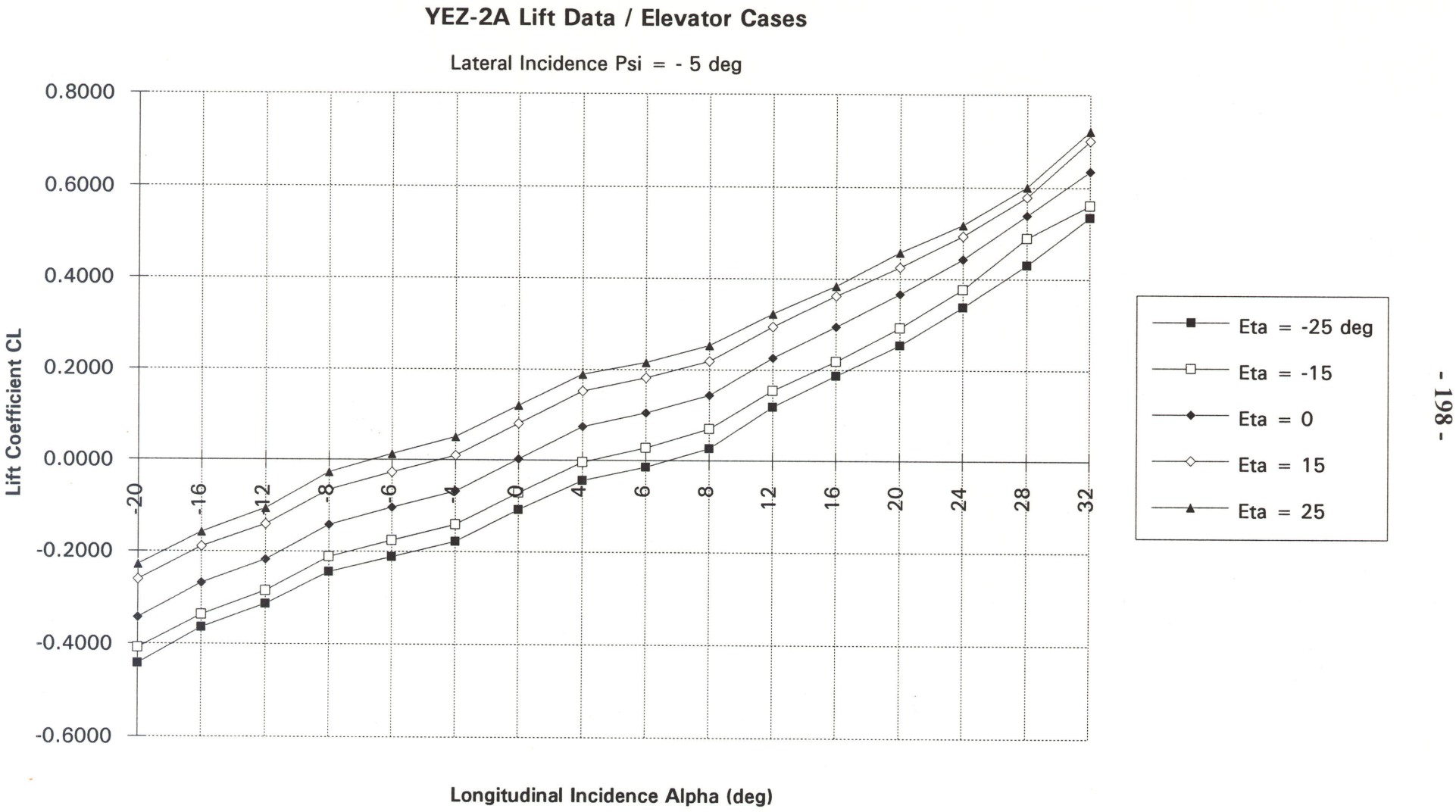


FIGURE A1.4.12

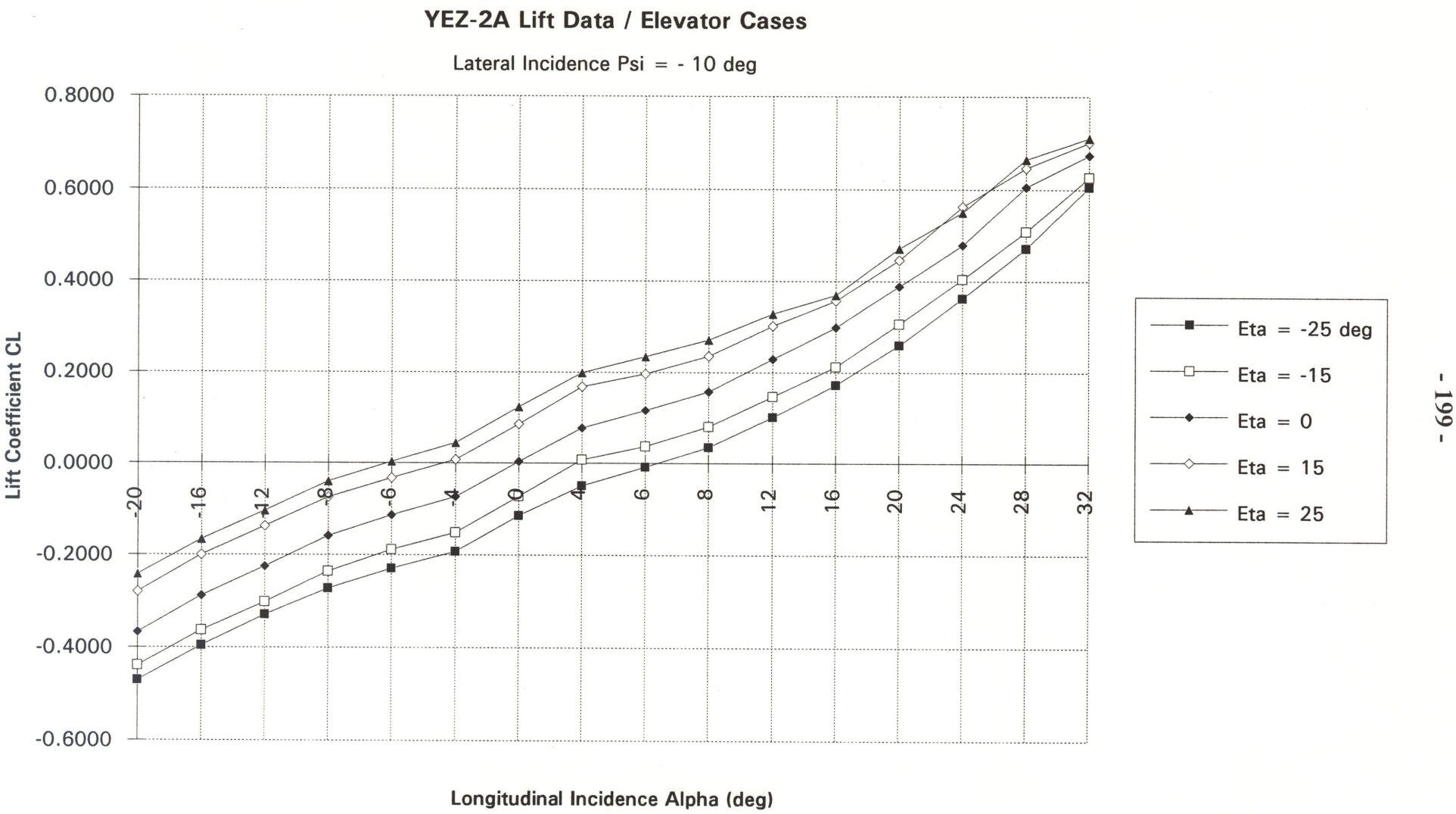


FIGURE A1.4.13

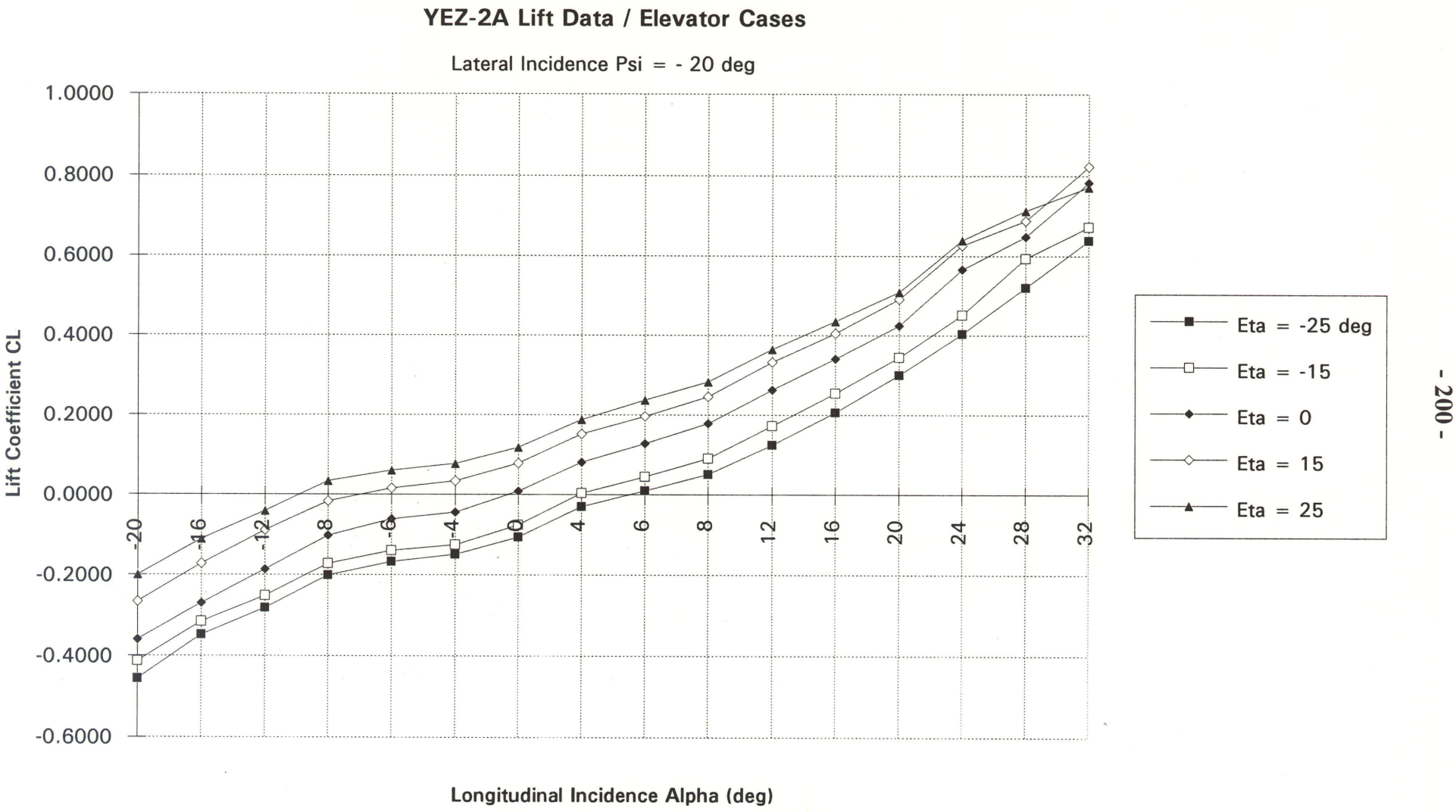


FIGURE A1.4.14

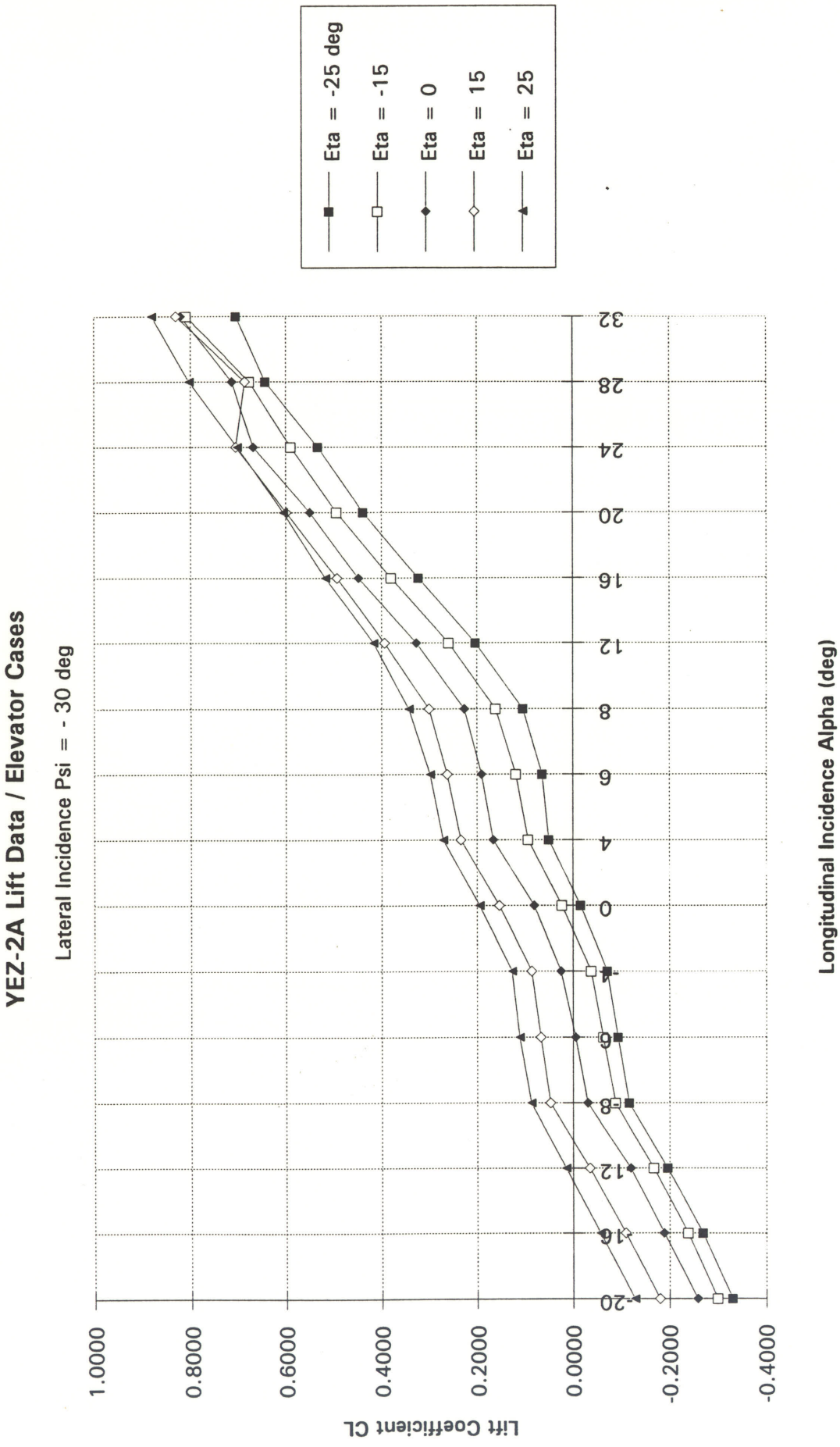


FIGURE A1.4.15

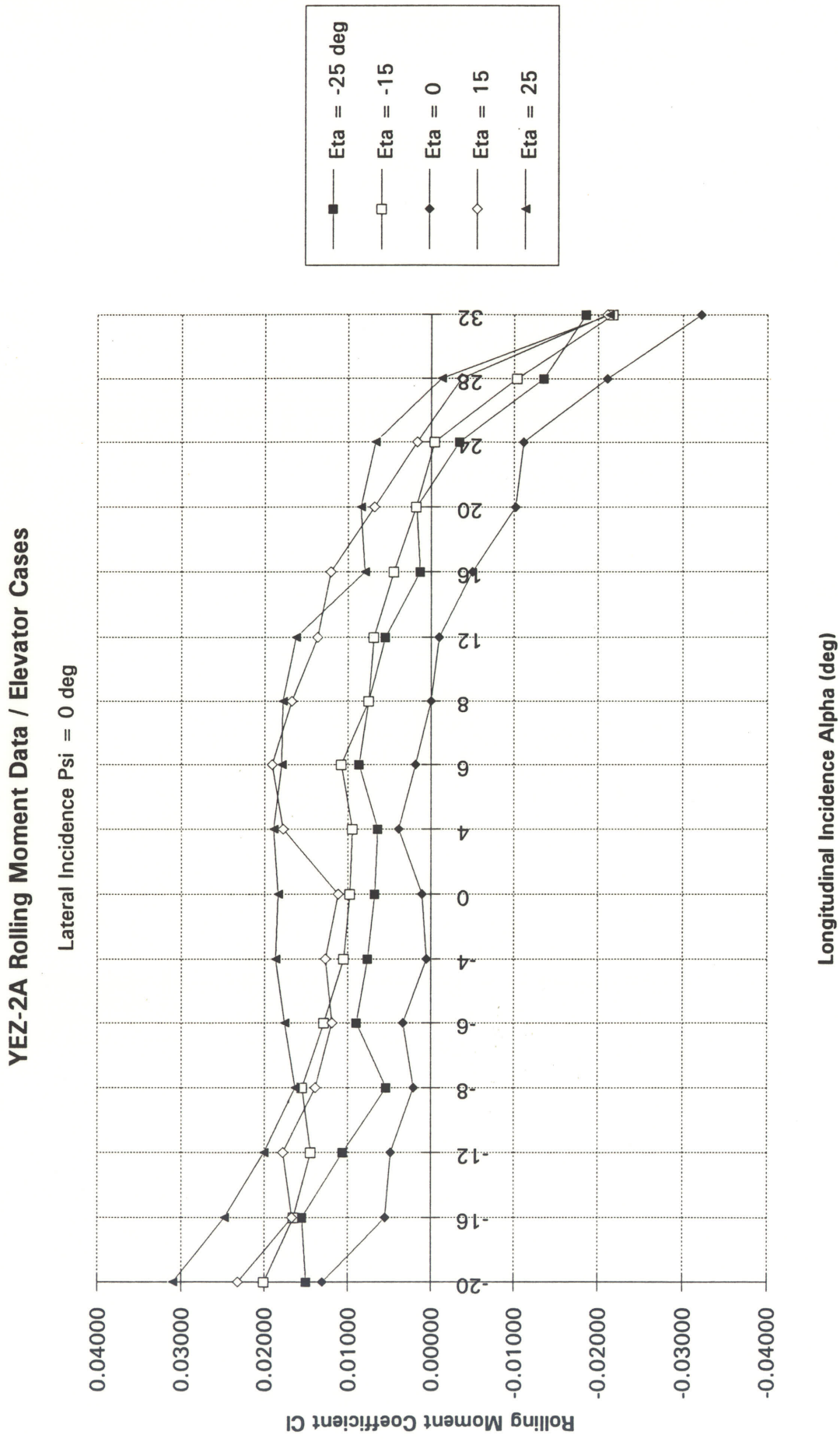


FIGURE A1.4.16

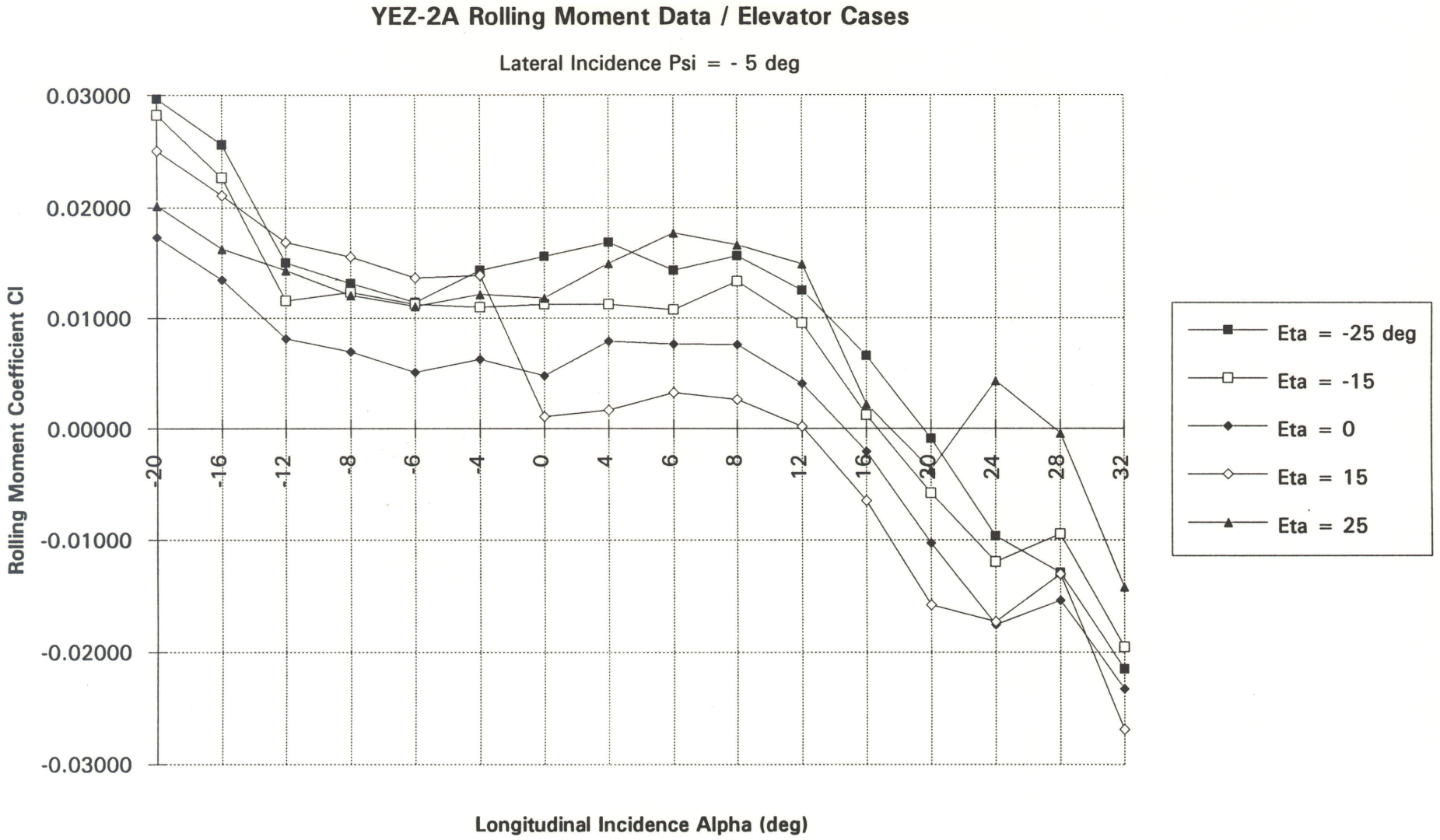


FIGURE A1.4.17

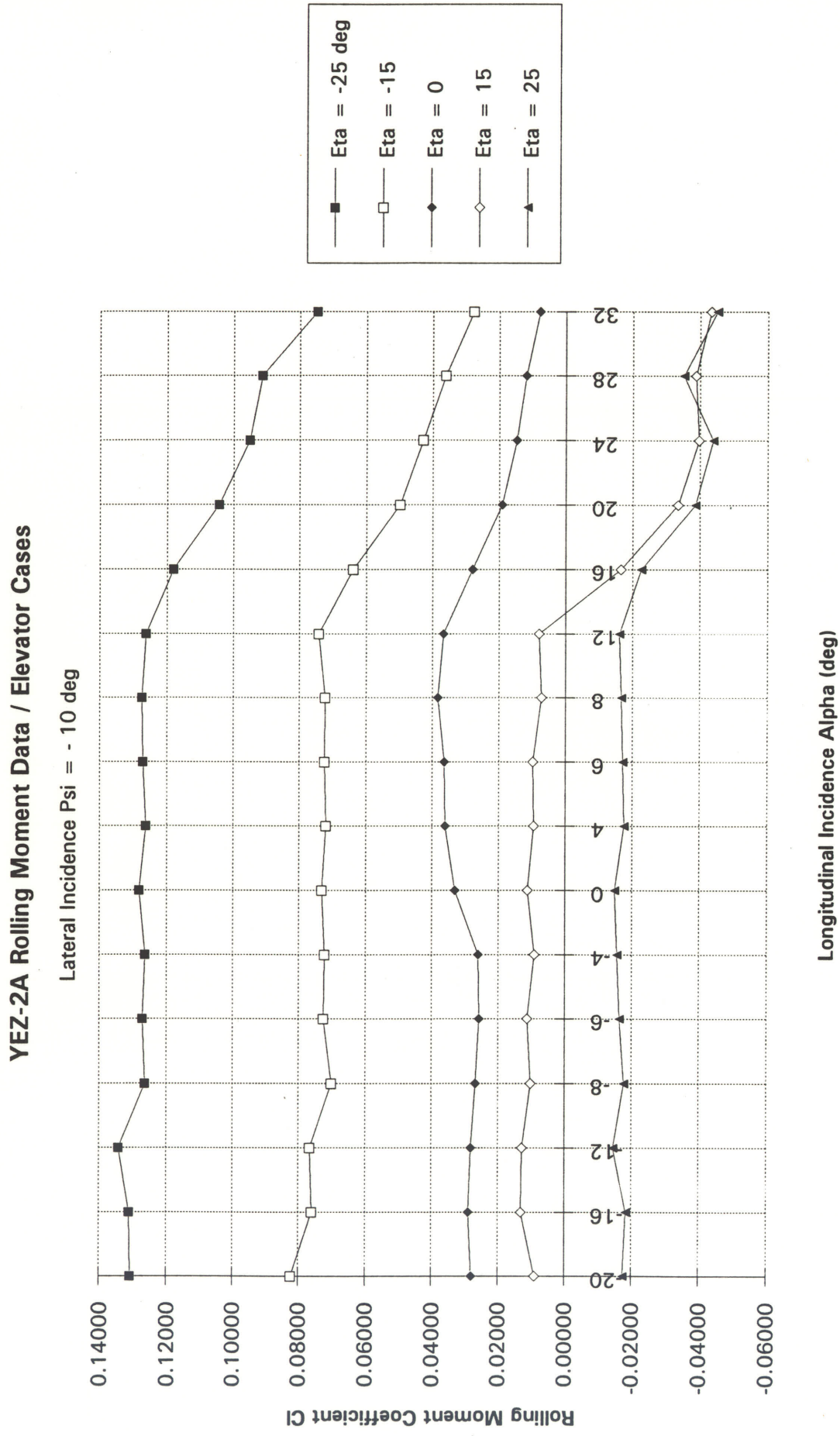


FIGURE A1.4.18

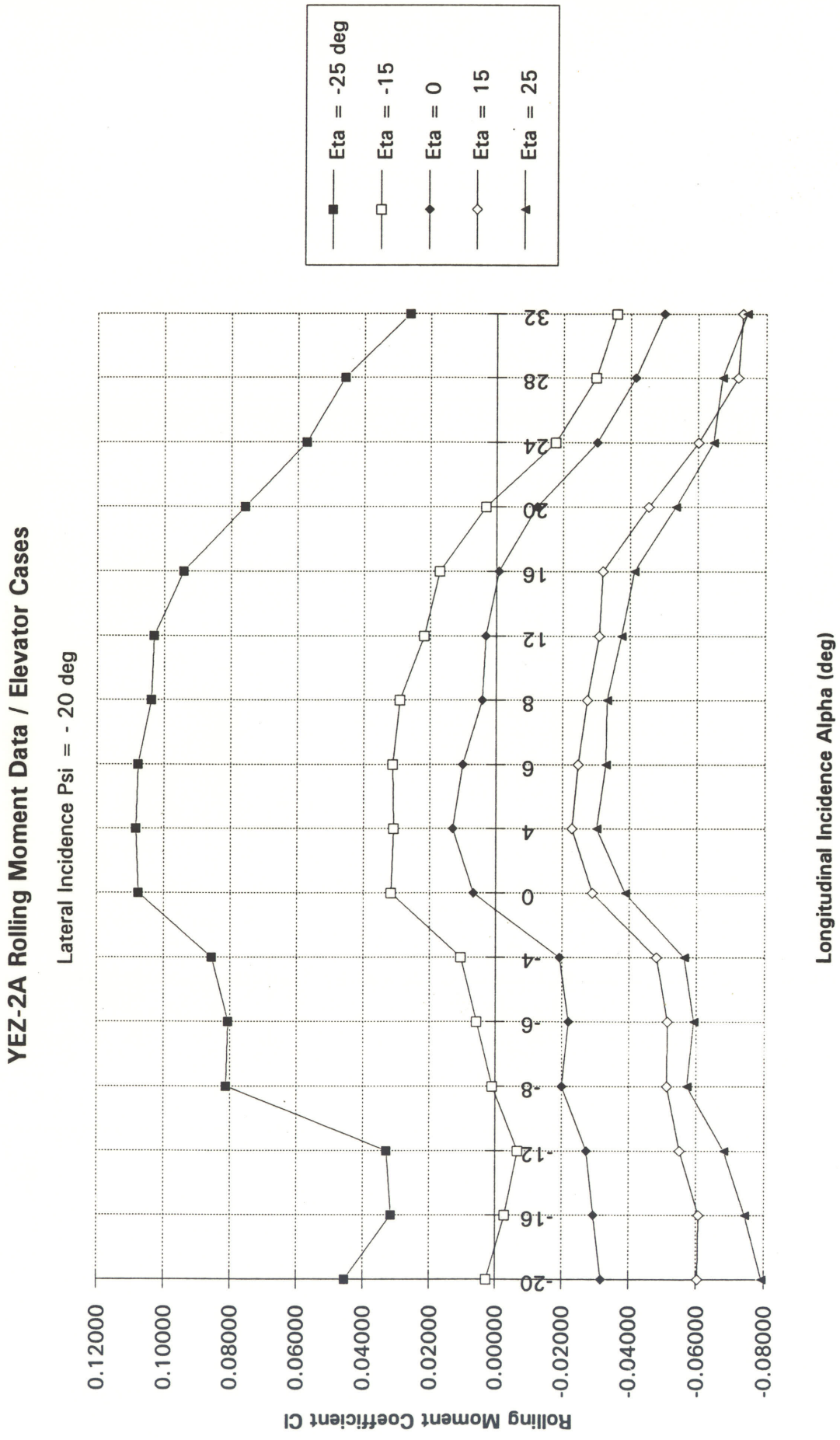


FIGURE A1.4.19

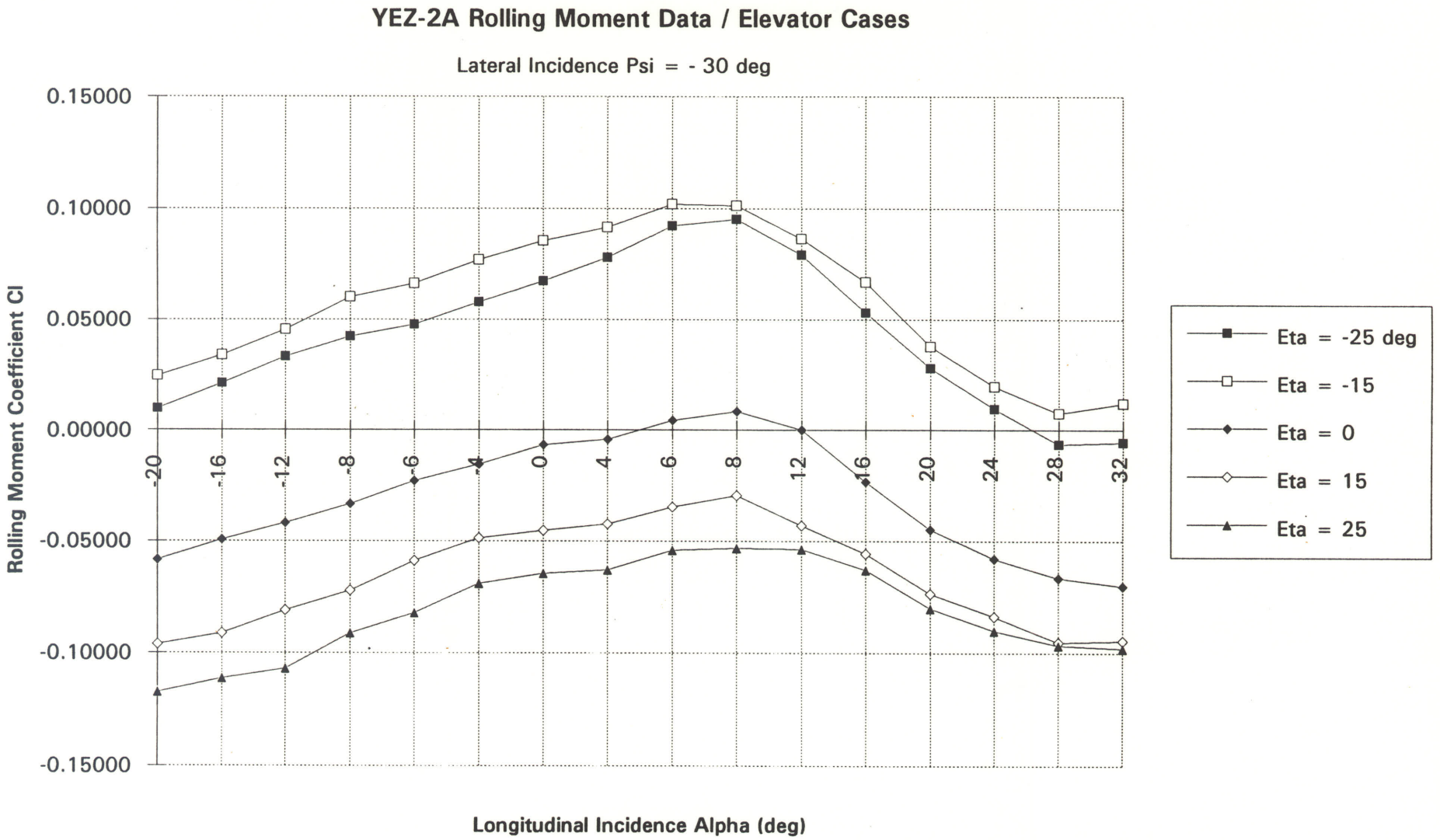


FIGURE A1.4.20

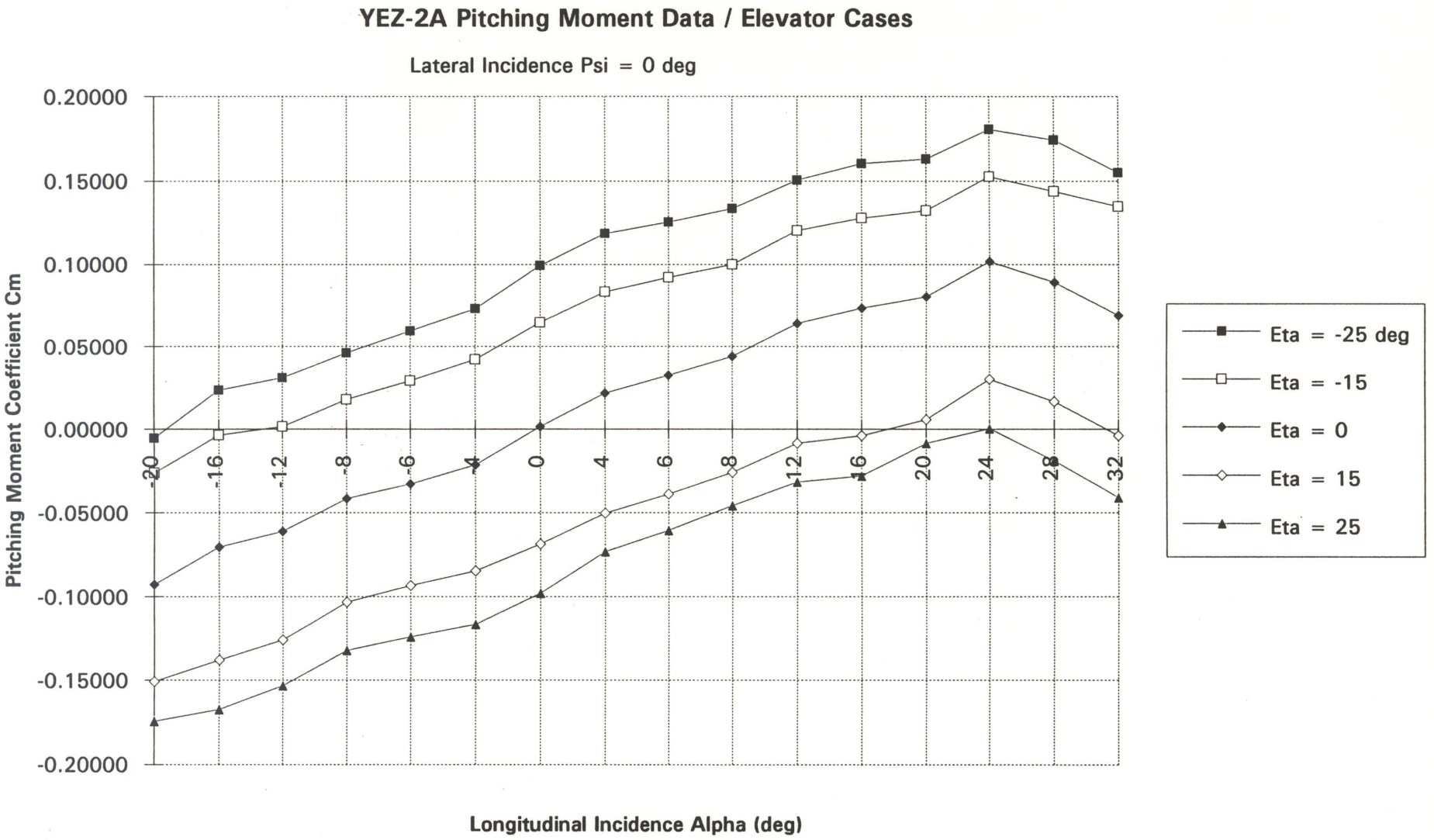


FIGURE A1.4.21

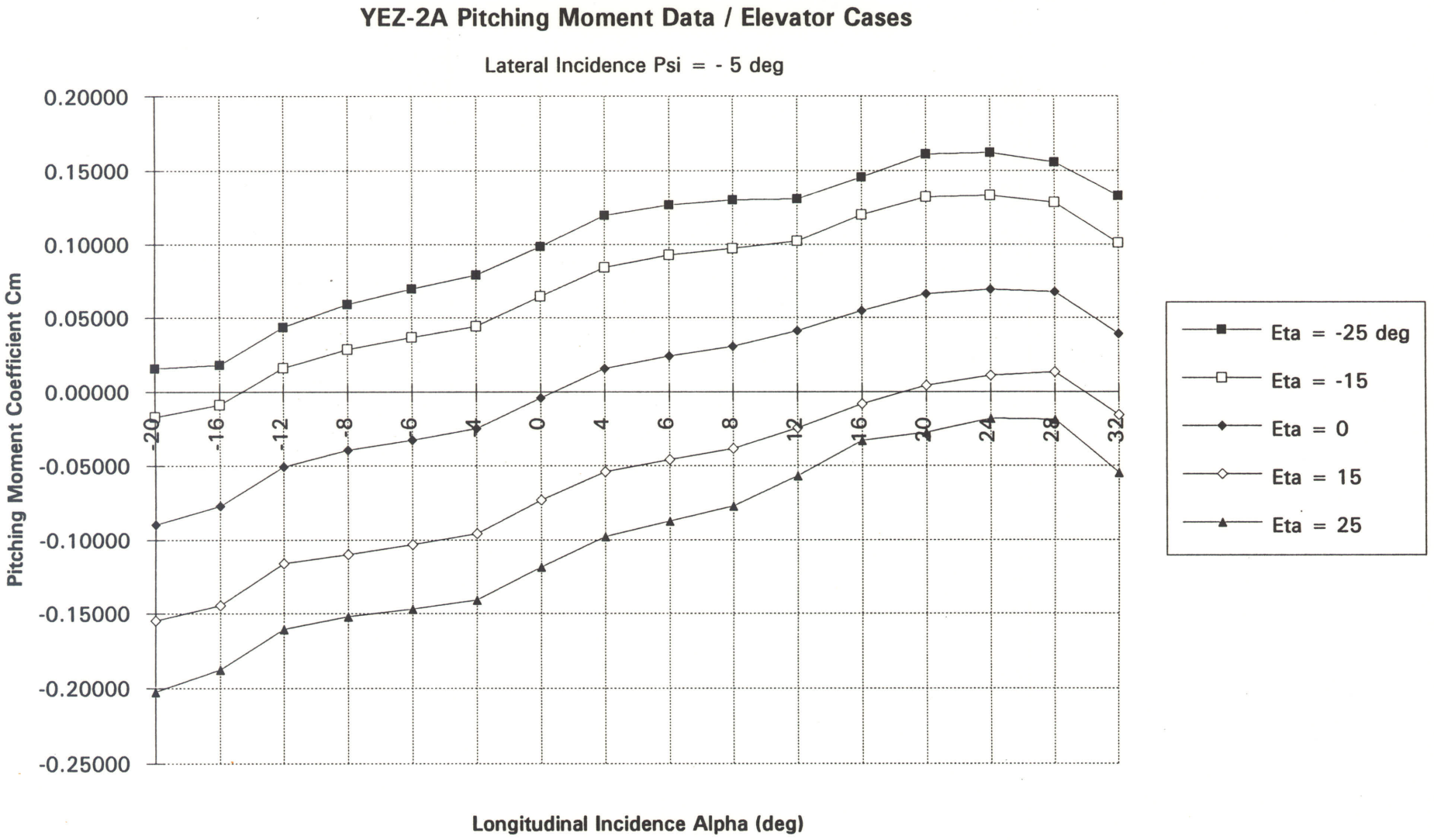


FIGURE A1.4.22

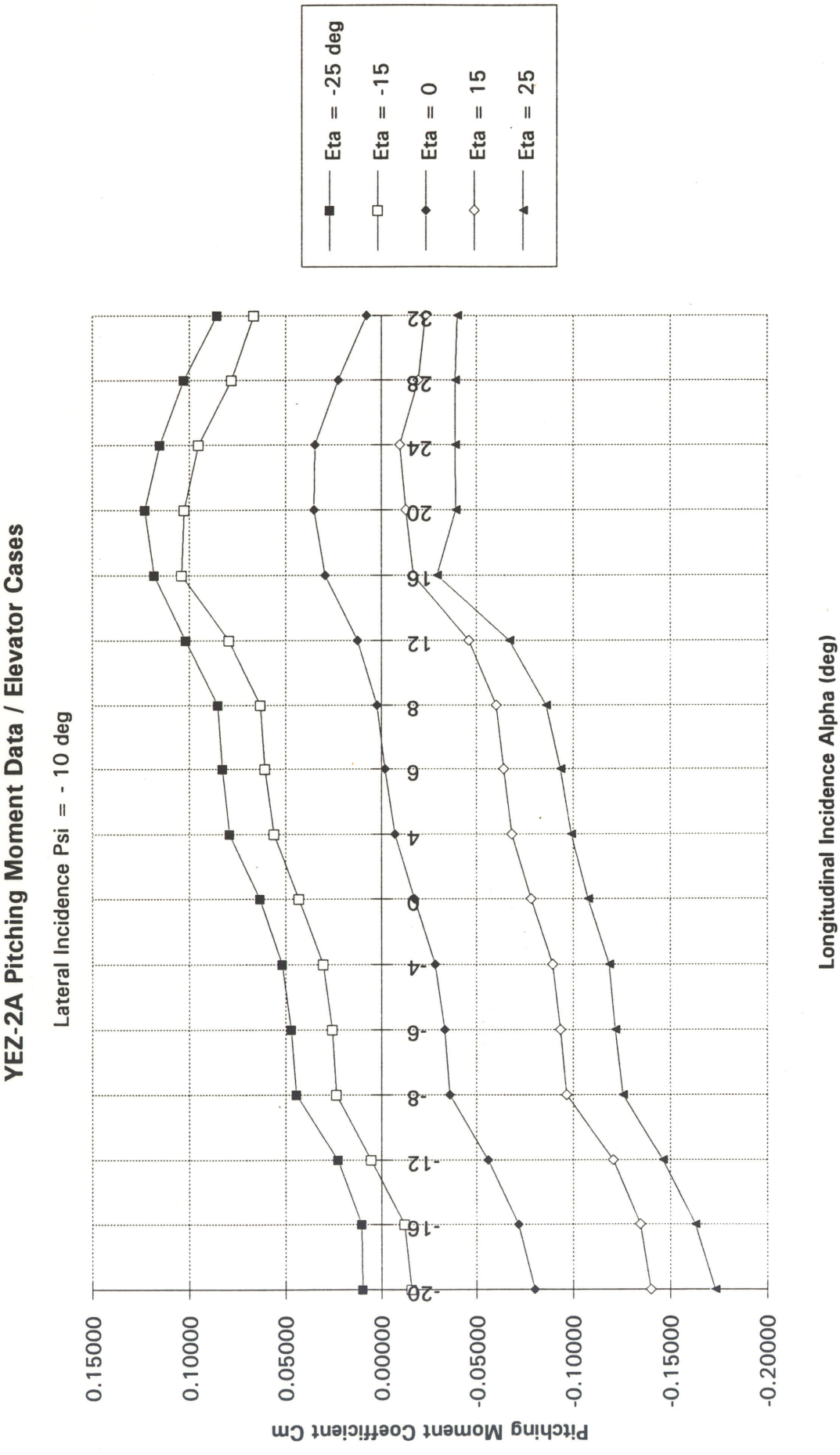


FIGURE A1.4.23

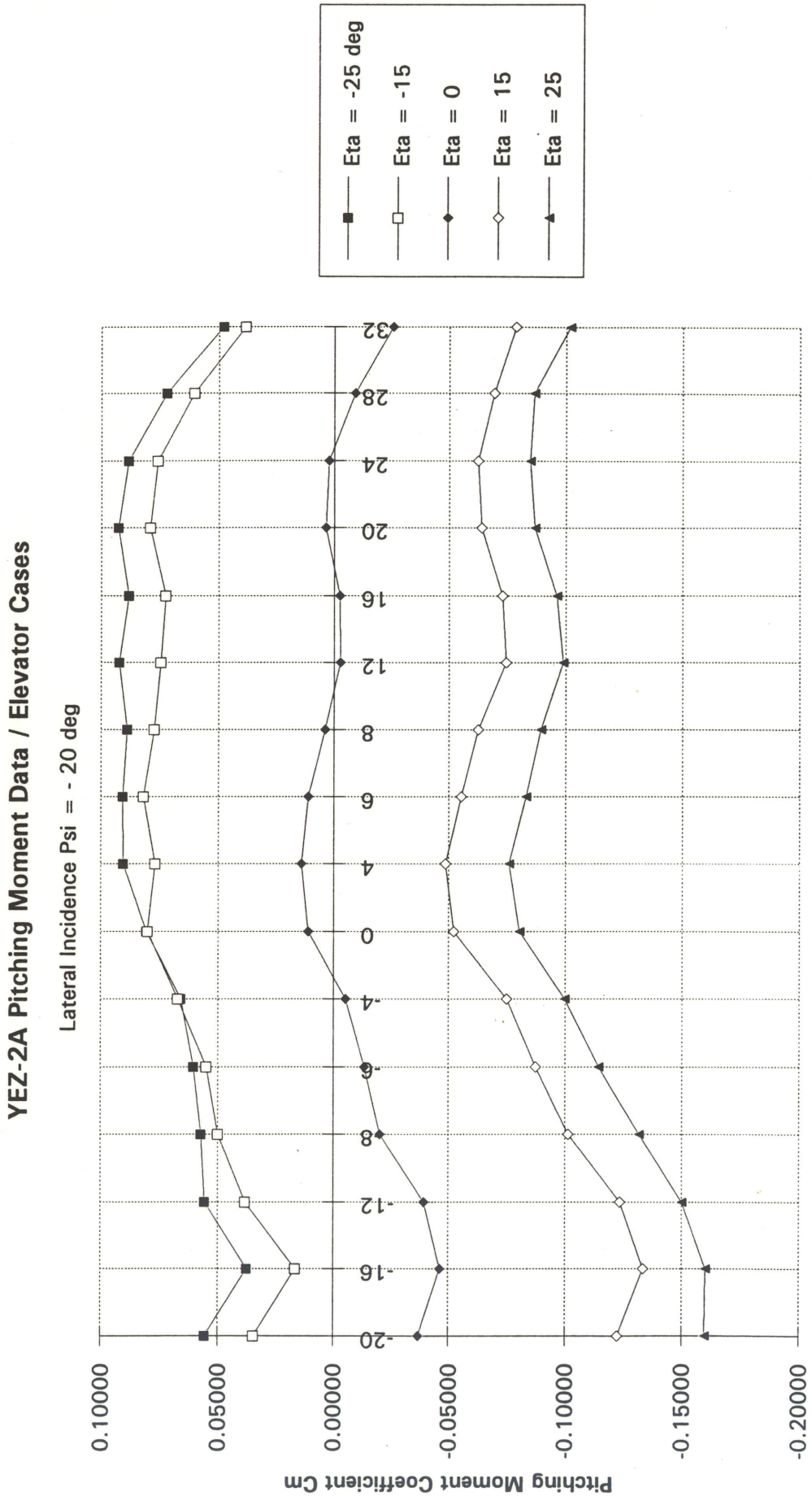


FIGURE A1.4.24

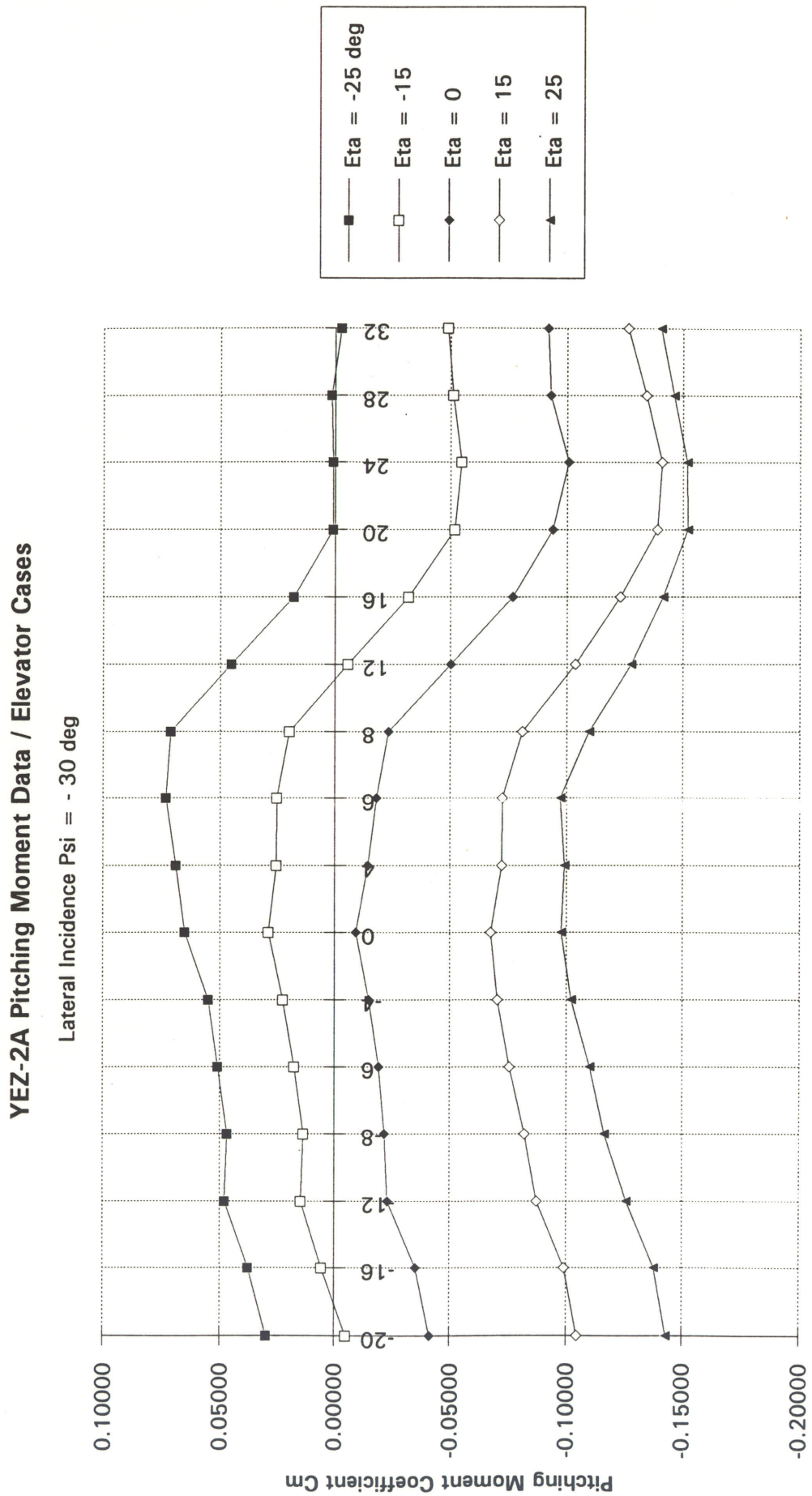


FIGURE A1.4.25

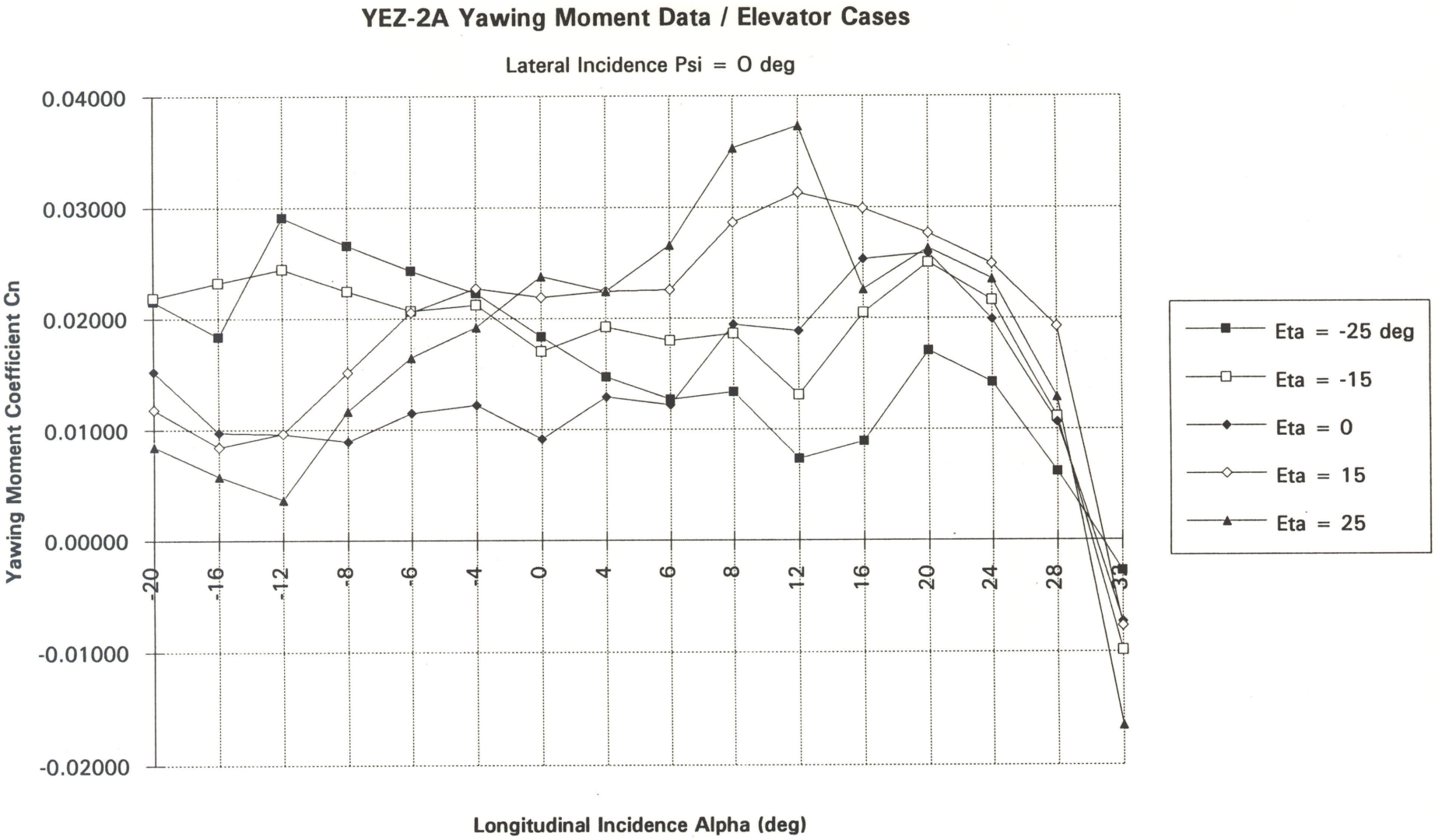


FIGURE A1.4.26

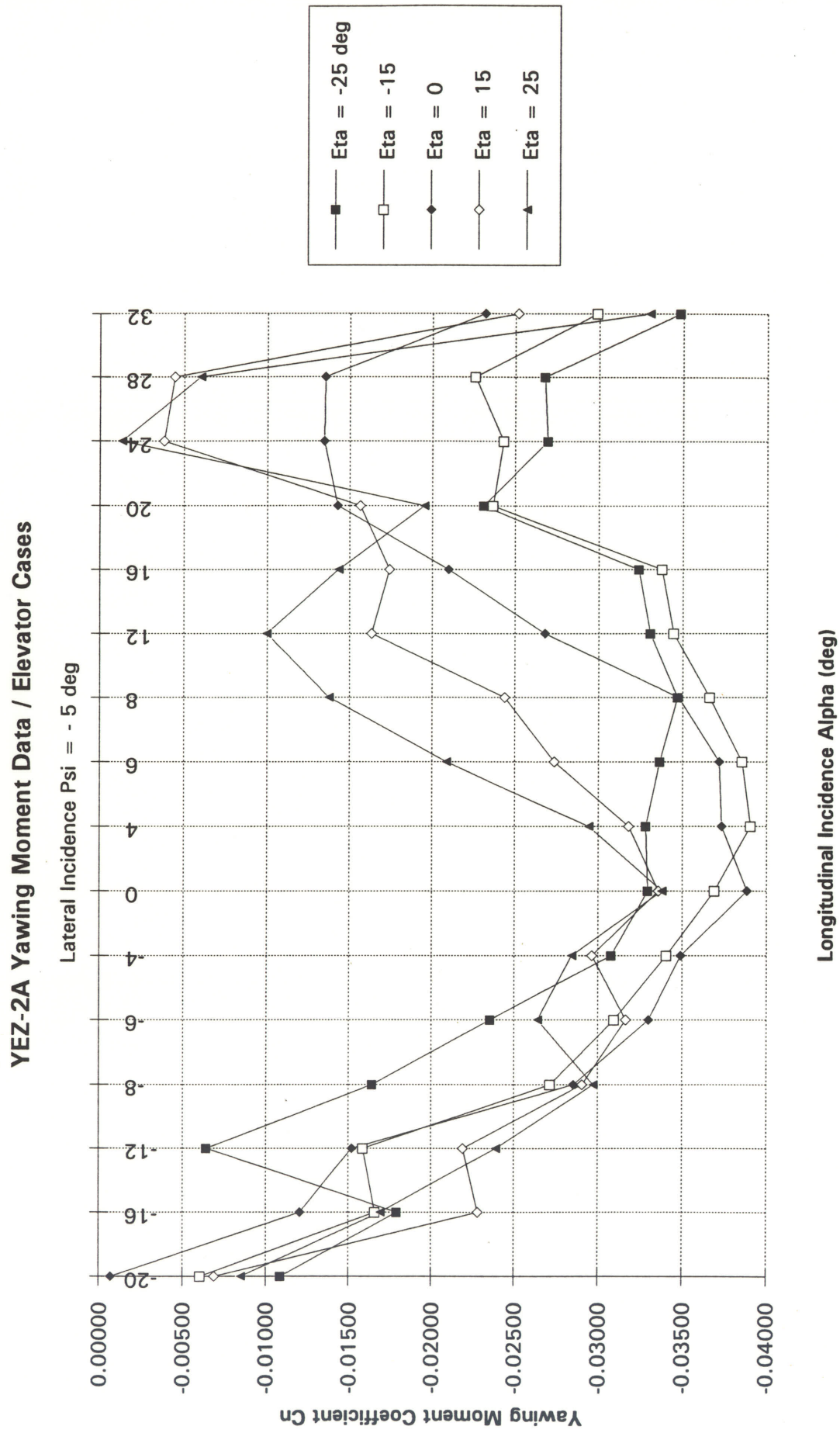


FIGURE A1.4.27

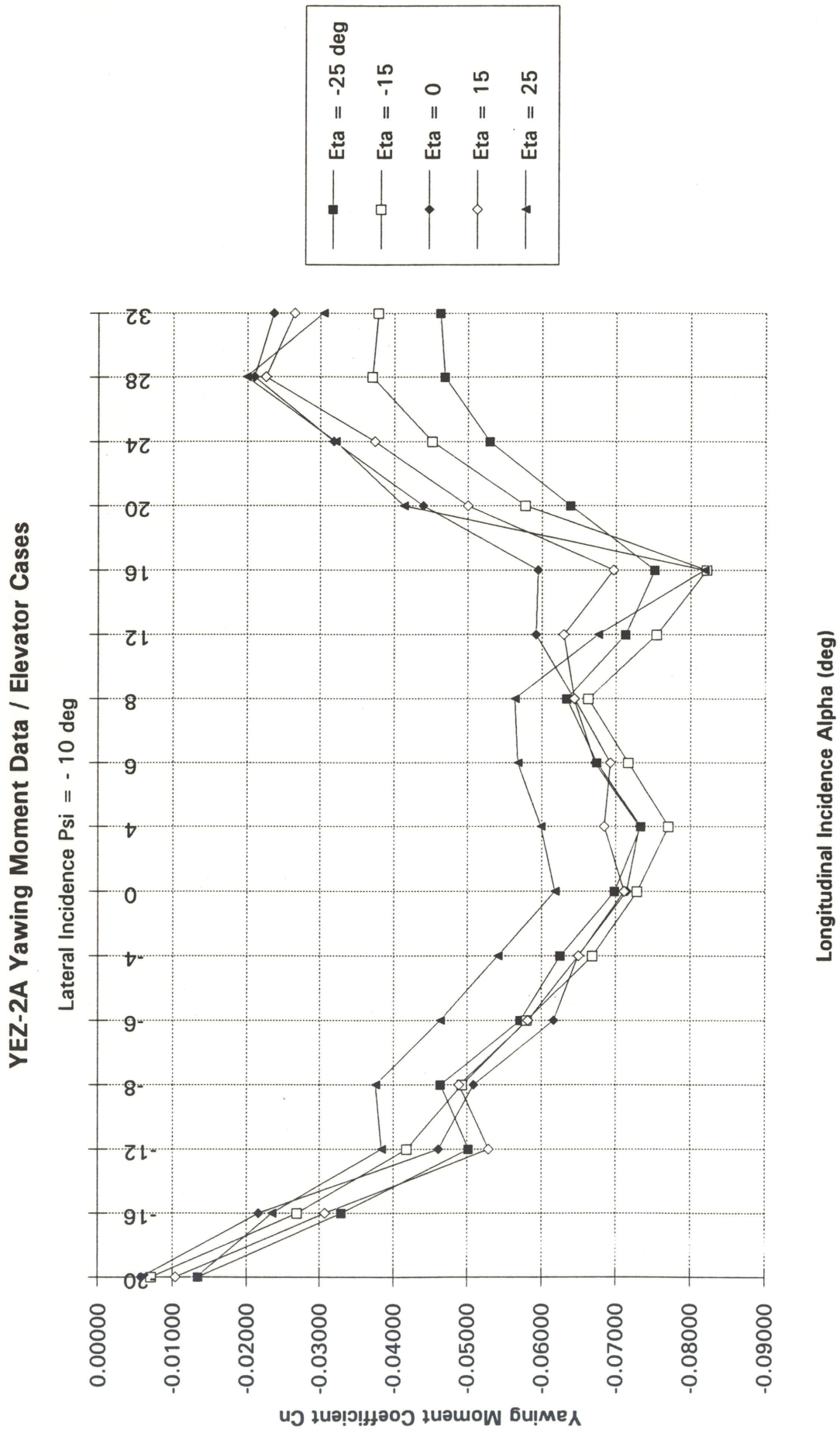


FIGURE A1.4.28

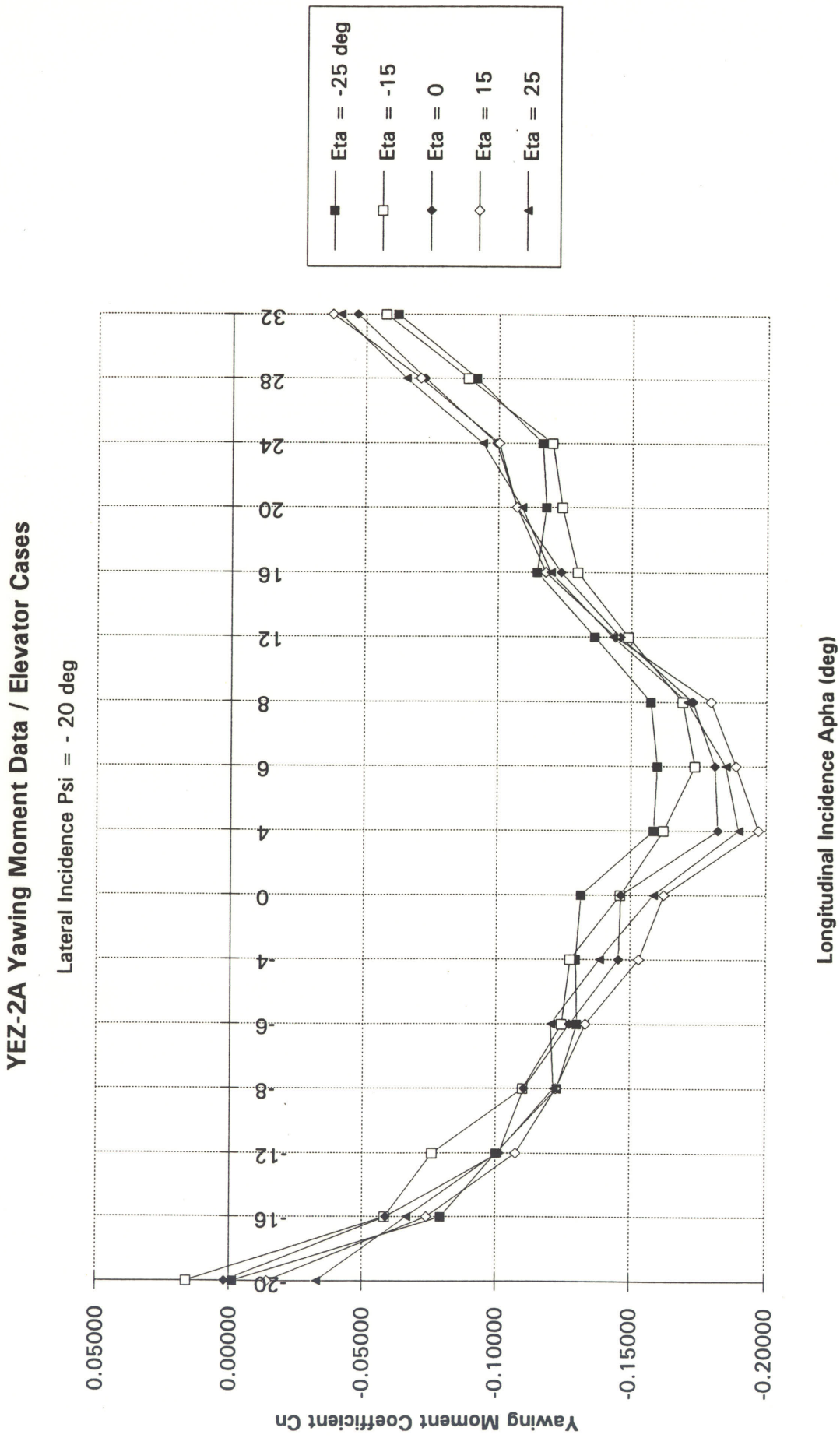


FIGURE A1.4.29

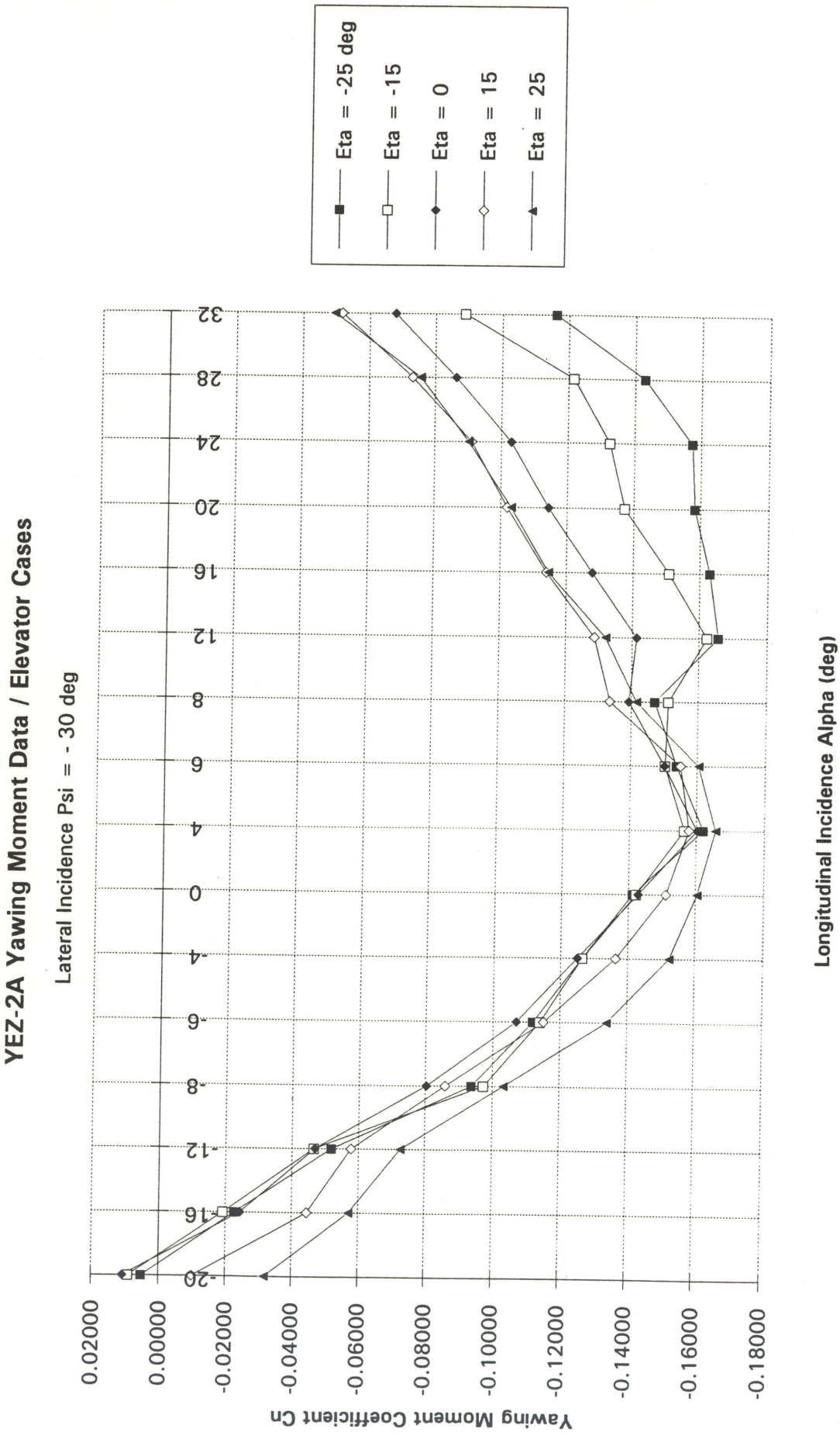


FIGURE A1.4.30

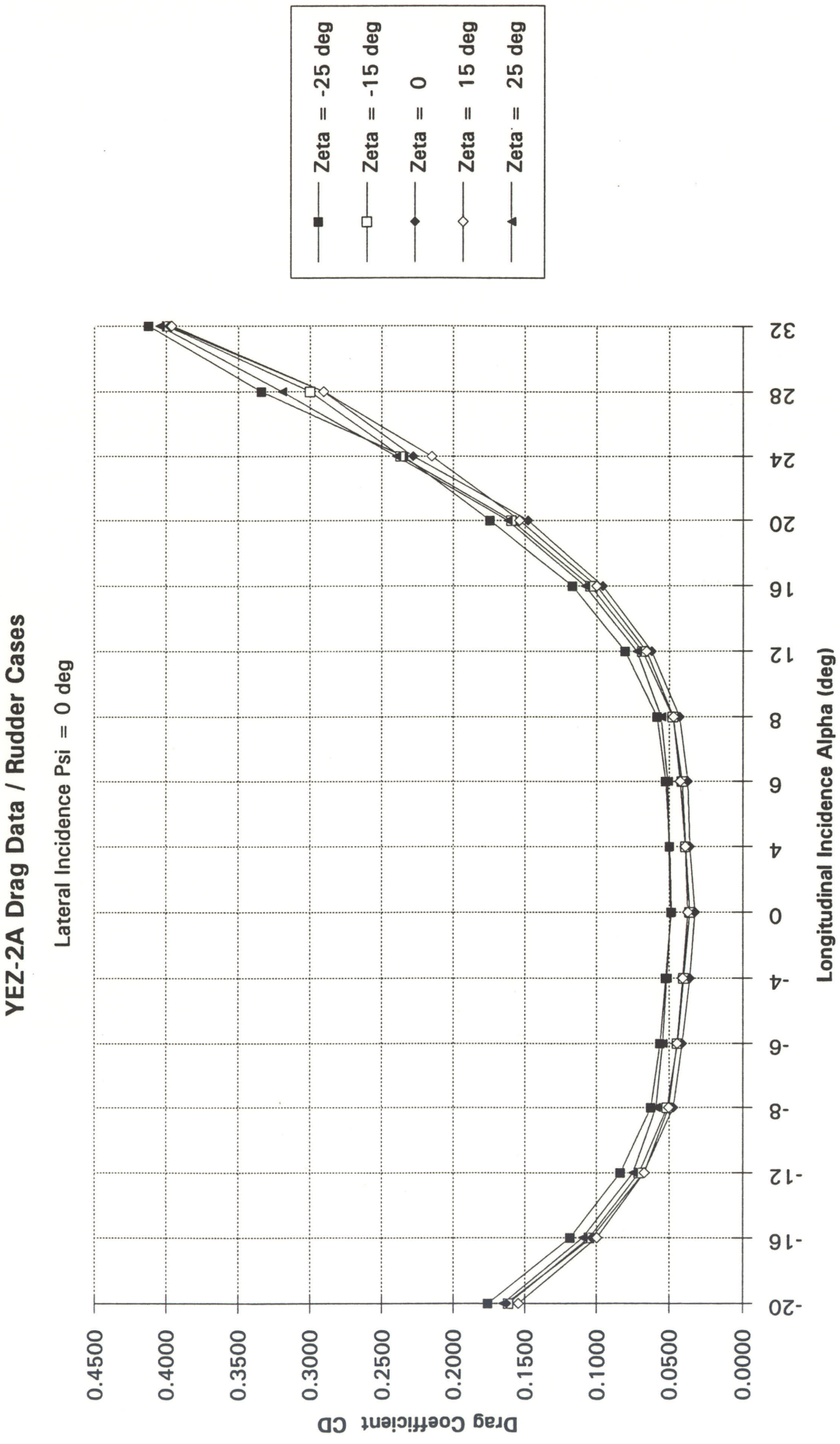


FIGURE A1.4.31

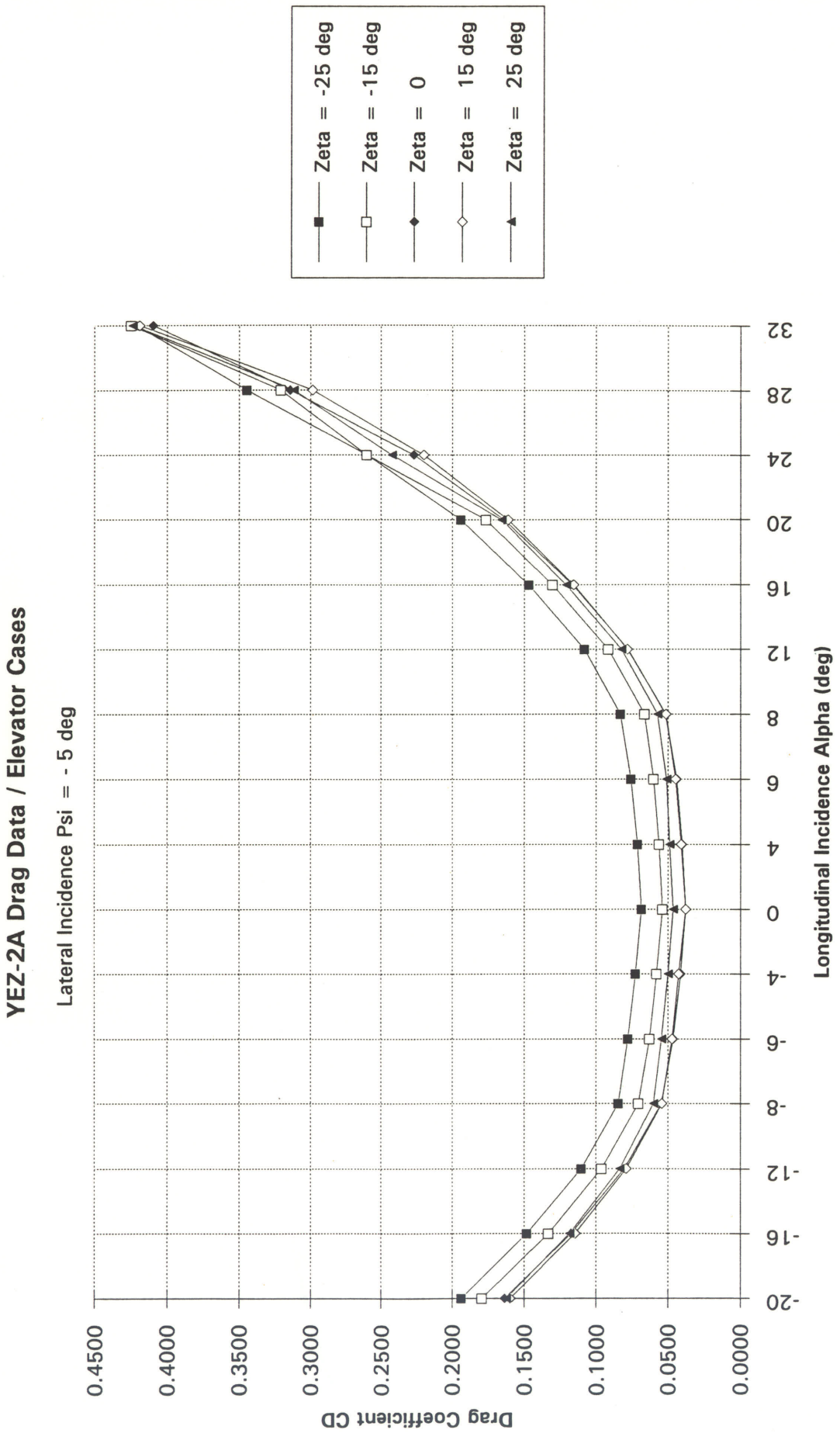


FIGURE A1.4.32

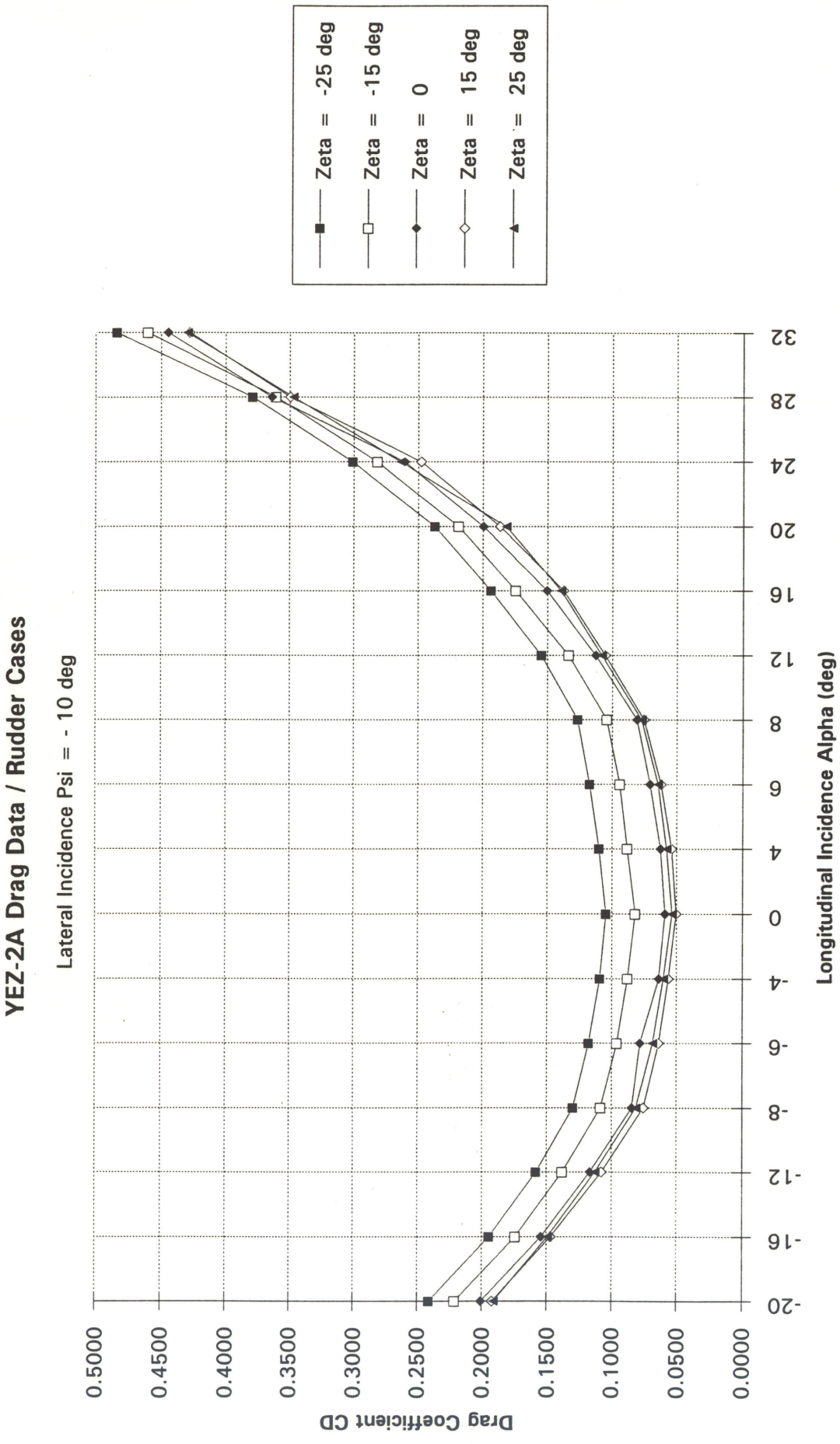


FIGURE A1.4.33

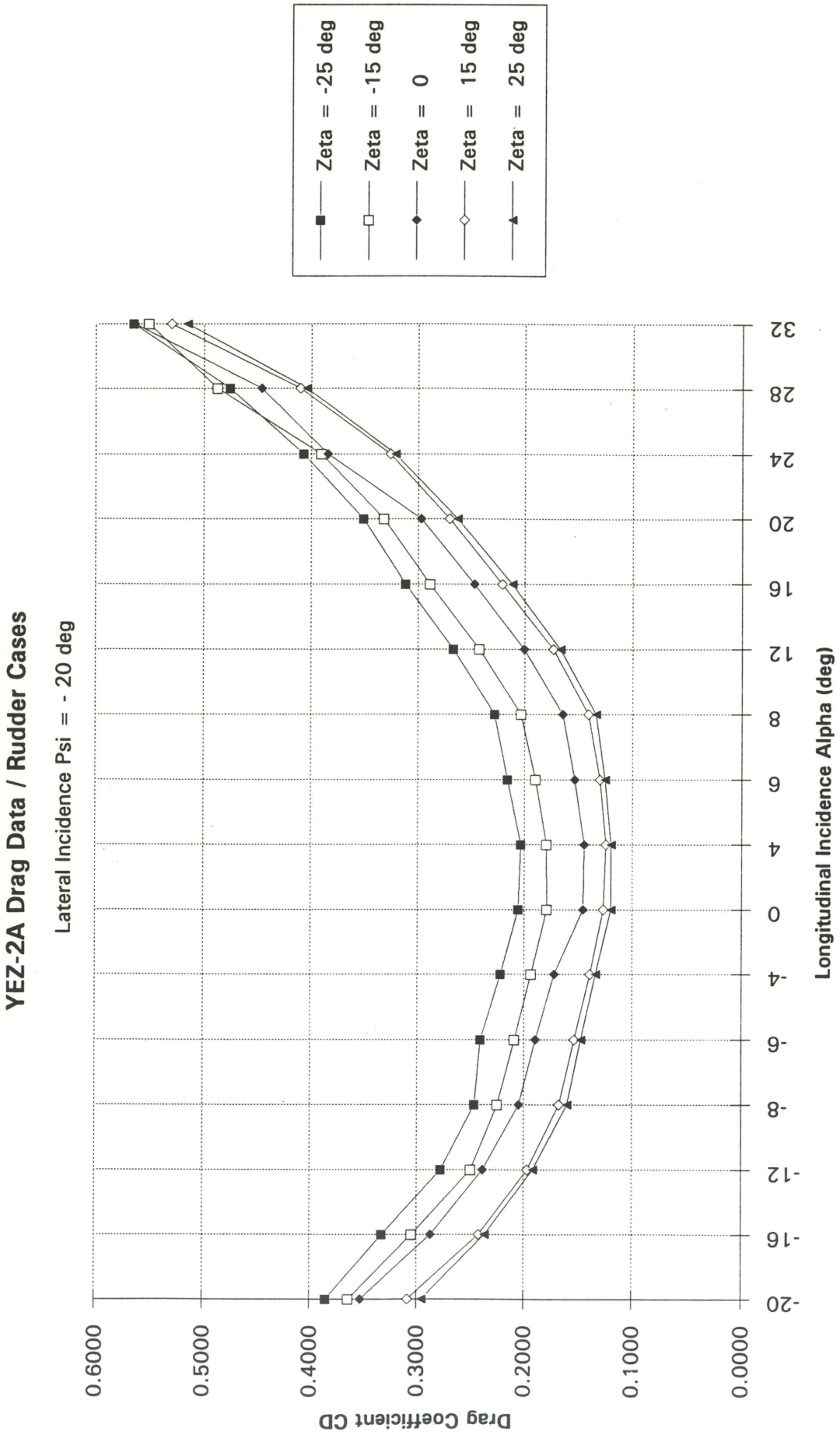


FIGURE A1.4.34

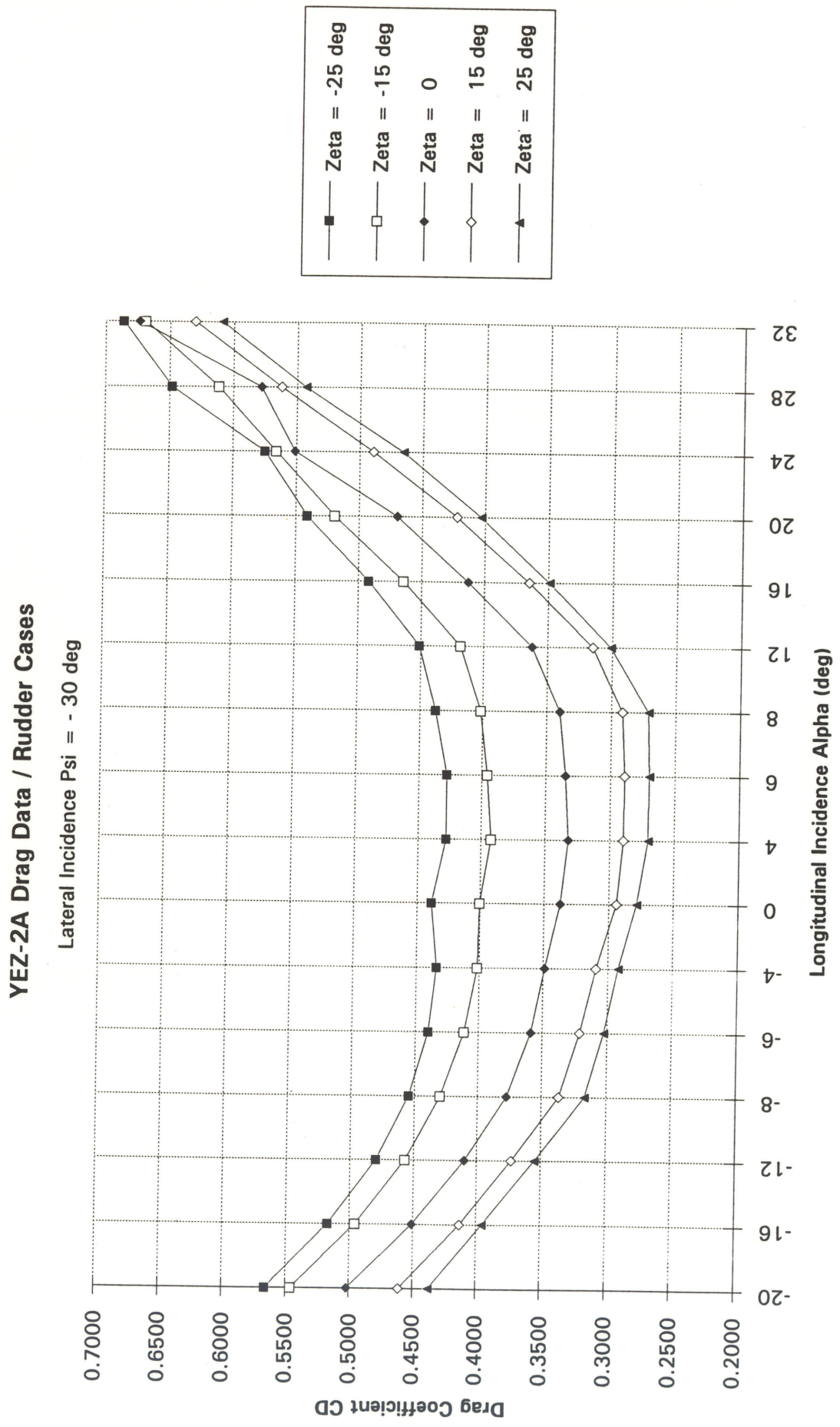


FIGURE A1.4.35

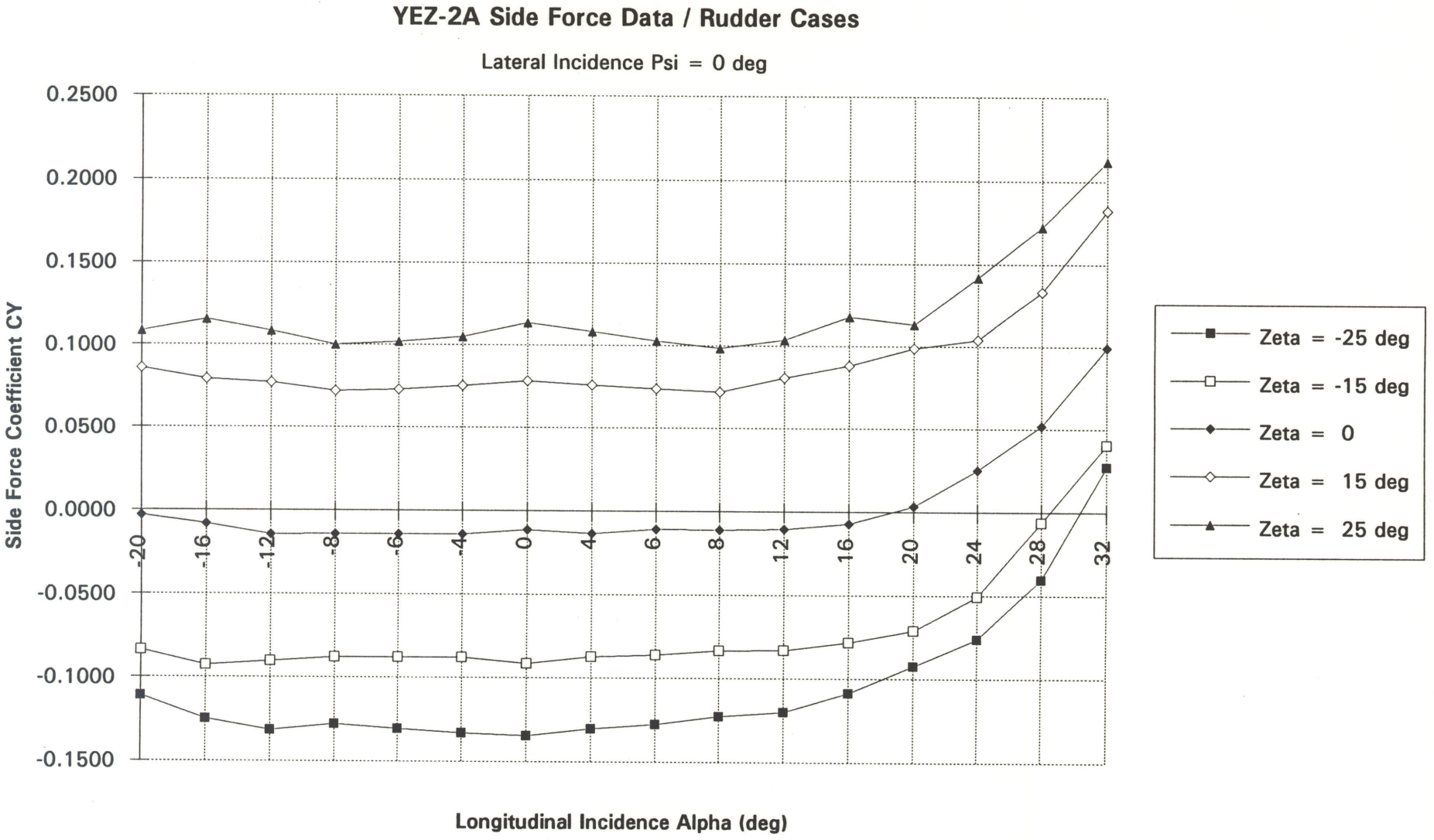


FIGURE A1.4.36

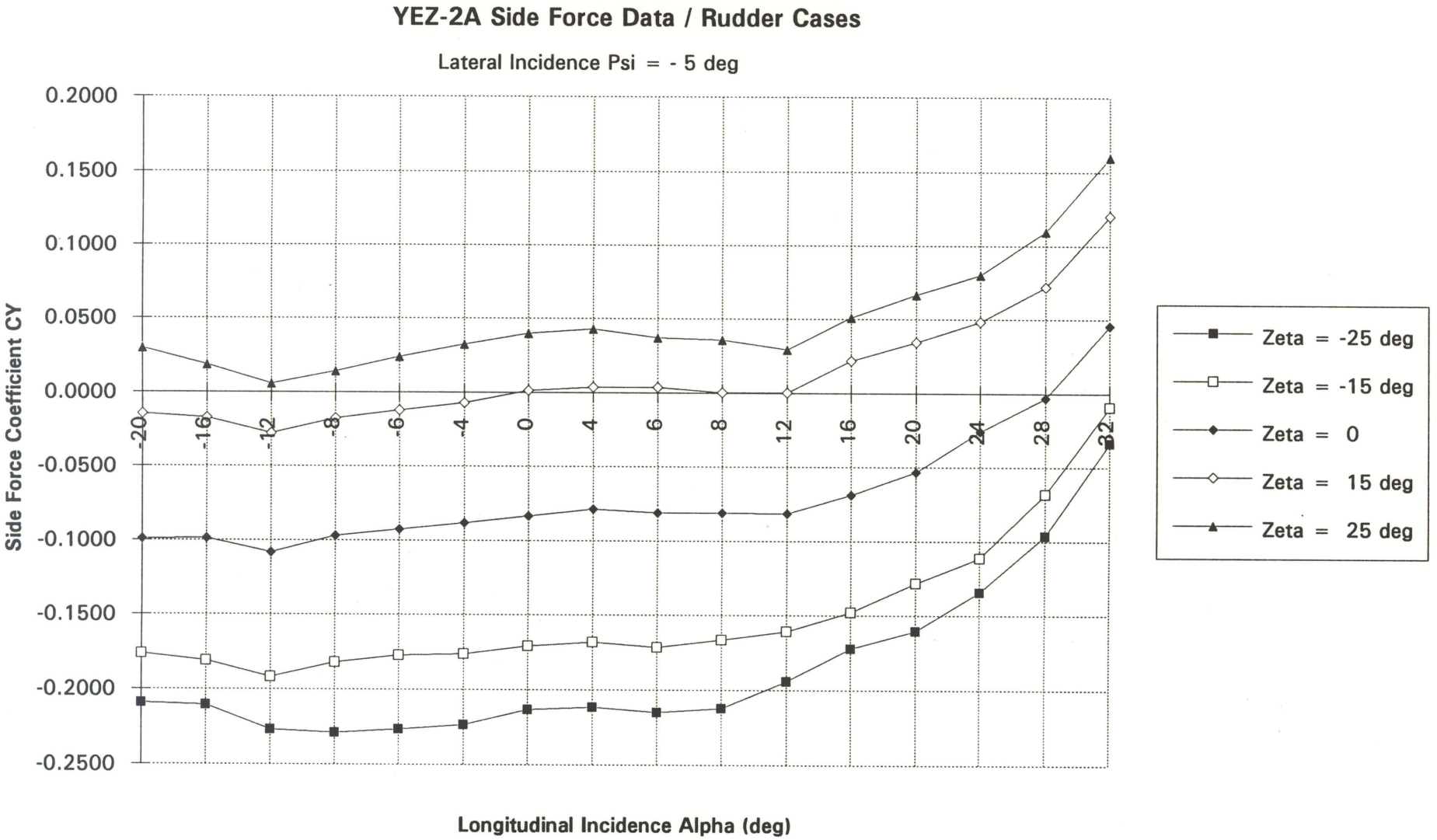


FIGURE A1.4.37

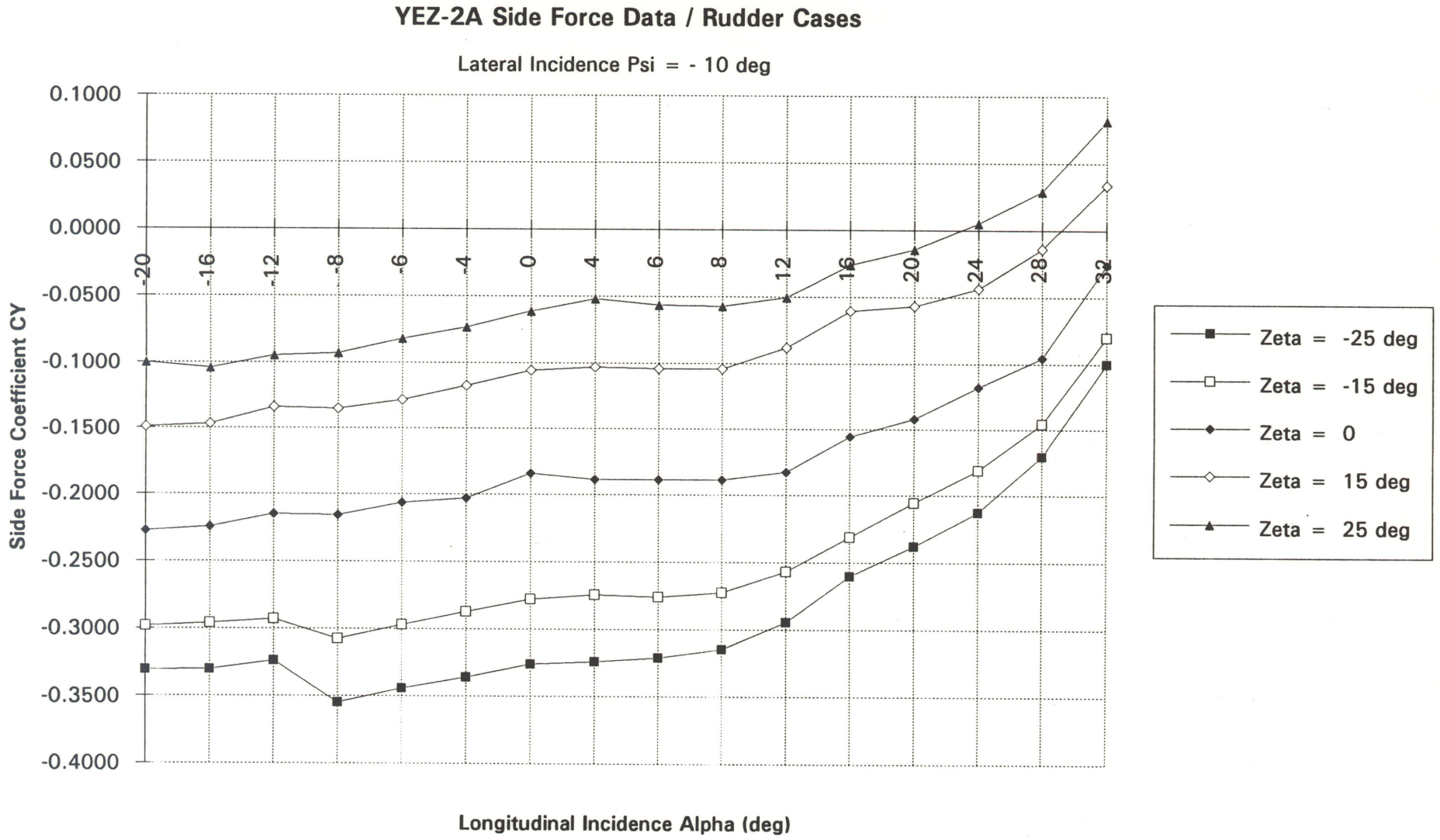


FIGURE A1.4.38

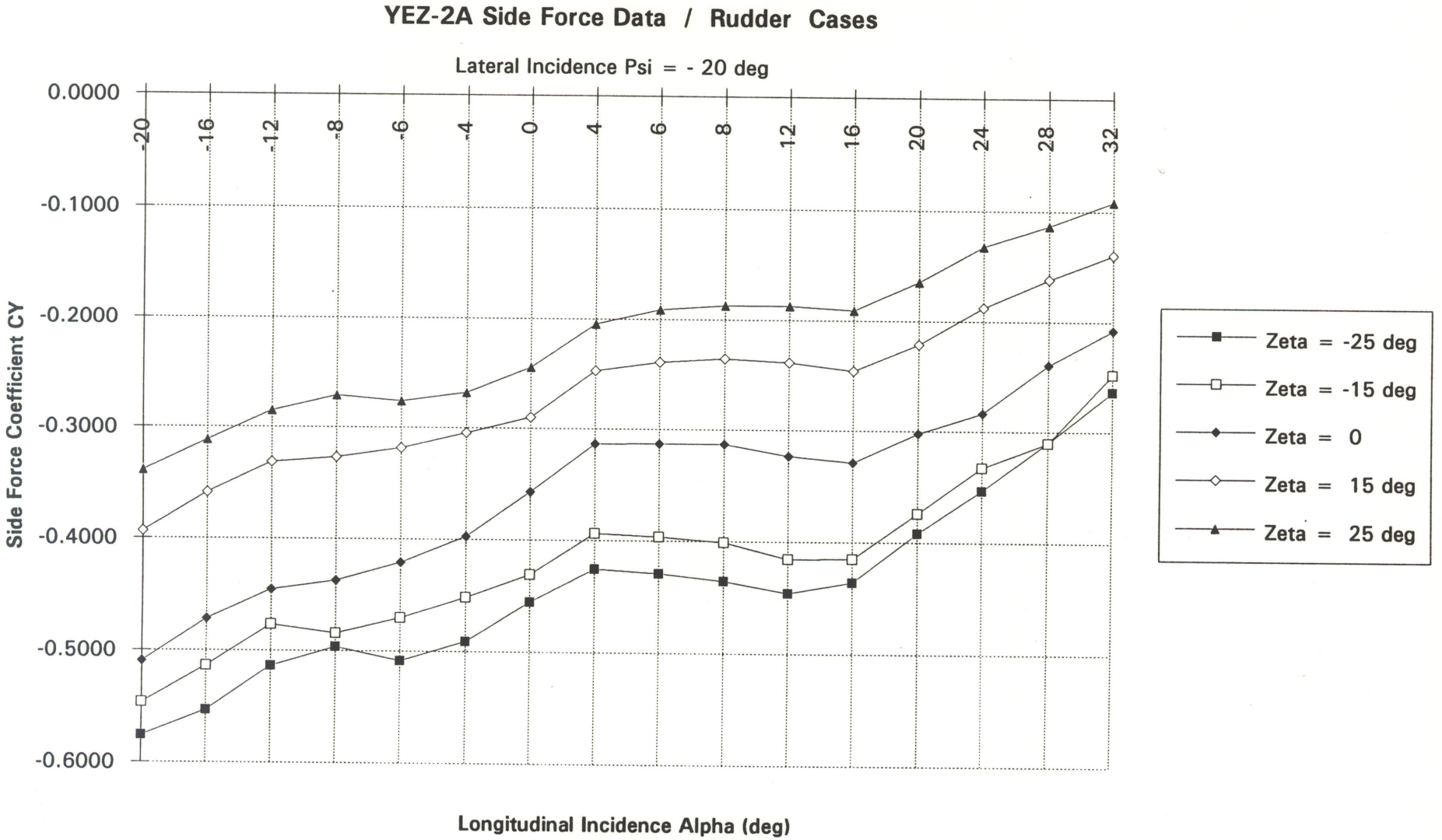


FIGURE A1.4.39

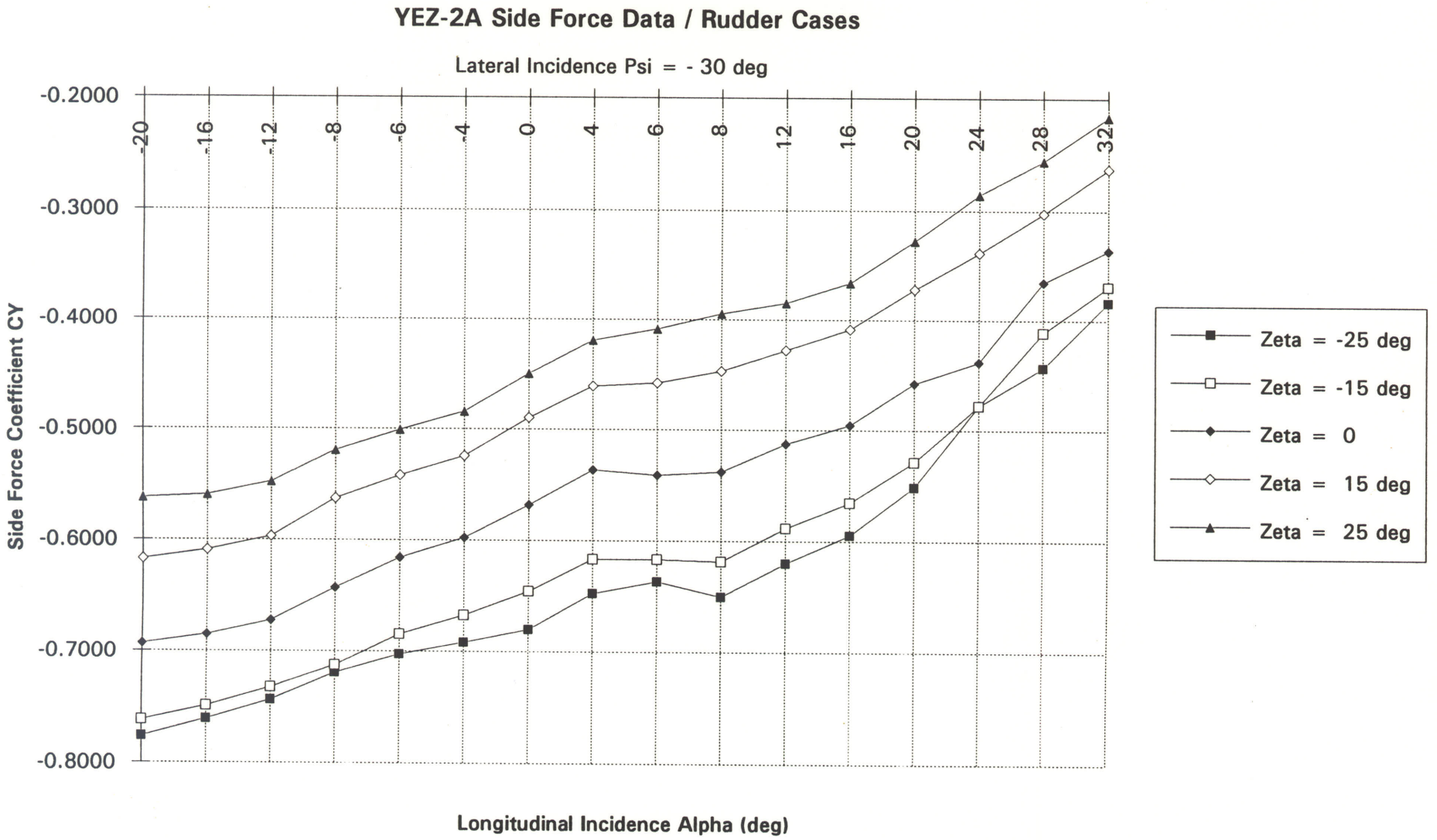


FIGURE A1.4.40

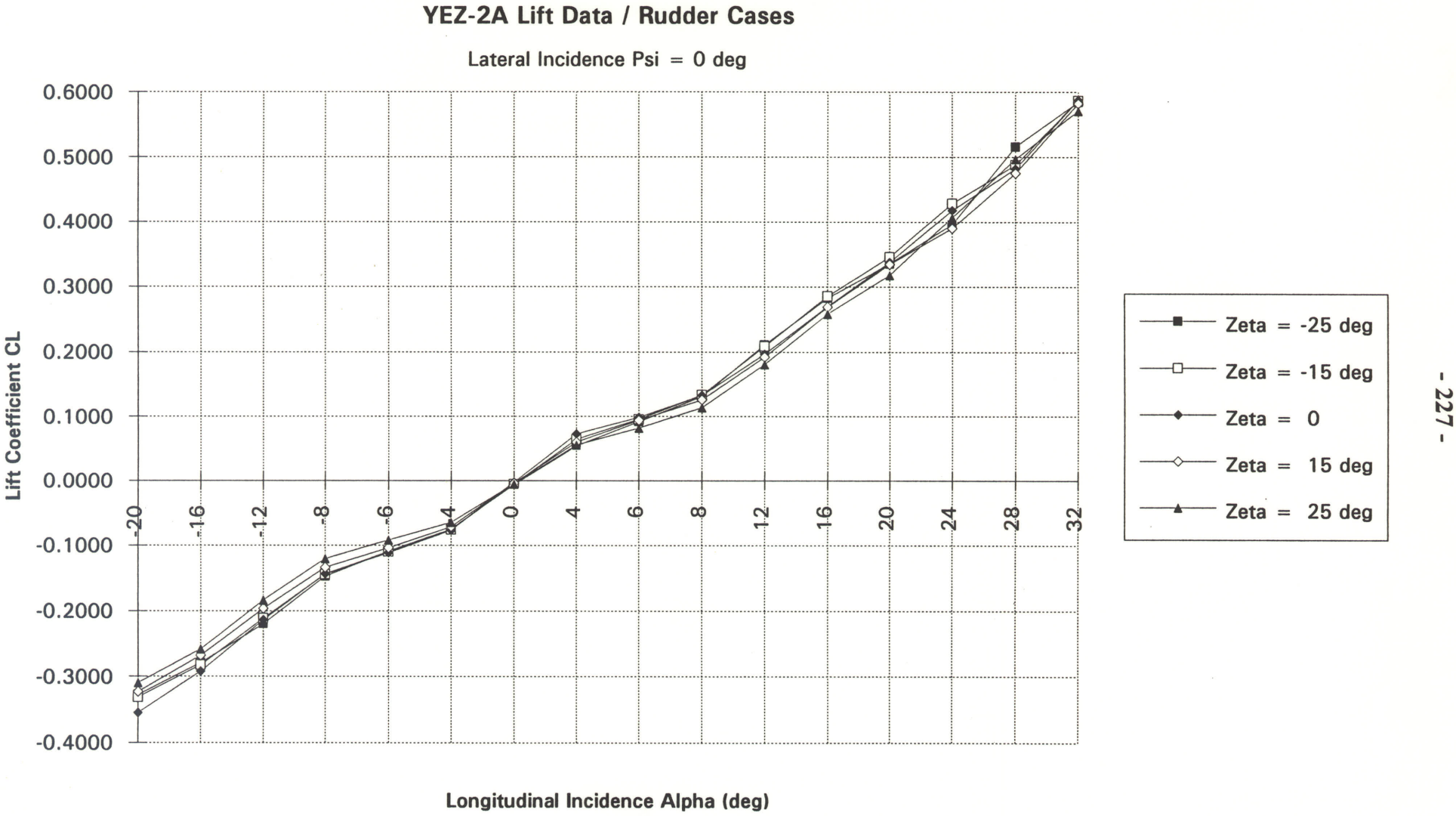


FIGURE A1.4.41

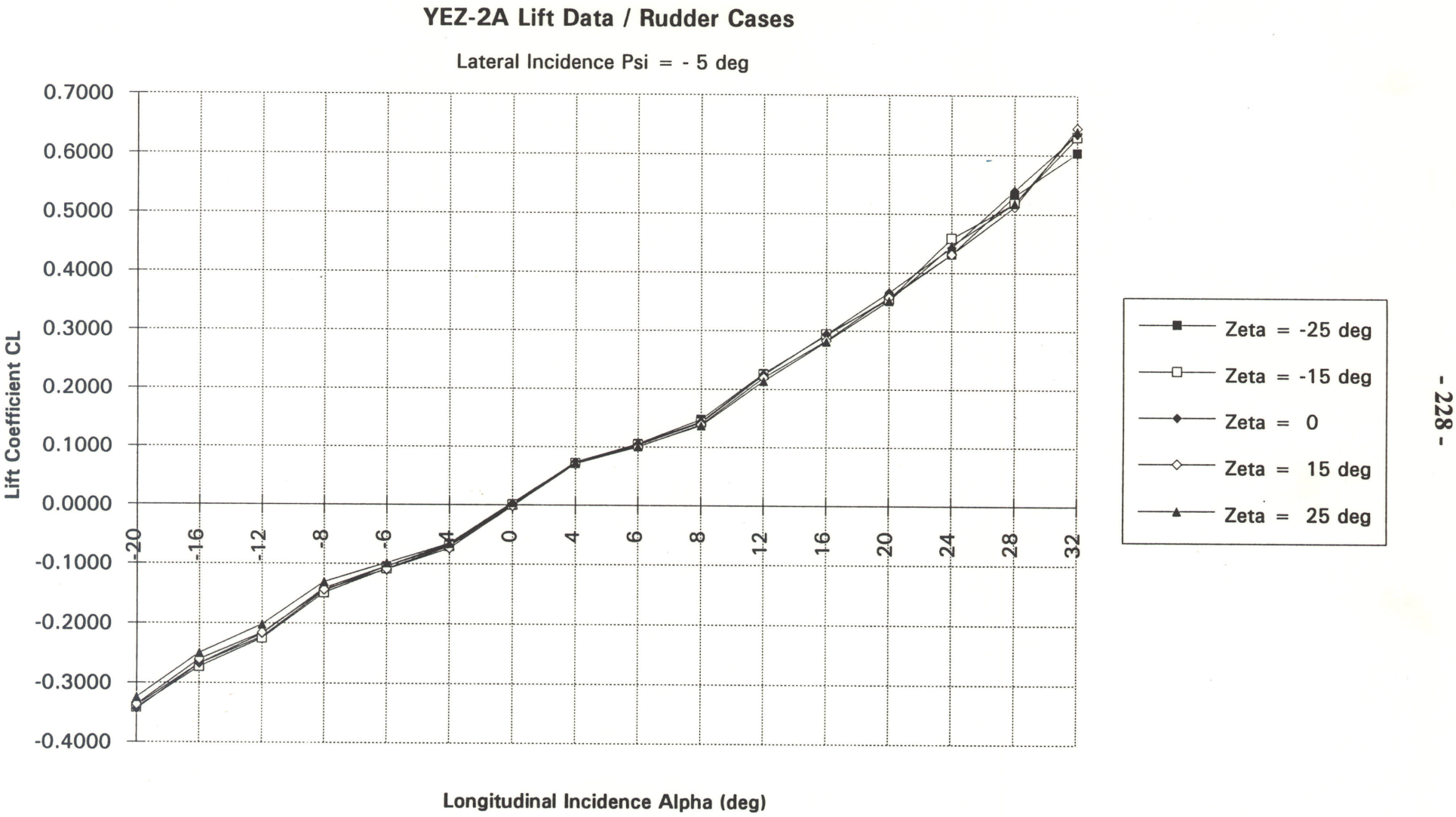


FIGURE A1.4.42

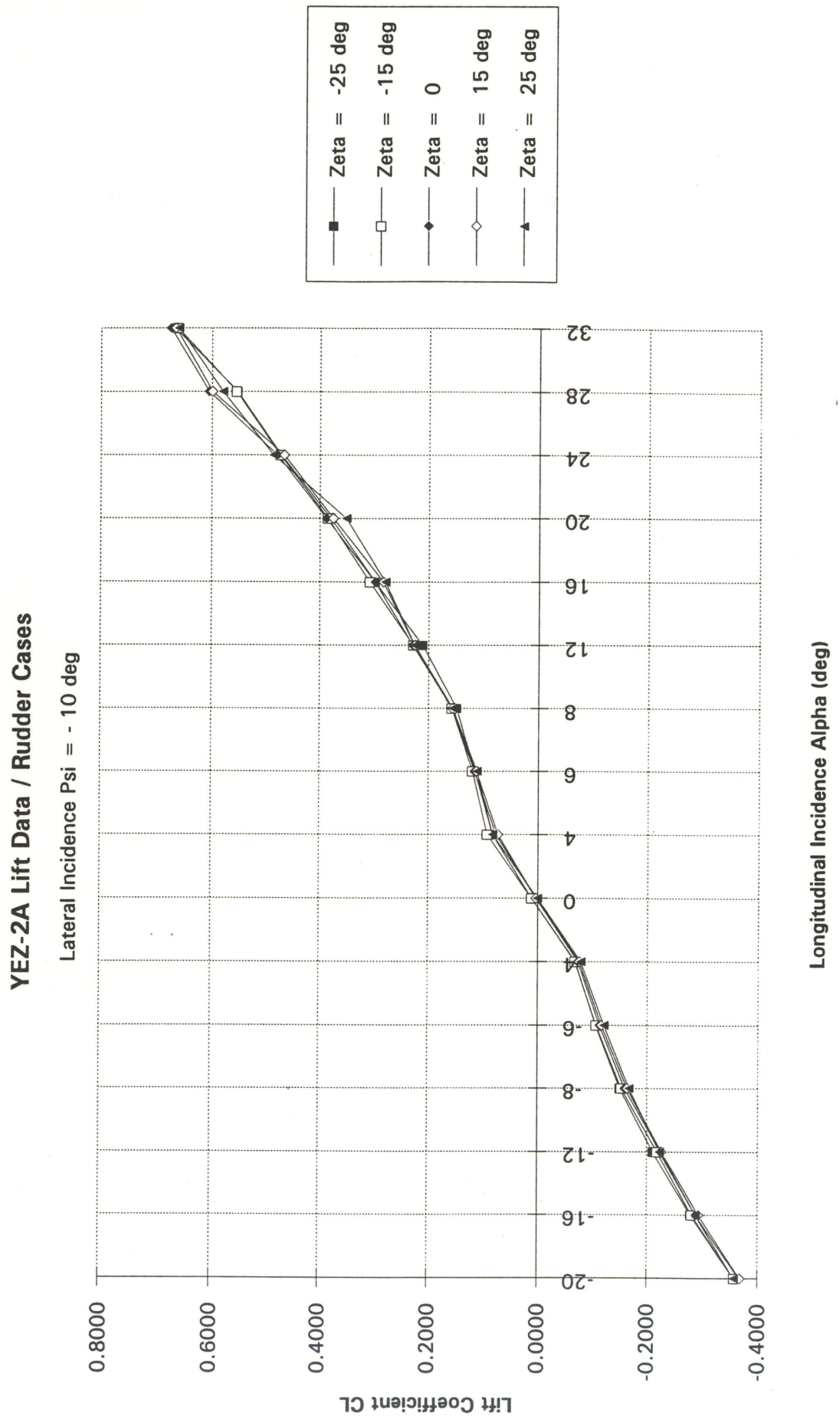


FIGURE A1.4.43

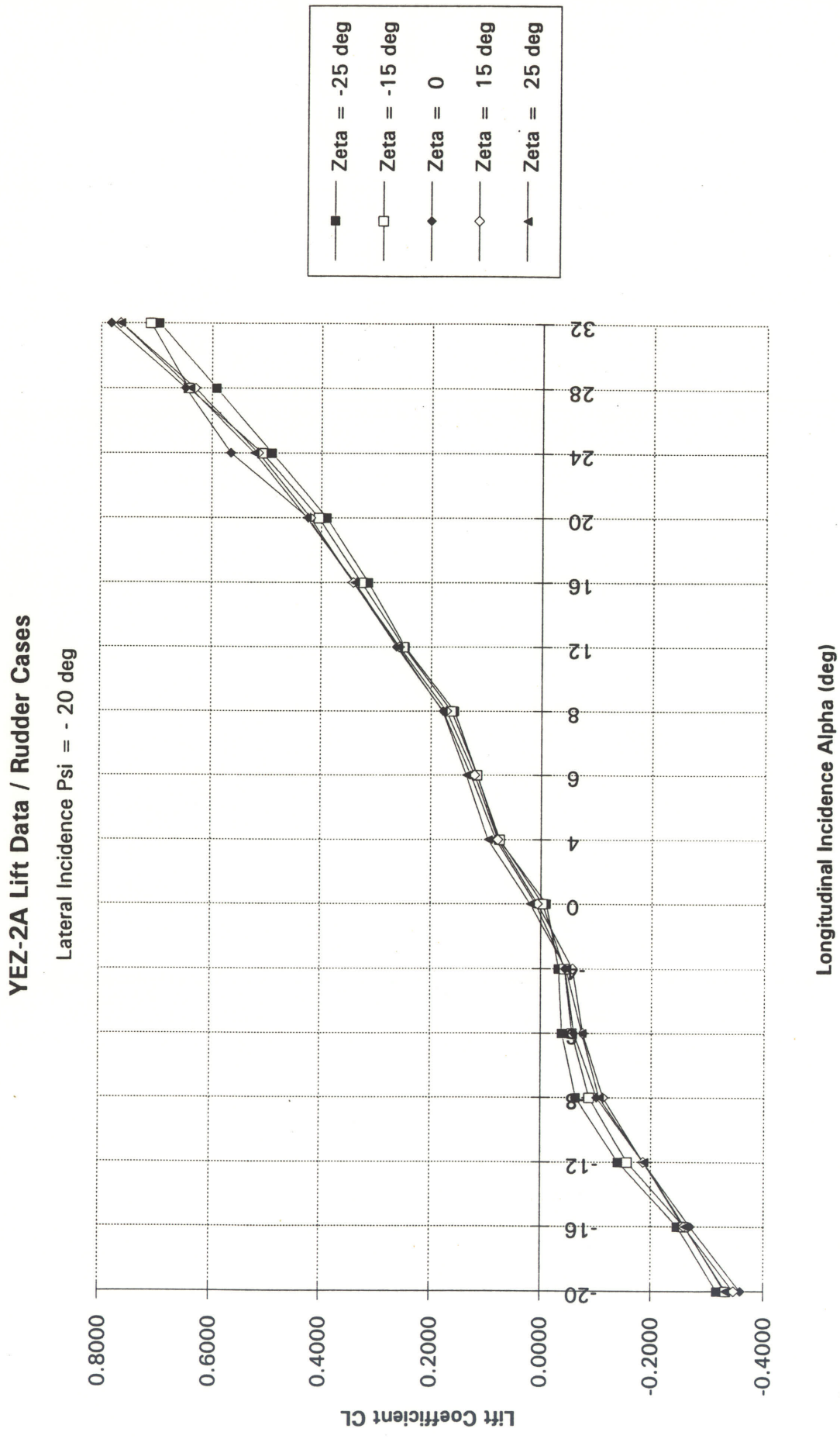


FIGURE A1.4.44

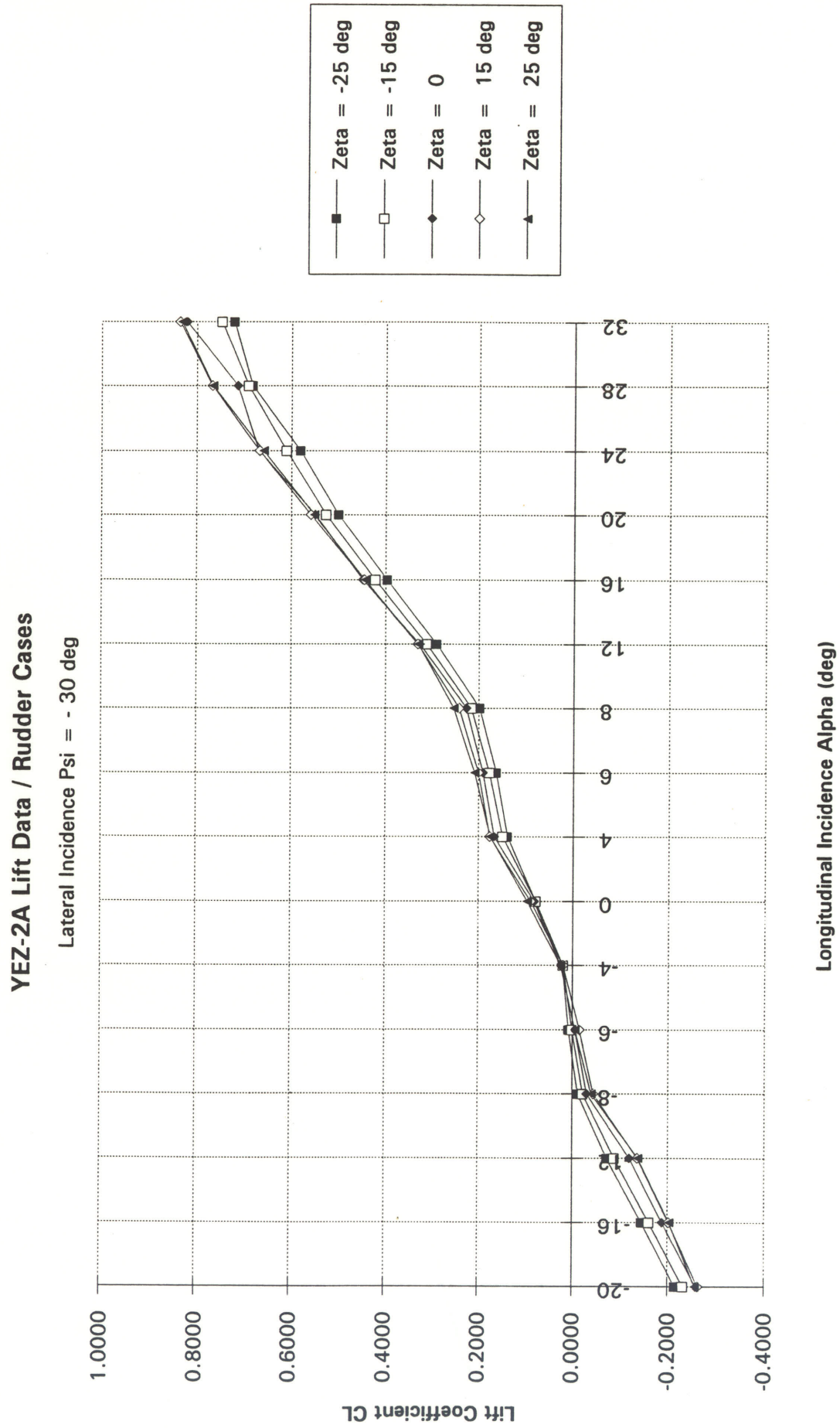


FIGURE A1.4.45

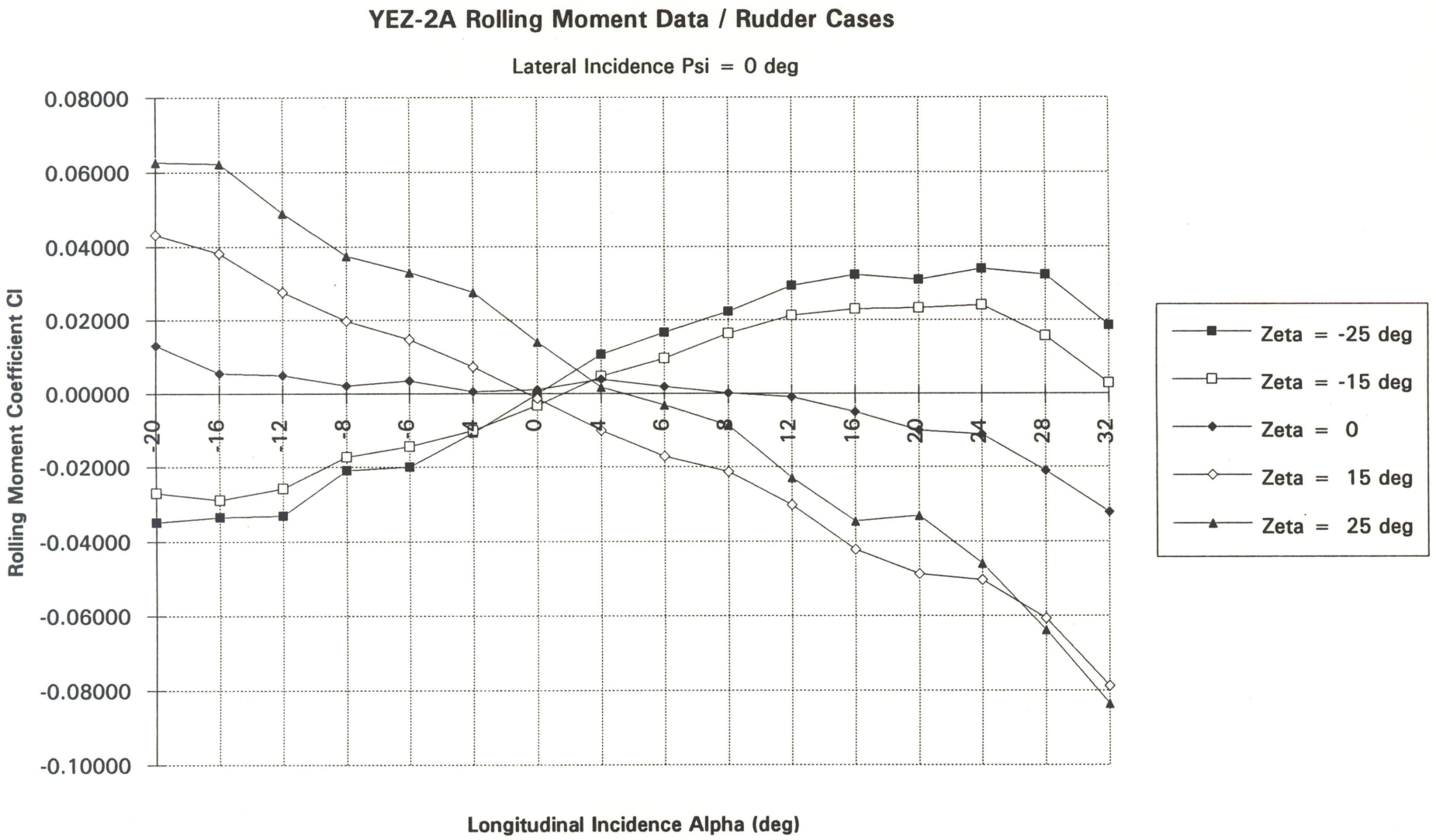


FIGURE A1.4.46

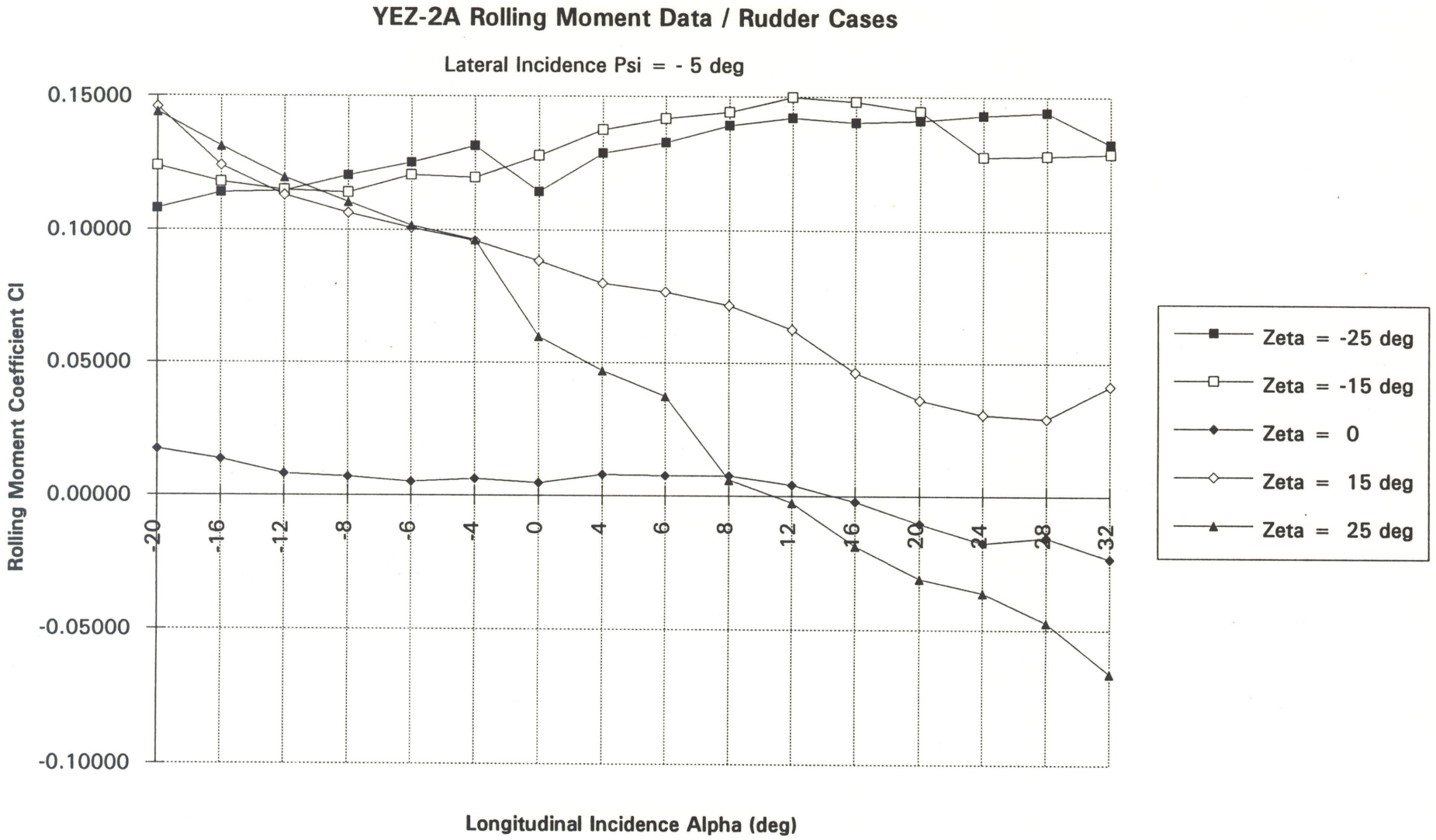


FIGURE A1.4.47

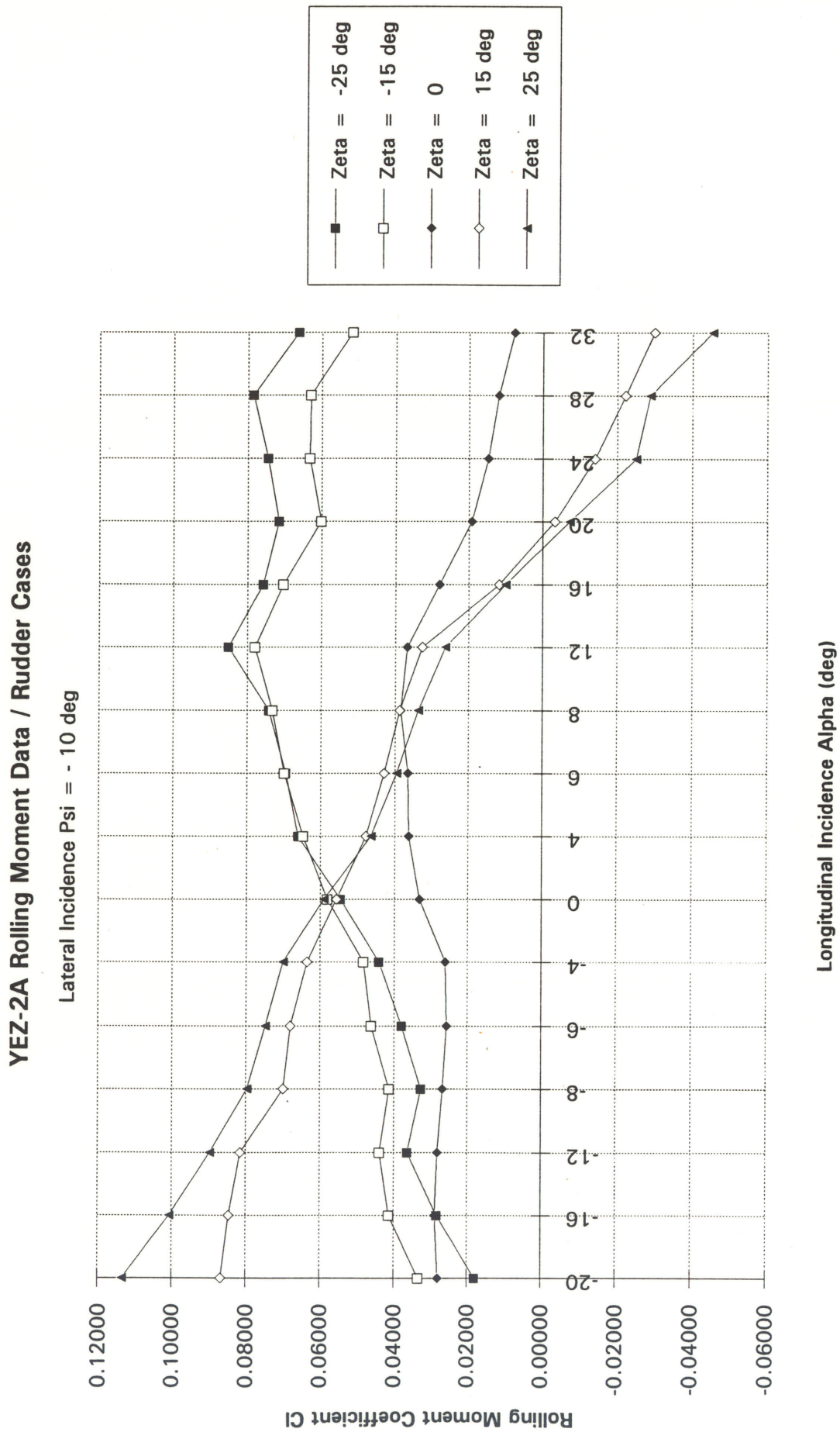


FIGURE A1.4.48

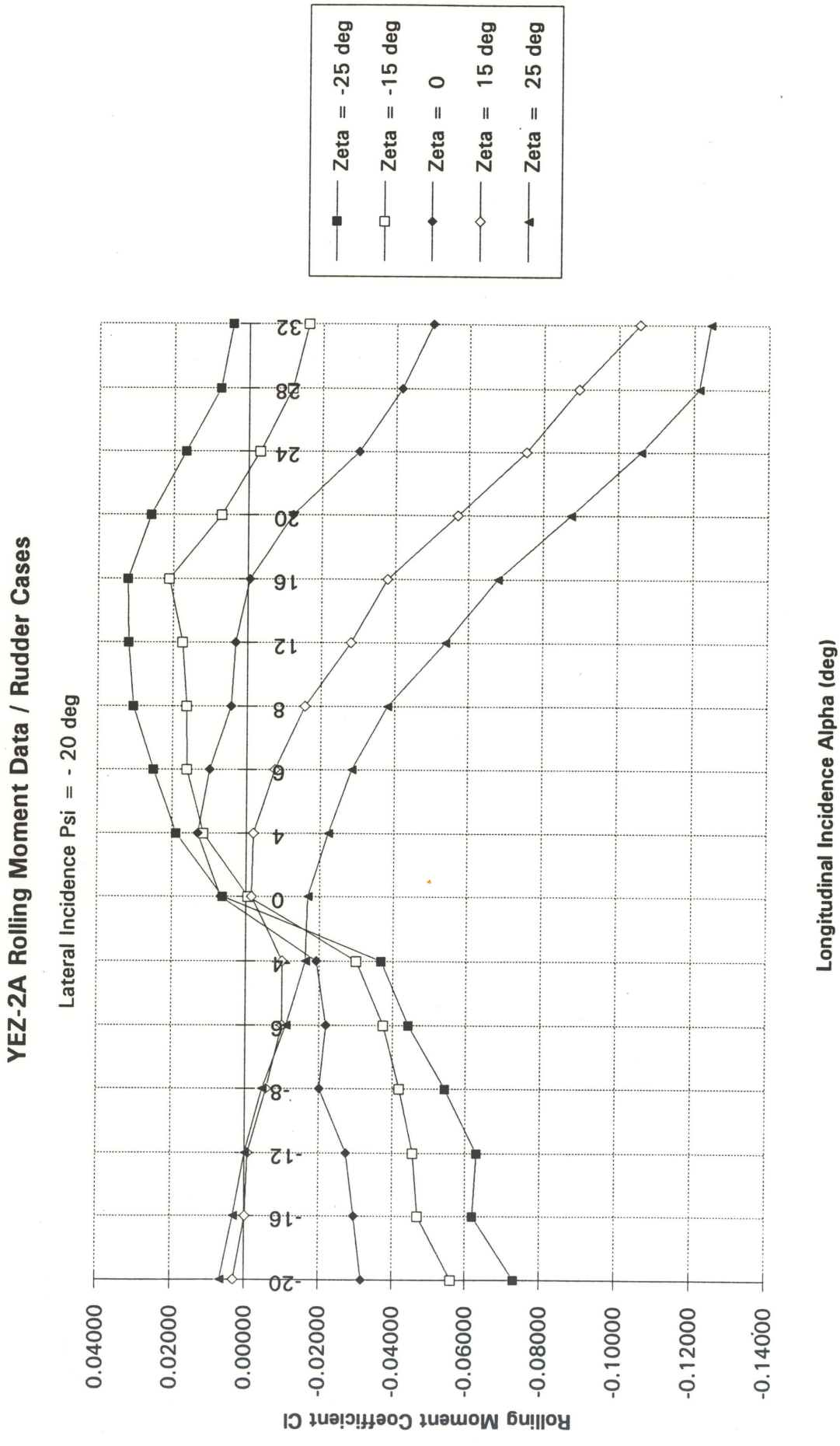


FIGURE A1.4.49

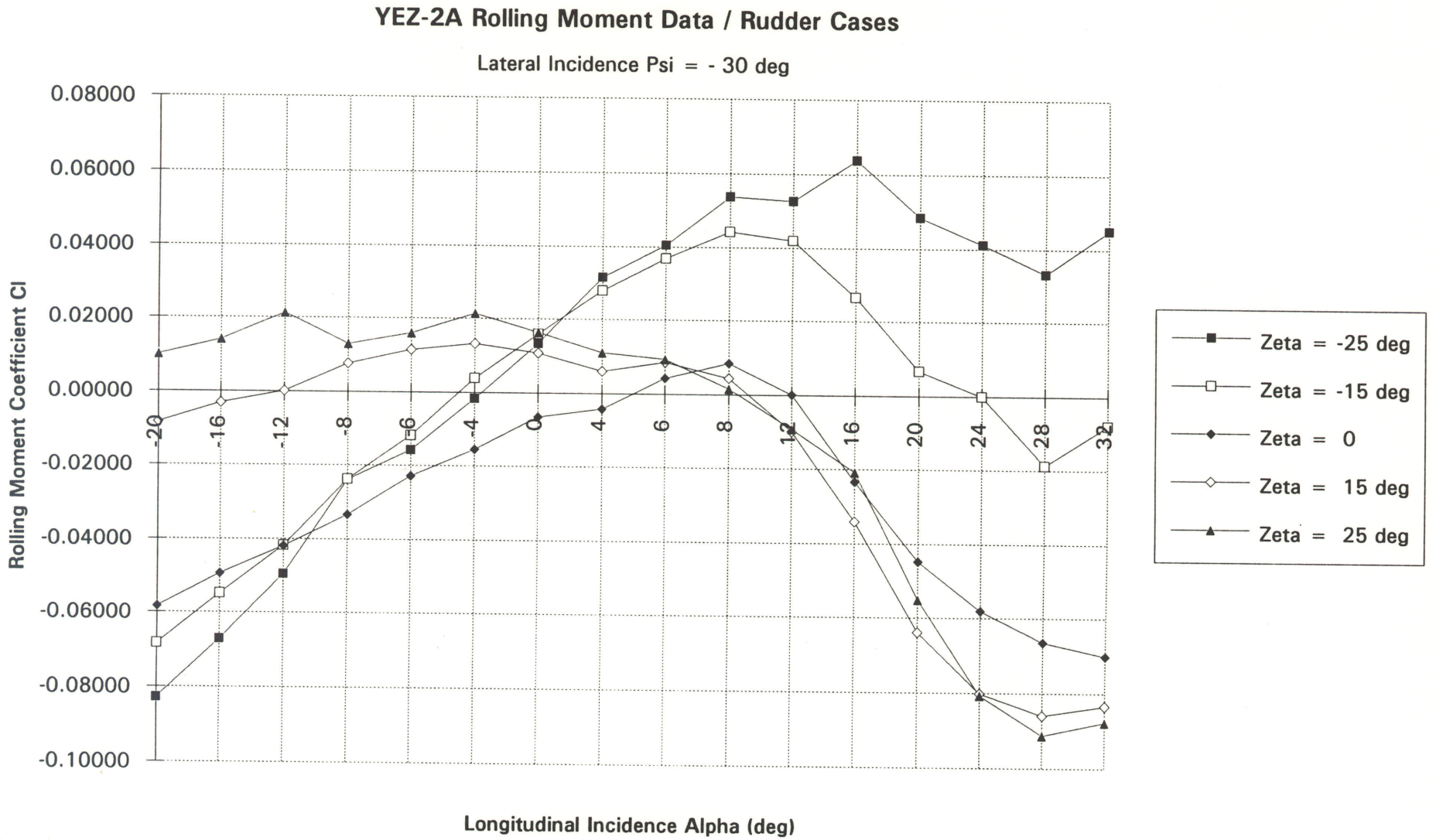


FIGURE A1.4.50

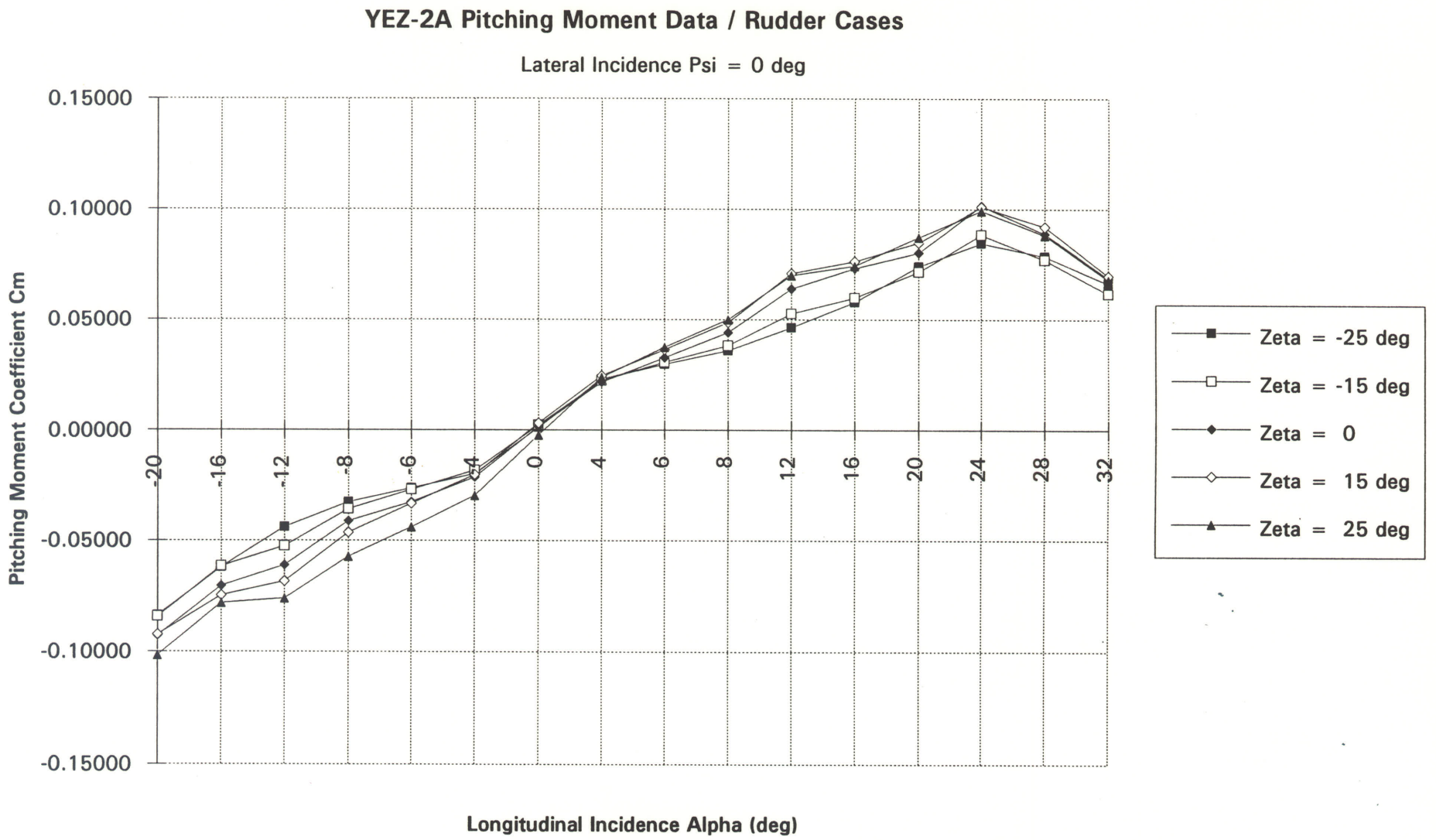


FIGURE A1.4.51

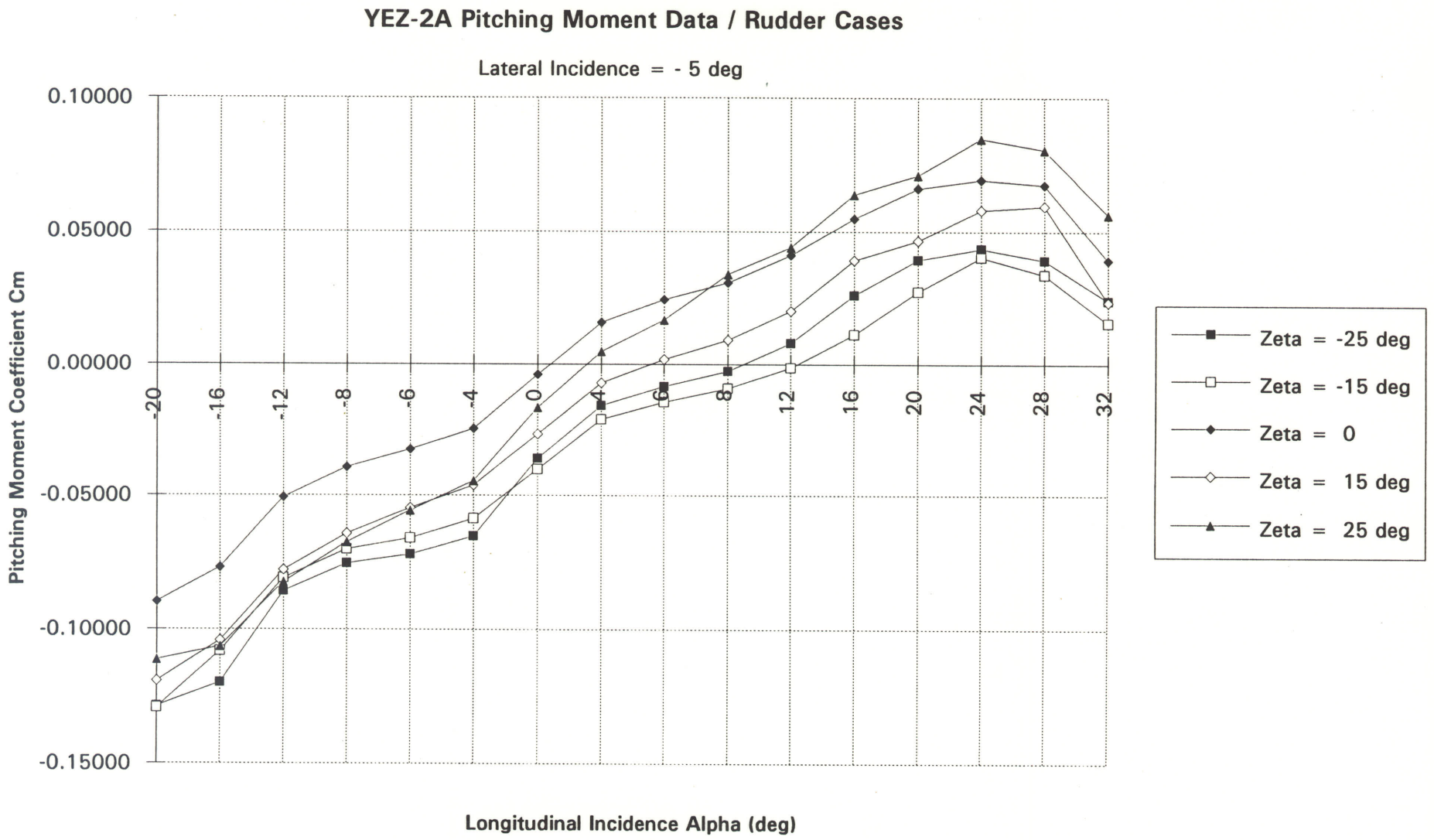


FIGURE A1.4.52

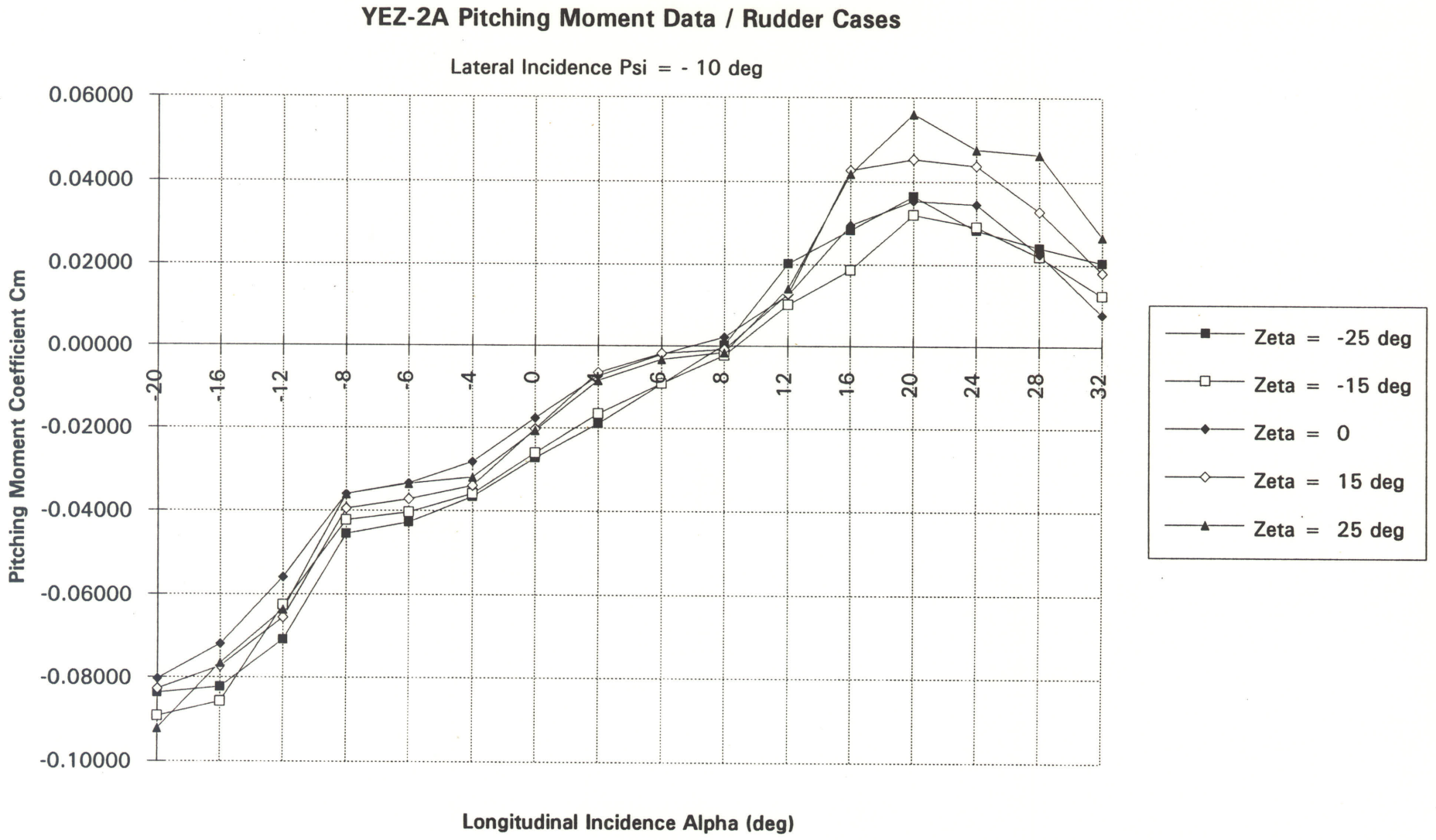


FIGURE A1.4.53

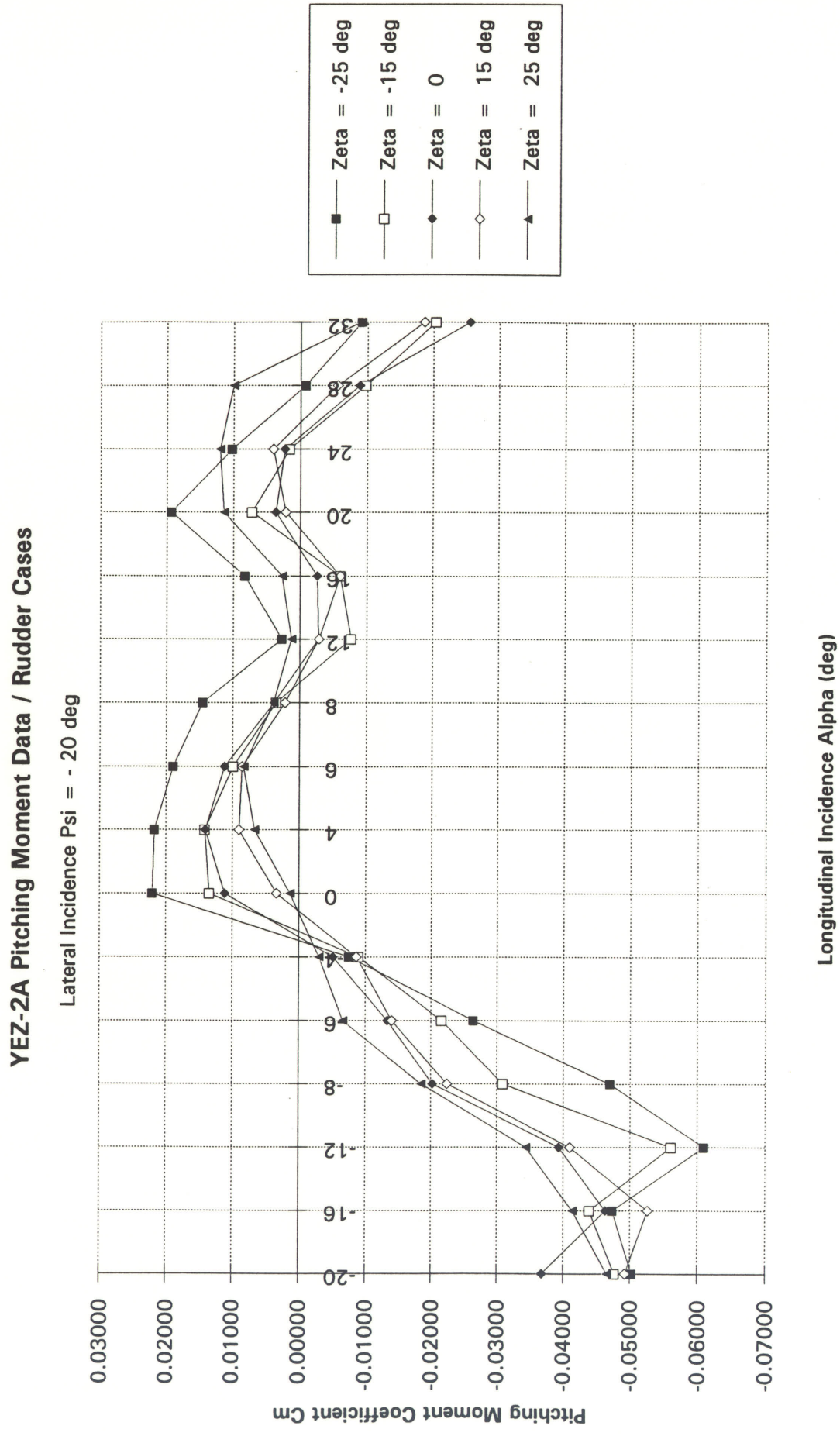


FIGURE A1.4.54

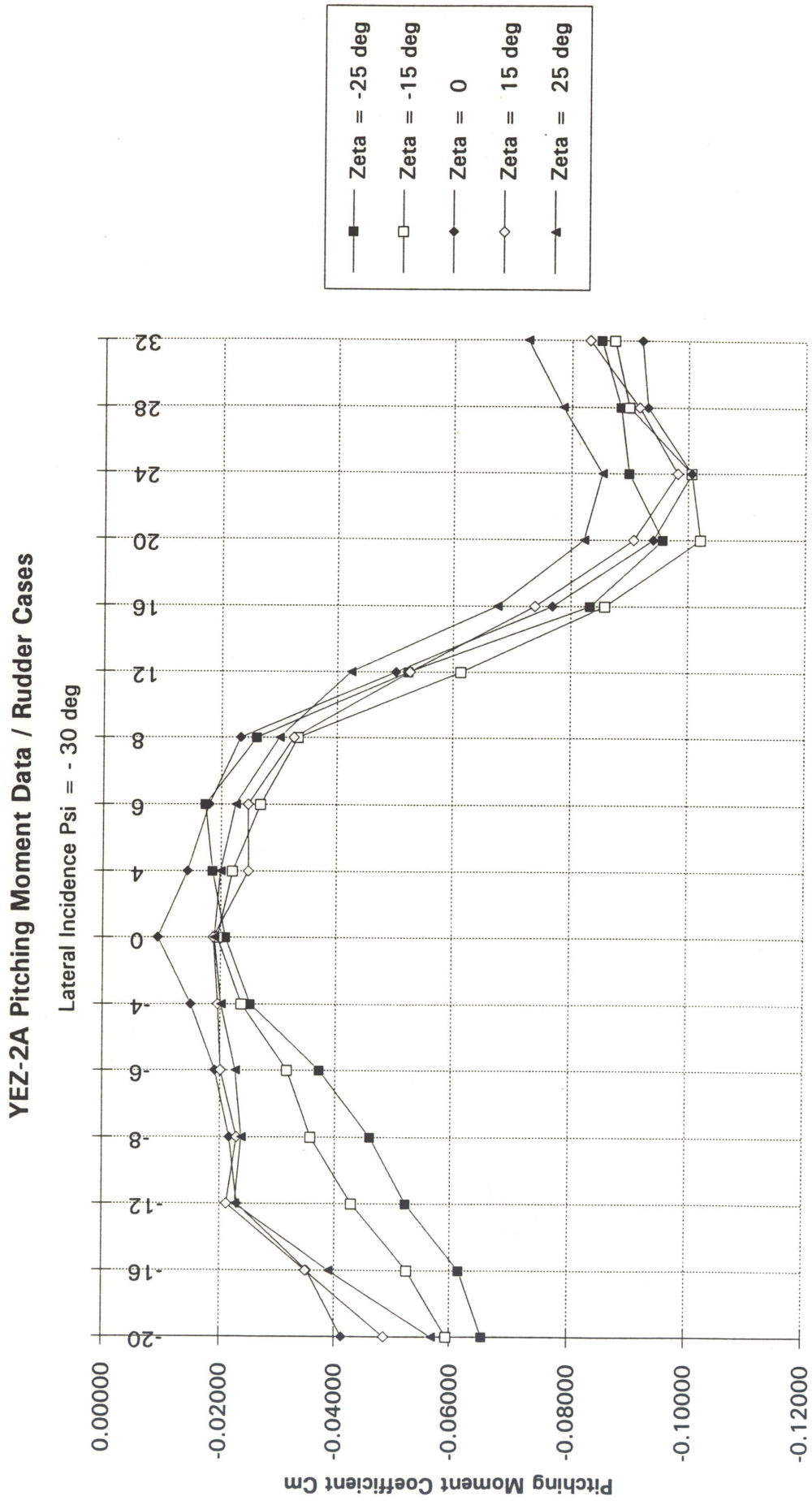


FIGURE A1.4.55

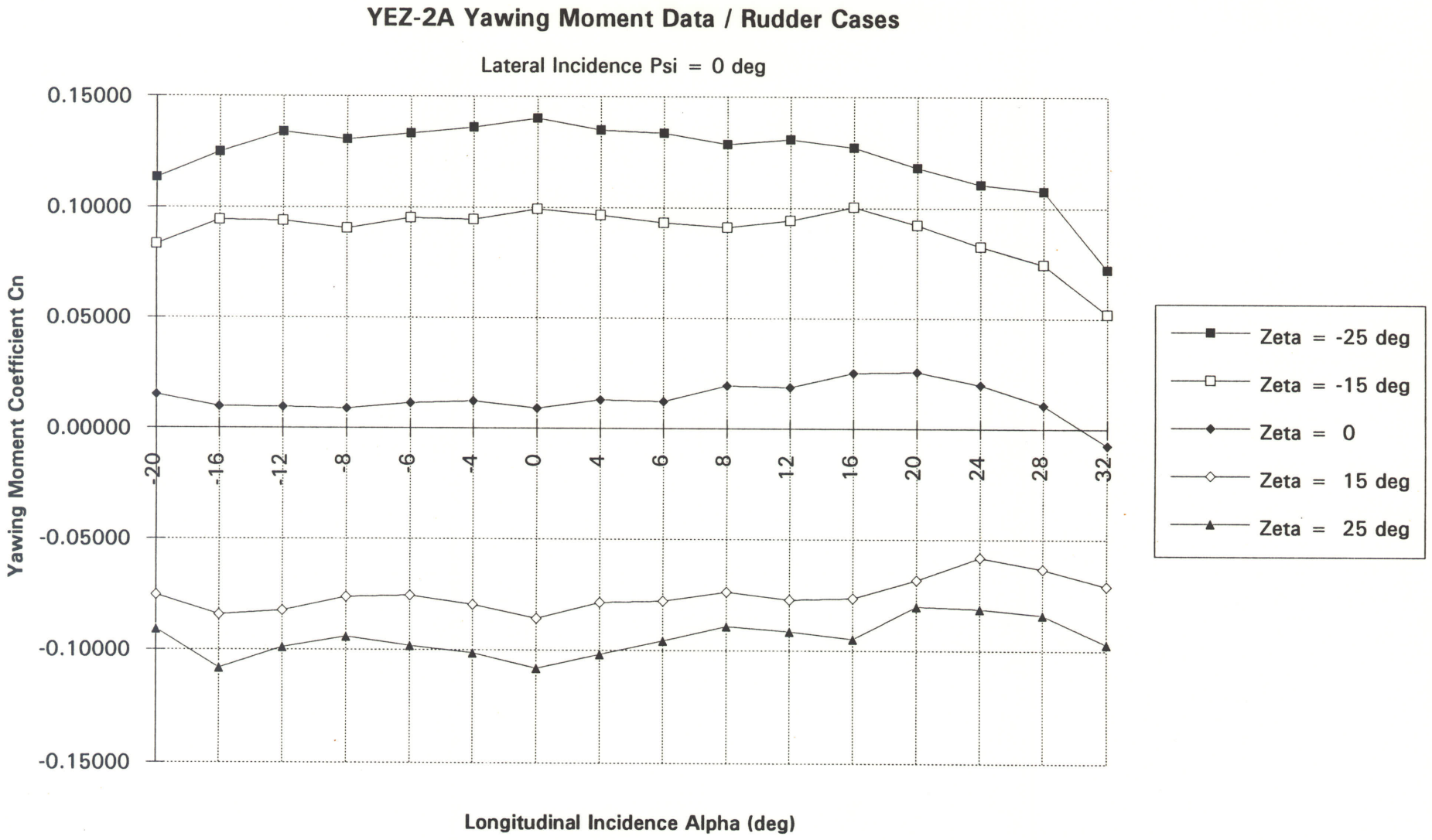


FIGURE A1.4.56

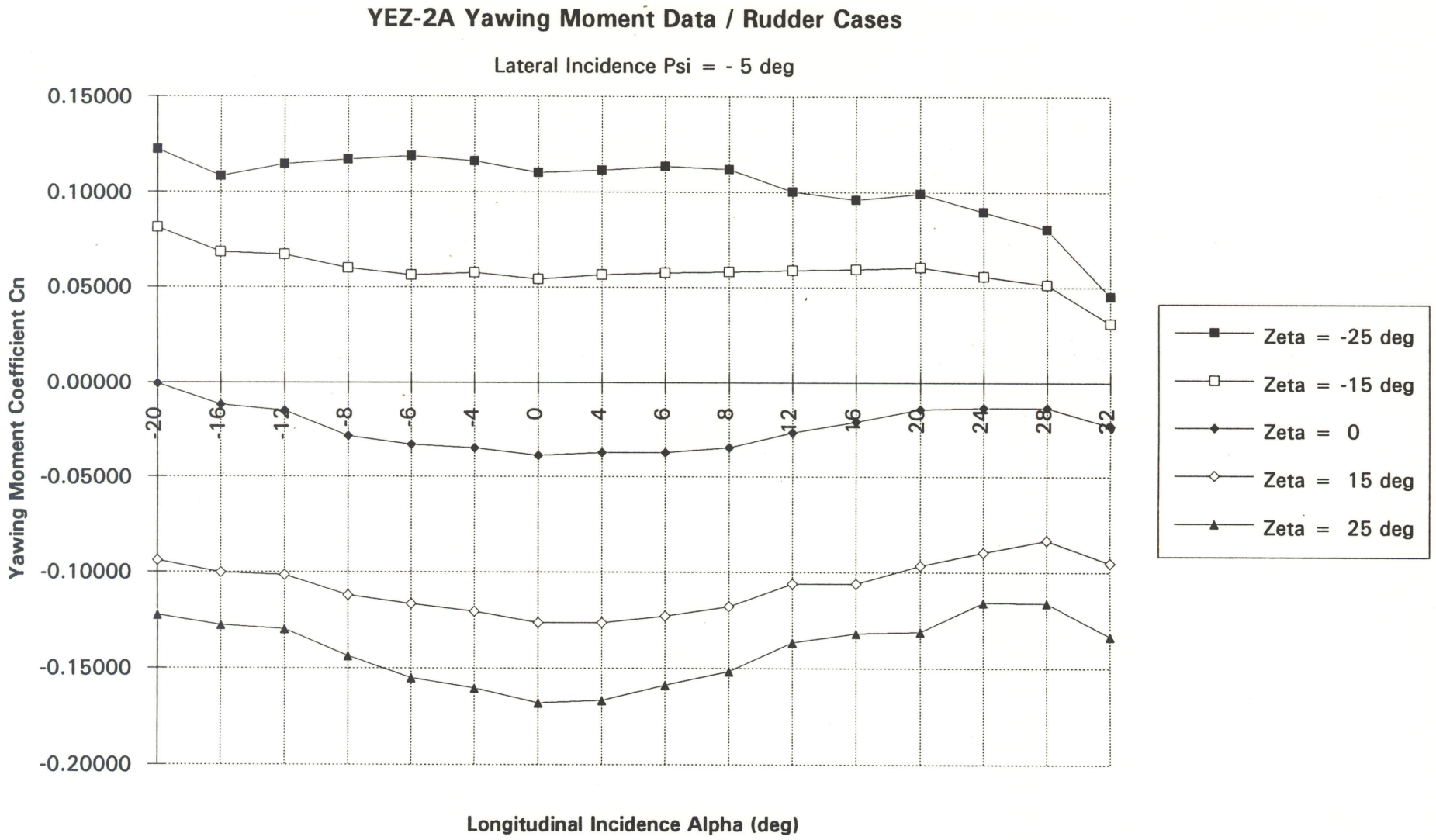


FIGURE A1.4.57

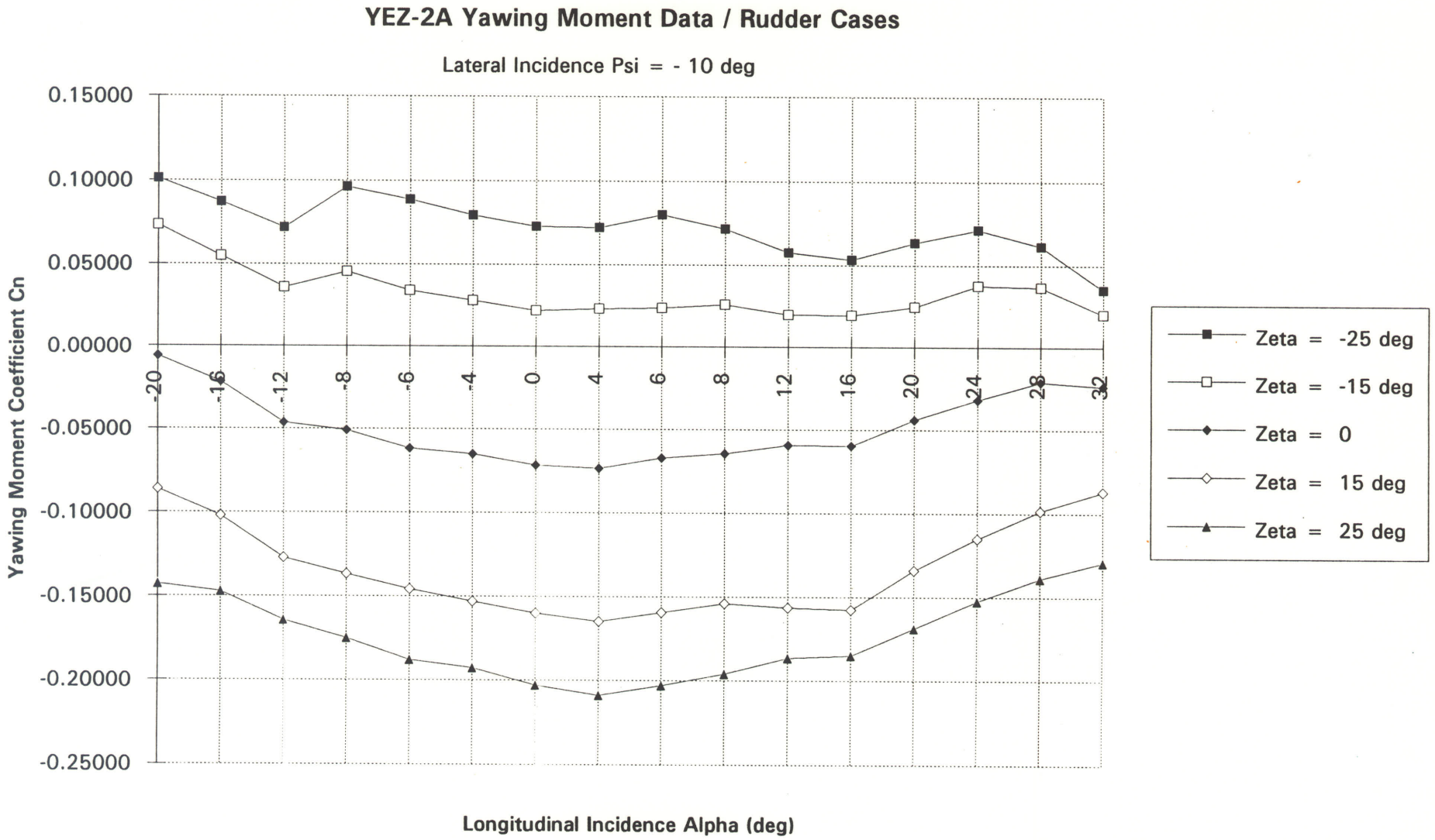


FIGURE A1.4.58

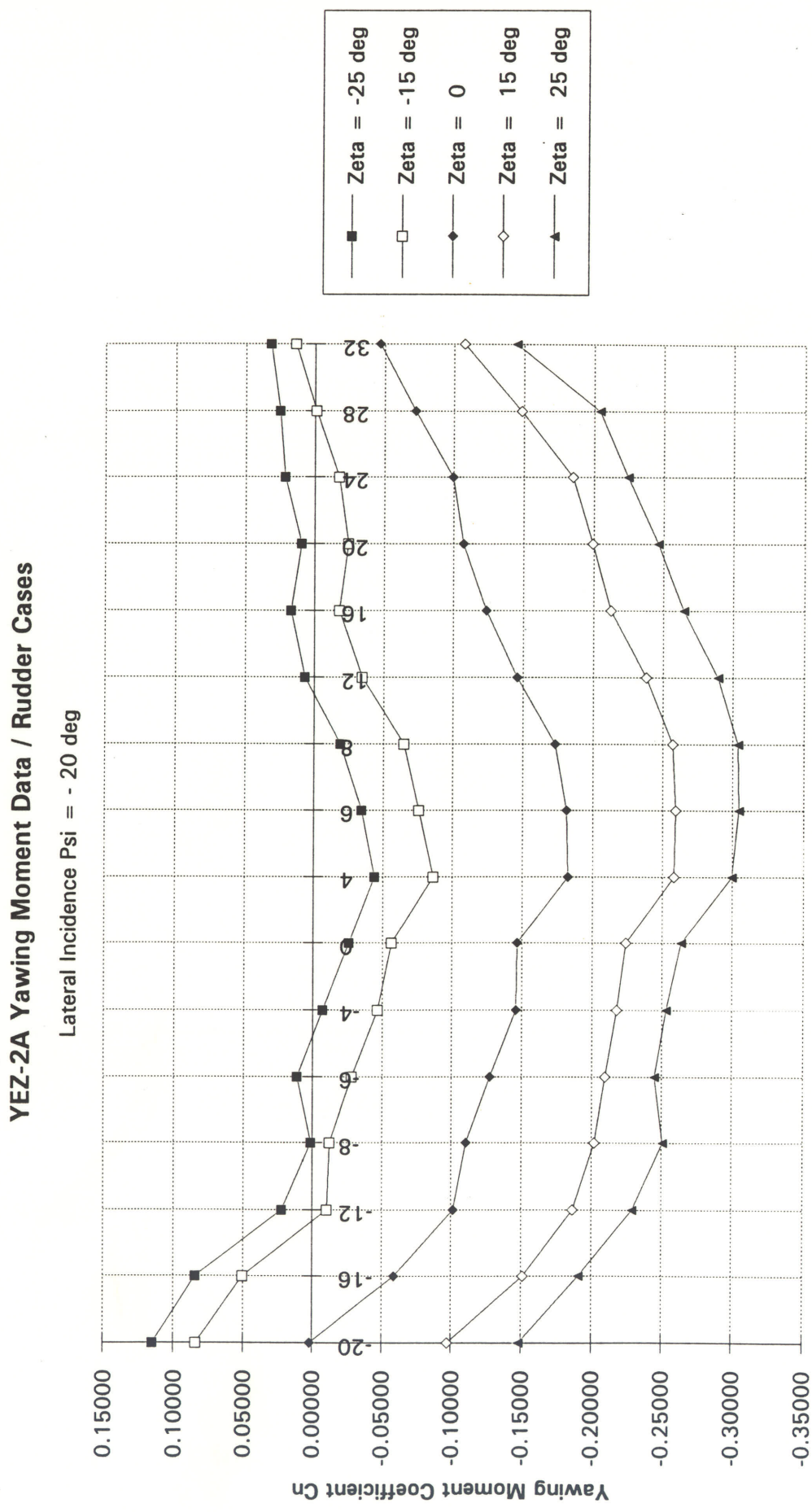


FIGURE A1.4.59

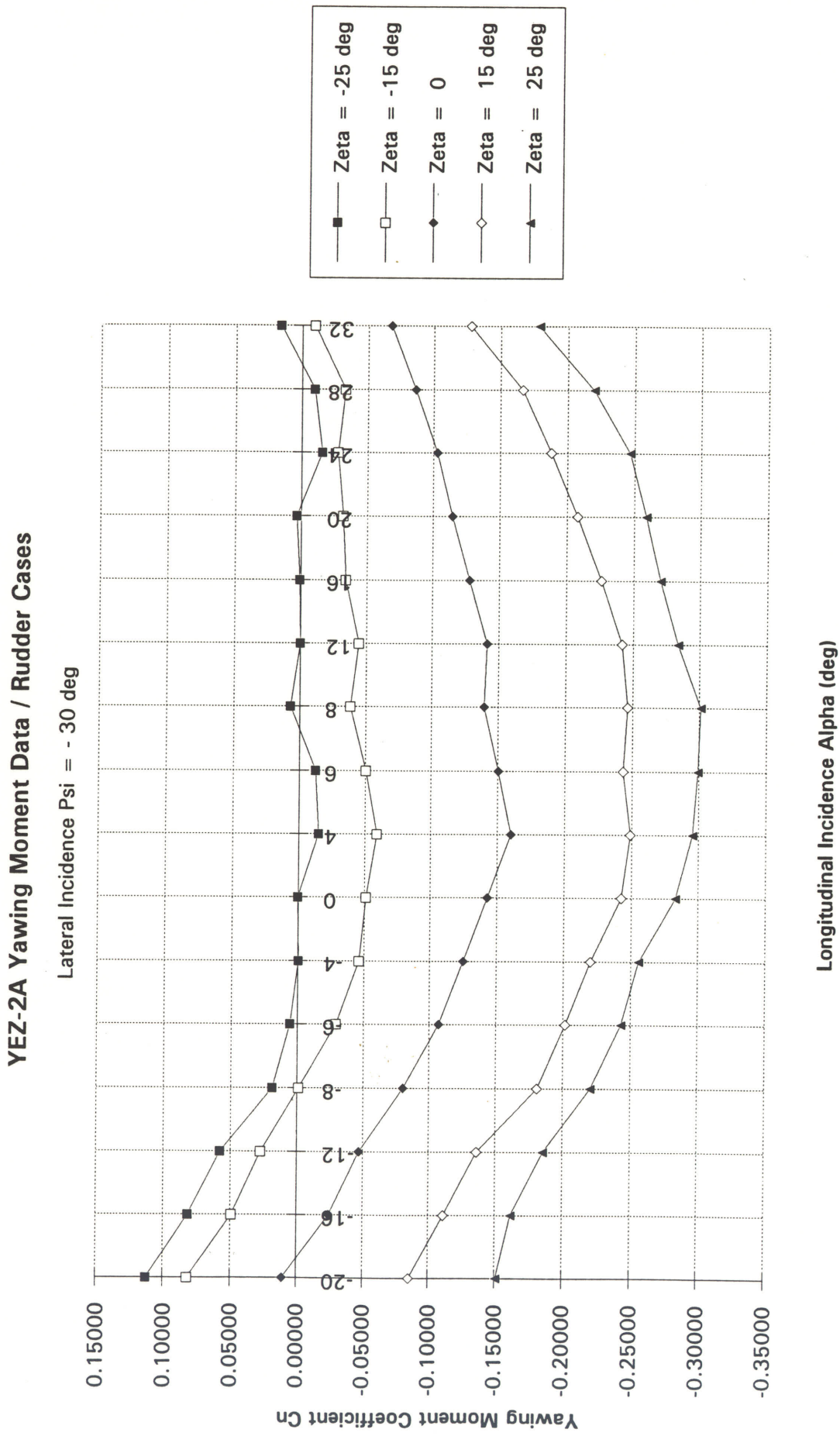


FIGURE A1.4.60

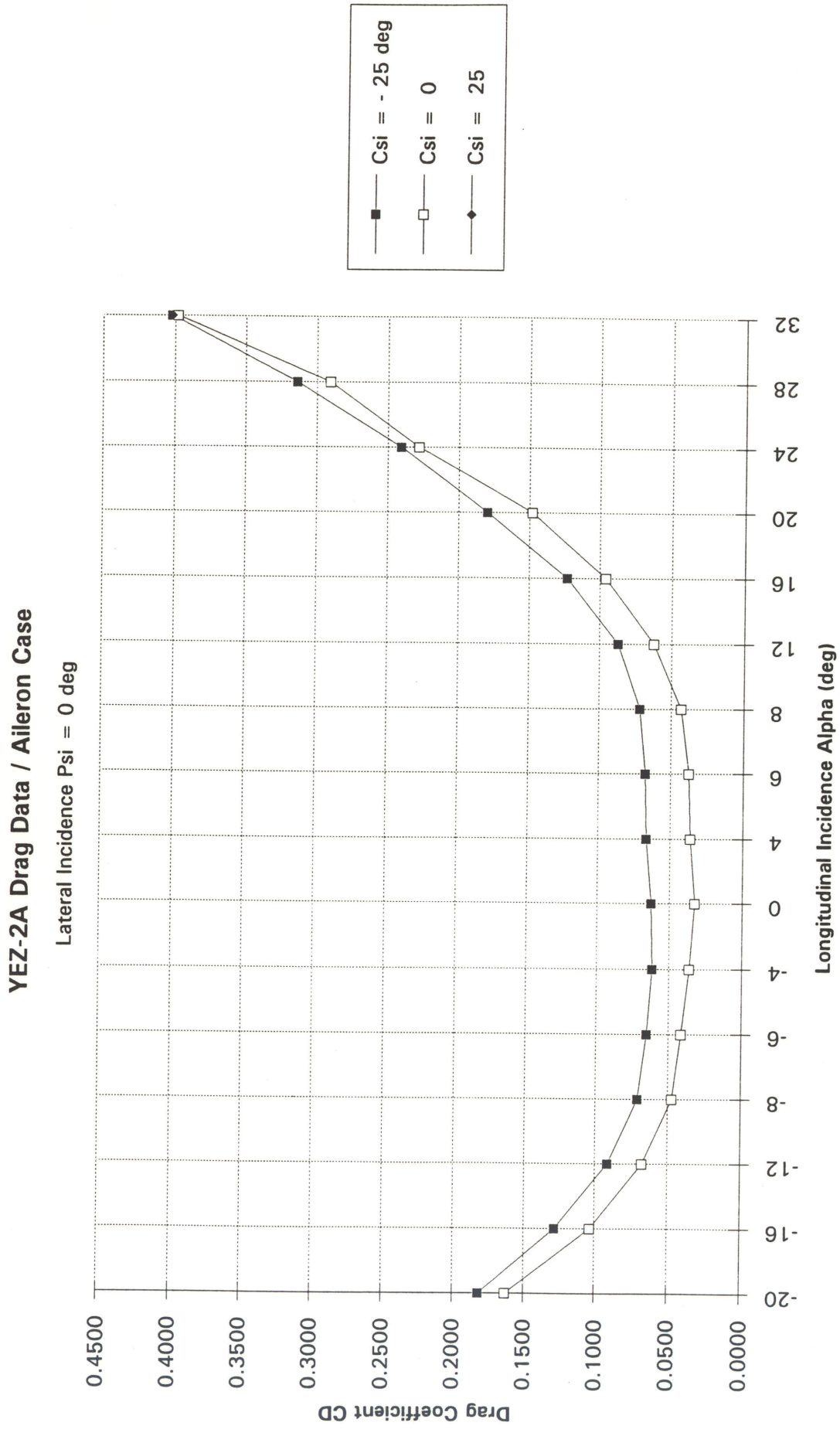


FIGURE A1.4.61

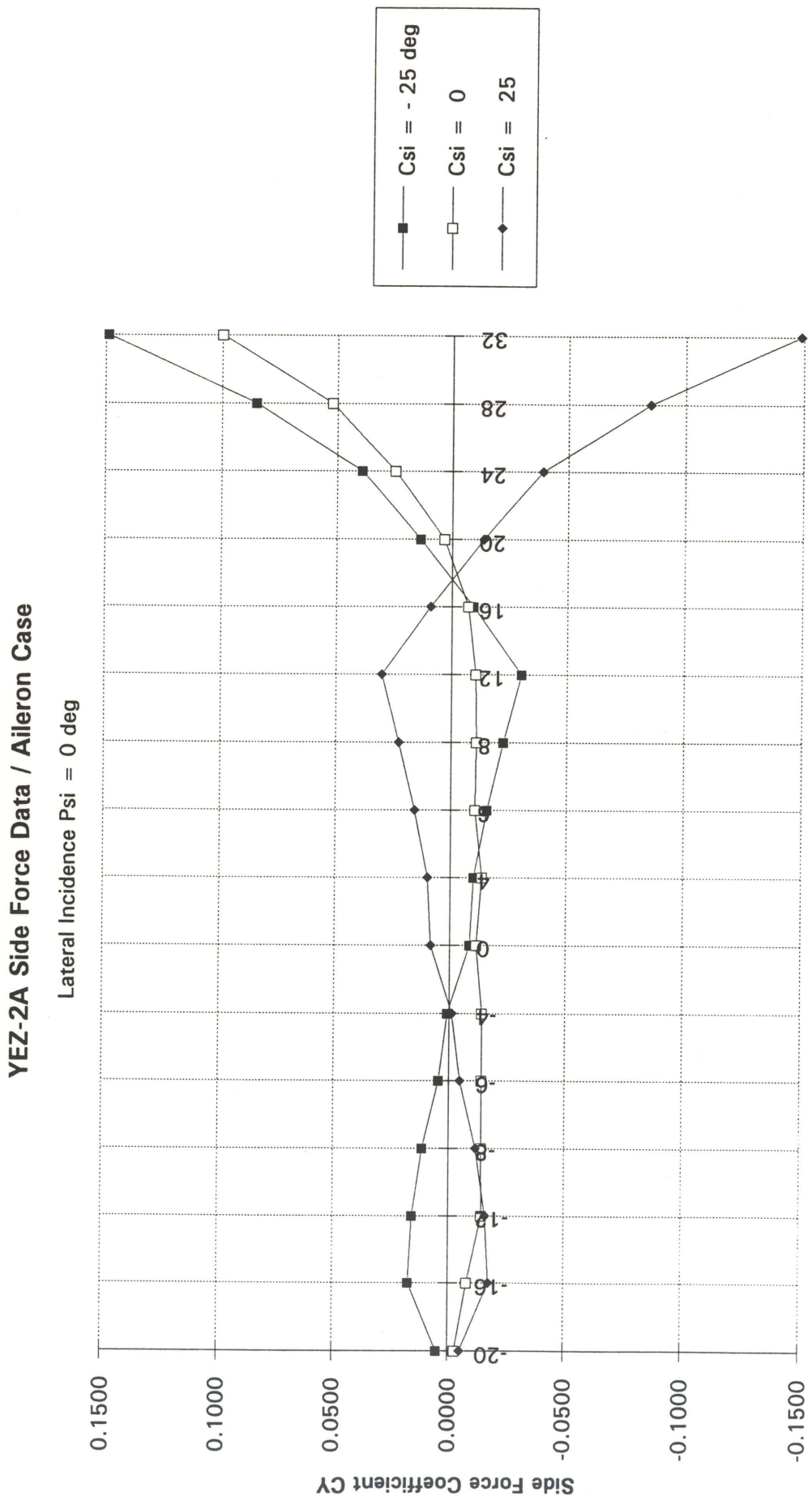


FIGURE A1.4.62

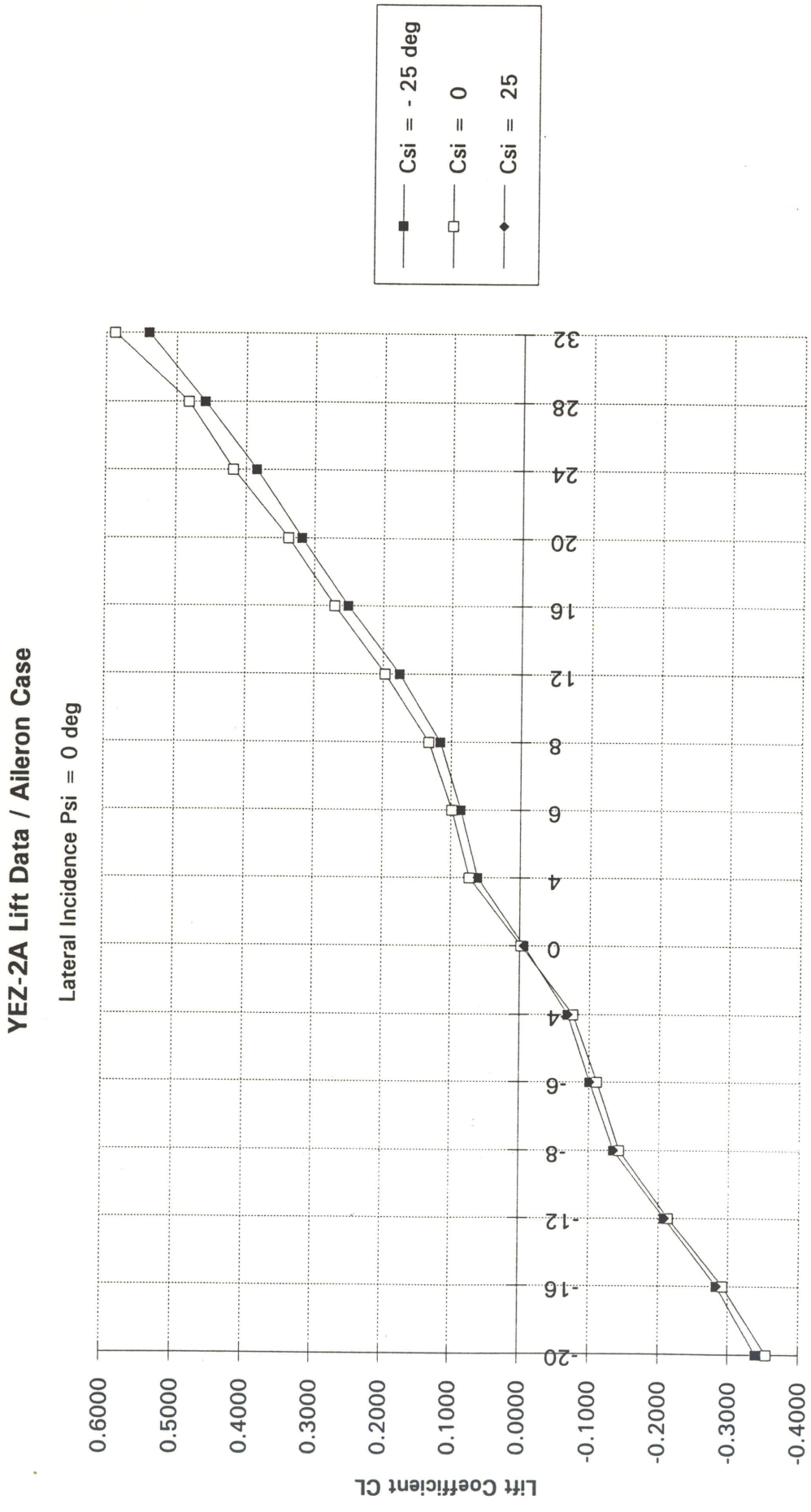


FIGURE A1.4.63

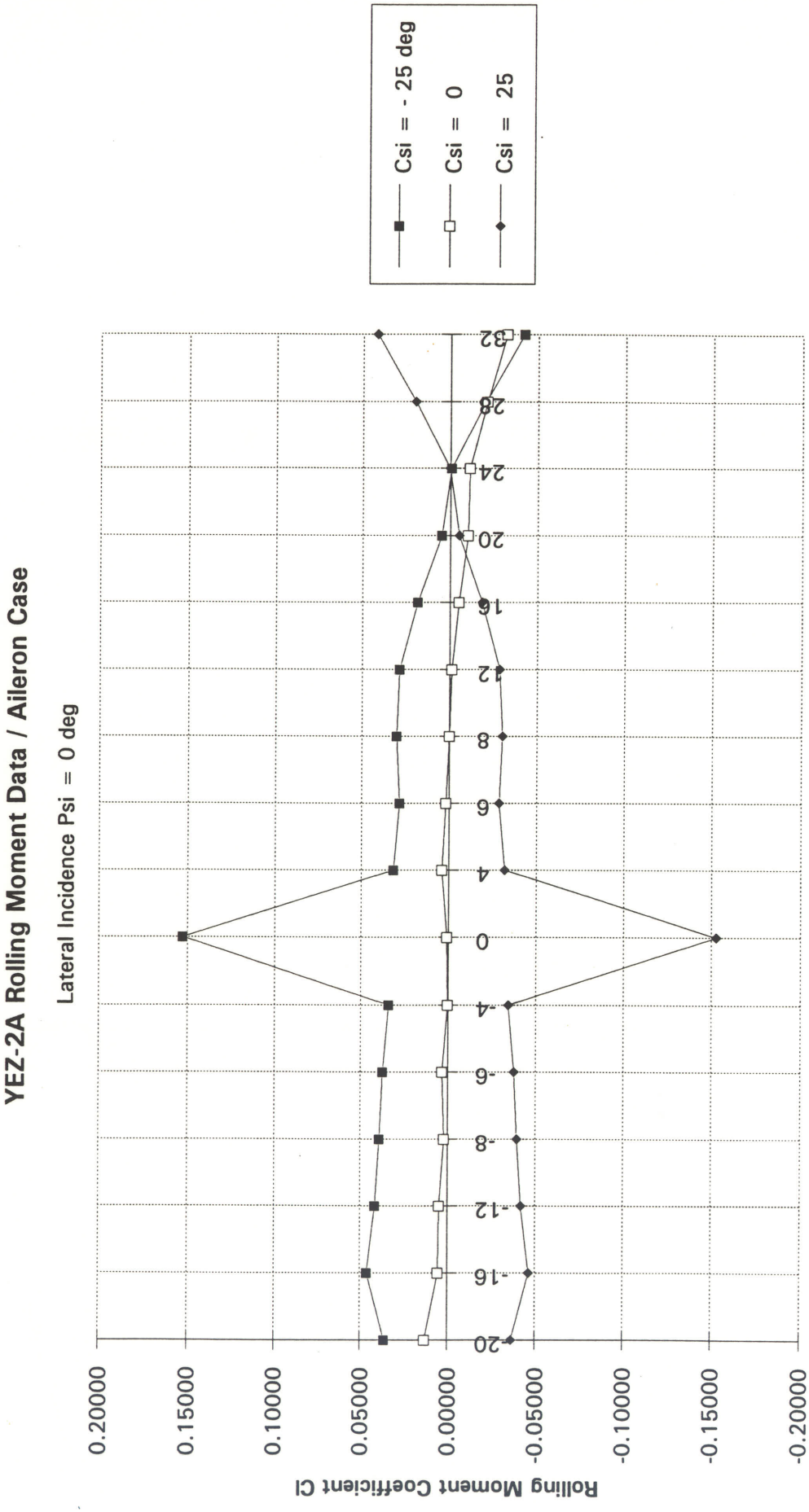


FIGURE A1.4.64

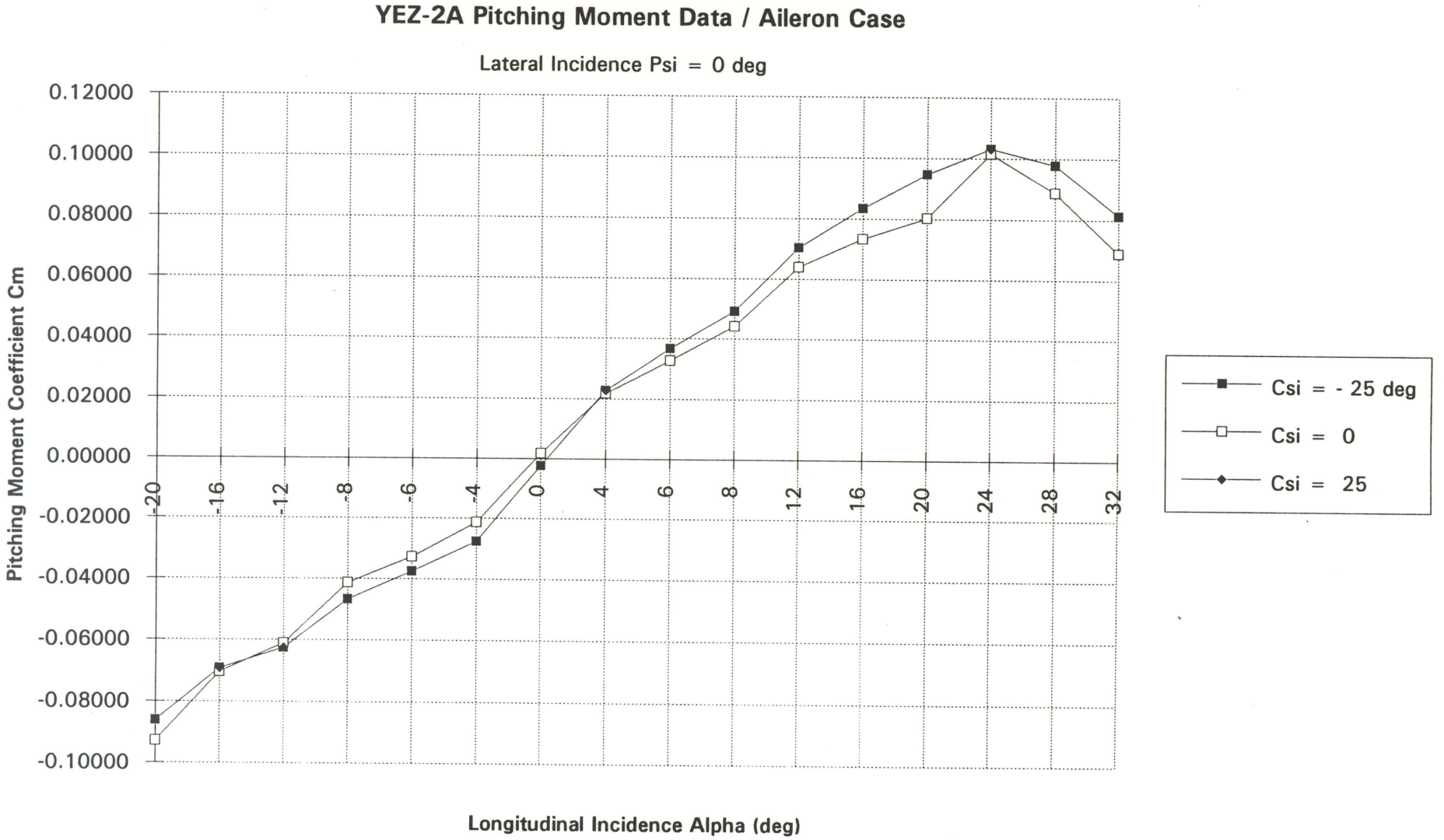


FIGURE A1.4.65

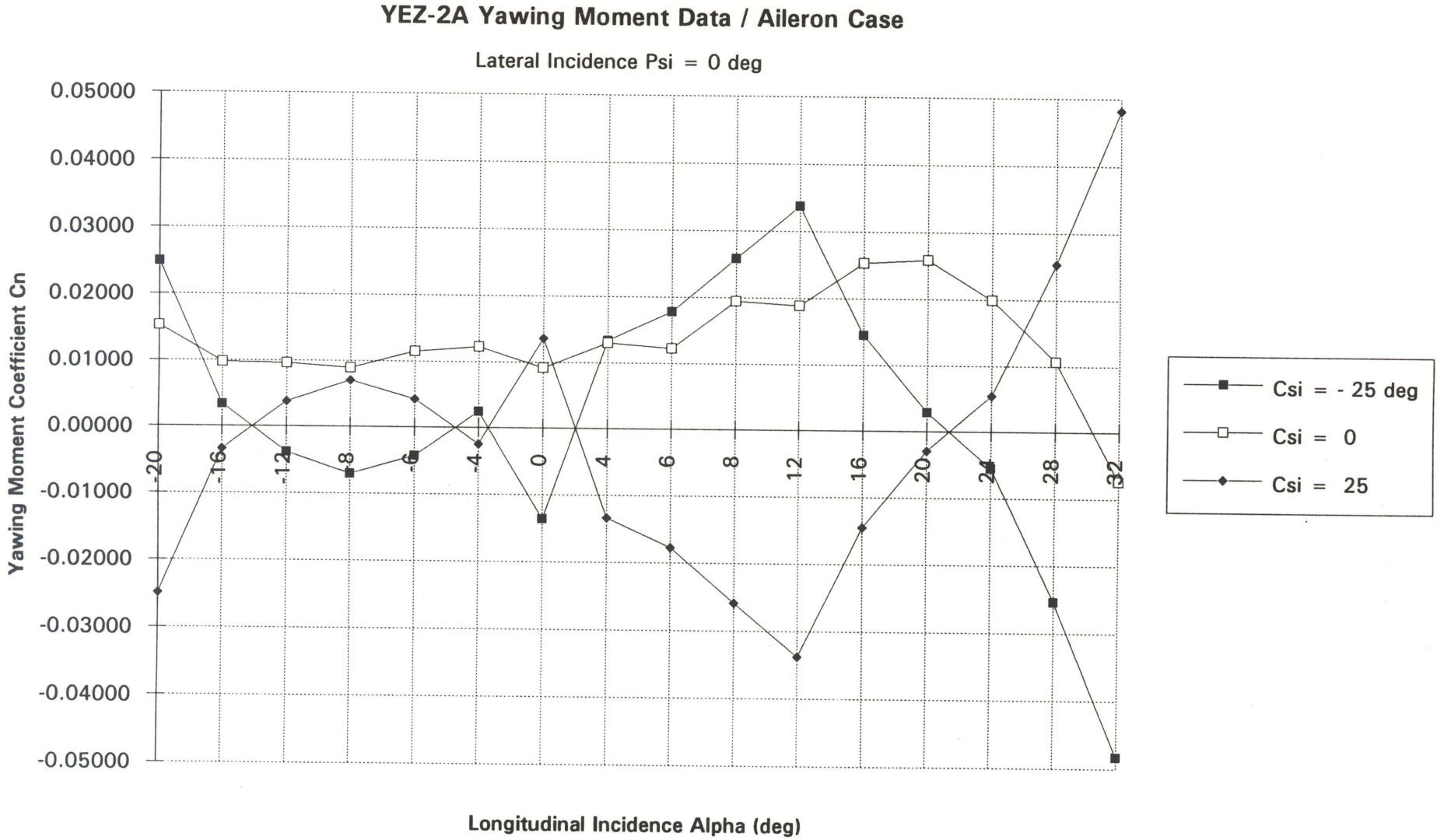


FIGURE A1.4.66

A1.5 Task 3 Results

The following Table A1.5.1 presents the results of the dynamic wind tunnel tests carried out as part of Task 3. The damping or rotary aerodynamic stability derivatives are stated in terms of the standard non-dimensional coefficients m_q, m_w, n_r and n_v, where

$$m_q = \frac{M_q}{0.5 \times \rho \times U^2 \times S \times b^2}$$

$$m_w = \frac{M_w}{0.5 \times \rho \times U^2 \times S \times b}$$

$$n_r = \frac{N_r}{0.5 \times \rho \times U^2 \times S \times b^2}$$

$$n_v = \frac{N_v}{0.5 \times \rho \times U^2 \times S \times b}$$

$M_q = \partial M/\partial q$ $M_w = \partial M/\partial w$ $N_r = \partial N/\partial r$ $N_v = \partial n/\partial v$

ρ = Air density (Kg/m^3)

U = Air speed in wind tunnel test section (m/s)

S = Airship model volume raised to the power 2/3

b = Airship model length (m)

It is important to notice that the results quoted for the other airships in Table A1.5.1 were, as far as could be determined, stated in terms of the same coefficients and non-dimensionalization factors as given above.

There are also three columns of results. This is because there were two attempts at carrying out the Task 3 tests. In the first one, only the free oscillation method yielded reasonable results, whereas in the second attempt the free and the forced oscillation methods

Comparison Between Task 3 Results and Estimates for other Airships

Aerodynamic Stability Derivative		Estimates from Reference 44			Task 3 Results for the YEZ-2A Airship Model		
American Notation	British Notation	ZR-1	ZR-4	Inverted Y-Tail Blimp	Free Oscillation/ 1st	Free Oscillation 2nd	Forced Oscillation
Cm_q	m_q	-0.1782	-0.2290	-0.3010	-0.256	-0.211	-0.238
Cm_α	m_w	0.2108	0.1710	0.0831	0.110	0.169	0.177
Cn_r	n_r	-0.1563	-0.2352	-0.2834	-0.258	-0.223	-0.220
Cn_β	n_v	-0.2180	-0.1710	-0.1188	-0.180	-0.213	-0.203

Notes: 1. ZR-1 is the US Navy designation for the "Shenandoah"

2. ZR-4 is the US Navy designation for the "Akron".

3. The "Inverted Y-tail blimp" is very similar to the existing Aerotek airship.

T A B L E A1.5.1

yielded acceptable results (See Ref. 38). For the YEZ-2A flight dynamics simulation, the results of the first free oscillation test were employed.

A1.6 YEZ-2A Mass and Inertia Tables

The following Tables A1.6.1-3 present the masses and inertias for three conditions, i.e.,

Case 1: ISA, sea level, neutral buoyancy
Case 2: ISA, sea level, 2268 Kg light
Case 3: ISA, sea level, 7118 Kg heavy

The data presented in the three Tables was supplied by the Weights Department of Airship Industries based on the current best estimates for the various YEZ-2A constituent elements. The last row of each table contains the data relevant to the flight dynamics simulation: Total airship mass, CG position (with reference to the the gas envelope bow) and moments and product of inertia with reference to the CG.

The CG position of the air ballonets was also determined from the X, Y and Z columns of each table, at the row corresponding to each of the four ballonets. This information was required in the initial trimming procedure of the simulation (See Section 4.9).

INERTIA ANALYSIS FOR NASP

PROJECT	NASP-ODM	: ISA +/- =	0
ANALYSIS REFERENCE	A-A-EQ	:ALTITUDE =	0M
ANALYSIS TITLE	CASE 1	:BALLONET =	60%
	03-MAY-89	:HEAVN'SS =	0KG

NOTE: ----- INERTIAS IN KG.M^2 MASS IN KG C. OF G. IN METRES

DESCRIPTION	MASS	X	Y	Z	IX	IY	IZ	IXZ	MXZ
ENVELOPE, TOTAL	11013.62	53.05	0	-0.45844	1631753	11007487	10649937	0	-2.68E+05
GONDOLA EMPTY-TOTAL	33917.42	58.47	0.02	-19.39	279665	1565888	1451667	0	-3.85E+07
TAIL FINS,C/S & SUSPENSN	2908.42	109.96	0.00	0.00	422402	283658	283658	0	0.00E+00
PRESSURE GROUP-HULL	370.13	57.20	0.00	-13.59	40313	74228	109147	0	-2.88E+05
FLIGHT CONTROLS-HULL	322.05	111.41	0.00	-0.27	1170	7300	6130	0	-9.69E+03
INSTRUMENTS+NAVN-HULL	63.50	56.39	0.00	0.00	0	0	0	0	0.00E+00
PNEUMATICS-HULL	42.55	52.12	0.00	-11.89	0	0	0	0	-2.64E+04
ELECTRICAL-HULL	49.89	91.94	0.00	-2.45	1357	23027	15069	0	-1.12E+04
AUXILIARY GEAR-HULL	93.89	28.62	0.00	-13.69	1986	41409	39423	0	-3.68E+04
	0.00	0.00	0.00	0.00	0	0	0	0	0.00E+00
	0.00	0.00	0.00	0.00	0	0	0	0	0.00E+00
	0.00	0.00	0.00	0.00	0	0	0	0	0.00E+00
	0.00	0.00	0.00	0.00	0	0	0	0	0.00E+00
	0.00	0.00	0.00	0.00	0	0	0	0	0.00E+00
	0.00	0.00	0.00	0.00	0	0	0	0	0.00E+00
	0.00	0.00	0.00	0.00	0	0	0	0	0.00E+00
	0.00	0.00	0.00	0.00	0	0	0	0	0.00E+00
	0.00	0.00	0.00	0.00	0	0	0	0	0.00E+00
	0.00	0.00	0.00	0.00	0	0	0	0	0.00E+00
	0.00	0.00	0.00	0.00	0	0	0	0	0.00E+00
	0.00	0.00	0.00	0.00	0	0	0	0	0.00E+00
SUB-TOTAL, EMPTY WEIGHT	48781.47	60.63	0.01	-13.73	6.030E+06	2.551E+07	2.141E+07	1.510E+06	-4.06E+07
PAYLOAD	8131.63	59.59	0.00	-19.44	93182	231909	274548	14134	-9.42E+06
	0.00	0.00	0.00	0.00	0	0	0	0	0.00E+00
	0.00	0.00	0.00	0.00	0	0	0	0	0.00E+00
	0.00	0.00	0.00	0.00	0	0	0	0	0.00E+00
	0.00	0.00	0.00	0.00	0	0	0	0	0.00E+00
	0.00	0.00	0.00	0.00	0	0	0	0	0.00E+00
SUB-TOTAL, T.O.W.	56913.10	60.48	0.01	-14.54	6.350E+06	2.597E+07	2.169E+07	1.566E+06	-5.01E+07
HELIUM	14222.59	60.26	0.00	0.00	1495506	12607266	12607266	0	0.00E+00
AIR, FWD BALLONET	5227.11	25.30	0.00	-7.07	259154	259154	404678	0	-9.35E+05
AIR, AFT BALLONET	5227.11	95.10	0.00	-6.31	259154	259154	404678	0	-3.14E+06
AIR, PANNIER, STBD	2613.25	60.20	13.21	-1.52	60247	282761	247871	0	-2.39E+05
AIR, PANNIER, PORT	2613.25	60.20	-13.21	-1.52	60247	282761	247871	0	-2.39E+05
	0.00	0.00	0.00	0.00	0.00	0.00	0.00	0.00	0.00E+00
	0.00	0.00	0.00	0.00	0.00	0.00	0.00	0.00	0.00E+00
	0.00	0.00	0.00	0.00	0.00	0.00	0.00	0.00	0.00E+00
	0.00	0.00	0.00	0.00	0.00	0.00	0.00	0.00	0.00E+00
TOTAL	86816	60.39	0.01	-10.43	12470787	55472495	49248564	1648250	-5.47E+07

T A B L E A1.6.1 - The YEZ-2A mass and inertias for the ISA, sea level, neutral buoyancy condition, i.e., CASE 1.

INERTIA ANALYSIS FOR NASP

PROJECT	NASP-ODM	ISA +/- =	0
ANALYSIS REFERENCE	A-B-A	ALTITUDE =	0M
ANALYSIS TITLE	CASE 5	BALLONET =	60%
DATE	12-JAN-89	LIGHT'SS =	2268KG

NOTE: INERTIAS IN KG.M^2; MASS IN KG; C. OF G. IN METRES

DESCRIPTION	MASS	X	Y	Z	IX	IY	IZ	IXZ	MXZ
ENVELOPE, TOTAL	11013.62	53.05	0	-0.45844	1631753	11007487	10649937	0	-2.68E+05
GONDOLA EMPTY-TOTAL	33917.42	58.47	0.02	-19.39	279665	1565888	1451667	0	-3.85E+07
TAIL FINS,C/S & SUSPENSN	2908.42	109.96	0.00	0.00	422402	283658	283658	0	0.00E+00
PRESSURE GROUP-HULL	370.13	57.20	0.00	-13.59	40313	74228	109147	0	-2.88E+05
FLIGHT CONTROLS-HULL	322.05	111.41	0.00	-0.27	1170	7300	6130	0	-9.64E+03
INSTRUMENTS+NAVN-HULL	63.50	56.39	0.00	0.00	0	0	0	0	0.00E+00
PNEUMATICS-HULL	42.55	52.12	0.00	-11.89	0	0	0	0	-2.64E+04
ELECTRICAL-HULL	49.89	91.94	0.00	-2.45	1357	23027	15069	0	-1.12E+04
AUXILIARY GEAR-HULL	93.89	28.62	0.00	-13.69	1986	41409	39423	0	-3.68E+04
	0.00	0.00	0.00	0.00	0	0	0	0	0.00E+00
	0.00	0.00	0.00	0.00	0	0	0	0	0.00E+00
	0.00	0.00	0.00	0.00	0	0	0	0	0.00E+00
	0.00	0.00	0.00	0.00	0	0	0	0	0.00E+00
	0.00	0.00	0.00	0.00	0	0	0	0	0.00E+00
	0.00	0.00	0.00	0.00	0	0	0	0	0.00E+00
	0.00	0.00	0.00	0.00	0	0	0	0	0.00E+00
	0.00	0.00	0.00	0.00	0	0	0	0	0.00E+00
	0.00	0.00	0.00	0.00	0	0	0	0	0.00E+00
	0.00	0.00	0.00	0.00	0	0	0	0	0.00E+00
	0.00	0.00	0.00	0.00	0	0	0	0	0.00E+00
	0.00	0.00	0.00	0.00	0	0	0	0	0.00E+00
SUB-TOTAL, EMPTY WEIGHT	48781.47	60.63	0.01	-13.73	6.030E+06	2.551E+07	2.141E+07	1.510E+06	-4.06E+07
PAYLOAD	5863.63	60.35	0.00	-19.85	53490	195367	71662	6381	-7.02E+06
	0.00	0.00	0.00	0.00	0	0	0	0	0.00E+00
	0.00	0.00	0.00	0.00	0	0	0	0	0.00E+00
	0.00	0.00	0.00	0.00	0	0	0	0	0.00E+00
	0.00	0.00	0.00	0.00	0	0	0	0	0.00E+00
	0.00	0.00	0.00	0.00	0	0	0	0	0.00E+00
SUB-TOTAL, T.O.W.	54645.10	60.60	0.01	-14.39	6.280E+06	2.590E+07	2.148E+07	1.525E+06	-4.76E+07
HELIUM	14222.59	60.26	0.00	0.00	1495506	12607266	12607266	0	0.00E+00
AIR, FWD BALLONET	5227.11	25.30	0.00	-7.07	259154	259154	404678	0	-9.35E+05
AIR, AFT BALLONET	5227.11	95.10	0.00	-6.31	259154	259154	404678	0	-3.14E+06
AIR, PANNIER, STBD	2613.25	60.20	13.21	-1.52	60247	282761	247871	0	-2.39E+05
AIR, PANNIER, PORT	2613.25	60.20	-13.21	-1.52	60247	282761	247871	0	-2.39E+05
	0.00	0.00	0.00	0.00	0.00	0.00	0.00	0.00	0.00E+00
	0.00	0.00	0.00	0.00	0.00	0.00	0.00	0.00	0.00E+00
	0.00	0.00	0.00	0.00	0.00	0.00	0.00	0.00	0.00E+00
	0.00	0.00	0.00	0.00	0.00	0.00	0.00	0.00	0.00E+00
TOTAL	84548	60.47	0.01	-10.22	12287632	55288770	49039956	1582404	-5.22E+07

T A B L E A1.6.2 - The YEZ-2A mass and inertias for the ISA, sea level, 2268 Kg lightness condition, i.e., CASE 2.

INERTIA ANALYSIS FOR NASP

PROJECT	NASP-ODM	ISA +/- =	0				NOTE:	INERTIAS IN KG.M^2	
ANALYSIS REFERENCE	A-A-A	ALTITUDE =	0M				-----	MASS IN KG	
ANALYSIS TITLE	CASE 6	BALLONET =	60%					C. OF G. IN METRES	
DATE	12-JAN-89	HEAVN'SS =	7118KG						
DESCRIPTION	MASS	X	Y	Z	IX	IY	IZ	IXZ	MXZ
ENVELOPE, TOTAL	11013.62	53.05	0	-0.45844	1631753	11007487	10649937	0	-2.68E+05
GONDOLA EMPTY-TOTAL	33917.42	58.47	0.02	-19.39	279665	1565888	1451667	0	-3.85E+07
TAIL FINS,C/S & SUSPENSN	2908.42	109.96	0.00	0.00	422402	283658	283658	0	0.00E+00
PRESSURE GROUP-HULL	370.13	57.20	0.00	-13.59	40313	74228	109147	0	-2.38E+05
FLIGHT CONTROLS-HULL	322.05	111.41	0.00	-0.27	1170	7300	6130	0	-9.69E+03
INSTRUMENTS+NAVN-HULL	63.50	56.39	0.00	0.00	0	0	0	0	0.00E+00
PNEUMATICS-HULL	42.55	52.12	0.00	-11.89	0	0	0	0	-2.64E+04
ELECTRICAL-HULL	49.89	91.94	0.00	-2.45	1357	23027	15069	0	-1.12E+04
AUXILIARY GEAR-HULL	93.89	28.62	0.00	-13.69	1986	41409	39423	0	-3.68E+04
	0.00	0.00	0.00	0.00	0	0	0	0	0.00E+00
	0.00	0.00	0.00	0.00	0	0	0	0	0.00E+00
	0.00	0.00	0.00	0.00	0	0	0	0	0.00E+00
	0.00	0.00	0.00	0.00	0	0	0	0	0.00E+00
	0.00	0.00	0.00	0.00	0	0	0	0	0.00E+00
	0.00	0.00	0.00	0.00	0	0	0	0	0.00E+00
	0.00	0.00	0.00	0.00	0	0	0	0	0.00E+00
	0.00	0.00	0.00	0.00	0	0	0	0	0.00E+00
	0.00	0.00	0.00	0.00	0	0	0	0	0.00E+00
	0.00	0.00	0.00	0.00	0	0	0	0	0.00E+00
	0.00	0.00	0.00	0.00	0	0	0	0	0.00E+00
SUB-TOTAL, EMPTY WEIGHT	48781.47	60.63	0.01	-13.73	6.030E+06	2.551E+07	2.141E+07	1.510E+06	-4.06E+07
PAYLOAD	15249.63	58.67	0.00	-19.41	197737	326613	121920	13703	-1.74E+07
	0.00	0.00	0.00	0.00	0	0	0	0	0.00E+00
	0.00	0.00	0.00	0.00	0	0	0	0	0.00E+00
	0.00	0.00	0.00	0.00	0	0	0	0	0.00E+00
	0.00	0.00	0.00	0.00	0	0	0	0	0.00E+00
	0.00	0.00	0.00	0.00	0	0	0	0	0.00E+00
SUB-TOTAL, T.O.W.	64031.10	60.16	0.01	-15.08	6.603E+06	2.625E+07	2.157E+07	1.653E+06	-5.81E+07
HELIUM	14222.59	60.26	0.00	0.00	1495506	12607266	12607266	0	0.00E+00
AIR, FWD BALLONET	5227.11	25.30	0.00	-7.07	259154	259154	404678	0	-9.35E+05
AIR, AFT BALLONET	5227.11	95.10	0.00	-6.31	259154	259154	404678	0	-3.14E+06
AIR, PANNIER, STBD	2613.25	60.20	13.21	-1.52	60247	282761	247871	0	-2.39E+05
AIR, PANNIER, PORT	2613.25	60.20	-13.21	-1.52	60247	282761	247871	0	-2.39E+05
	0.00	0.00	0.00	0.00	0.00	0.00	0.00	0.00	0.00E+00
	0.00	0.00	0.00	0.00	0.00	0.00	0.00	0.00	0.00E+00
	0.00	0.00	0.00	0.00	0.00	0.00	0.00	0.00	0.00E+00
	0.00	0.00	0.00	0.00	0.00	0.00	0.00	0.00	0.00E+00
TOTAL	93934	60.18	0.01	-11.11	13103119	56130975	49131936	1811919	-6.28E+07

T A B L E A1.6.3 - The YEZ-2A mass and inertias for the ISA, sea level, 7118 Kg heaviness condition, i.e., CASE 3.

A1.7 Propulsion

The following Figure A1.7.1 depicts the Power versus RPM curve for the Diesel engines to be used in the YEZ-2A. It was supplied by Airship Industries based on the currently available engine manufacturer data (CRM of Italy). For the flight dynamics simulation, this curve was transformed into an ACSL TABLE, from which the available engine power was determined once an RPM value was specified (See Section 4.7).

For the 'sprint' turboprop engine, a flat figure of 1700 bhp was assumed. This corresponds to the maximum continuous power allowed for the General Electric CT7-7 engine to be used in the YEZ-2A. This figure was taken directly from the manufacturer's manual (Ref. 51).

A1.8 The Atmospheric Model

In order to determine the value of the air density ρ at each time step of the flight dynamics simulation, a model of the atmosphere based on the formulation of the International Standard Atmosphere (ISA) was implemented in a FORTRAN subroutine. For the determination of ρ, the value of the temperature in the standard ISA condition was first calculated from

$$T_s = T_0 + A \cdot H_p \qquad \text{(A1.8.1)}$$

where,

T_0 = Standard temperature at sea level = 288.15 K
A = ISA temperature gradient = -0.0065 K/m
H_p = Airship pressure height (m)

After that, the next step was the determination of ρ in the standard ISA condition, i.e.,

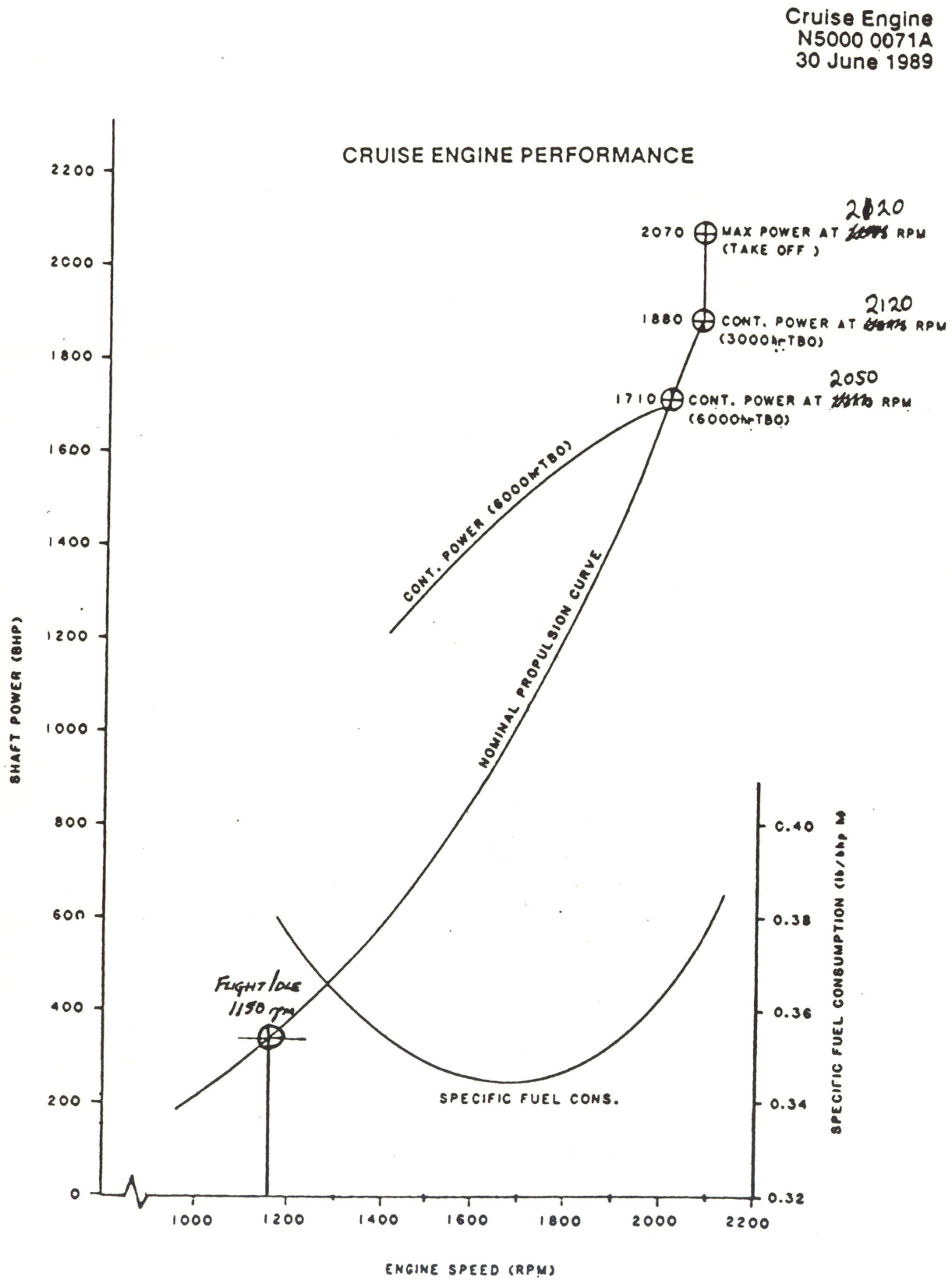


Figure A1.7.1 - Power available versus engine speed curve for the CRM Diesel engine to be used in the YEZ-2A airship.

$$\rho_s = \rho_0 \left(\frac{T_s}{T_0} \right)^{-\left(1 + \frac{g_0}{A \times R_A} \right)} \qquad \text{(A1.8.2)}$$

where,

g_0 = Acceleration due to gravity = 9.80665 m/s^2
R_A = Gas constant for air = 287.05287 N.m/Kg.K

Finally the value of the air density ρ in a possible off-ISA condition was determined from

$$\rho_A = \frac{\rho_s}{1 + \left(\frac{\Delta T}{T_s} \right)} \qquad \text{(A1.8.3)}$$

where,

ΔT = Temperature difference between the off-standard atmospheric condition and the ISA condition (K)

In the simulation program the values of ΔT and the initial height for the flight could be specified by the user.

A P P E N D I X - 2

Computer Simulation : Additional Algorithms and Procedures

A2.1 Introduction

The purpose of this Appendix is to present further information on some of the topics outlined in the description of the computer simulation (Chapter 4). Each of the following sections deals with a specific item and usually there is no connection between them. An attempt has therefore been made to make each section as self contained as possible.

A2.2 The Quaternion Method

The standard four parameter or 'quaternion' method was implemented in the computer simulation in order to determine, at each time step, the attitude geometry of the airship, as well as to permit the transformation of velocities between body and Earth (inertial) axes.

The purpose of the method is to obtain the Direction Cosine Matrix (DCM), which can then be used directly in the velocities transformation operation (See Section 4.2). Also, some of the elements of the DCM can be used to determine the vehicle's Euler angles, ϕ, θ and ψ which in turn describe its roll, pitch and yaw attitudes respectively (See Section 4.2).

The fundamental Quaternion equation (Ref. 42) is that which relates the four parameters e_0, e_1, e_2 and e_3 to the airship rates of roll, pitch and yaw, i.e., p, q and r respectively, in the following way:

$$\begin{bmatrix} \dot{e}_0 \\ \dot{e}_1 \\ \dot{e}_2 \\ \dot{e}_3 \end{bmatrix} = \frac{1}{2} \begin{bmatrix} -e_1 & -e_2 & -e_3 \\ e_0 & -e_3 & e_2 \\ e_3 & e_0 & -e_1 \\ -e_2 & e_1 & e_0 \end{bmatrix} \begin{bmatrix} p \\ q \\ r \end{bmatrix} \qquad \text{(A2.2.1)}$$

Equation (A2.2.1) was implemented in the Dynamic / Derivative region of the simulation program. By using the same INTEG function of ACSL as used for the other

state variables of the simulation, this equation was integrated to obtain the values of the four e-parameters.

The actual mechanization of the quaternion method algorithm started by setting the initial value of the e-parameters in the Initial region of the program. This was given by:

$$e_0 = \cos\frac{\psi}{2}\cos\frac{\theta}{2}\cos\frac{\phi}{2} + \sin\frac{\psi}{2}\sin\frac{\theta}{2}\sin\frac{\phi}{2} \quad \text{(A2.2.2)}$$

$$e_1 = \cos\frac{\psi}{2}\cos\frac{\theta}{2}\sin\frac{\phi}{2} - \sin\frac{\psi}{2}\sin\frac{\theta}{2}\cos\frac{\phi}{2} \quad \text{(A2.2.3)}$$

$$e_2 = \cos\frac{\psi}{2}\sin\frac{\theta}{2}\cos\frac{\phi}{2} + \sin\frac{\psi}{2}\cos\frac{\theta}{2}\sin\frac{\phi}{2} \quad \text{(A2.2.4)}$$

$$e_3 = \sin\frac{\psi}{2}\cos\frac{\theta}{2}\cos\frac{\phi}{2} - \cos\frac{\psi}{2}\sin\frac{\theta}{2}\sin\frac{\phi}{2} \quad \text{(A2.2.5)}$$

where, in these equations, the values of ϕ, θ and ψ are the initial values of the Euler angles, also specified in the Initial region of the simulation program, and which establish the airship attitude at the beginning of each simulation run.

The next step of the quaternion method called for the integration of Equation (A2.2.1) in the Dynamic / Derivative region of the program, as already mentioned. Once the new e-parameter values were obtained, the DCM could be determined from the relation

$$\text{DCM} = \left[\lambda_{ij}\right] =$$

$$= \begin{bmatrix} e_0^2+e_1^2-e_2^2-e_3^2 & 2\left(e_1e_2-e_0e_3\right) & 2\left(e_0e_2+e_1e_3\right) \\ 2\left(e_0e_3+e_1e_2\right) & e_0^2-e_1^2+e_2^2-e_3^2 & 2\left(e_2e_3-e_0e_1\right) \\ 2\left(e_1e_3-e_0e_2\right) & 2\left(e_0e_1+e_2e_3\right) & e_0^2-e_1^2-e_2^2+e_3^2 \end{bmatrix}$$

(A2.2.6)

Once the DCM was obtained in the ACSL coded form of

Equation (A2.2.6), the values of the Euler angles at the same time step of the simulation were obtained by implementing Equations (4.3-5) of Section 4.2.

The main advantage in using the quaternion method is the avoidance of the discontinuities in the trigonometric functions, e.g. tan 90°, which would otherwise happen if the traditional equations of ϕ, θ and ψ as functions of p, q and r were employed. It is also quite suitable to be implemented in a digital type of flight simulation as in the present case.

A2.3 From Wind Tunnel Axes to Body Axes

In the Aerodynamics section of the YEZ-2A flight dynamics simulation, the aerodynamic forces and moments acting on the vehicle due to its flight speed and longitudinal and lateral incidences (α and β respectively) were obtained by entering the TABLEs of non-dimensional coefficients as already explained in Section 4.5. The coefficients that were thus obtained from the TABLEs were effectively those resulting from the carrying out of Task 2.

This means that they are referred to the stationary wind tunnel axes system and need to be converted to the airship body axes system (Section 3.2.1). This axes transformation was implemented in the Aerodynamics section of the simulation by initially assuming that the wind tunnel axes are identical with inertial axes. Then, from Reference 47, the required transformation can be achieved by a rotation of α about the wind tunnel OY axis followed by a rotation of $-\beta$ about the new OZ axis. No rotation about OX is required since the YEZ-2A model was never tested at a bank angle different from zero (Fig. A2.3.1).

In the simulation, this solution was implemented by considering that if the transformation matrix of axes rotation about the wind tunnel OY is given by

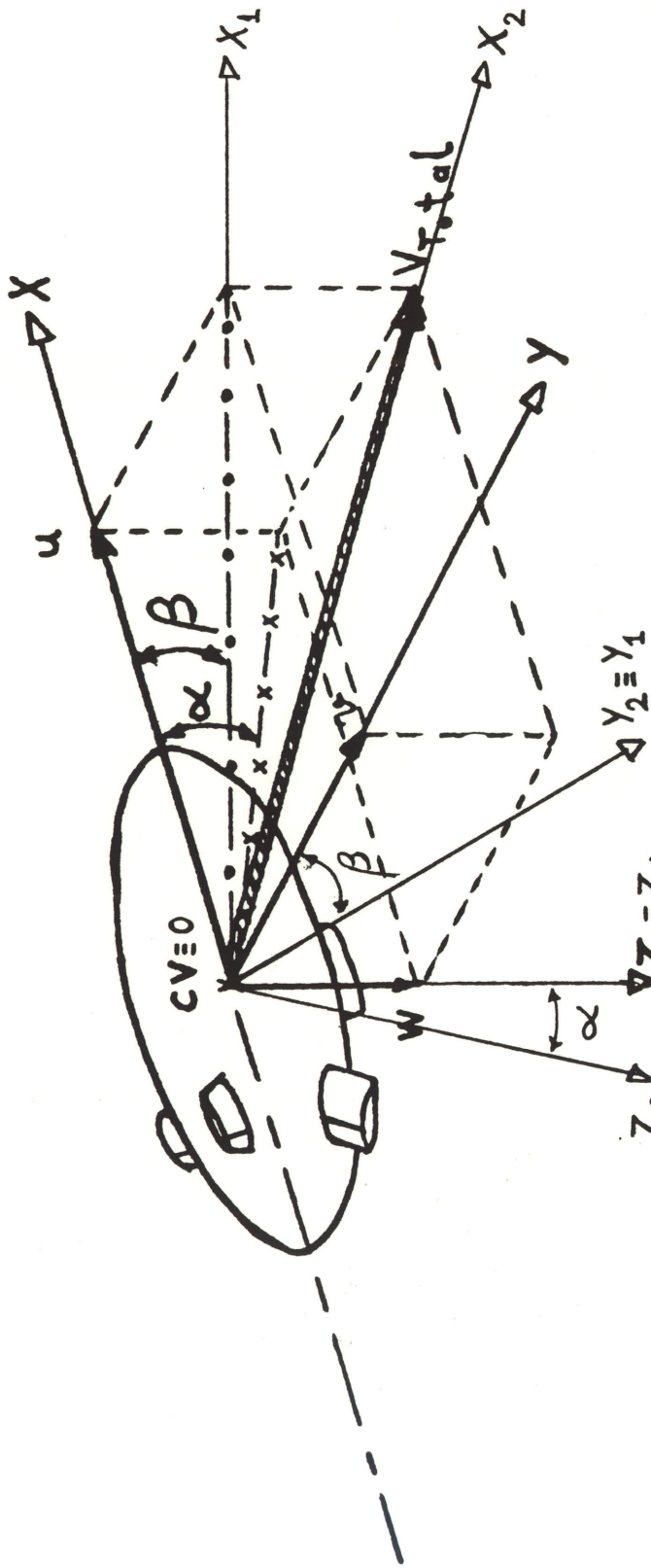


Figure A2.3.1 - If the wind tunnel axes are represented by (X_2, Y_2, Z_2), then a rotation through an angle α about OY_2, to obtain (X_1, Y_1, Z_1), followed by a rotation of $(-\beta)$ about OZ_1 will yield the airship body axes system (X,Y,Z).

$$S_\alpha = \begin{bmatrix} \cos\alpha & 0 & -\sin\alpha \\ 0 & 1 & 0 \\ \sin\alpha & 0 & \cos\alpha \end{bmatrix}_{\text{Body from Wind Tunnel}}$$

and the transformation matrix of the rotation about the new OZ axes is given by

$$T_{-\beta} = \begin{bmatrix} \cos(-\beta) & \sin(-\beta) & 0 \\ -\sin(-\beta) & \cos(-\beta) & 0 \\ 0 & 0 & 1 \end{bmatrix}_{\text{Body from Wind Tunnel}}$$

then the complete transformation required is obtained by multiplying S_α by $T_{-\beta}$, i.e.,

$$S_\alpha T_{-\beta} = \begin{bmatrix} \cos\alpha.\cos\beta & -\cos\alpha.\sin\beta & -\sin\alpha \\ \sin\beta & \cos\beta & 0 \\ \sin\alpha.\cos\beta & -\sin\alpha.\sin\beta & \cos\alpha \end{bmatrix} \quad \text{(A2.3.1)}$$

In the simulation, after the six force and moment coefficients were obtained from the TABLEs, the equivalent body axes coefficients were obtained by carrying out the transformation

$$\begin{bmatrix} C_X \\ C_Y \\ C_Z \end{bmatrix}_{\text{Body Axes}} = S_\alpha T_{-\beta} \begin{bmatrix} -C_D \\ C_Y \\ -C_L \end{bmatrix}_{\text{Wind Tunnel Axes}} \quad \text{(A2.3.2)}$$

for the case of the forces along OX, OY and OZ, and the transformation

$$\begin{bmatrix} C_l \\ C_m \\ C_n \end{bmatrix}_{\text{Body Axes}} = S_\alpha T_{-\beta} \begin{bmatrix} C_l \\ C_m \\ C_n \end{bmatrix}_{\text{Wind Tunnel Axes}} \quad \text{(A2.3.3)}$$

in the case of the moments about OX, OY and OZ.

Equations (A2.3.2-3) were implemented in the Aerodynamics section of the simulation, in each of the code segments devoted to calculating the coefficients for the 'no ruddervator deflection' sector, the 'elevator' type of deflection sector and the 'rudder' type of deflection sector (See Section 4.5.3). In the 'aileron' type of deflection code sector, a slightly different kind of solution had to be adopted.

A2.4 The Solution to the Aileron Case

In the Aerodynamics section of the YEZ-2A simulation program, the calculation of the three force and three moment non-dimensional coefficients due to any amount of 'aileron' type of ruddervator deflection (See Section 4.5.3) had to follow a slightly different approach than that used in the 'no deflection', 'elevator' and 'rudder' case sections (See previous Section). The reason for that lied in the fact that effectively only one set of results were obtained, in the course of the Task 2 tests, with the four ruddervators deflected in an 'aileron' type of configuration, which was a $\xi = 25^{\circ}$ case at $\beta = 0$ (See Section A1.4 of Appendix-1).

The solution to this slight limitation in the aerodynamic data base was found in Reference 47. By studying the section on artillery shell body axes system it was decided that the aileron TABLEs would be constructed with two input variables only, i.e., α_T and ξ, unlike the other TABLEs which had three input variables, i.e., α, β and 0 (no deflection) or η (elevator) or ζ (rudder). By neglecting the effects of the YEZ-2A airship model gondola, the total incidence α_T, where,

$$\alpha_T = \tan^{-1}\left(\frac{\sqrt{v^2 + w^2}}{u}\right) \qquad \text{(A2.4.1)}$$

was used instead of separate longitudinal (α) and lateral

(β) incidences (Fig. A2.4.1).

An axes system $\left(X_2, Y_2, Z_2\right)$ was then conceived, in addition to the established system of body axes (X, Y, Z), where OX_2 coincides in direction with the flight velocity vector V_{Total}, OZ_2 is perpendicular to it but parallel to the Lift force line, and OY_2 is perpendicular to both of them. The relationship between the forces and moments measured by the wind tunnel axes (with the Task 2 data processing sign corrections already incorporated - See Ref. 37) and those that would result from the $\left(X_2, Y_2, Z_2\right)$ axes system can be expressed as

$$\begin{bmatrix} X_2 \\ Y_2 \\ Z_2 \end{bmatrix}_{\text{Forces}} = \begin{bmatrix} -\text{Drag} \\ \text{Side Force} \\ -\text{Lift} \end{bmatrix}_{\text{Wind Tunnel}} \quad \text{and}$$

$$\begin{bmatrix} X_2 \\ Y_2 \\ Z_2 \end{bmatrix}_{\text{Moments}} = \begin{bmatrix} \text{Rolling Moment} \\ \text{Pitching Moment} \\ \text{Yawing Moment} \end{bmatrix}_{\text{Wind Tunnel}} \qquad \text{(A2.4.2)}$$

In order to transform from the $\left(X_2, Y_2, Z_2\right)$ axes to body axes two operations are required: A rotation through an angle α_T of X_2 and Z_2 about Y_2, followed by a rotation through an angle ε of Y_2 and Z_1 about X.

If we call $V^* = \sqrt{v^2 + w^2}$ then the first stated axes transformation operation will yield

$$\begin{bmatrix} X_1 \\ Y_1 \\ Z_1 \end{bmatrix} = \begin{bmatrix} \cos \alpha_T & 0 & -\sin \alpha_T \\ 0 & 1 & 0 \\ \sin \alpha_T & 0 & \cos \alpha_T \end{bmatrix} \begin{bmatrix} X_2 \\ Y_2 \\ Z_2 \end{bmatrix} \qquad \text{(A2.4.3)}$$

and the second operation will finally give

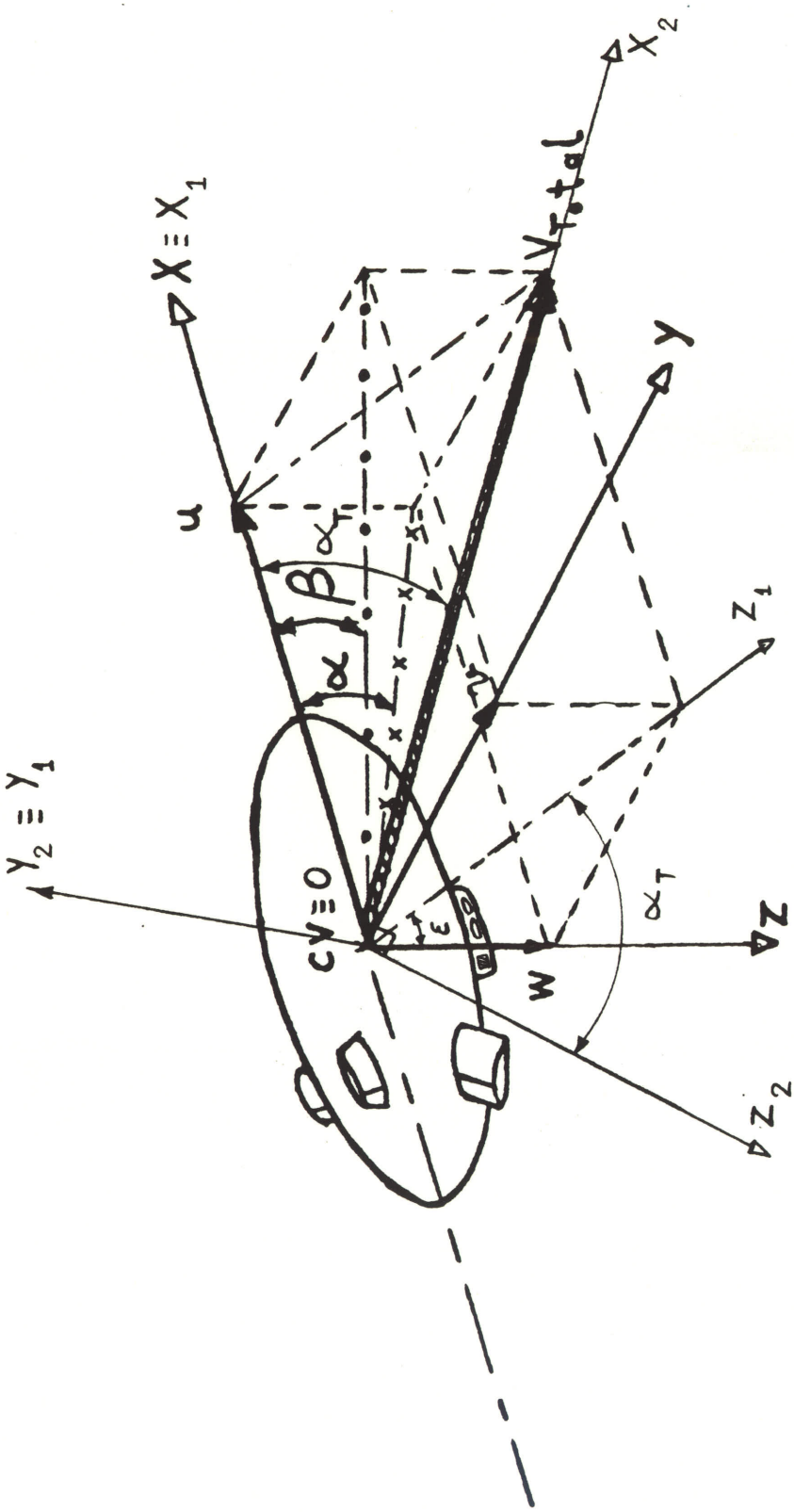


Figure A2.4.1 - Axes transformation between the (X_2, Y_2, Z_2) system and the established airship system of body axes (X, Y, Z). The former is effectively a Lift and Drag system of orthogonal axes and the (X_1, Y_1, Z_1) system is obtained after rotating (X_2, Z_2) about OY_2 through an angle α_T.

$$\begin{bmatrix} X \\ Y \\ Z \end{bmatrix} = \begin{bmatrix} 1 & 0 & 0 \\ 0 & w/V^* & v/V^* \\ 0 & -v/V^* & w/V^* \end{bmatrix} \begin{bmatrix} X_1 \\ Y_1 \\ Z_1 \end{bmatrix} \qquad \text{(A2.4.4)}$$

In the program implementation, Equations (A2.4.2-4) were all combined to give the final wind tunnel to body axes transformations

$$\begin{bmatrix} X \\ Y \\ Z \end{bmatrix}_{\substack{\text{Forces} \\ \text{in} \\ \text{Body Axes}}} = \begin{bmatrix} u/V_{Total} & 0 & -V^*/V_{Total} \\ v/V_{Total} & w/V^* & uv/V^*V_{Total} \\ w/V_{Total} & -v/V^* & uw/V^*V_{Total} \end{bmatrix} \begin{bmatrix} -\text{Drag} \\ \text{Side Force} \\ -\text{Lift} \end{bmatrix}$$

$$\begin{bmatrix} X \\ Y \\ Z \end{bmatrix}_{\substack{\text{Moments} \\ \text{in} \\ \text{Body Axes}}} = \begin{bmatrix} u/V_{Total} & 0 & -V^*/V_{Total} \\ v/V_{Total} & w/V^* & uv/V^*V_{Total} \\ w/V_{Total} & -v/V^* & uw/V^*V_{Total} \end{bmatrix} \begin{bmatrix} \text{Rolling M.} \\ \text{Pitching M.} \\ \text{Yawing M.} \end{bmatrix}$$

(A2.4.5)

where the substitutions

$$\cos \alpha_T = u/V_{Total}$$

$$\sin \alpha_T = V^*/V_{Total}$$

were implemented.

In this way, the forces and moments in body axes were obtained in the 'aileron' sector of the Aerodynamics program section. For the construction of the axes transformation matrix only the set of body axes velocity components were required, as was the case in the other three sectors ('elevator', 'rudder' and 'no deflection') as explained in the previous item.

A2.5 The Solution to the $\beta < 0$ Problem

Due to the YEZ-2A airship inherent symmetry about its vertical plane (OXZ), the scope of the Task 2 wind

tunnel test programme included only zero and positive values of lateral incidences (See Appendix-1). The Aerodynamics section of the simulation program had therefore to incorporate some additional features in order to deal with this problem, which affected the 'elevator', 'rudder' and 'no deflection' code sections. The 'aileron' section was formulated in a slightly different way (See previous item) and was not affected.

The heart of the problem laid in the fact that the aerodynamic forces and moments TABLEs of non-dimensional coefficients had only zero or positive values of the lateral incidence β as an input (independent) variable. Clearly, if the flight condition implied only $\beta \geq 0$ values, no further corrective action on the TABLE generated values of C_D, C_Y, C_L, C_l, C_m and C_n would be required.

The first step in the solution algorithm was therefore a check on the sign of β. This was implemented in the 'elevator', 'rudder' and 'no surface deflection' code sectors. If at each time step of the simulation run the condition $\beta \geq 0$ were satisfied, program execution continued normally.

If however a $\beta < 0$ condition was detected, the solution had to follow the following steps:

i. Reverse the sign of β in order to be able to enter the coefficient TABLEs.

ii. In the 'rudder' code sector, reverse also the sign of ζ, in case there is any amount of rudder deflection in the total tail configuration deflection. This step is required as a direct consequence of the previous one, in order to construct the aerodynamic 'mirror' image of the airship in the now $\beta > 0$ condition.

iii. After the forces and moments coefficients have been obtained from the TABLEs, reverse the signs of the side force (C_Y), the rolling moment (C_l) and the yawing moment (C_n) coefficients.

iv. In the 'rudder' sector only, reverse again the sign of ζ, restoring therefore its original sign before carrying out operation iii above.

In the actual implementation of the algorithm just outlined, a further refinement had to be incorporated. As the force and moment coefficient data contained points only for the $\beta \geq 0$ condition, and as the values of any of the three coefficients that had to have their signs reversed in the algorithm described (C_Y, C_l and C_n) are unlikely to be zero when $\beta = 0$, strong non-linearities would arise near the origin (when β has just gone slightly below zero) if the coefficient signs were simply reversed.

The solution was to incorporate, in the same code section that did the sign reversal, a summation of twice the value of the coefficient in question at the $\beta = 0$ condition. This program section (item iii of the algorithm description on this page) was therefore expressed as

$$C_Y(\beta, \Delta, \alpha) \equiv -C_Y(\beta, \Delta, \alpha) + 2 \times C_Y(0, \Delta, \alpha)$$

$$C_l(\beta, \Delta, \alpha) \equiv -C_l(\beta, \Delta, \alpha) + 2 \times C_l(0, \Delta, \alpha)$$

$$C_n(\beta, \Delta, \alpha) \equiv -C_n(\beta, \Delta, \alpha) + 2 \times C_n(0, \Delta, \alpha)$$

where,

Δ is the control surface deflection (η in the 'elevator' program code sector, ζ in the 'rudder'

sector or zero in the 'no surface deflection' sector)

The importance of these modifications was realized when, in the earlier versions of the simulation program, it had not been incorporated and spurious results were generated, especially in the airship modes investigation (See Appendix-3). The tailoring of the simulation concept and coding to the peculiar characteristics of the aerodynamic data base was, by consequence, a prominent aspect of the construction and validation of the simulation program.

A2.6 Tail Deflection Configuration Due to Pilot Demand

The standard YEZ-2A simulation program, as used in the flight dynamics simulation, was conceived in a such a way that it required the input, by the user, of the amount of control surface deflection for each of the four ruddervators (See Section 4.5.2).

However, a second version of the program was developed in which the intention was to arrive at a total tail deflection configuration based on the amounts of 'elevator' and 'rudder' deflection demanded by the airship pilot, as airships, unlike conventional aircraft, do not have pilot roll control demands. If the pilot demand for 'elevator' type of deflection is called η_{dem} and that for 'rudder' is called ζ_{dem} then the problem was to find the four unknowns represented by the amount of deflection of each ruddervator, i.e., δ_1, δ_2, δ_3 and δ_4 (See Fig. 4.4).

At this stage, the problem can be regarded as having two equations, i.e.,

$$\frac{\delta_1 + \delta_2 + \delta_3 + \delta_4}{4} = \eta_{dem} \qquad \text{(A2.6.1)}$$

$$\frac{\delta_1 - \delta_2 + \delta_3 - \delta_4}{4} = \zeta_{dem} \qquad \text{(A2.6.2)}$$

In order to find the solution in terms of the ruddervator deflection angles, two more equations are required. The choice was then made to impose the conditions that would permit the solution of the problem: First, that an aileron type of demand would always be zero, as is usually the case in lighter-than-air flying controls, and second that the deflection of the controls must be done in such a way that the elevator type of demand comes in first followed by the rudder type. These concepts were implemented by means of the following respective equations:

$$-\delta_1 + \delta_2 + \delta_3 - \delta_4 = \xi_{dem} = 0 \qquad \text{(A2.6.3)}$$

$$\delta_1 + \delta_2 - \delta_3 - \delta_4 = 0 \qquad \text{(A2.6.4)}$$

Equations (A2.6.1-4) provided therefore the solution to the total tail deflection configuration as a function of pilot demand. It was implemented in one of the simulation program versions, where the user just had to input values for η_{dem} and ζ_{dem}. The δ_i values were then determined by the algorithm that solved the four equations given. As already pointed out in Chapter 4, this is only one possible way of finding a solution, amongst many that can and should be tried.

A P P E N D I X - 3

Derivation of the YEZ-2A Modes of Motion

A3.1 Introduction

The purpose of this Appendix is to present the derivation of the YEZ-2A characteristic modes of motion. The method adopted is that based on the use of eigenvalues and eigenvectors (Refs. 52 and 53) since, from a mathematical point of view, it is as rigorous as any other method and it also facilitates the visualization of the vehicle motion after a disturbance.

This type of solution to the problem was made possible by the use of the ANALYZ package that is part of ACSL. It is operated by instructing the ACSL system, at the desired point of the state space, to 'freeze' all the state variables and then release the ones that are relevant to the analysis being pursued. Next, a command to produce the eigenvalues and the eigenvectors for that condition will generate the output with the value of the those parameters as well as the system Jacobian (equivalent to an A-matrix of a linear system).

In the present investigation, the method described was applied at the simulation time t = 0, just after longitudinal trim had been achieved (See Section 4.9). It was carried out for a number of flight speeds, starting at the hover condition, where a 'speed' of 0.01 m/s had to be specified in order to avoid division by zero during program execution, and going up in steps to 30 m/s. This is estimated to cover most of the useful range of flight speeds of the YEZ-2A.

The experiment was divided, for each flight speed condition, into the longitudinal and the lateral cases. In the former case the relevant ('released') variables were u, w, q and θ, whereas in the latter case the variables in question were v, p, r and ϕ. Although θ and ϕ were not state variables as such, for the small perturbation procedure involved in producing the system Jacobian the following approximations were used:

$$\frac{\theta}{2} \cong e_2$$

$$\frac{\phi}{2} \cong e_1$$

where,

e_i are two of the quaternion method e-parameters (See Section A2.2 of Appendix-2, Equations A2.2.3 and A2.2.4)

The following section lists the eigenvalues and eigenvectors found for the Case 1 situation, i.e., neutral buoyancy, ISA, sea level conditions.

A slight nuisance was found in the fact that the ACSL manual (Ref. 54) does not specify the solution algorithm used to obtain the eigenvectors. As there is no unique set of eigenvectors that will satisfy an eigenvalue problem, it was assumed, by looking at the results, that the ACSL system normalized each eigenvector set by selecting the associated state variable that yields an eigenvector modulus of one (including the complex eigenvectors) for that variable in that set. If this assumption is true, then the amplitude units of each eigenvector will be those of the state variable to which it belongs divided by the units of the eigenvector used for normalization in that set. As it turned out it appears that in most cases the state variables selected were either u or w, in the longitudinal case, and v in the lateral case.

In any event, if it is eventually found out that this assumption was wrong, it will not affect the mode derivation method here employed, as in this type of investigation it is the relative magnitude of the eigenvectors in each set that really matters.

In the next section, the actual airship modes applicable to each case have been named (in accordance

with an early investigation based solely on the analysis of the system Jacobian at various speeds for the Skyship-600 airship, Ref. 55), although only in the following Sections A3.3 and A3.4 are they actually derived. Section A3.5 presents the results of a brief investigation on non-neutral buoyancy effects and the last Section A3.6 compares the results found in the present investigation with those published elsewhere for other airships.

A3.2 Eigenvalues and Eigenvectors

Table A3.2.1 - Longitudinal Eigenvectors, YEZ-2A
Speed = Hover, Case 1
ω = Frequency, ζ = Damping

M O D E	Surge	Heave	Pendulum Oscillation
EIGENVALUES (rad/s)	-7.64E-6	-7.59E-5	-2.21E-4 ± 0.293i
ω (rad/s)			0.293
ζ			7.52E-4
EIGENVECTORS			
u	-1.0	8.20E-4	-0.00363 ∓ 0.979i
w	-0.00460	1.0	-0.00440 ∓ 0.00380i
q	7.62E-12	-1.17E-9	3.75E-4 ± 0.102i
θ	-4.99E-7	7.74E-6	-0.174 ± 5.08E-4i

Table A3.2.2 - Lateral Eigenvectors, YEZ-2A
Speed = Hover, Case 1
ω = Frequency, ζ = Damping

M O D E	Sideslip Subsidence	Yaw Subsidence	Roll Oscillation
EIGENVALUES (rad/s)	-6.40E-5	-4.70E-4	-6.40E-5 ± 0.727i
ω (rad/s)			0.727
ζ			8.81E-5
EIGENVECTORS			
v	1.0	0.925	-0.00317 ± 0.977i
p	6.06E-10	1.87E-7	-5.80E-4 ± 0.175i
r	-0.00557	-0.380	-5.05E-6 ± 0.00304i
ϕ	-4.74E-6	-1.99E-4	-0.120 ∓ 4.10E-4i

Table A3.2.3 - Longitudinal Eigenvectors, YEZ-2A
Speed = 5 m/s, Case 1
ω = Frequency, ζ = Damping

M O D E	Surge	Pitch Subsidence	Pendulum Oscillation
EIGENVALUES (rad/s)	-0.00565	-0.0392	-0.108 ± 0.264i
ω (rad/s)			0.285
ζ			0.379
EIGENVECTORS			
u	1.0	0.00518	0.222 ∓ 0.318i
w	0.00462	1.0	-0.578 ∓ 0.714i
q	-1.58E-6	-3.23E-4	-0.0235 ± 0.0325i
θ	1.40E-4	0.00412	-0.0370 ∓ 0.0596i

Table A3.2.4 - Lateral Eigenvectors, YEZ-2A
Speed = 5 m/s, Case 1
ω = Frequency, ζ = Damping

M O D E	Sideslip Subsidence	Yaw Subsidence	Roll Oscillation
EIGENVALUES (rad/s)	-0.0315	-0.232	-0.0322 ± 0.728i
ω (rad/s)			0.728
ζ			0.0443
EIGENVECTORS			
v	1.0	-0.946	0.218 ± 0.953i
p	1.46E-4	-0.0351	0.0454 ± 0.168i
r	-0.00557	0.312	-0.0161 ± 0.00281i
ϕ	-0.00231	0.0758	0.114 ∓ 0.0326i

Table A3.2.5 - Longitudinal Eigenvectors, YEZ-2A
Speed = 7.5 m/s, Case 1
ω = Frequency, ζ = Damping

M O D E	Surge	Pitch Subsidence	Pendulum Oscillation
EIGENVALUES (rad/s)	-0.00847	-0.0643	-0.159 ± 0.222i
ω (rad/s)			0.273
ζ			0.584
EIGENVECTORS			
u	1.0	0.0116	0.199 ± 0.146i
w	0.00422	1.0	0.861 ∓ 0.442i
q	-3.57E-6	-9.09E-4	-0.0199 ∓ 0.0154i
θ	2.11E-4	0.00707	0.0442 ∓ 0.0131i

Table A3.2.6 - Lateral Eigenvectors, YEZ-2A
Speed = 7.5 m/s, Case 1
ω = Frequency, ζ = Damping

M O D E	Sideslip Subsidence	Yaw Subsidence	Roll Oscillation
EIGENVALUES (rad/s)	-0.0474	-0.345	-0.0493 ± 0.728i
ω (rad/s)			0.730
ζ			0.0676
EIGENVECTORS			
v	1.0	-0.962	-0.479 ± 0.852i
p	3.29E-4	0.0586	-0.0764 ± 0.156i
r	-0.00557	-0.251	-0.00344 ∓ 5.65E-6i
ϕ	-0.00347	-0.0848	0.110 ± 0.0450i

Table A3.2.7 - Longitudinal Eigenvectors, YEZ-2A
Speed = 10 m/s, Case 1
ω = Frequency, ζ = Damping

M O D E	Surge	Pitch Subsidence	Pendulum Oscillation
EIGENVALUES (rad/s)	-0.0113	-0.110	-0.200 ± 0.134i
ω (rad/s)			0.240
ζ			0.832
EIGENVECTORS			
u	-1.0	0.0317	0.144 ± 0.0210i
w	-0.00366	1.0	-0.591 ± 0.793i
q	6.42E-6	-0.0286	0.0144 ∓ 0.00166i
θ	-2.84E-4	0.0130	-0.0229 ± 0.0195i

Table A3.2.8 - Lateral Eigenvectors, YEZ-2A
Speed = 10 m/s, Case 1
ω = Frequency, ζ = Damping

M O D E	Sideslip Subsidence	Yaw Subsidence	Roll Oscillation
EIGENVALUES (rad/s)	-0.0632	-0.457	-0.0674 ± 0.728i
ω (rad/s)			0.732
ζ			0.0921
EIGENVECTORS			
v	-1.0	-0.972	0.412 ∓ 0.887i
p	-5.87E-4	-0.0723	0.0605 ∓ 0.162i
r	0.00557	0.204	0.00360 ± 7.03E-4i
ϕ	0.00465	0.0834	-0.114 ∓ 0.0310i

Table A3.2.9 - Longitudinal Eigenvectors, YEZ-2A
Speed = 15 m/s, Case 1
ω = Frequency, ζ = Damping

M O D E	Surge	Pitch Subsidence	Pendulum Oscillation
EIGENVALUES (rad/s)	-0.0169	-0.584	-0.0906 ± 0.0904i
ω (rad/s)			0.128
ζ			0.708
EIGENVECTORS			
u	1.0	-0.242	-0.0346 ± 0.0373i
w	0.00198	-0.970	-0.653 ∓ 0.755i
q	-1.49E-5	0.0244	0.00291 ∓ 0.00398i
θ	4.38E-4	-0.0209	-0.0190 ± 0.00299i

Table A3.2.10 - Lateral Eigenvectors, YEZ-2A
Speed = 15 m/s, Case 1
ω = Frequency, ζ = Damping

M O D E	Sideslip Subsidence	Yaw Subsidence	Roll Oscillation
EIGENVALUES (rad/s)	-0.0953	-0.677	-0.106 ± 0.727i
ω (rad/s)			0.735
ζ			0.144
EIGENVECTORS			
v	-1.0	-0.982	0.852 ± 0.480i
p	-0.00134	-0.0971	0.159 ± 0.0658i
r	0.00557	0.147	-0.00263 ± 0.00318i
ϕ	0.00704	0.0717	0.0288 ∓ 0.113i

Table A3.2.11 - Longitudinal Eigenvectors, YEZ-2A
Speed = 20 m/s, Case 1
ω = Frequency, ζ = Damping

M O D E	Surge	Pitch Subsidence	Pendulum Oscillation
EIGENVALUES (rad/s)	-0.0226	-0.863	-0.0789 ± 0.0927i
ω (rad/s)			0.122
ζ			0.648
EIGENVECTORS			
u	-1.0	0.271	0.0458 ∓ 0.0160i
w	5.46E-4	0.962	-0.147 ± 0.988i
q	2.77E-5	-0.0275	-0.00406 ± 0.00221i
θ	-6.10E-4	0.0159	0.0177 ± 0.00683i

Table A3.2.12 - Lateral Eigenvectors, YEZ-2A
Speed = 20 m/s, Case 1
ω = Frequency, ζ = Damping

M O D E	Sideslip Subsidence	Yaw Subsidence	Roll Oscillation
EIGENVALUES (rad/s)	-0.128	-0.893	-0.147 ± 0.722i
ω (rad/s)			0.737
ζ			0.199
EIGENVECTORS			
v	-1.0	-0.985	-0.704 ± 0.680i
p	-0.00243	-0.107	-0.101 ± 0.136i
r	0.00557	0.117	-0.00127 ∓ 0.00436i
ϕ	0.00951	0.0601	0.104 ± 0.0491i

Table A3.2.13 - Longitudinal Eigenvectors, YEZ-2A
Speed = 25 m/s, Case 1
ω = Frequency, ζ = Damping

M O D E	Surge	Pitch Subsidence	Pendulum Oscillation
EIGENVALUES (rad/s)	-0.0282	-1.12	-0.0775 ± 0.0909i
ω (rad/s)			0.119
ζ			0.649
EIGENVECTORS			
u	1.0	-0.283	0.0423 ± 0.0184i
w	-0.00412	-0.959	-0.884 ± 0.464i
q	-4.55E-5	0.0287	-0.00441 ∓ 9.58E-4i
θ	8.06E-4	-0.0128	0.00892 ± 0.0166i

Table A3.2.14 - Lateral Eigenvectors, YEZ-2A
Speed = 25 m/s, Case 1
ω = Frequency, ζ = Damping

M O D E	Sideslip Subsidence	Yaw Subsidence	Roll Oscillation
EIGENVALUES (rad/s)	-0.161	-1.108	-0.188 ± 0.712i
ω (rad/s)			0.736
ζ			0.256
EIGENVECTORS			
v	-1.0	-0.987	-0.0645 ± 0.977i
p	-0.00390	-0.113	0.0235 ± 0.166i
r	0.00558	0.101	-0.00348 ∓ 0.00345i
ϕ	0.0121	0.0508	0.105 ∓ 0.0442i

Table A3.2.15 - Longitudinal Eigenvectors, YEZ-2A
Speed = 30 m/s, Case 1
ω = Frequency, ζ = Damping

M O D E	Surge	Pitch Subsidence	Pendulum Oscillation
EIGENVALUES (rad/s)	-0.0339	-1.368	-0.0802 ± 0.0871i
ω (rad/s)			0.118
ζ			0.677
EIGENVECTORS			
u	-1.0	-0.290	0.0342 ∓ 0.0327i
w	0.00914	-0.957	-0.0301 ± 0.998i
q	7.08E-5	0.0294	-0.00243 ± 0.00373i
θ	-0.00104	-0.0107	0.0185 ∓ 0.00312i

Table A3.2.16 - Lateral Eigenvectors, YEZ-2A
Speed = 30 m/s, Case 1
ω = Frequency, ζ = Damping

M O D E	Sideslip Subsidence	Yaw Subsidence	Roll Oscillation
EIGENVALUES (rad/s)	-0.196	-1.132	-0.230 ± 0.697i
ω (rad/s)			0.734
ζ			0.313
EIGENVECTORS			
v	-1.0	-0.988	-0.875 ∓ 0.441i
p	-0.00582	-0.115	-0.161 ∓ 0.0349i
r	0.00558	0.0906	0.00509 ∓ 0.00110i
ϕ	0.0149	0.0436	0.0117 ± 0.111i

A3.3 Derivation of the Longitudinal Modes

The eigenvalue and eigenvector tables of the previous section have shown that as far as the longitudinal stability of the YEZ-2A airship is concerned there are basically three modes of motion. Following a longitudinal type of disturbance, two of the modes are of the subsidence type, represented by the negative real eigenvalues, whereas the third mode is of the oscillatory type, represented by the complex eigenvalue.

Since all the eigenvalues have a negative real part, it can be concluded that they are all stable modes, although only marginally so in the hover condition and at the slow end of the flight speed range. In fact, it is perhaps safer to assume that the real part of the hover eigenvalues are effectively zero, as the figures shown in Table A3.2.1 were obtained by specifying a flight speed of 0.01 m/s in order to avoid division by zero. The plot of the eigenvalues in the complex plane for the various values of flight speed is presented in Chapter 5.

The derivation of the longitudinal modes was carried out by simply analyzing the relative magnitudes (and phase relations in the case of complex quantities) of the eigenvectors associated with each eigenvalue. Three values of flight speed were selected, in support of the mode demonstrations presented in Chapter 5:

* Hover

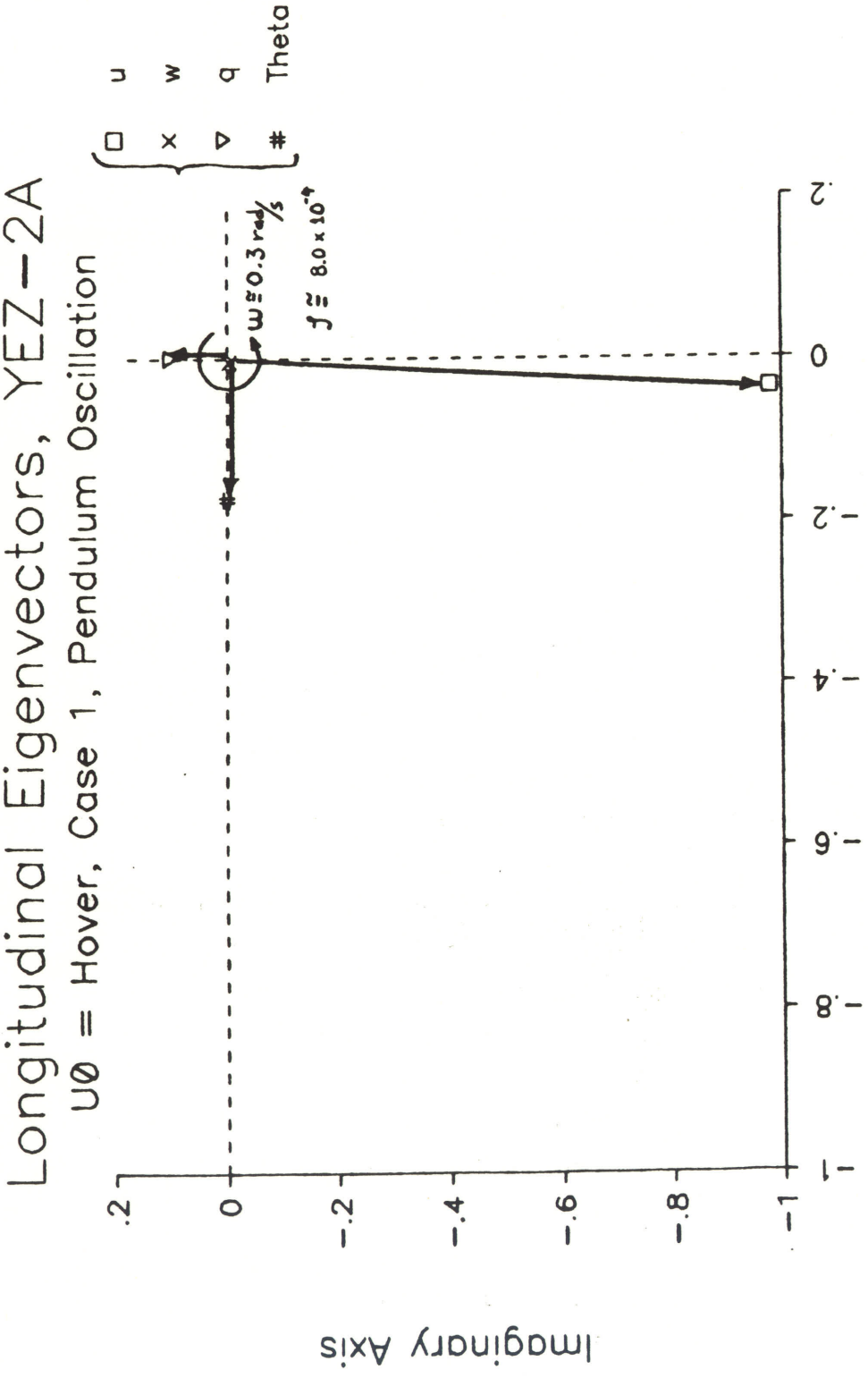
The first hover eigenvalue ($s_1 = -7.6 \times 10^{-6}$) is a negligibly small negative real number and has, associated with it, only two eigenvectors with significant magnitude values: The first is that associated with the u-velocity change, which has reached the top absolute value of one, and the second is the w-velocity change, with a relatively small value (only 0.5% of the u-velocity). It can therefore be concluded that this mode of motion affects primarily the u-velocity component, i.e., the

longitudinal disturbance will result in the final steady state u-velocity being a finite value that will be reached in approximately exponential fashion. This mode is therefore called the u-velocity 'surge' mode or simply 'surge'.

The second eigenvalue ($s_2 = -7.6 \times 10^{-5}$) is again a negligibly small negative real number and has associated with it only one eigenvector with a significant magnitude value. Since that eigenvector is the one corresponding to the w-velocity, it means that the longitudinal disturbance will result in a vertical displacement of the airship, when both the new steady state vertical velocity as well as the new height will be finite values, that will be reached in approximately exponential fashion. This mode is therefore called the 'heave' mode.

The last longitudinal eigenvalue is a complex number, which means that it is an oscillatory mode of motion, with an angular frequency ω of approximately 0.3 rad/s and very little damping indeed. In order to try to visualize this type of motion the associated eigenvectors have been plotted in the complex plane (Fig. A3.3.1). If the eigenvectors are then allowed to rotate at the frequency ω so as to produce results in the amplitude versus time plane (Ref. 56), it can be concluded that the resulting vehicle motion will be composed mainly of oscillations in the u-velocity (about the average value of 0.01 m/s), accompanied by oscillations in pitch rate (q) and pitch angle (θ). The phase shift between u and q is approximately of 180°, but what is perhaps even more important, the phase shift between q and θ is of the order of 90°, which configures a 'pendulum' type of oscillation. The type of motion predicted by this analysis is therefore an oscillation in pitch, following a longitudinal disturbance, with negligible height changes, and therefore it has been named the pendulum mode. Unfortunately, in the hover condition there does

FIGURE A3.3.1


Longitudinal Eigenvectors, YEZ-2A
U0 = Hover, Case 1, Pendulum Oscillation
u
w
q
Theta
ω=0.3 rad/s
ζ≅ 8.0 x 10⁻²
Imaginary Axis
Real Axis
.2
0
-.2
-.4
-.6
-.8
-1

not seem to be much damping available to reduce the amplitude of this motion, at least in the open loop vehicle condition.

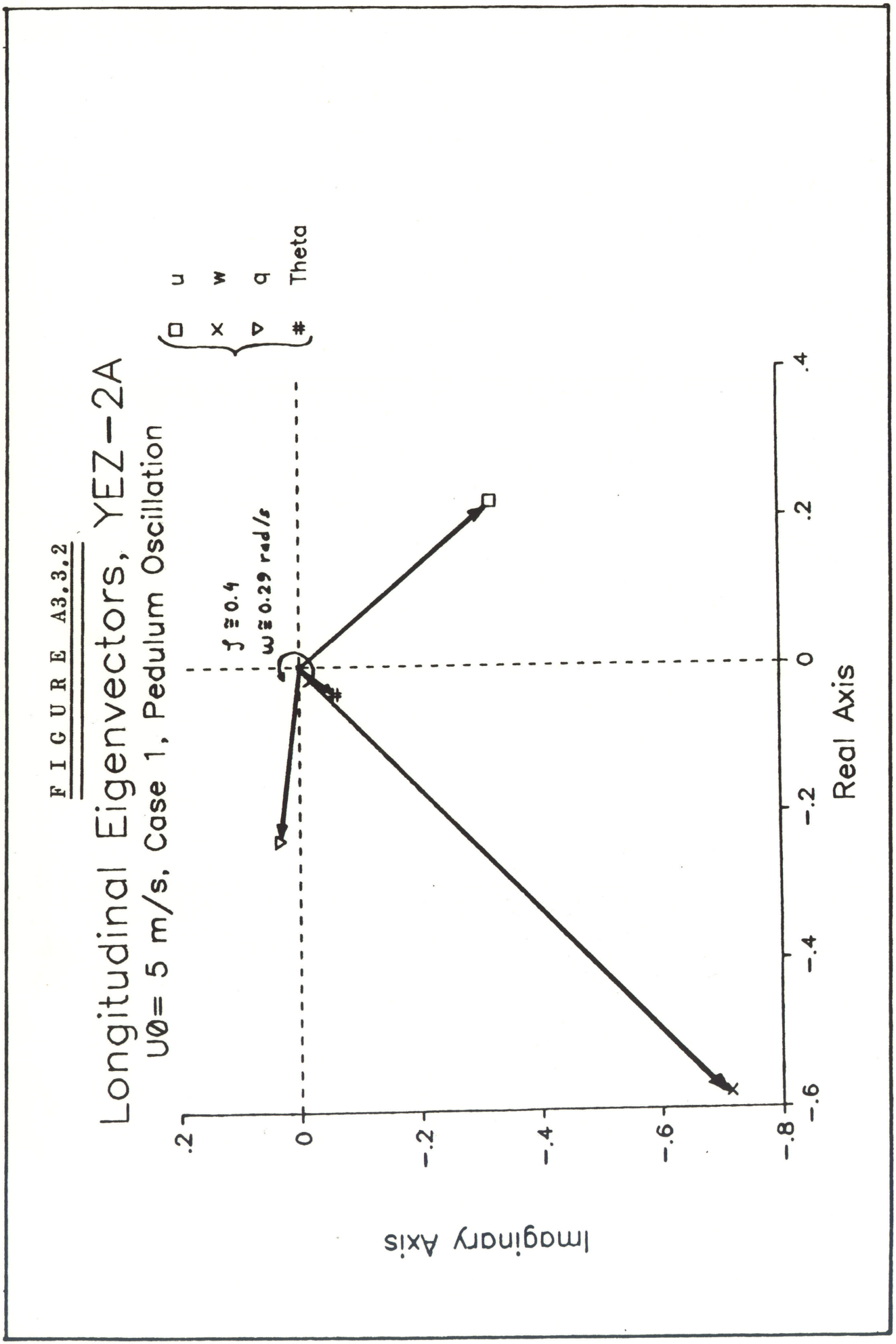
* Flight Speed = 5 m/s

Table A3.2.3 shows that the increase in speed from the hover condition to 5 m/s generated some slight changes in the YEZ-2A modes. The magnitudes of the eigenvectors associated with the first eigenvalue (s_1 = -0.00565), a negative real number, imply that this is a marginally stable mode with the u-velocity eigenvector being the significant response parameter in this case. It has therefore all the characteristics of the hover surge mode already described.

The second eigenvalue (s_2 = -0.039) should also imply a marginally stable mode. An analysis of the magnitudes of the eigenvectors associated with it shows that a small longitudinal disturbance will be followed by a slow change of the vertical velocity (and the longitudinal incidence α for that matter) until a final steady state value is reached in approximately exponential fashion. However, in comparison with what happened in the hover condition, in this case there will be also some exponential variation in the pitch angle, as shown by the magnitude of the θ eigenvector (which becomes even more significant as the speed goes up) and therefore this mode has been named the 'pitch subsidence' mode.

The third eigenvalue is, as before, a complex number. The ω value has gone down just a little bit, whereas the damping (ζ) has improved considerably. The plot of the associated eigenvectors in the complex plane (Fig. A3.3.2) shows that although a pendulum type of oscillation is still present (q lags behind θ by just under 90°), a heave oscillation coupled with it is now to be expected. In addition, the heave oscillation is in

FIGURE A3.3.2


Longitudinal Eigenvectors, YEZ-2A
U0= 5 m/s, Case 1, Pedulum Oscillation
ζ ≅ 0.4
ω ≅ 0.29 rad/s
u
w
q
Theta
Imaginary Axis
Real Axis
.2
0
-.2
-.4
-.6
-.8
.4
.2
0
-.2
-.4
-.6

phase with the pitch angle oscillation, which means that the changes in longitudinal incidence (α) happen more or less at the same time as the changes in vehicle attitude (θ), a coincidence that makes sense at the slow end of the flight speed range.

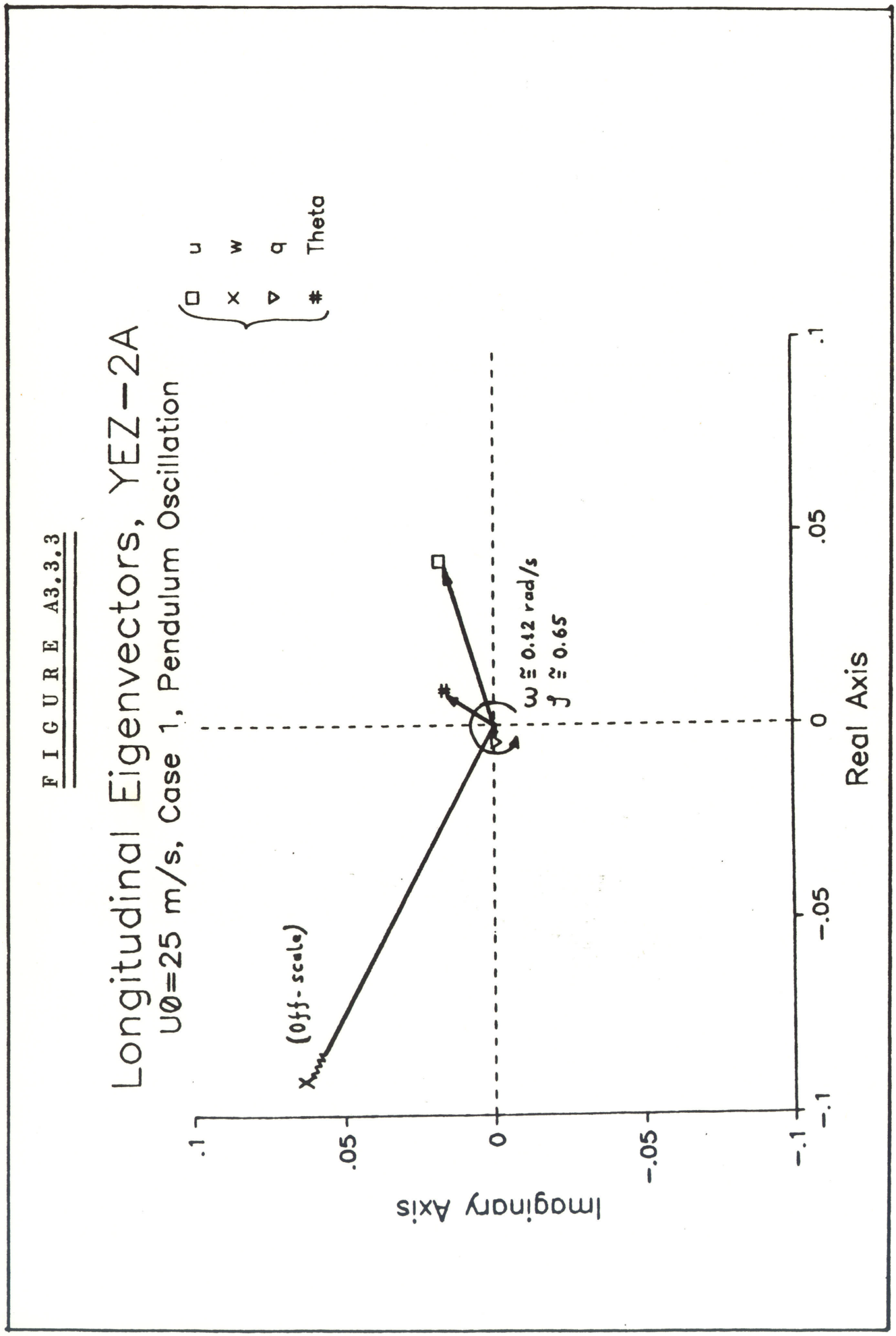
* Flight Speed = 25 m/s

Table A3.2.13 shows some changes in the modes of motion of the YEZ-2A more or less in the directions already detected in the previous case when compared to the hover condition. The first eigenvalue ($s_1 = -0.028$) implies a slightly more stable mode than before, where the most significant eigenvector is still that associated with the u-velocity. Therefore, much in the same fashion as in the hover condition, this is termed the surge mode.

The second eigenvalue ($s_2 = -1.12$) shows a dramatic improvement in stability over the previous case. An inspection of its associated eigenvectors shows that the nature of the mode has changed only slightly in the sense that now a small longitudinal disturbance will result in the expected heave subsidence (or, equivalently, a longitudinal incidence α exponential convergence to a final steady state value) accompanied by relatively fast (since the eigenvalue is larger now), approximately exponential, convergence to the final steady state values of u-velocity, pitch rate q and pitch angle θ. The q-associated eigenvector value has grown considerably over the previous case, substantiating the prediction that the final longitudinal attitude θ will be reached much sooner than before.

Finally, the complex eigenvalue predicts an oscillatory mode that has some marked changes over the previous cases. The plot of the eigenvectors in the complex plane (Fig. A3.3.3) shows that in spite of some form of pendulum oscillation being still present (the phase difference between q and θ has now grown over 90°),

FIGURE A3.3.3


Longitudinal Eigenvectors, YEZ-2A
U0=25 m/s, Case 1, Pendulum Oscillation
u
w
q
Theta
(off-scale)
ω ≅ 0.12 rad/s
ζ ≅ 0.65
Imaginary Axis
Real Axis
.1
.05
0
-.05
-.1

the greatest emphasis is now on the heave / longitudinal incidence α type of oscillation. On the other hand the mode as a whole is now considerably slower (w is now less than half the previous value) and heavily damped. In summary, a small longitudinal disturbance at U0 = 25 m/s is likely to cause just a small vertical oscillatory displacement, accompanied by even smaller oscillations in pitch, and the whole motion is likely to die out in a very short time indeed. At this fast end of the speed range the mode denomination of pendulum oscillation is clearly a misnomer.

A3.4 Derivation of the Lateral Modes

The eigenvalue and eigenvector tables of Section A3.2 show that the lateral modes of motion of the YEZ-2A are constituted by two subsidence and one oscillatory mode, very much in line with what happened in the longitudinal case. Again all the eigenvalues have a negative real part and therefore they should be all stable modes, although as before, the stability in the hover condition can be assumed to be neutral in view of the forward speed of 0.01 m/s that had to be specified in this case. The plot of the lateral eigenvalues in the complex plane for the range of flight speeds is presented in Chapter 5.

The derivation of the lateral modes was carried out much in the same way as for the longitudinal case, i.e., by simply analyzing the relative magnitudes (and phase relations when appropriate) of the eigenvectors associated with each eigenvalue. Two values of flight speed were selected, in support of the mode demonstrations presented in Chapter 5:

* Hover

The first hover eigenvalue ($s_1 = -6.4 \times 10^{-5}$) from Table A3.2.2 is a negative real number and has,

associated with it, only two eigenvectors with significant values: The first is that associated with the proper lateral disturbance, i.e., the v-velocity, which has reached the top normalized value of one, and the second is that associated with the yaw rate r, which is effectively very small indeed. It can therefore be concluded that following a small lateral type of perturbation, a very small yaw rate will contribute to a new sideslip angle which will be reached in approximately exponential fashion. This mode was therefore called 'sideslip subsidence'.

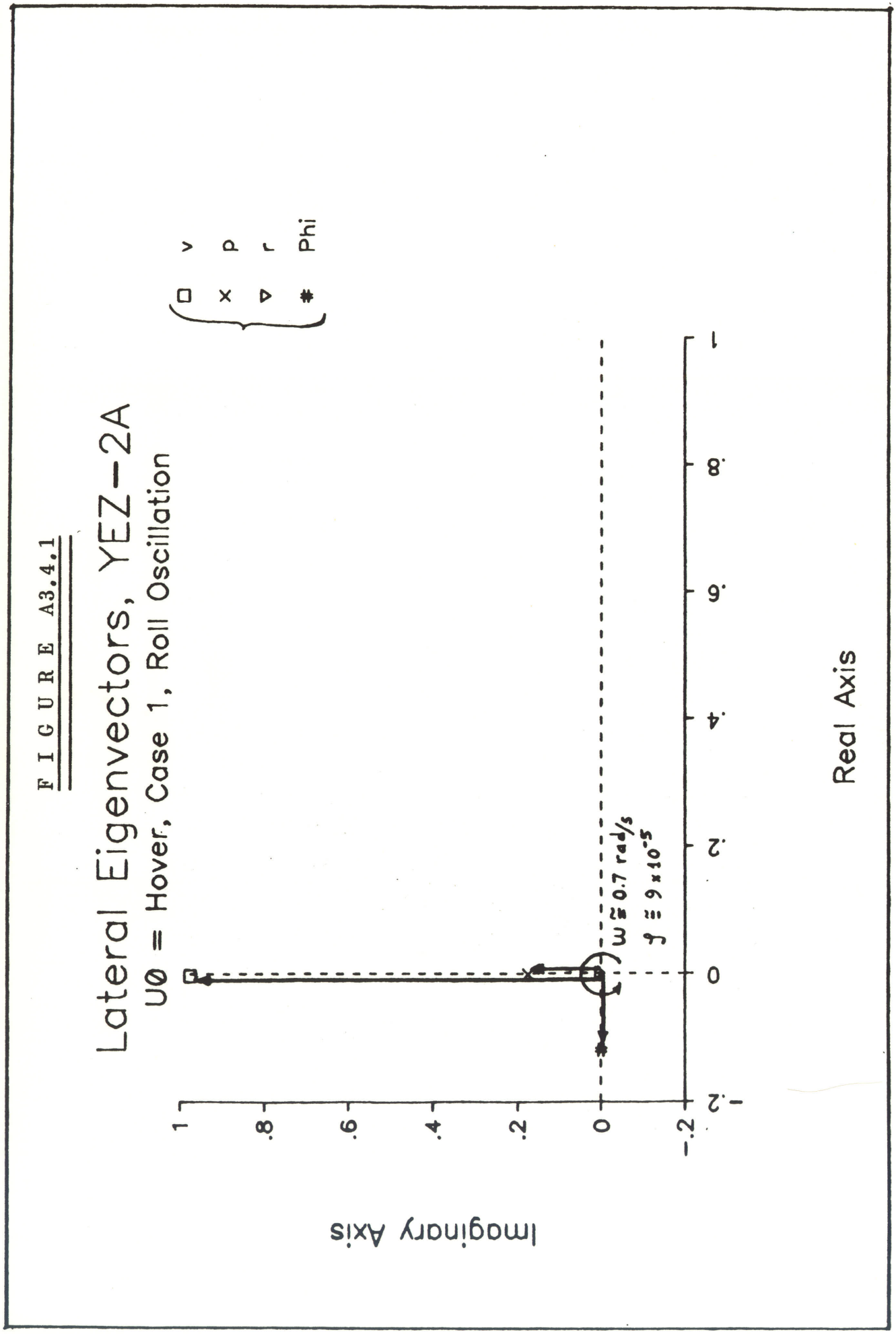
The second eigenvalue ($s_2 = -4.7 \times 10^{-7}$) has, associated with it, only two eigenvectors with significant magnitude values: v and r, i.e., the same vectors of the previous mode, although now r is relatively much more important now. As this mode appears to be at least one order of magnitude faster than the previous one it was denominated 'yaw subsidence'.

The third and last hover eigenvalue is a complex number with negligible negative real part. The significant eigenvectors in this case are those associated with the roll rate p and the roll angle ϕ. When they are plotted in the complex plane (Fig. A3.4.1) it can be seen that p is in phase with the lateral disturbance represented by the sideslip velocity v (or equivalently the lateral incidence β) and has a 90° phase shift when compared to the bank angle ϕ. It can therefore be concluded that, following a small lateral perturbation, the airship will develop an oscillatory motion about the OX body axis, with an angular frequency of about 0.7 rad/s and very little damping. For these reasons this mode was called 'roll oscillation'.

* Flight Speed = 5 m/s

The results presented in Table A3.2.4 show some noticeable stability improvements over the previous hover

FIGURE A3.4.1

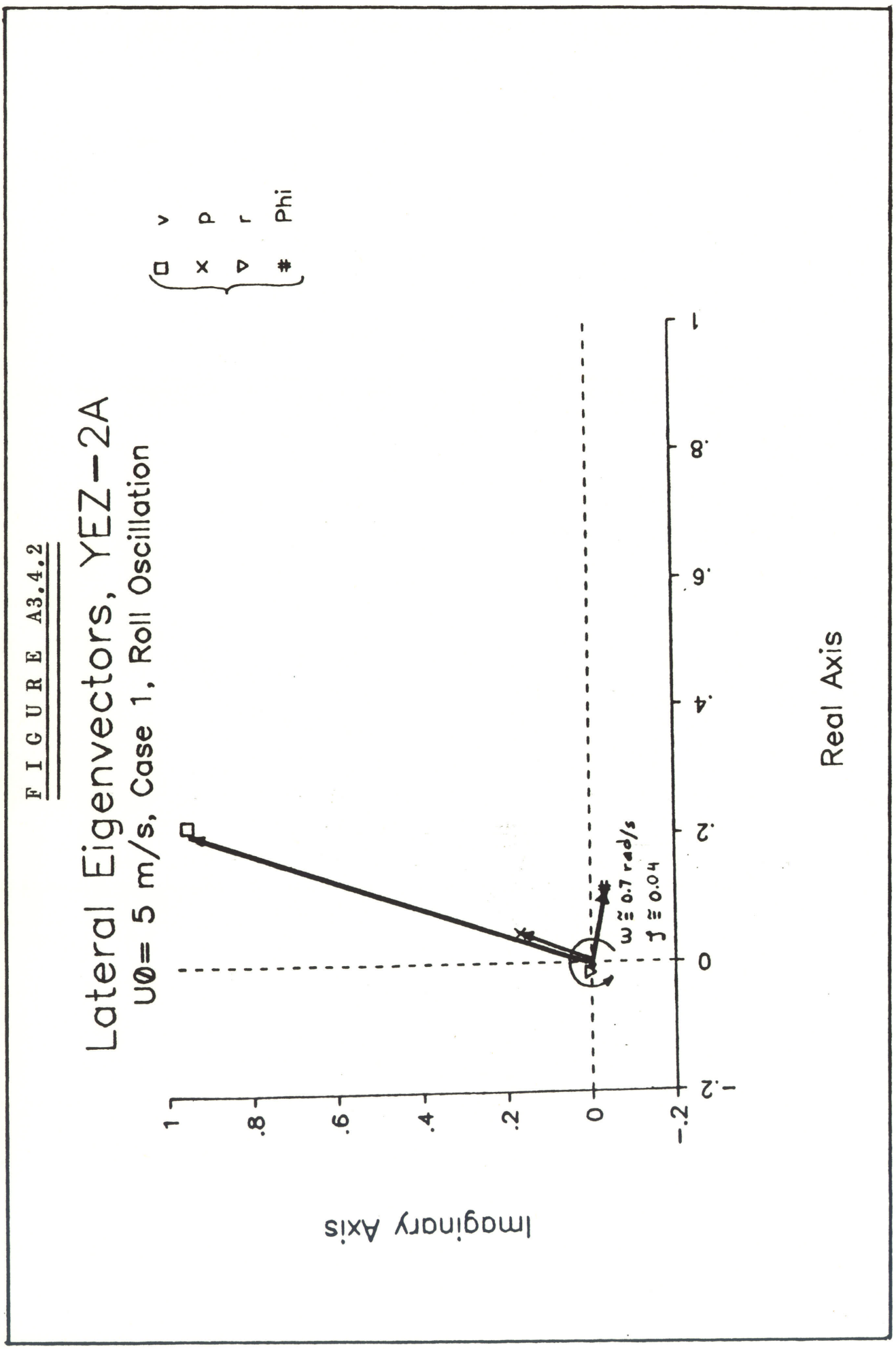

Lateral Eigenvectors, YEZ-2A
U0 = Hover, Case 1, Roll Oscillation
v
p
r
Phi
ω ≅ 0.7 rad/s
ζ ≅ 9 x 10⁻⁵
Imaginary Axis
Real Axis
1
.8
.6
.4
.2
0
-.2
-1
-.8
-.6
-.4
-.2
0
.2
.4
.6
.8
1

condition case. The first eigenvalue (s_1 = -0.0315) suggests a marginally stable mode and has, associated with it, the same two significant eigenvectors as before: The v-velocity and the yaw rate r. It can therefore be concluded that this mode of motion remains essentially the same as in the hover condition, i.e., it is a slow acquisition of a new sideslip angle β following a disturbance in sideslip. Hence the name 'sideslip subsidence', although it appears that now some very slight banking motion will also develop, in the usual approximate exponential fashion, in view of the magnitude of the ϕ-associated eigenvector.

The second eigenvalue (s = -0.232) is also a negative real number and appears to be a much faster mode than the first. The associated eigenvectors show that most, if not all of them, have enough in terms of magnitude to be able to contribute to the mode characteristics, although the yaw rate r is the dominant eigenvector. It can therefore be concluded that following a small sideslip disturbance, the kind of motion that will develop is constituted by a relatively rapid exponential convergence to a new yaw rate r, accompanied by a small banking motion about the OX body axis. Hence the mode designation of 'yaw subsidence'.

The third eigenvalue is a complex number with negative real part. The plot of its associated eigenvectors (Fig. A3.4.2) show essentially the same characteristics as in the hover condition, with the difference that the amount of damping has now risen to a nonetheless still small value of $\zeta \cong 0.04$. It can therefore be concluded that a lateral small perturbation will result in the oscillatory type of motion already described as roll oscillation with some small degree of damping now being incorporated.

FIGURE A3.4.2


Lateral Eigenvectors, YEZ-2A
U0= 5 m/s, Case 1, Roll Oscillation
v
p
r
Phi
ω ≅ 0.7 rad/s
ζ ≅ 0.04
Imaginary Axis
Real Axis
1
.8
.6
.4
.2
0
-.2
-.2
0
.2
.4
.6
.8
1

* Flight Speed = 25 m/s

An inspection of the results presented in Table A3.2.14 show that, in essence, the increase in forward speed has not resulted in any change in the nature of the YEZ-2A lateral modes of motion. The only differences that are noticeable can be summarized as:

i. The subsidence modes have become much faster now.

ii. The roll oscillation has still the same angular frequency as before, although the damping has increased substantially, in spite of being still a rather small value, even if compared just with the one obtained for the longitudinal oscillatory mode.

A3.5 Non-neutral Buoyancy Effects

In the course of probing into the airship modes of motion, a short investigation was carried out with model parameters set for two non-neutral buoyancy cases, i.e., Cases 2 and 3 (See Section A1.6 of Appendix-1). The former is a 2268 Kg of lightness condition, whereas the latter refers to a 7118 Kg of heaviness condition, both at sea level, ISA conditions.

The main problem found in trying to run the simulation model with a non-neutral buoyancy condition was associated with the fact that the airship had now to be longitudinally trimmed, at run-time, manually in order to prevent it from going into a descent path (heaviness case) or into an ascending one (lightness case). This took the form of trying out different power settings and elevator angles, i.e., the ruddervators were deflected in an elevator like fashion, in order to achieve straight and level flight. After this had been accomplished, the

simulation run was stopped and the ANALYZ package of ACSL was applied in the way already described in Section A3.1.

The results thus achieved are presented in the following Tables A3.5.1-4.

Table A3.5.1 - Longitudinal Eigenvectors, YEZ-2A
Speed = 18 m/s, Case 2, Height = 110 m
η_{Trim} = + 20°, $\theta_{Trim} \cong \alpha_{Trim} \cong$ -9.5°
ω = Frequency, ζ = Damping

M O D E	Surge	Pitch Subsidence	Pendulum Oscillation
EIGENVALUES (rad/s)	-0.0285	-0.745	-0.0739 ± 0.0926i
ω (rad/s)			0.118
ζ			0.624
EIGENVECTORS			
u	1.0	-0.426	-0.179 ∓ 0.0211i
w	0.0921	-0.905	-0.422 ± 0.889i
q	5.48E-4	0.0254	0.00281 ± 0.00354i
θ	-0.00952	-0.0169	-0.0189 ∓ 2.88E-5i

Table A3.5.2 - Lateral Eigenvectors, YEZ-2A
Speed = 18 m/s, Case 2, Height = 110 m
η_{Trim} = + 20°, $\theta_{Trim} \cong \alpha_{Trim} \cong$ -9.5°
ω = Frequency, ζ = Damping

M O D E	Sideslip Subsidence	Yaw Subsidence	Roll Oscillation
EIGENVALUES (rad/s)	-0.167	-0.798	-0.165 ± 0.641i
ω (rad/s)			0.662
ζ			0.250
EIGENVECTORS			
v	-1.0	-1.0	-0.194 ∓ 0.970i
p	-0.00744	-0.0710	-0.0973 ∓ 0.0691i
r	0.00263	0.0725	0.00164 ∓ 2.87E-4i
ϕ	0.0227	0.0477	-0.0318 ± 0.0834i

Table A3.5.3 - Longitudinal Eigenvectors, YEZ-2A
Speed = 25 m/s, Case 2, Height = 12.5 m
η_{Trim} = + 1.6°, $\theta_{Trim} \cong \alpha_{Trim} \cong$ -2.3°
ω = Frequency, ζ = Damping

M O D E	Surge	Pitch Subsidence	Pendulum Oscillation
EIGENVALUES (rad/s)	-0.0305	-1.084	-0.0785 ± 0.0747i
ω (rad/s)			0.108
ζ			0.724
EIGENVECTORS			
u	1.0	-0.321	-0.0460 ± 7.07E-4i
w	0.0374	-0.947	-0.777 ∓ 0.627i
q	4.01E-5	0.0282	-0.00105 ∓ 0.00399i
θ	-6.03E-4	-0.0120	-0.00841 ± 0.0153i

Table A3.5.4 - Lateral Eigenvectors, YEZ-2A
Speed = 25 m/s, Case 2, Height = 12.5 m
η_{Trim} = + 1.6°, $\theta_{Trim} \cong \alpha_{Trim} \cong$ -2.3°
ω = Frequency, ζ = Damping

M O D E	Sideslip Subsidence	Yaw Subsidence	Roll Oscillation
EIGENVALUES (rad/s)	-0.168	-1.07	-0.198 ± 0.629i
ω (rad/s)			0.659
ζ			0.301
EIGENVECTORS			
v	-1.0	-1.0	-0.619 ± 0.764i
p	-0.00608	-0.102	-0.0361 ± 0.145i
r	0.00532	0.0841	-5.20E-4 ∓ 0.00457i
ϕ	0.0169	0.0443	-0.104 ∓ 0.00634i

Table A3.5.5 - Longitudinal Eigenvectors, YEZ-2A
Speed = 29 m/s, Case 3, Height = -9.0 m
$\eta_{Trim} = -0.005°$, $\theta_{Trim} \cong \alpha_{Trim} \cong 4.3°$
ω = Frequency, ζ = Damping

M O D E	Surge	Pitch Subsidence	Pendulum Oscillation
EIGENVALUES (rad/s)	-0.0365	-1.25	-0.0585 ± 0.0651i
ω (rad/s)			0.088
ζ			0.669
EIGENVECTORS			
u	-0.99	0.225	0.304 ∓ 0.0141i
w	0.167	0.974	0.0463 ∓ 0.952i
q	1.51E-5	-0.0304	-0.00146 ∓ 0.00246i
θ	-1.76E-4	0.0103	0.0136 ± 0.00269i

Table A3.5.6 - Lateral Eigenvectors, YEZ-2A
Speed = 29 m/s, Case 3, Height = -9.0 m
$\eta_{Trim} = +0.005°$, $\theta_{Trim} \cong \alpha_{Trim} \cong 4.3°$
ω = Frequency, ζ = Damping

M O D E	Sideslip Subsidence	Yaw Subsidence	Roll Oscillation
EIGENVALUES (rad/s)	-0.159	-1.27	-0.207 ± 0.617i
ω (rad/s)			0.650
ζ			0.312
EIGENVECTORS			
v	-1.0	-0.981	-0.934 ∓ 0.292i
p	-0.00680	-0.151	-0.145 ∓ 0.0970i
r	0.00619	0.114	0.00612 ∓ 0.00178i
ϕ	0.0174	0.0489	-0.0301 ± 0.109i

A comparison between the results presented in the Tables of Section A3.2 and Tables A3.5.1-6 shows essentially that:

i. The order of magnitude of the eigenvalues and the nature of the YEZ-2A modes of motion, as expressed by the associated eigenvectors, remained substantially the same, both for the 'lightness' Case 2 as for the 'heaviness' Case 3.

ii. Generally speaking, the effects associated with a non-neutral buoyancy condition, where these could be detected, appear to be linked with a slight slowing down of the modes of motion, coupled with a slight increase in the mode damping. This latter effect is more noticeable in the lateral cases.

In summary therefore it can be said that the nature of the aerodynamic stability modes of motion of the airship did not change due to a non-neutral buoyancy condition. The slight changes detected were mostly of a beneficial consequence to controllability, although the vehicle attitudes required in order to achieve longitudinal trim are likely to result in marked increases in fuel consumption due to higher drag.

Finally, it must be remembered that these results and conclusions were produced in the course of a short investigative process and therefore were not aimed at exhausting the subject. The number of possibilities of, for instance, combining thrust setting with ruddervator deflection angle in order to achieve the required longitudinal trim condition is virtually limitless. Changes in other flight governing parameters can and should also be attempted.